

Håkon Steinholt Bygdås

Evaluation of protective groups for purines in synthesis of CSF1R inhibitors

Master's thesis in Chemical Engineering and Biotechnology

Supervisor: Bård Helge Hoff

Co-supervisor: Thomas Ihle Aarhus

June 2019

Håkon Steinholt Bygdås

Evaluation of protective groups for purines in synthesis of CSF1R inhibitors

Master's thesis in Chemical Engineering and Biotechnology
Supervisor: Bård Helge Hoff
Co-supervisor: Thomas Ihle Aarhus
June 2019

Norwegian University of Science and Technology
Faculty of Natural Sciences
Department of Chemistry



Norwegian University of
Science and Technology

I hereby declare that the work done in this thesis is independent and in accordance with the exam regulations of the Norwegian University of Science and Technology.

Trondheim, June 17, 2019

Håkon Steinholt Bygdås
Håkon Steinholt Bygdås

Acknowledgements

This master's thesis has been carried out at the Department of Chemistry at The Norwegian University of Science and Technology in the spring of 2019. It has been supervised by Professor Bård Helge Hoff and PhD Candidate Thomas Ihle Aarhus.

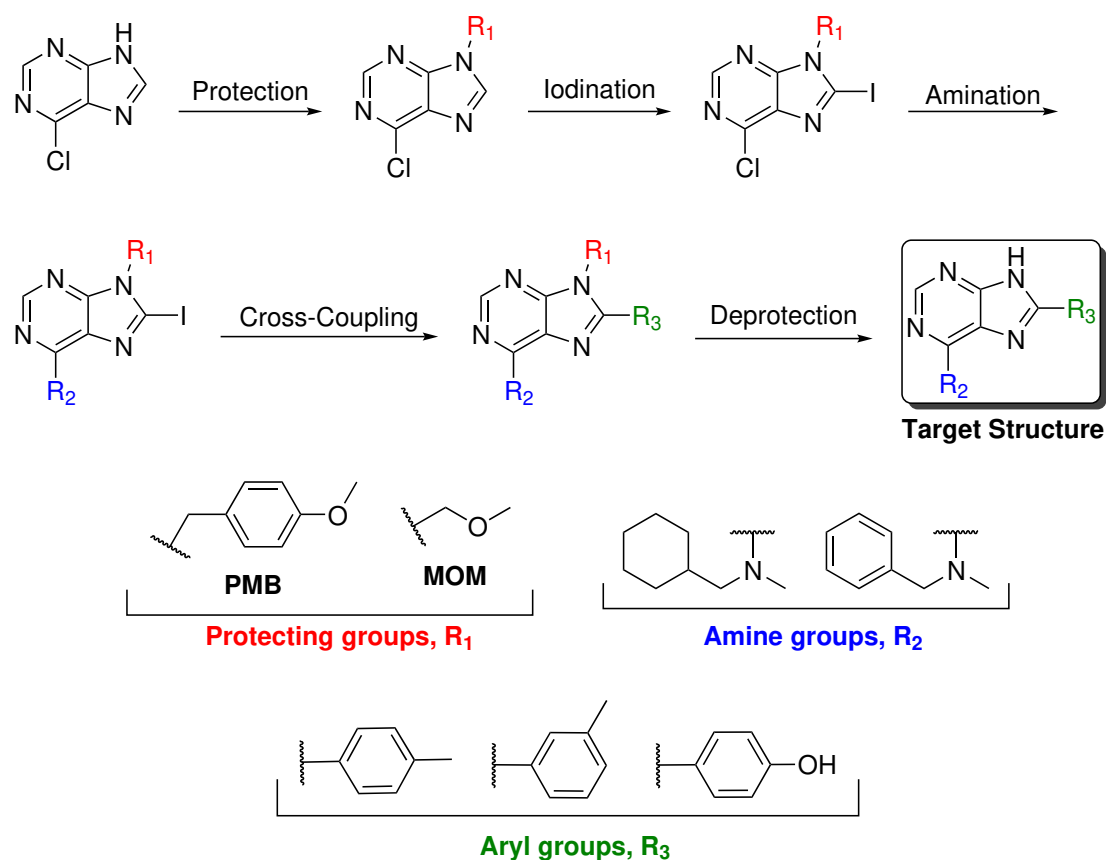
First of all, I would like to thank my supervisors for all their patience and guidance. Their door was always open if I needed it, regardless of the time of day, or how minor my problems might have been. I would also like to give a special thanks to Head Engineer Torun Margareta Melø for all help in the NMR lab, Engineer Susanna Vila Gonzales and Engineer Julie Asmussen for the help with the MS analyses, and Roger Aarvik for providing chemicals and a good mood.

Last but not least, I would like to thank my friends and family for supporting me throughout my years in Trondheim.

Abstract

The colony stimulating factor 1 (CSF1) is overexpressed in several diseases such as cancers, inflammatory diseases and bone diseases. Recent studies have shown that inhibition of the colony stimulating factor one receptor kinase (CSF1R) can aid in treatment of these conditions.

Ongoing work in the research group has shown that purine based molecules are excellent inhibitors of CSF1R. The purpose of this thesis was to investigate synthetic protocols towards 6-amino-8-arylpurines, by utilizing *p*-methoxybenzyl (PMB) and methoxymethyl (MOM) as protecting groups.



The PMB protected purine was synthesized during the pre-master's project, and exhibited poor *N*9 regioselectivity, resulting in only a 45% yield. Successive iodination with NIS gave the iodinated building block in 62% yield, and further functionalization through amination and Suzuki cross-coupling proceeded with

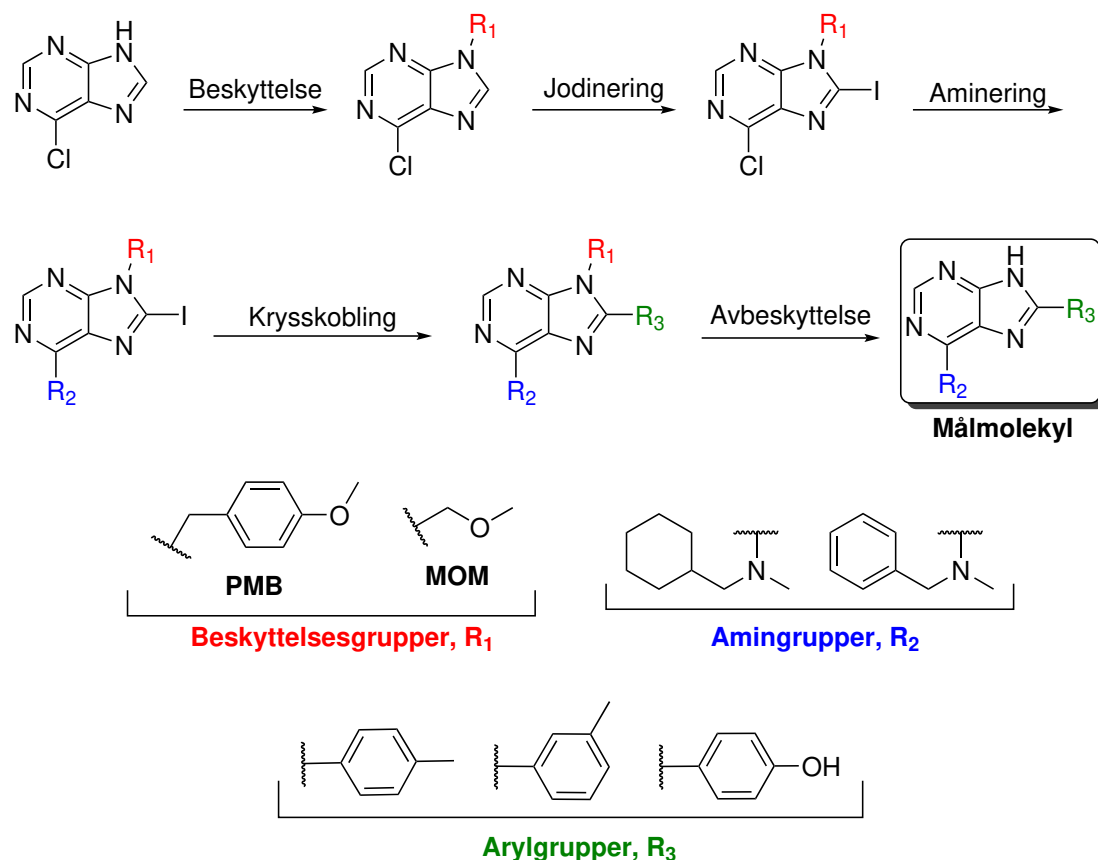
ease. Multiple deprotection methods were attempted, and debenzylation through catalytic hydrogenation and transfer hydrogenolysis proved futile. Successful *N*-debenzylation was achieved with AlCl₃ at high temperature, yielding the targeted 6-amino-8-arylpurine in 11% overall yield.

In an attempt to achieve higher regioselectivity and easier deprotection, MOM was selected as an alternative protecting group. *N*-Alkylation with MOMCl was completely regioselective, and yields up to 86% was achieved. Subsequent iodination through metallation reactions gave yields between 25-36%. Thermal amination and Suzuki cross-coupling were both good reactions, and deprotection was achieved with HCl in MeOH. The targeted 6-amino-8-tolylpurine was isolated in 18% overall yield, while the phenol analog was isolated in 4% overall yield due to partial decomposition.

Sammendrag

Kolonistimmulerende faktor 1 (CSF1) er ofte overuttrykt i flere typer kreft, betennelsesykdommer og beinsykdommer. Studier har vist at hemning av den kolonistimmulerende faktor 1 reseptor kinasen (CSF1R) kan gi økt effekt av behandling for disse sykdommene.

Pågående arbeid i forskningsgruppen har vist at purinbaserte molekyler er utmerkede CSF1R inhibitorer. Formålet med denne masteroppgaven er å undersøke synteseprotokoller mot 6-amino-8-arylpuriner, ved bruk av *p*-metoksybenzyl (PMB) og metoksymetyl som beskyttelsesgrupper.



Det PMB beskyttede purinet ble syntetisert i førmasterprosjektet, og lav *N*9 regiosektivitet resulterte i bare 45% utbytte. Jodinerings med NIS gav den jodinererte byggesteinen i 62% utbytte, og påfølgende funksjonalisering ved aminering og Suzuki-krysskobling gikk uten problemer. Flere avbeskyttingsmetoder ble testet,

og debenzylering igjennom katalytisk hydrogenering og overføringshydrogenolyse var fåfengt. Vellykket *N*-debenzylering ble oppnådd med AlCl_3 ved høy temperatur, og gav det ønskede 6-amino-8-arylpurinet i 11% totalutbytte.

I et forsøk på å oppnå økte regioselektivitet og enklere avbeskytting ble MOM testet som en alternativ beskyttelsesgruppe. *N*-Alkylering med MOMCl var fullstendig regioselektiv, og utbytter opp til 86% ble oppnådd. Påfølgende jodinerings via metallering gav utbytter mellom 26-36%. Termisk aminering og Suzuki krysskobling var gode reaksjoner, og avbeskytting ble oppnådd med HCl i MeOH. Det ønskede 6-amino-8-tolylpurinet ble isolert i 18% totalutbytte, mens fenol analogen ble isolert i 4% totalutbytte på grunn av delvis dekomponering.

Contents

Background and Aim	1
Introduction and Theory	3
2.1 Colony Stimulating Factor 1 Receptor	3
2.2 Previous Work In the Research Group	4
2.3 Purines	6
2.4 Synthesis of 6-Amino-8-Arylpurines	8
2.5 Protecting Groups	10
2.5.1 Tetrahydropyran (THP)	10
2.5.2 Benzylic Groups	10
2.5.3 Methoxymethyl (MOM)	11
2.6 Nucleophilic Aromatic Substitution	11
2.7 Suzuki-Miyaura Cross-Coupling	12
Results and Discussion	15
3.1 Introduction of the Protecting Group and Synthesis of Compound 3	15
3.2 Iodination	18
3.2.1 Synthesis of Compound 4	18
3.2.2 Synthesis of Compound 5	19
3.3 Amination	22
3.3.1 Synthesis of Compound 6	23
3.3.2 Synthesis of Compounds 8, 9 and 10	25
3.4 Cross-Coupling and Synthesis of Compounds 12, 15, 17 and 18 . . .	29
3.4.1 Suzuki	29
3.4.2 Negishi	32
3.5 Debenzylation and Synthesis of Compounds HSB2 and HSB3	33
3.5.1 Hydrogenation	33
3.5.2 Acid Protocols	35
3.6 MOM Deprotection and Synthesis of Compounds HSB4 and HSB5 .	38

3.7	Structure Elucidation	42
3.7.1	General Remarks	43
3.7.2	Compound 3	44
3.7.3	Compound 10	47
3.7.4	Compound 12	49
3.7.5	Compound 15	52
3.7.6	Compound 17	54
3.7.7	Compound 18	56
3.7.8	Compound HSB2	58
3.7.9	Compound HSB4	60
3.7.10	Compound HSB5	62
3.7.11	IR-Spectroscopy	64
Conclusion and Further Work		69
4.1	Conclusion	69
4.2	Further Work	73
Experimental		76
5.1	General Information	76
5.2	Protection	77
5.3	Iodination	79
5.4	Amination	83
5.5	Suzuki Cross-Coupling	85
5.6	Negishi Cross-Coupling	90
5.7	Deprotection	91
Appendices		
Spectroscopic Data for Compound 3		A-1
Spectroscopic Data for Compound 4		A-9
Spectroscopic Data for Compound 5		A-10
Spectroscopic Data for Compound 6		A-12

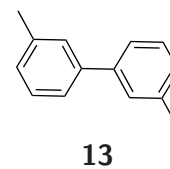
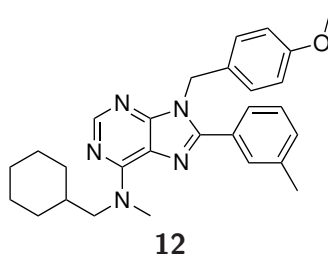
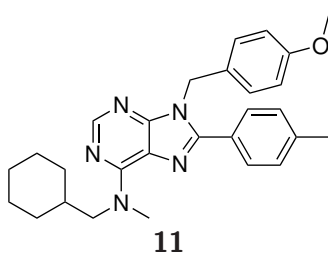
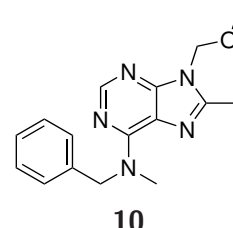
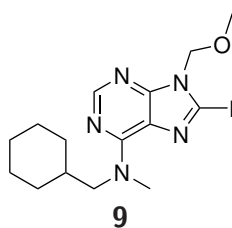
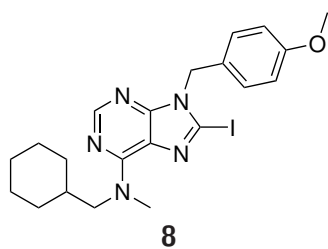
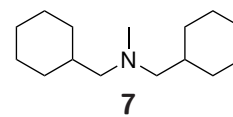
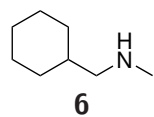
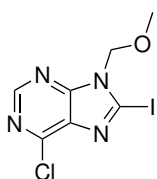
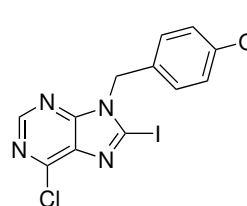
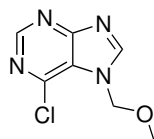
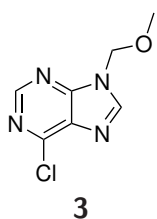
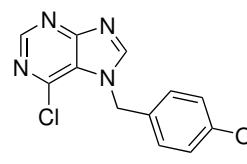
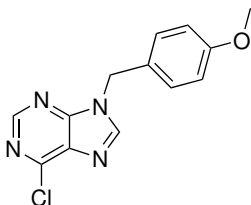
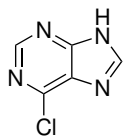
Spectroscopic Data for Compound 8	A-14
Spectroscopic Data for Compound 9	A-15
Spectroscopic Data for Compound 10	A-16
Spectroscopic Data for Compound 12	A-23
Spectroscopic Data for Compound 15	A-33
Spectroscopic Data for Compound 17	A-41
Spectroscopic Data for Compound 18	A-48
Spectroscopic Data for Compound 20	A-55
Spectroscopic Data for Compound HSB2	A-58
Spectroscopic Data for Compound HSB4	A-65
Spectroscopic Data for Compound HSB5	A-74

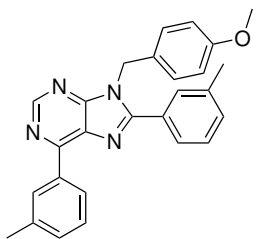
Symbols and Abbreviations

\approx	Approximately
δ	Chemical Shift [ppm]
ν	Frequency [cm^{-1}]
^1H NMR	Proton Nuclear Magnetic Resonance
^{13}C NMR	Carbon Nuclear Magnetic Resonance
BuLi	Butyllithium
br	Broad
conc.	Concentrated
COSY	Correlation Spectroscopy
CSF1	Colony Stimulating Factor 1
CSF1R	Colony Stimulating Factor 1 Receptor
d	Doublet
DMB	Dimethoxybenzene
DMF	Dimethylformamide
DMSO	Dimethyl Sulfoxide
DNA	Deoxyribonucleic Acid
dppf	1,1'-Ferrocenediyl-bis(diphenylphosphine)
EGFR	Epidermal Growth Factor Receptor
eq	Equivalents
EtOAc	Ethyl Acetate
GC	Gas Chromatography
h	Hours
hept	Heptet
hex	Hextet
HMBC	Heteronuclear Multiple Bond Correlation
HRMS	High Resolution Mass Spectroscopy
HSQC	Heteronuclear Single Bond Correlation
IC_{50}	Half Maximal Inhibitory Concentration
IL-34	Interleukin-34
int.	Integral

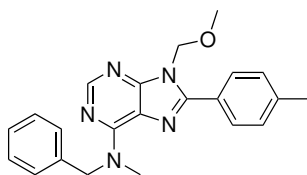
IR	Infrared
J	Coupling Constant [Hz]
LDA	Lithium Diisopropylamide
m/z	Mass per Charge
m	Meta
m	Multiplet
MOM	Methoxymethyl
mp.	Melting Point
MS	Mass Spectroscopy
mult.	Multiplicity
NIS	<i>N</i> -Iodosuccinimide
NMR	Nuclear Magnetic Resonance
<i>o</i>	Ortho
<i>p</i>	Para
pent	Pentet
Pd	Palladium
PK	Protein Kinase
PMB	<i>p</i> -Methoxybenzyl
ppm	Parts per Million
R_f	Retention Factor
rt	Room Temperature
s	Singlet
S_NAr	Nucleophilic Aromatic Substitution
THF	Tetrahydrofuran
THP	Tetrahydropyran
TLC	Thin Layer Chromatography
TMP	Tetramethylpiperidine
TMS	Trimethylsilyl
t	Triplet

Numbered Compounds

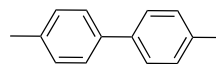




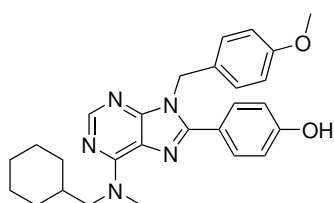
14



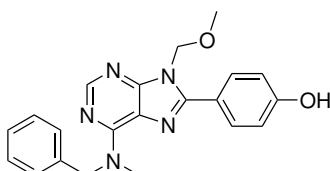
15



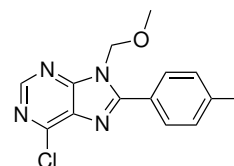
16



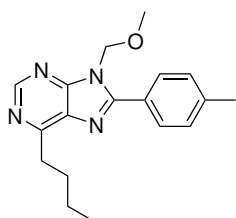
17



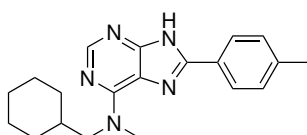
18



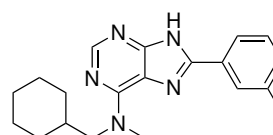
19



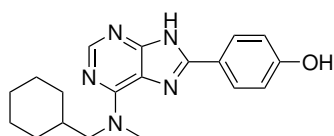
20



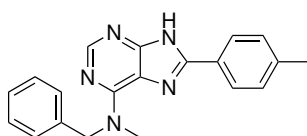
HSB1



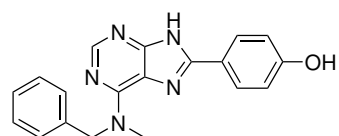
HSB2



HSB3



HSB4



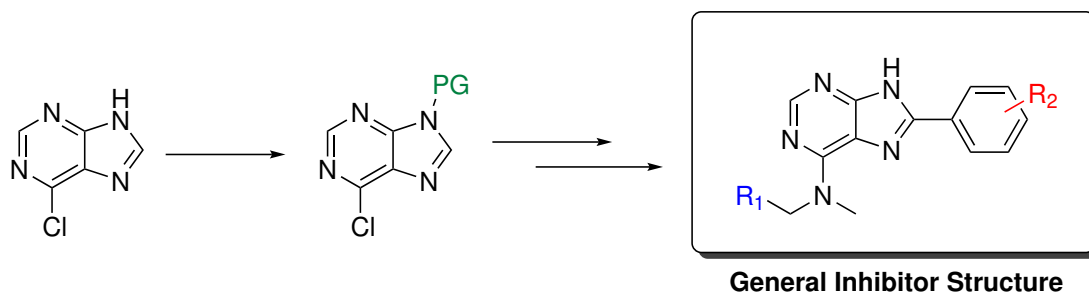
HSB5

1 Background and Aim

Cancer is the leading cause of death in the developed world, and over seven million people die of cancer every year.¹

Protein kinases mediate most of the signal transduction in eukaryotic cells.^{2,3} Dysregulation of the signaling pathways have been linked to cancers and various other disease states.^{4,5} As a consequence, kinases have become emerging drug targets.⁵ One such kinase is the colony stimulating factor 1 receptor (CSF1R), which is overexpressed in some cancers and bone disease.⁶ However, there are currently no drugs on the market.^{6,7}

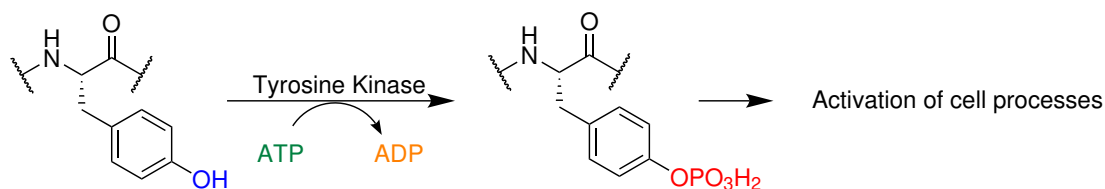
Previous work in the research group has seen the potential of purine based CSF1R inhibitors. The aim of this thesis is to investigate the use of *p*-methoxybenzyl and methoxymethyl as protecting groups in synthetic protocols towards 6-amino-8-arylpurines.



2 Introduction and Theory

2.1 Colony Stimulating Factor 1 Receptor

The colony stimulating factor 1 receptor (CSF1R) is a type III tyrosine kinase receptor that regulates the survival, proliferation, differentiation and function of the cells of the mononuclear phagocyte lineage.^{8,9} It consists of an extracellular and an intracellular domain connected by a transmembrane domain.⁹ Binding of ligands to the extracellular domain results in receptor dimerization and intermolecular phosphorylation, see Scheme 2.1.⁸ There are two known ligands that control activation of the kinase: colony stimulating factor 1 (CSF1), and interleukin-34 (IL-34).⁶



Scheme 2.1: Phosphorylation mechanism.¹⁰

During phosphorylation, a phosphoryl group is transferred to a target protein, changing the activity of the protein.¹¹ It has been shown that a number of diseases are linked to changes in regulation of phosphorylation reactions.^{4,6} This includes the overexpression of CSF1, which has been implicated in the proliferation of osteoclasts, growth and metastasis of cancer, and several inflammatory diseases.⁶ Inhibition of the CSF1R protein or the ligands may prove effective in treatment of the associated diseases.^{6,12}

CSF1R inhibition have already shown some promising results. Xu *et al.* reported improved effects of radiation of prostate cancer cells with use of selective CSF1R inhibitors.¹³ Promising results have also been seen in improving quality of life in mice with inflammatory diseases,¹⁴ as well as slowing the progress of Alzheimer's disease in mice.¹⁵

There are currently only two inhibitors targeting the CSF1 ligand in clinical trials, and no inhibitors targeting IL-34.¹⁶ No inhibitors are currently on the market.^{6,7} Examples of some CSF1R inhibitors are shown in Figure 2.1.¹⁶⁻¹⁸

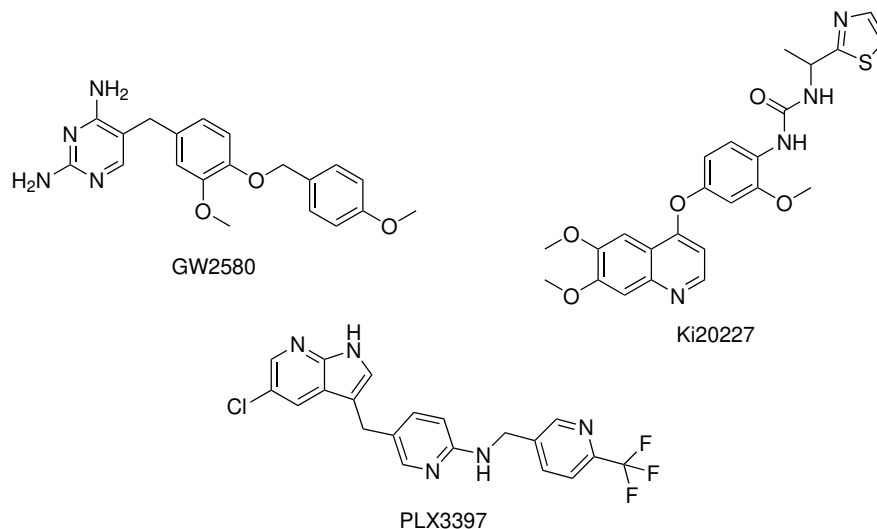


Figure 2.1: Examples of CSF1R inhibitors.¹⁶⁻¹⁸

2.2 Previous Work In the Research Group

The previous focus of the research group was the development of inhibitors for the epidermal growth factor receptor (EGFR), a kinase that is involved in breast,¹⁹ pancreatic,²⁰ ovarian,²¹ and non-small-cell lung cancer.^{22,23} Structures based on the thieno-,²⁴ furo-²⁵ and pyrrolopyrimidines,²⁶ with variations in the C4- and C6-positions have shown promising IC_{50} values in *in vitro* enzymatic assays, some under 1 nM.^{24,26} The base structure is shown in Figure 2.2.

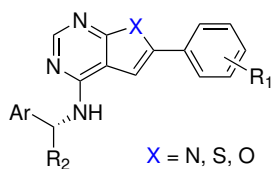


Figure 2.2: General structure of molecules previously synthesized in the research group.²⁵

As a part of this work the molecules were tested against other kinases, and some of these molecules showed promising inhibition against the CSF1R kinase. More

molecules were synthesized with the focus on CSF1R inhibition giving rise to promising purine based structures, see Figure 2.3.²⁷

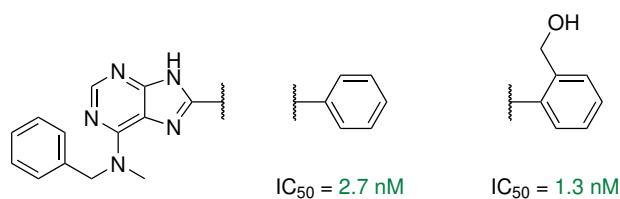
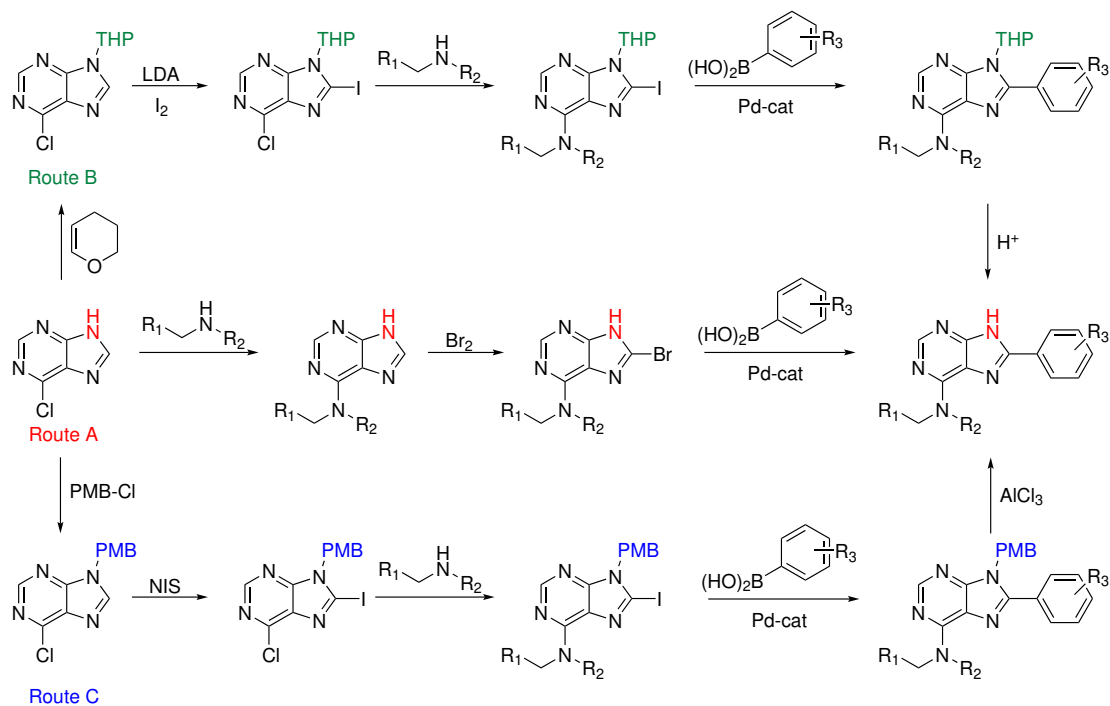


Figure 2.3: Previously synthesized purine based CSF1R inhibitors.²⁷

The group has previously investigated three main routes towards the purine based inhibitor structures, see Scheme 2.2. Route A was initially used, and relies on bromination followed by Suzuki cross-coupling on the unprotected purine. Difficulties with coupling reactions in the presence of free NH groups are known,^{28,29} and the Suzuki reaction proved to be extremely slow. THP protection at the *N*9-position solved the problem,²⁷ and most of the inhibitors have been made following route B. However, major drawbacks include low yields of the iodination, and moderate stability in subsequent reactions.²⁷ Switching to benzylic protecting groups for route C, resulted in a high yielding iodination reaction using NIS.^{27,30} But less regioselective *N*-alkylation was achieved,²⁷ and harsher deprotection conditions were needed.³⁰ The purpose of this thesis is to investigate MOM as an alternative protecting group, and further develop deprotection protocols for route C.



Scheme 2.2: Previously investigated routes towards 6,8-disubstituted purines.

2.3 Purines

Purines are found as the structural units of the nucleobases adenine and guanine in DNA.^{31,32} The nucleobases form nucleosides and nucleotides,³¹ which can act as hormones and neurotransmitters, as well as being active in intracellular signaling and many metabolic systems.³² In addition to this, purine antimetabolites have been used in the treatment of autoimmune diseases,³³ and purine analogs have shown to possess antimicrobial,³⁴ antifungal,³⁵ antitumor,³⁶ antitubercular,³⁷ antiviral and cardiotoxic properties.^{38,39} This makes the purine structure vastly important in both biology and as a basis for new potential lead structures in medicinal chemistry.³⁴

Purines are heterocyclic molecules consisting of a fused pyrimidine and imidazole ring, as shown in Figure 2.4.⁴⁰ Due to the electron-localizing effects of the nitrogen, the pyrimidine is a π -electron deficient system.⁴¹ The imidazole ring has both a single bonded, and doubly bonded nitrogen and is an electron rich system.⁴² The overall electron density profile of the unsubstituted purine is produced

by sharing of the π -electrons of the imidazole ring to the pyrimidine moiety.⁴¹ Introducing electron withdrawing or donating substituents to the ring system will further alter this distribution.⁴¹

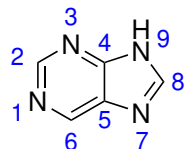
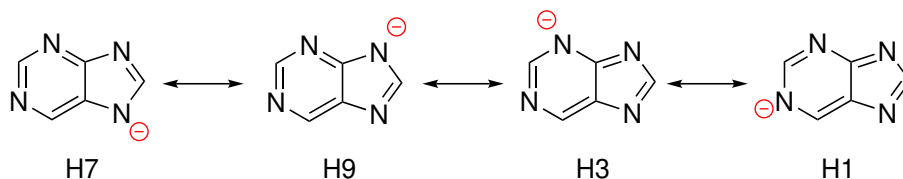


Figure 2.4: Numbering of atoms in the purine ring system.⁴⁰

With the electron withdrawing effects of the nitrogen, the neighbouring carbon atoms in the ring has a pronounced electrophilic character. Substituents in these positions can be replaced by nucleophilic attack, and the 8-carbon atom is the most electron deficient and will react first, followed by the C6 and C2 substituents.^{32,41} In the presence of an electron donating group, the C8-position also shows some nucleophilic character and the purine can react in electrophilic as well as nucleophilic reactions.⁴¹

Purines can undergo *N*-alkylation, as the nitrogen in the molecule can act as a nucleophile.⁴¹ *N*-Alkylation often gives both the *N*9 and *N*7 isomers, where the former is usually the major product.^{43,44} Factors known to influence the *N*9:*N*7 ratio, is the purine and reactant structure, reaction temperature, and what type of base and solvent are used.^{43,45}

When the purine is deprotonated, the negative charge will be delocalized, as shown in Scheme 2.3. Alkyl-addition to the *N*3 or *N*1 ion will give a less aromatic product, making the *N*9 and *N*7 isomers more favourable.



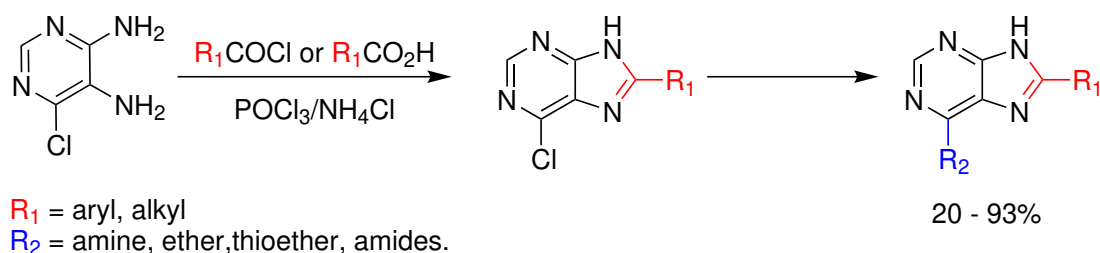
Scheme 2.3: Resonance of deprotonated purine.

The nucleophilic character of the nitrogen may prove difficult in electrophilic reactions targeted towards other ring atoms, and the *N*9 and *N*7 purine should in these cases be protected.

2.4 Synthesis of 6-Amino-8-Arylpurines

A wide variety of substituted purines can be synthesized from 4,5-diaminopyrimidine with a one carbon reagent, known as a Traube type condensation reaction.^{41,46} The availability of different cyclization reagents allows for preparation of virtually any type of substituted purine. Some of the most common reagents are acid chlorides,⁴⁷ carboxylic acids,⁴⁶ chloroformic esters,⁴⁸ carboxamides and ureas.^{49,50} Due to the harsh reaction conditions needed for ring closing, side reactions with other groups on the pyrimidine must be considered. If 6-halopurines are to be used as an intermediate towards 6-aminopurines, special reagents need to be used to avoid hydrolysis of the halogen during the Traube reaction.⁴¹ Catalysis by Ag/SiO₂ have effectively been used for one-pot formation of 8-substituted-9*H*-purines in excellent yields under mild, eco-friendly conditions.⁵¹

Ibrahim *et al.* reported a two step synthetic route giving 6-amino-8-arylpurines in yields up to 93%.⁵² The synthesis involved Traube type condensation of 6-chloro-4,5-diaminopyrimidine followed by nucleophilic aromatic substitution or Pd-catalysed amination. A general reaction pathway is shown in Scheme 2.4.

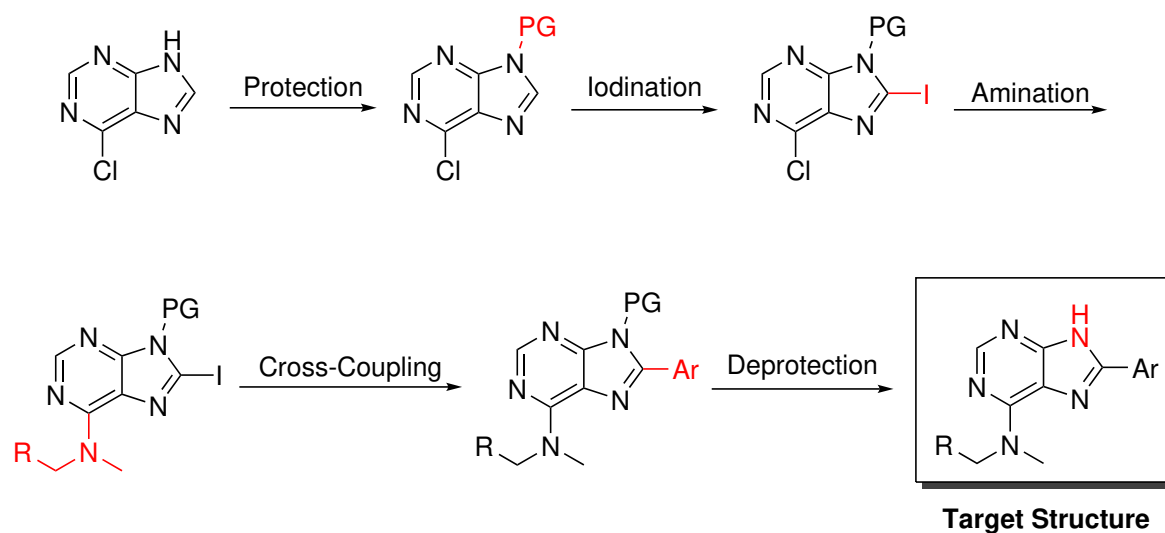


Scheme 2.4: Synthesis of 6-amino-8-arylpurines by Ibrahim *et al.*⁵²

6-Amino-8-arylpurines can alternatively be made in a three step synthesis from the readily available 6-chloropurine. Functionalization of the purine skeleton can be achieved by substituting the C2, C6 or C8 hydrogen with good leaving groups.⁴¹

Halogenation is often used for this purpose, and regioselective functionalization can be carried out by transition metal catalysed or S_NAr type reactions.^{53,54}

It has been documented that Suzuki cross-coupling reaction and nucleophilic aromatic substitution might fail if the purine nitrogen is unprotected.^{28,29,55} Synthesis of 6-amino-8-arylpurines from 6-chloropurine deploying *p*-methoxybenzyl (PMB), and methoxymethyl (MOM) as protecting groups are the selected routes for this project. Introduction of the protective group is followed by iodination to give the 6-chloro-8-iodopurine intermediate. Amine is introduced by nucleophilic aromatic substitution, and Pd-catalysed Suzuki cross-coupling followed by deprotection gives the desired product. The synthetic route of 6-amino-8-arylpurine through the *N*-protected analog is shown in Scheme 2.5.



Scheme 2.5: Synthesis of 6-amino-8-arylpurine from 6-chloropurine.

2.5 Protecting Groups

As previously mentioned, protecting the *N*-position in the purine may be necessary to prevent unfavourable decoration of the purine scaffold. Protection of purines with tetrahydropyran (THP), methoxymethyl (MOM) and benzyl derivatives like *p*-methoxybenzyl (PMB) have been reported in the literature,^{56–59} see Figure 2.5

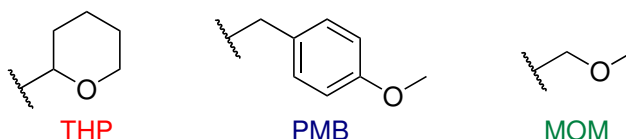


Figure 2.5: Various *N*9 protecting groups for purines.

2.5.1 Tetrahydropyran (THP)

THP is a popular protecting group due to its ease of introduction and removal, as well as its stability in a variety of reaction conditions.^{57,58} However, halogenation of THP protected purines have been associated with poor yields because of by-product formation.^{60,61} Previous work in the research group have shown that the halogenation step is much improved with benzyl protected purines.²⁷

2.5.2 Benzylic Groups

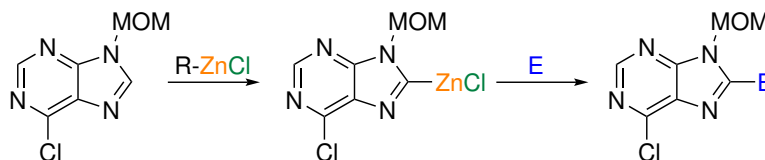
Benzylic protecting groups are widely used in the protection of nitrogen containing heterocycles.^{58,62} *N*-Protection of purines have previously been reported by Wang *et al.*⁵⁹ The 9-benzyl-purines were synthesized by reacting various purines with the appropriate benzyl chloride derivative.⁶³ Qu *et al.* synthesized 6-substituted 9-benzyl purines from 6-halo-9-benzylpurines employing S_NAr -type reactions.⁶⁴ Successful Suzuki cross-coupling reactions on 2-, 6- and 8-halo-9-benzylpurines have been reported by Dvořák *et al.*⁶⁵ The protecting groups are stable, but may require forceful conditions to remove, and only a small number of debenylation procedures are available.

One of the most common ways of debenylation is by Pd-catalysed hydrogenation.⁶⁶ This method is not viable if the protected compounds contain reactive

groups that can be reduced as well.⁶² An alternative method employs a strong acid such as trifluoroacetic acid (TFA) or Lewis acid such as AlCl_3 .^{67,68} Anisole is often used in these reactions to trap the benzyl cation.⁶⁹ Methods employing strong acids can also be problematic if the molecule contains other reactive groups, and AlCl_3 may lead to side reactions like Friedel Craft alkylation.^{62,70} Other methods employing sodium metal in ammonia,⁷¹ or KOtBu in DMSO in the presence of oxygen have also been reported.^{62,72}

2.5.3 Methoxymethyl (MOM)

MOM is a third alternative protection group, and is quite stable.⁵⁸ Crestey *et al.* synthesized MOM protected purines by reacting the unprotected purine with MOMCl in presence of K_2CO_3 . Halogenation at the C8-position was achieved by zincation with $\text{TMPZnCl}\cdot\text{LiCl}$ and subsequent trapping with iodine. Arylation was then completed through a Suzuki cross-coupling, or directly on the zincated species with a Negishi cross-coupling, see Scheme 2.6.⁵⁷ Deprotection is commonly achieved with acid or BBr_3 in CH_2Cl_2 .⁵⁸



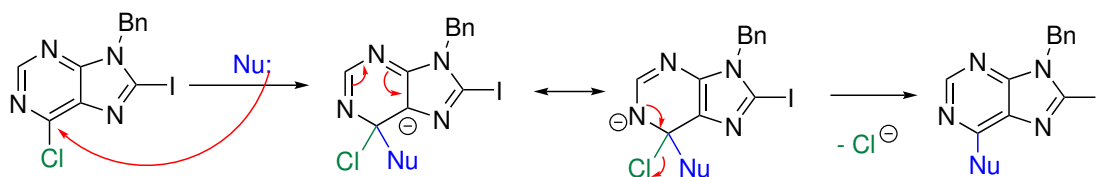
Scheme 2.6: General reaction scheme of the selective zincation of purines, and subsequent trapping with an electrophile.^{57,73}

2.6 Nucleophilic Aromatic Substitution

Nucleophilic aromatic substitution is an $\text{S}_{\text{N}}\text{Ar}$ type reaction, which is one of the most used reaction types in medicinal chemistry.⁷⁴ These reactions have high chemoselectivity, and is believed to follow an addition-elimination mechanism.⁷⁵ The nucleophilic attack leads to formation of an anionic σ -complex called the Meisenheimer complex.^{76,77} This is followed by departure of the leaving group and reformation of the aromaticity of the ring.⁷⁸

The reaction rate is dependent on the strength of nucleophile and the leaving group ability. Halides are the most popular leaving groups, and the reactivity increases with electronegativity; thus, making the reactivity series: $F > Br \approx Cl > I$.⁷⁹ Both the departure of the leaving group and the reactivity of the nucleophile is dependent on the solvent. In aprotic solvents the nucleophile is activated and the rate-determining step is often the departure of the leaving group.⁸⁰ This is backed up by simulations done by Acevedo and Jorgensen which show that the Meisenheimer complex is more stable than reactants in aprotic solvents.⁸¹

Halopurines undergo S_NAr -type reactions with a variety of nucleophiles.³² Nucleophilic displacement of leaving groups at C2, C6, and C8 work with relative ease. A proposed mechanism for nucleophilic aromatic substitution of 6-chloro-8-iodo-9-benzylpurine is shown in Scheme 2.7.



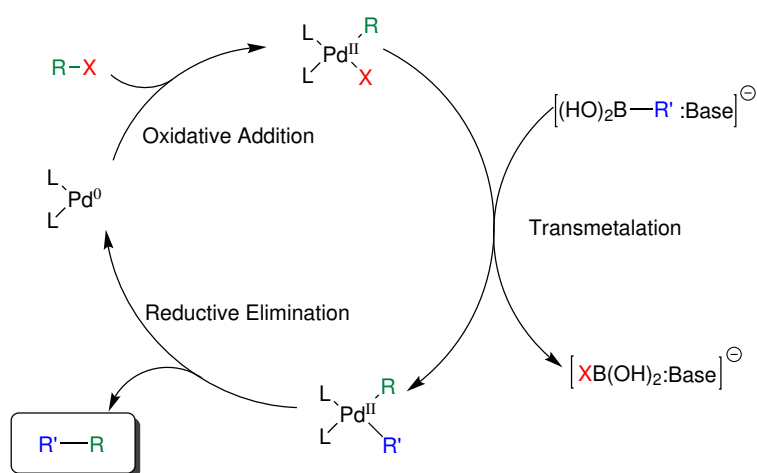
Scheme 2.7: Proposed mechanism for nucleophilic aromatic substitution of 6-halo-9-benzylpurine.

2.7 Suzuki-Miyaura Cross-Coupling

The Suzuki cross-coupling reaction is a Pd-catalysed cross-coupling between organoboronic acids and aryl/vinyl halides, in the presence of a base. Due to its versatility and chemoselectivity, it is one of the most used reactions in medicinal chemistry.^{74,82} It is easy to understand the wide usage of the reaction. A variety of different organoboronic acids are commercially available, and the organohalides tolerate a wide range of functional groups.^{82,83} The reaction can proceed under mild conditions and tolerates water. A high regio- and chemoselectivity is often achieved, and the inorganic by-products are easily removed.^{83,84}

Some disadvantages are decomposing of the boronic acid, and side reactions, such as homocoupling, and dehalogenation.^{84,85} The presence of oxygen in the reaction mixture can lead to homocoupling and oxidation.⁸⁶ Degassing of the solvent is often taken as a preliminary measure.⁸⁶ Dehalogenation is a prominent competing reaction often making it difficult to isolate the product.^{85,87} Jedinák *et al.* discovered that the dehalogenation process is caused by the base.⁸⁵

The mechanism involves the three usual steps for a Pd-catalysed cross-coupling: oxidative addition, transmetalation, and reductive elimination. A general mechanism is shown in Scheme 2.8.^{84,88}



Scheme 2.8: General mechanism for the Suzuki-Miyaura cross-coupling reaction.^{84,88}

In the oxidative addition step the organohalide bond is broken and two new bonds form with Pd, increasing its oxidation state by two. This equilibrium is expected to lean towards the addition product when strong electron donating ligands are used.⁸³ In the transmetalation step the migration of the organo-group from the boronic acid to the Pd complex takes place. The base is a requirement for the reaction to take place. It has been shown that the base attacks the boronic acid to form an anionic intermediate, which can then attack the Pd complex and initiate the migration.^{83,88} The catalyst is reformed in the reductive elimination step, where a bond is formed between the organo-substituents as they detach from the Pd.⁸⁸

Bulky and electron rich ligands have been shown to have high reactivity and selectivity.⁸⁹ Because of this, dialkylbiarylphosphine ligands are heavily used.⁹⁰ Some common ligands and catalysts are shown in Figure 2.6.

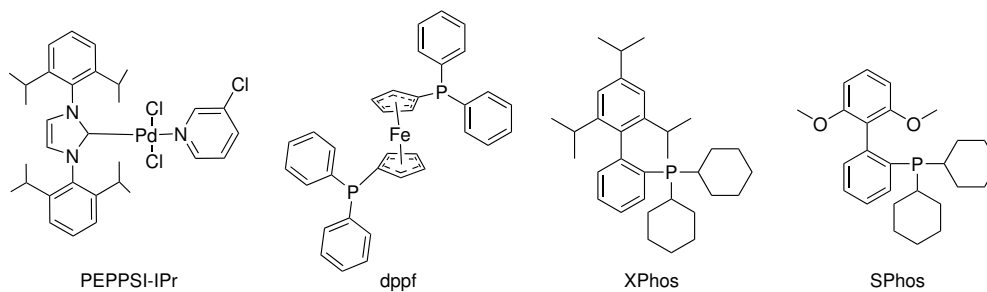


Figure 2.6: Some common phosphine ligands.^{85,90}

3 Results and Discussion

In order to prepare complex purines functionalized at the 6- and 8- positions, protection of *N*9 or *N*7 is needed. Previous work in the research group has involved using tetrahydropyran (THP) or benzyl protecting groups. THP shows high selectivity towards introduction at the *N*9-position, and is readily deprotected under mild acidic conditions.^{27,56,91} However, challenges in the halogenation step, involving by-product formation and difficulties during work-up, result in mediocre yields.^{27,60,61} While the benzyl derivatives are easier to halogenate, they show poor selectivity in the *N*-alkylation step, and require harsh deprotection conditions.^{27,30}

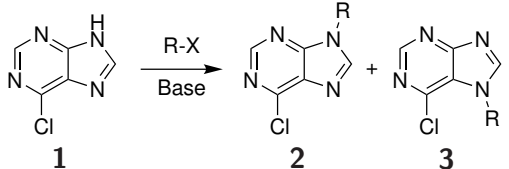
The aim of this project is to investigate the use of methoxymethyl (MOM) and *p*-methoxybenzyl (PMB) as protecting groups in the synthesis of 6-amino-8-aryl purines. Functionalization of PMB protected purines was investigated during the pre-master's project.³⁰ In this thesis the focus will be on functionalization of the MOM protected derivatives and finding milder *N*-debenzylation protocols.

The initial parts of this chapter covers the synthesis of the various building blocks, including protection, iodination, amination, cross-coupling and deprotection. This is followed by structure elucidation of the synthesized compounds.

3.1 Introduction of the Protecting Group and Synthesis of Compound 3

A protecting group is introduced at the *N*9-position of 6-chloropurine (**1**) to prevent difficulties with Pd catalyzed and S_NAr type reactions.^{28,29,55} The reaction conditions and data for the synthesis of compounds **2** and **3** from compound **1** are given in Table 3.1.

Table 3.1: Overview of reaction conditions and data for *N*-alkylation of compound **1** with PMB-Cl and MOM-Cl, yielding compound **2**, **2b**, and **3**.

						R	
						2	PMB-
						3	MOM-
Compound	Scale	Solvent	Rx time	T	Conv. ^a	Ratio <i>N9:N7</i> ^b	Yield ^c
	[g]		[h]	[°C]	[%]		[%]
2 ^d	3.04	DMF	25	rt	98	2:1	45
3	0.15	DMF	44	60	>99	1:0	37
3	1.03	DMF	23	40	>99	1:0	65
3	0.13	EtOAc	25	40	>99	1:0	67
3	0.12	THF	25	40	>99	1:0	61
3	3.03	THF	24	40	>99	1:0	86

^a Conversion determined by ¹H NMR spectroscopy.

^b *N9:N7* ratio determined by ¹H NMR spectroscopy.

^c Isolated yields of the *N9* isomer.

^d Synthesized in the pre-master's project.³⁰

Compound **2** was synthesized in the pre-master's project following the procedure of Wang *et al.*⁵⁹ 6-Chloropurine **1** was reacted with *p*-methoxybenzyl chloride in the presence of K₂CO₃ to give **2** in 45% yield. The low yield stems primarily from the lack of selectivity towards the *N9* isomer.

As an alternative to the PMB and THP protecting groups, *N*-alkylation of compound **1** using chloromethyl methyl ether was attempted. The reaction was done based on the procedure of Crestey *et al.*⁵⁷ MOMCl was added dropwise to a solution of compound **1** and NEt₃ to yield compound **3**. A small scale reaction was conducted at rt. using DMF as solvent, but after 24 h full conversion was not observed. The temperature was therefore increased to 60 °C, and full conversion was achieved after a total of 44 h. The MOM protected purine **3** was isolated in

37% yield. Loss of product was observed both during work-up and purification, indicating that the product is somewhat soluble in water and has affinity for silica. ^1H NMR analysis revealed no formation of the *N7* isomer, see Figure 3.1. Due to the small scale, the low yield is likely due to loss of product during work-up and purification, and with a 100% selectivity the reaction has higher potential than the PMB analog.

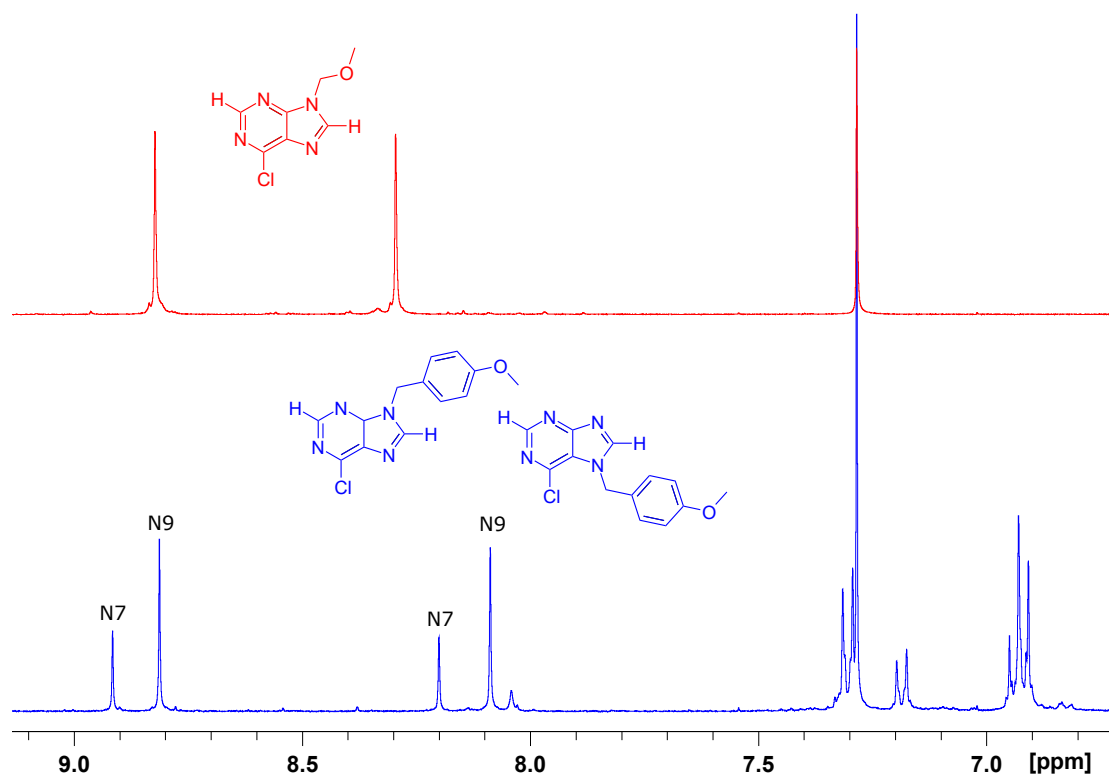


Figure 3.1: ^1H NMR (400 MHz, CDCl_3) spectra of crude products from the synthesis of compounds **2** and **3**. The C2 and C8 proton signals show the corresponding *N9/N7* ratios.

The reaction was scaled up, and with a reaction temperature of 40 °C full conversion was achieved after 23 h. Traces of DMF was seen in the compound both after work-up and purification by silica-gel column chromatography. The solvent traces were removed under vacuum at 120 °C giving compound **3** in 65% yield. The increase in yield is probably due to more care being taken during the work-up and purification. Since DMF is miscible with water, emulsions were formed during work-up. Solvent traces could increase the solubility of the product in the aqueous

phase and contribute to lowering the yield.

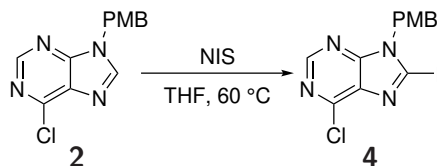
Two test reactions using THF and EtOAc as solvents were conducted. The same reactivity and selectivity was seen in both solvents. With no DMF the removal of solvents and work-up was easier, but no overall gain in yield was achieved. A final scaled-up reaction was conducted using THF as solvent, resulting in compound **3** being isolated in 86% yield. This is a considerable higher yield than previously achieved. Less loss during extraction was observed, possibly due to the lack of DMF traces making it easier to avoid emulsions and achieve a clean separation. Since the reaction is quenched with K_2CO_3 , the resulting unprotonated NEt_3 can be removed *in vacuo*, and it might be possible to further increase the yield by skipping the work-up and proceeding directly to purification.

3.2 Iodination

Iodination of the purine at the C8-position allows for further functionalization through cross-coupling reactions. Benzyl protected purines have previously been iodinated using *N*-iodosuccinimide (NIS) through what is expected to be an electrophilic aromatic substitution reaction.^{27,30,92} Halogenation of MOM protected purines are usually done through a metallation reaction.⁵⁷

3.2.1 Synthesis of Compound **4**

Following the procedure by Guthmann *et al.*,⁹² compound **2** - previously synthesized in the pre-master's project³⁰ - was reacted with NIS in THF at 60 °C to give compound **4**, see Scheme 3.1.



Scheme 3.1: Reaction conditions for iodination of compound **2**.

Full conversion was observed after 22 h and purification gave compound **4** in 62% yield. The yield is comparable to previous reactions.³⁰ No by-products were

observed. Due to the polar nature of the compound, it has some affinity towards the aqueous phase and silica,⁹³ and the mediocre yield is likely due to loss of compound during work-up and purification.

3.2.2 Synthesis of Compound 5

Iodination of compound **3** through both *ortho* lithiation and zincation were investigated. An overview of reaction conditions are given in Table 3.2.

Table 3.2: Overview of reaction conditions and data for the synthesis of compound **5**.

M-R	Scale	Rx time	T	Conv. ^a	Yield ^b
	[g]	[h]	[°C]	[%]	[%]
LDA	0.3	1.5	-78	94	37
TMPZnCl·LiCl	0.3	16	rt.	64	25
TMPZnCl·LiCl	0.9	27	rt.	70	39

^a Conversion determined by ¹H NMR spectroscopy.

^b Isolated yields.

Initially, the iodination was attempted by *ortho* lithiation following the procedure by Ibrahim *et al.*⁶¹ Lithiation of compound **3** was performed with LDA in a solution of THF at -78 °C. I₂ in THF was added, and the solution was stirred for 1.5 h. The resulting work-up proved difficult, with the formation of multiple insoluble solids and troublesome emulsions. The product **5** was isolated in 37% yield, and 3% starting material was recovered. Multiple by-products were observed with TLC analysis, but were difficult to separate from the product by silica-gel column chromatography. Similar results were observed with the iodination of the THP protected analog.^{27,60} Both the formation of by-products and the difficulties in the work-up is expected to be the main contributors to the poor yield.

After the mediocre results with *ortho* lithiation, iodination of the MOM protected purine **3** was attempted using zincation as described by Crestey *et al.*⁵⁷ This procedure has reported yields of up to 98% for the synthesis of compound **5**. The hindered amide base 2,2,6,6-tetramethylpiperidine (TMP) was used as the basis for the zincation agent, and TMPZnCl·LiCl was synthesized according to the procedure of Mosrin *et al.*⁷³ TMP was deprotonated using *n*-BuLi, before ZnCl₂ was added. After stirring the solution for 1 h, solvents were removed and the residue dissolved in dry THF to give a concentration of 1.2 M. Compound **3** was stirred for 40 minutes with 1.2 equivalents of the TMP base, before 1.2 equivalents of I₂ was added. ¹H NMR analysis showed 37% conversion after 2.5 h. The reported reaction time is 1 h,⁵⁷ and an additional 1.1 equivalent of TMPZnCl·LiCl and 0.7 equivalents of I₂ was added. After an additional 15 h, the reaction was stopped, and ¹H NMR analysis showed 64% conversion. The reaction was quenched with Na₂S₂O₃ and the following work-up proved difficult with the formation of troublesome emulsions. Purification by silica-gel column chromatography gave the iodinated purine **5** in 25% yield, and 27% of starting material was recovered.

The main contributing factors to the low yield is the low conversion, as well as the difficulties during work-up. Due to the hygroscopic nature of ZnCl₂, and the water and air sensitive nature of the metalation agent, it is expected that the low conversion was caused by poor preparation and inaccurate concentration of the TMP salt. Because of the polar functionalities, some loss of product is always expected during work-up and purification. It was deemed more expedient to achieve full conversion and proper preparation of the TMP base before the work-up procedure was scrutinized.

Before the TMP salt was remade, ZnCl₂ was dried at 140 °C under vacuum for 15 h, and measurements were made under inert atmosphere. In an effort to ascertain an accurate concentration, the TMPZnCl·LiCl solution was titrated. The titration was initially attempted with the readily available *N*-benzylbenzamide in dry THF at 0 °C, in accordance with Burchat *et al.*⁹⁴ No colour change was

observed and the titration was reattempted at rt. Again, no colour change was observed. The base is likely too weak to successfully deprotonate the benzamide. The titrant was changed to benzoic acid with 4-(phenylazo)-diphenylamine as indicator, and the titration was performed as described by Hammet *et al.*,⁹⁵ and Mosri *et al.*⁷³ Upon addition of the TMP base, only a slight gradual colour change was observed. After addition of nearly two equivalents TMPZnCl·LiCl, no clear endpoint was observed. A test titration was performed with LDA in which every drop gave a definite colour change that immediately vanished, and a clear distinguishable endpoint was reached. This indicates that the synthesized TMP base is too weak or the concentration too low for the titration methods.

Since the concentration could not be determined by titration, concentration determination by quantitative NMR was attempted. By deuterating all the TMP salt in a sample of known volume, the ratio between the NH and CH₃ peaks would give the conversion ratio of TMP to TMPZnCl·LiCl. Combined with an internal standard, an accurate concentration of the TMP base should be obtained. DMSO-*d*₆ was chosen as the readily available aprotic solvent to avoid proton exchange and obtain a clear NH peak. However, the DHO peak overlapped with the amine peak, and an accurate concentration could not be determined.

Considering an accurate concentration could not be ascertained, compound **3** was reacted with a large excess of TMPZnCl·LiCl. After 27 h, 70% conversion was reached, and the reaction quenched. Changing solvent from Et₂O to CH₂Cl₂ during extraction reduced the amount of emulsions, but a multitude of poorly soluble solids were formed. ¹H NMR analysis revealed the formation of some by-products which were difficult to separate from the product with silica-gel column chromatography. Compound **5** was isolated in 39% yield, and 3% starting material was recovered.

Taking more care in keeping dry conditions and additional drying of the ZnCl₂ seems to have improved the quality of the TMP base as a higher conversion was

achieved. It is possible that this could further be increased by drying TMP with molecular sieves or by distilling it prior to use. Additionally, changing the procedure to ensure inert conditions while removing volatiles could also increase the yield. Considering the TMP base was seemingly too weak for the recommended titration methods, it is possible that the reactivity of the base rather than the conversion from TMP is the limiting factor in the iodination. Lower reactivity would mean longer reaction times, and full conversion to the zincated intermediate should be ensured before an electrophile is added. This could be done by quenching an analytical sample with an electrophile like I₂, before running TLC or GC analysis. Other zincation or metallating agents could also be considered. Stathakis *et al.*⁹⁶ reported the synthesis of the air-stable TMPZnOPiv·LiCl with a successful metallation yield of 78%.

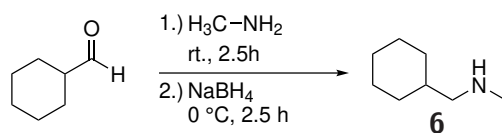
One of the reasons for changing the protecting group from THP was to seek an improvement in the iodination step. As it stands, the NIS iodination of compound **2** exceeds its THP analog, while the iodination of compound **3** exhibits some of the same challenges, with comparable yields.^{27,60} However, there are multiple instances of similar or identical reactions being reported with high yields.^{57,73,96} This indicates that with some more work into finding an efficient work-up procedure and higher quality TMP base, the reaction could far outshine even the PMB iodination.

3.3 Amination

Thermal amination was used for regioselective functionalization at the C6-position of the purine moiety. The reaction is thought to proceed through an S_NAr mechanism, with nucleophilic attack from the selected amine and assistance from a co-base. The purines were functionalised with 1-cyclohexyl-*N*-methylethylamine (**6**) and *N*-methyl-1-phenylethylamine, using Hünigs base as a co-base.

3.3.1 Synthesis of Compound 6

Compound **6** was synthesized from cyclohexanecarbaldehyde and methylamine in a reductive amination reaction. The reaction was done in accordance with previous experiments by Ehrhardt *et al.*,⁹⁷ using NaBH₄ as a reduction agent, see Scheme 3.2.



Scheme 3.2: Reaction conditions for synthesis of compound **6**.

The reaction was done in a 3 g scale using methanol as solvent. After 1.5 h ¹H NMR showed 97% conversion of the aldehyde. The first step of the reaction is reversible, and small traces of water in the deuterated solvent could cause some of the imine to convert back to the aldehyde. The DMSO-*d*₆ was dried for 24 h using molecular sieves prior to use. However, to ensure full conversion, the reaction was left for another hour before NaBH₄ was added.

Borane salts were removed by adjusting the pH to 0 using conc. HCl, converting the product to its HCl salt and extracting with H₂O. Readjusting to pH 11 with NaOH and extracting with CH₂Cl₂ gave a white solid. Compound **6** is usually a clear liquid at rt, indicating that the product could be a salt. Comparing the ¹H NMR spectra of the crude product and a standard sample of the amine showed a slight difference in the shifts of the CH₂ and CH₃ groups. Additionally, the signal from the amine group was not present in the crude product, see Figure 3.2.

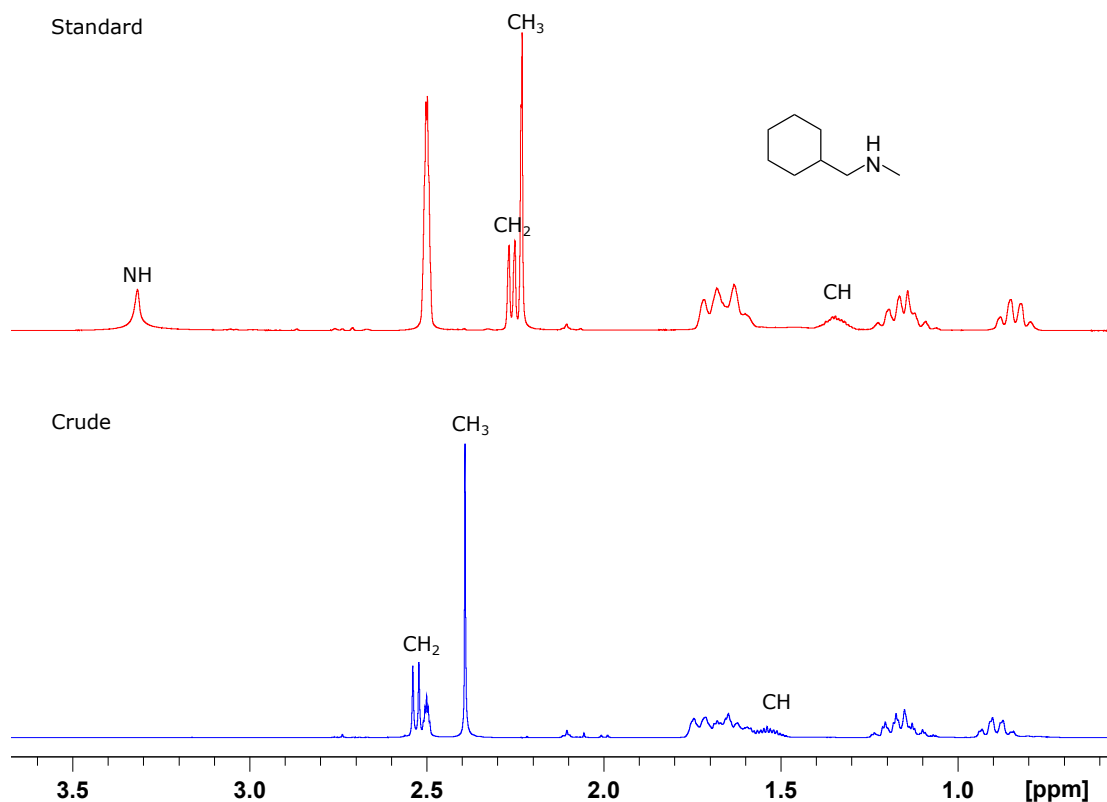
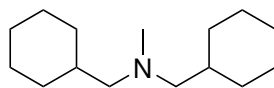


Figure 3.2: ¹H NMR (400 MHz, DMSO-*d*₆) of a standard solution of 1-cyclohexyl-*N*-methylmethanamin and the crude product.

The lack of signal for the amine proton and the change in chemical shift of neighbouring groups is a clear sign that the compound exists as a borane or HCl salt. Dissolving the compound in H₂O gave a solution with pH 11, indicating that the compound is not an HCl, but a borane salt. Concentrated HCl was added and the solution was stirred at pH 0 for 1 h to ensure the dissolution of all borane salts. The ensuing work-up gave compound **6** in 45% yield as a clear liquid. ¹H NMR analysis revealed small amounts of by-product formation. Previous work in the research group has isolated and identified the by-product as 1-cyclohexyl-*N*-(cyclohexylmethyl)-*N*-methylmethanamine (**7**), see Figure 3.3.⁹⁸ Purity of the amine **6** was determined by ¹H NMR analysis to be over 95%, and no further purification was deemed necessary.



7

Figure 3.3: Observed by-product in the synthesis of compound **6**.⁹⁸

With a boiling point of 144 °C,⁹⁹ the amine **6** is quite volatile. It is likely that some of the product is lost during removal of solvents. Material could also be lost during extraction due to it being somewhat water soluble or if a sufficient conversion from the borane or HCl salt was not achieved. Changing the work-up to ensure the full conversion from the borane salt and limit the amount of extractions could increase the yield. This could possibly be achieved by employing ion-exchange resins.

3.3.2 Synthesis of Compounds **8**, **9** and **10**

The 6-aminopurines **8**, **9** and **10** were synthesized from compounds **4** and **5** at 60 °C in 1,4-dioxane. An overview of reaction conditions and data are given in Table 3.3.

Table 3.3: Overview of reaction conditions and data for thermal amination of compounds **4** and **5** with 1-cyclohexyl-*N*-methylmethanamine or *N*-methyl-1-phenylmethanamine.

		R₁	R₂
8		PMB	C ₆ H ₁₁ -
9		MOM	C ₆ H ₁₁ -
10		MOM	C ₆ H ₅ -

Compound	Scale	Rx time	T	Conv.^a	Yield^b
	[mg]	[h]	[°C]	[%]	[%]
8	847	24	60	98	90
9	52	25	60	9	nd ^c
10	50	2	60	>99	nd ^c
10	500	2	60	>99	83

^aConversion determined by ¹H NMR. ^bIsolated yields. ^cNot determined.

Compound **8** was synthesized in 90% yield using the same procedure as in the pre-master's project.³⁰ ¹H NMR of the crude mixture revealed the product to be pure and no further purification was necessary.

Synthesis of compound **9** was attempted by reacting compound **5** with **6** at 60 °C. After 25 h, ¹H NMR showed only 9% conversion. No by-products were observed, only signals pertaining to the starting material and the intended product. Purification by silica-gel column chromatography was attempted, but TLC showed co-elution of the two compounds and no separation was achieved. HRMS analysis gave an *m/z* of 416.0948 [M+H]⁺ with a calculated value of 416.0947, confirming the molecular formula C₁₅H₂₃N₅OI and indicating that compound **9** was formed. The reaction was performed under the same conditions as the amination of compound **4**. Nucleophilic aromatic substitutions require an electron deficient aromatic system to proceed.⁷⁸ It seems unlikely that the MOM group should have a more drastic effect on the electron-profile of the pyrimidine moiety in comparison to the PMB group. Considering the reaction was conducted in only 50 mg scale, one possibility is that the reaction vessel was not gas tight and most of the volatile amine evaporated. Due to a shortage of compound **6**, the experiment was not redone.

It was deemed unnecessary to make more of compound **6**, and instead the amination of compound **5** was conducted using *N*-methyl-1-phenylmethanamine. Thermal amination on purines using *N*-methyl-1-phenylmethanamine have previously been done in the research group.²⁷ A switch to aliphatic amines was made due to a statistical correlation between toxicity and a high fraction of sp² carbons.¹⁰⁰ As the main purpose of this thesis is not to investigate the biological activity or toxicity of the compounds, this is not viewed as a problem. Additionally, the challenges in achieving a selective deprotection without debenzylating the phenylamine moiety is assumed not to be present with the MOM protecting group.

Initially, a test reaction in 50 mg scale was conducted, and full conversion of **5** to **10** was observed after 2 h. The reaction was scaled up to 500 mg, giving compound **10** in 83% yield after work-up. No further purification was necessary. The yield was slightly lower than for the PMB analog. This is possibly because the smaller MOM group increases water solubility and subsequent loss of material during work-up.

While the yields are comparable, the amination reaction times for the PMB and MOM analogs differ with more than 20 h. Considering the reaction follows an S_NAr type mechanism, the rate is dependent upon both the nucleophile and the aromatic electrophile.⁸⁰ Due to inductive effect, the aliphatic amine **6** is expected to be slightly more nucleophilic than the phenylamine, and should give similar or quicker reaction times. Previous work in the research group has shown reaction times as low as 2 h for the same reaction.²⁷ As previously discussed in the synthesis of compound **6**, there were challenges in achieving full conversion of the amine salt. Remaining salt impurities could affect the reactivity of the amine, and it is likely that the extended reaction time is caused by poor quality of the starting material.

¹H NMR analysis of the products showed peak broadening for the signals at 3.28 and 4.03 for compound **8**, 3.30 and 4.08 for compound **9**, and 3.45 ppm and 5.28 ppm for compound **10**, see Figure 3.4. Complete NMR spectra are given in E and G.

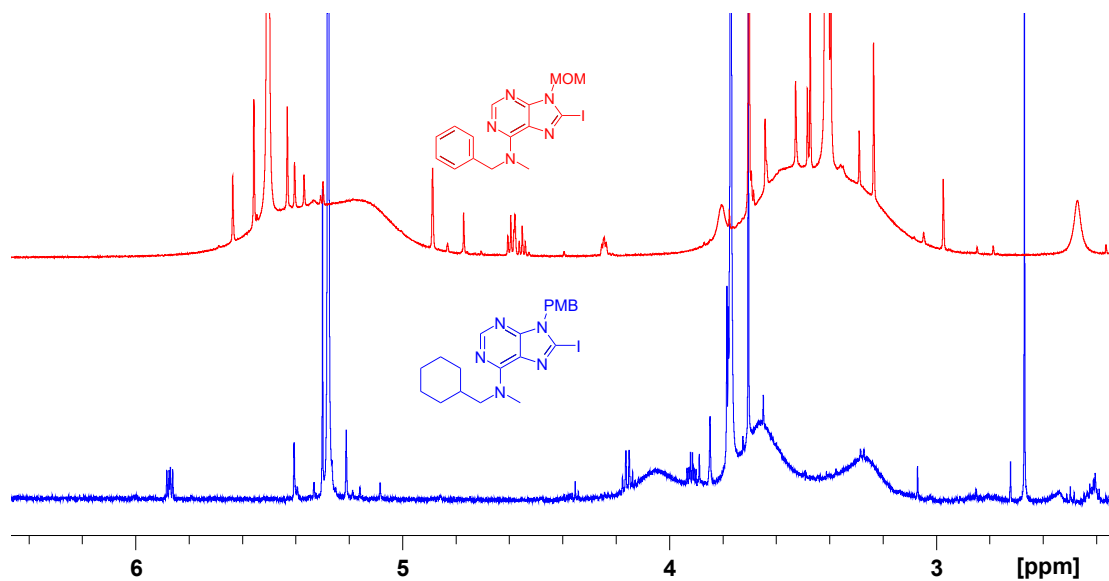
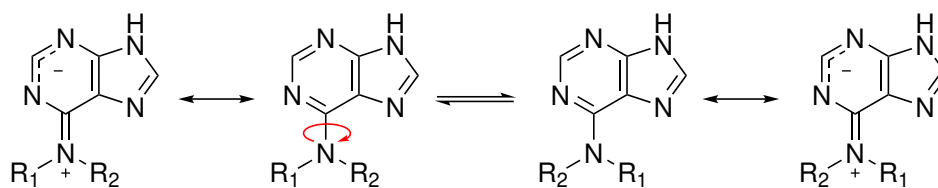


Figure 3.4: Peak broadening in ^1H NMR analysis of compounds **8** and **10**.
400 MHz, CDCl_3 .

Peak broadening is normally a result of chemical or conformational exchange, and has been observed in purines bearing an amine functionality in the C6 position.^{101,102} Pitner *et al.* proposed a partial double bond character between the C6 carbon and the amine functionality.¹⁰¹ This double bond character leads to formation of two rotational isomers, which results in broadening. An illustration of the rotamers and the resonance-formed double bond character is shown in Scheme 3.3.



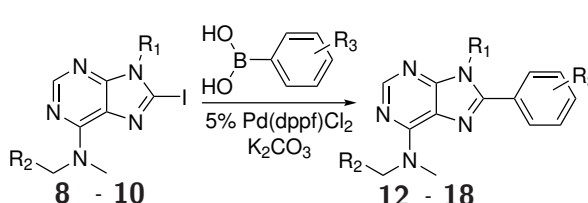
Scheme 3.3: Rotational isomers for 6-amino purines.^{101,102}

3.4 Cross-Coupling and Synthesis of Compounds **12**, **15**, **17** and **18**

3.4.1 Suzuki

Functionalization at the C8-position of the iodinated purines were done through Suzuki cross-coupling reactions, based on a procedure described by Bugge *et al.*¹⁰³ Compounds **12** to **18** were synthesized from the 8-iodopurines **8** and **10**, with the corresponding boronic acid and Pd(dppf)Cl₂ as the chosen catalyst. A mixture of 1,4-dioxane and H₂O was used as the solvent system, and all reactions were conducted at 80 °C. An overview of reaction conditions and data are given in Table 3.4.

Table 3.4: Overview of reaction conditions and data for the Suzuki cross-coupling of compounds **8** and **10**, yielding compounds **12** to **18**.

		R ₁	R ₂	R ₃
12	PMB	C ₆ H ₁₁ -	<i>m</i> -CH ₃	
15	MOM	C ₆ H ₅ -	<i>p</i> -CH ₃	
17	PMB	C ₆ H ₁₁ -	<i>p</i> -OH	
18	MOM	C ₆ H ₅ -	<i>p</i> -OH	

Compound	Scale	1,4-dioxane:H ₂ O	Rx time	Conv. ^a	Yield ^b
	[mg]		[min]	[%]	[%]
12	509	2:1	30	>99	84
15	100	1:1	30	>99	86
17	198	2:1	30	>99	91
18	200	2:1	30	>99	61

^aConversion determined by ¹H NMR.

^bIsolated yields.

Compound **12** was obtained from the Suzuki coupling between compound **8** and *m*-tolylboronic acid. Full conversion was observed after 30 minutes and purification by silica-gel column chromatography gave the desired compound in 84% yield.

The formation of two by-products was observed. ^1H NMR revealed the primary by-product to be 3,3'-dimethyl-1,1'-biphenyl (**13**) which was isolated in 10 mg, see Figure 3.5. This compound is the result of homocoupling of the boronic acid, and is normally expected due to the use of a slight excess of boronic acid. ^1H NMR analysis of the second by-product showed no amine substituent in the C6-position of the purine. However, three methyl groups at 3.79 ppm, 2.52 ppm and 2.44 ppm, and multiple new peaks in the aromatic region were observed. The splitting pattern of the aromatic peaks are quite complex, but two singlets with an integral of 1H at 8.64 ppm 7.58 ppm were noted. Together with the missing broad amine peaks, and the extra methyl group this indicates the presence of two distinct *m*-tolyl substituents. HRMS analysis gave an m/z ratio of 421.2028 $[\text{M}+\text{H}]^+$ corresponding to a molecular formula of $\text{C}_{27}\text{H}_{25}\text{N}_4\text{O}$ further supporting 9-(4-methoxybenzyl)-6,8-di-*m*-tolyl-9*H*-purine (**14**) as the by-product, see Figure 3.5. Only 8 mg of the impure by-product was isolated, and it is expected that compound **14** was formed by a Suzuki di-coupling on impurities of compound **4** in the starting material.

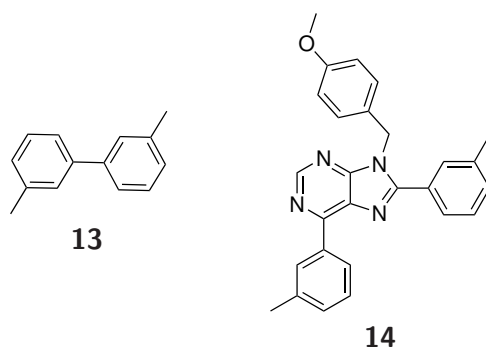


Figure 3.5: Suggested by-products in the Suzuki coupling of compound **8**.

Considering that full conversion of the starting material was observed and only 8 mg and 10 mg of the respective by-products were isolated, the formation of by-products is not considered a major factor in decreasing the overall yield.

Compound **15** was obtained from the cross-coupling between compound **10** and *p*-tolyl boronic acid. Full conversion was achieved after 30 minutes and the desired compound was isolated in 86% yield, which is comparable to the PMB analog. Formation of the homocoupled by-product **16** was observed, and 2.6 mg of the

compound was isolated, see Figure 3.6.

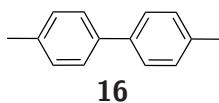


Figure 3.6: By-product formed in the Suzuki coupling of compound **10**.

The tolyl substituents of compounds **11** to **15** were chosen to provide an easy substrate for the investigation of various deprotection methods. In an effort to test possible deprotection protocols on substrates more relevant to the biological research, cross-coupling reactions with (4-hydroxyphenyl)boronic acid were performed.

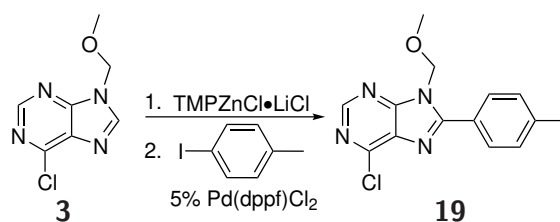
Compound **17** was synthesized from compound **8** and (4-hydroxyphenyl)boronic acid in 91% yield. No by-products were observed. The same molar equivalents of boronic acid was used as in the previous experiments. Pd-catalyzed homocoupling of boronic acids is dependent on the presence of an oxidant, and is linked to amount of dissolved oxygen in the reaction.^{86,104} To limit bi-aryl formation solvents were degassed by a subsurface nitrogen sparge in an ultrasound bath for minimum 0.5 h, prior to all Suzuki reactions. It is possible that the disparity in homocoupling is due to a difference in degassing time. However, the electron density of the aryl boronic acids have shown to influence the rate of the trans-metallation and reductive elimination steps, as well as the stability of the associated complexes.¹⁰⁵ Although the direct impact is difficult to ascertain, it is possible that the presence of an electron withdrawing group contributed to the reduced by-product formation.

Cross-coupling between compound **10** and (4-hydroxyphenyl)boronic acid gave compound **18** in 61% yield. No by-products were observed, and the compound was purified by silica-plug filtration. The yield is considerably lower than previous reactions. It is suspected that the mediocre yield is due to an increased loss of product during work-up and purification, caused by the increase in polarity with both the hydroxyl and MOM substituents present.

3.4.2 Negishi

Functionalization of the purine moiety at the C8-position is currently a two step process, through a iodination and a successive Suzuki cross-coupling. Using the TMP zincation agent discussed in section 3.2.2, a Negishi cross-coupling could be performed.^{57,73} This would reduce the required steps by one, and could potentially increase the overall yield.

The Negishi coupling between compound **3** and 4-iodotoluene was attempted based on the procedure of Crestey *et al.*⁵⁷ Since the preferred ligand (*o*-furyl)₃P was not available, Pd(dppf)Cl₂ was used instead, as it has proven to be both selective and reactive in other cross-coupling reactions with purines.^{27,30} The same TMPZnCl·LiCl as described in section 3.2.2 was used as zincation agent, see Scheme 3.4.



Scheme 3.4: Overview of reaction conditions for the attempted Negishi cross-coupling of compound **3** with 4-iodotoluene.

Compound **3** was stirred in a solution of TMPZnCl·LiCl and the catalyst for 1.75 h before 4-iodotoluene was added. After an additional 1.5 hours TLC analysis showed full conversion. ¹H NMR analysis of the crude mixture showed formation of a by-product and traces of the starting material, but not the intended product. The by-product was isolated by silica-gel column chromatography. NMR and HRMS analysis indicates the formation of 6-butyl-9-(methoxymethyl)-9*H*-purine (**20**), see Figure 3.7.

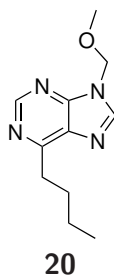


Figure 3.7: Product of the Negishi cross coupling of compound **3**.

Compound **20** was most likely formed from coupling between compound **3** and unreacted traces of *n*-BuLi in the TMPZnCl·LiCl solution. Since the catalyst was added before the TMPZnCl·LiCl, it is possible that most of the zincated purine intermediate had reacted before the 4-iodotoluene was added. The choice of solvent and catalyst must be made such that the catalyst can be added in solution together with the aryl halide. Additional care should be made in reducing the excess of *n*-BuLi when preparing the zincation agent, in order to reduce the possibility of competing reactions.

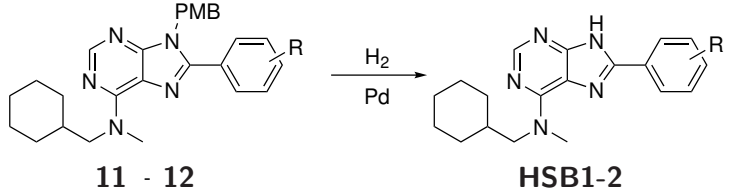
Due to the previously experienced difficulties in producing the zincation agent, the experiment was not repeated.

3.5 Debenzylation and Synthesis of Compounds HSB2 and HSB3

3.5.1 Hydrogenation

Deprotection of PMB was achieved in the pre-master's project using various acid protocols at high temperature. Milder debenzylation protocols are of interest as many of the promising inhibitors utilize more labile substituents at the C8-position. Merz *et al.* reported successful deprotection of *N*-benzylated dialkoxypyrroles using Pd-catalyzed hydrogenation at 20 bar in glacial AcOH.⁶⁷ The available equipment only allowed for hydrogen pressure up to 6 atm, so hydrogenation of compounds **11** and **12** at 1 and 6 atm was attempted, reaction conditions are shown in Table 3.5.

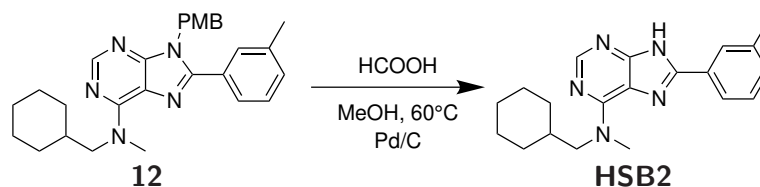
Table 3.5: Overview of reaction conditions of the attempted hydrogenation of compounds **11** and **12**. Reactions were done in glacial AcOH with 10% Pd/C and 15% Pd(OH)₂/C.

		<table border="1"> <thead> <tr> <th></th> <th>R</th> </tr> </thead> <tbody> <tr> <td>11</td> <td><i>p</i>-CH₃</td> </tr> <tr> <td>12</td> <td><i>m</i>-CH₃</td> </tr> </tbody> </table>			R	11	<i>p</i> -CH ₃	12	<i>m</i> -CH ₃
	R								
11	<i>p</i> -CH ₃								
12	<i>m</i> -CH ₃								
Compound	P	Cat.	Scale	Rx time	Conv. ^a				
	[atm]		[mg]	[h]	[%]				
11	1	Pd/C	30	28	< 1				
11	6	Pd/C	30	24	<1				
12	6	Pd(OH) ₂ /C	30	23	<1				
12	6	Pd(OH) ₂ /C + Pd/C	30	23	<1				

^aConversion determined by ¹H NMR spectroscopy.

Reactions were done according to the procedure described by Merz *et al.*⁶⁷ The debenzoylation was first attempted at atmospheric pressure, yielding no conversion after 24 h. Increasing the pressure to 6 atm had no effect. Since any further pressure increase was impossible with the current system, another approach had to be considered. Another commonly used catalyst for debenzoylation by hydrogenolysis is Pearlman's catalyst,⁵⁸ and Li *et al.* reported in 2006 higher debenzoylation rates for all tested compounds using a 1:1 mixture of Pd/C and Pearlman's.¹⁰⁶ The deprotection was reattempted using 1 molar eq. Pd(OH)₂/C, and 1 eq. 1:1 mixture of Pd/C with Pd(OH)₂/C. After 24 h at 6 atm H₂ pressure no conversion was observed. The debenzoylation reported by Merz *et al.* was conducted at a considerably higher pressure than 6 atm,⁶⁷ and it is possible the *N*-debenzoylation of purines could proceed at a higher pressure or temperature. Due to the limitations of the available equipment this was not attempted, and other methods had to be explored.

Debenzylation by catalytic hydrogenation has been reported as a slow process,¹⁰⁷ and transfer hydrogenolysis has found to be a suitable alternative.¹⁰⁸ Deprotection of compound **12** was attempted according to the procedure described by Elamin *et al.*,¹⁰⁹ see Scheme 3.5.



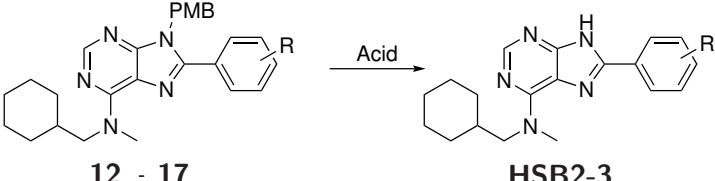
Scheme 3.5: Reaction conditions for transfer hydrogenolysis of compound **12**.

Compound **12** was dissolved in methanol with 4 vol% concentrated formic acid, with 1 eq. Pd/C at rt. under an N₂-atmosphere. No conversion was observed after 48 hours, and the temperature was increased to 60 °C. After an additional 24 hours, the reaction had still not proceeded. Other hydride transfer agents like NaBH₄ or use of other catalysts, i.e ruthenium based catalysts, could prove successful. Due to time constraints and the successful MOM deprotection, no further attempts at debenzylation were attempted.

3.5.2 Acid Protocols

Previously successful debenzylation attempts include the TFA and AlCl₃ protocols described by Merz *et al.*⁶⁷ and Girardet *et al.*,⁶⁸ respectively.³⁰ Due to formation of excessive by-products with the TFA protocol, deprotection using AlCl₃ was preferred.³⁰ Due to reports of multiple successful *N*-debenzylation with TFA,^{58,110,111} additional protocols were tested. Deprotection of compounds **12** and **17** were done using the previously successful protocol based on Girardet *et al.*^{30,68} Reaction conditions are shown in Table 3.6.

Table 3.6: Overview of reaction conditions and data for deprotection of compounds **12** and **17** using AlCl₃ and TFA.

						R
12 - 17		HSB2-3		12	17	<i>m</i> -CH ₃ <i>p</i> -OH
Compound	Scale	Acid	T	Rx time	Conv. ^a	Yield ^b
	[mg]		[°C]	[h]	[%]	[%]
12	50	TFA	60	22	<1	nd. ^c
12	27	AlCl ₃	160	3	>99	53
17	35	AlCl ₃	160	3	>99	nd. ^c

^a Conversion determined by ¹H NMR spectroscopy.

^b Isolated yields.

^c Not determined.

Miki *et al.*¹¹⁰ reported successful debenzoylation of indoles with TFA using dimethoxybenzene (DMB) as an additive. Because of limited availability, DMB was substituted with anisole, which has a similar ability to trap the benzyl cation.⁶⁹ Compound **12** was dissolved in CH₂Cl₂ with 5 eq. TFA and 3 eq. anisole at rt. TLC analysis showed no conversion after 1 h and the reaction was continued at reflux. After an additional 21 h TLC and ¹H NMR analysis revealed <1% conversion and the reaction was stopped. It seems evident that benzyl groups bind stronger to the purine ring than with similar compounds, and harsher conditions are needed for *N*-debenzoylation. Further deprotections were done with the previously successful AlCl₃ protocol.

Compound **12** was dissolved in 1,2-dichlorobenzene with a large excess of AlCl₃, and stirred at 160 °C for 3 hours. ¹H NMR analysis showed full conversion, and the formation of multiple unknown by-products. Purification by silica-gel column chromatography gave compound **HSB2** in 53% yield. The formation of by-products is likely due to the harsh conditions, and the main contributing fac-

tor to the mediocre yield. With the free amine proton an increase in bonding interactions with silica groups is expected. Due to the small scale of the reaction, loss of compound during purification could have significant impact on the yield.

^1H NMR analysis of the purified compound revealed low integrals for the cyclohexane ring in the amine group. Since all signals and integrals were correct in the crude product, this could indicate partial decomposition during purification. However, HRMS and ^{13}C NMR analysis revealed no signals for compounds other than the expected product **HSB2**. Due to limited amount of material no further analysis was possible, and the reason for the low integrals is still unknown.

Synthesis of compound **HSB3** was conducted in a similar fashion; however, no clear separation between compounds was observed with TLC analysis. The deprotection was assumed to follow similar kinetics as the deprotection of the toluene analog, and was stopped after 3 h. ^1H NMR analysis showed full conversion, and formation of multiple by-products. Formation of the desired compound was not possible to ascertain from analysis of the crude mixture. Remaining traces of solvent and some by-products were removed by silica-plug filtration. Further ^1H NMR analysis revealed the disappearance of the PMB signals, and a singlet at 13.01 ppm corresponding to the *N*9 proton in an unprotected purine. Signals akin to those from the amine and aryl substituents were also observed, which indicates that the deprotection proceeded and the desired product was formed. However, due to the small scale and insufficient separation on TLC further purification proved futile. With multiple signals from impurities in both the aromatic and aliphatic region, accurate structure determination was not possible.

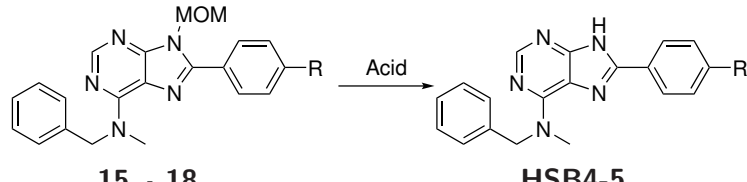
Formation of by-products were seen in both Lewis acid catalyzed deprotections. AlCl_3 is a strong Lewis acid and can react in Friedel-Craft alkylations.^{78,112} 1,2-Dichlorobenzene is an electron deficient aromatic and should not exhibit high reactivity in electrophilic aromatic substitutions. However, it is possible that some by-product formation is due to Friedel-Craft type side reactions. The mechanism

as proposed by Watanabe *et al.*,¹¹² involves the coordination of AlCl₃ to the nitrogen with subsequent departure and trapping of the benzyl group. Presence of substituents that react with the Lewis acid was reported to slow down or hinder the reaction, and by-products from attack by the benzyl cation has previously been observed.¹¹² More severe by-product formation was seen in the deprotection of the *p*-hydroxy derivative **17**. AlCl₃ can form aluminum alkoxides with alcohols, which makes the Lewis acid less active,¹¹² and changes the reactivity of the hydroxyl group. It is possible that the formation of aluminum alkoxides either directly facilitates formation of by-products or decomposition, or slows down the reaction enough to allow time for more side reactions.

3.6 MOM Deprotection and Synthesis of Compounds HSB4 and HSB5

Cleavage of the MOM group is normally achieved by treatment with acid, and have been achieved at mild conditions.⁵⁸ Deprotection of compounds **15** and **18** using HCl and TFA were investigated. The reaction conditions and results are shown in Table 3.7.

Table 3.7: Overview of reaction conditions and data for deprotection of compounds **15** and **18**.

		R				
15 - 18		15	CH ₃			
		18	OH			
Compound	Scale [mg]	Acid	T [°C]	Rx time [h]	Conv. ^a [%]	Yield ^b [%]
15	13	TFA	rt.	2	>99	nd. ^c
15	10	HCl	rt.	24	<1	nd. ^c
15	19	HCl	60	3	>99	74
18	40	HCl	60	3	>99	20

^a Conversion determined by ¹H NMR spectroscopy. ^b Isolated yields. ^c Not determined.

Initially, two protocols conducted at rt. were tested. Deprotection with TFA were done according to the procedure described by Mayrargue *et al.*¹¹³ Compound **15** was dissolved in equal parts CH₂Cl₂ and TFA. TLC analysis showed complete conversion after 2 h. ¹H NMR analysis revealed a doubling of the signals corresponding to the C2 proton at 8.48 ppm and the tolyl CH₃ group at 2.44 ppm. Additional singlets at 5.83 ppm, 5.18 ppm, 3.98 ppm, 3.39 ppm were also observed. Remnants of the deprotected MOM group are expected to form volatiles, and the unknown signals in the 3 - 5 ppm region were thought to belong to non-deprotected compounds. However, HRMS analysis only revealed signals corresponding to the molecular formula of the expected product.

Since there was no pH adjustment after the completed reaction, the product could exist in a protonated form. Due to purines having multiple tautomeres, there are multiple possible protonation sites.^{114,115} The predominant tautomeric form is both solvent and substituent dependent.^{114,116,117} Because of the lack of the broad amine signals, it is hypothesized that the imine tautomer of the amino substituted purine is dominant. Protonation would then occur at N1,¹¹⁵ and stabilize against rapid isomerisation. This would indicate that the unknown ¹H NMR signals at 5.83 ppm, 5.18 ppm, 3.98 ppm, 3.39 ppm belong to the CH₂ and CH₃ groups of the two rotameres. The amine tautomer is usually more predominant in more polar solvents.¹¹⁴ Upon ¹H NMR analysis of the product in DMSO-*d*₆, no doubling of signals was observed. The unknown signals between 3-5 ppm had vanished, and the broad amine signals reappeared, see Figure 3.8. This supports the hypothesis that the compound exists as the protonated imine tautomer in CDCl₃. Full characterisation by NMR analysis shows that the desired 6-amino-8-aryl purine **HSB4** was formed.

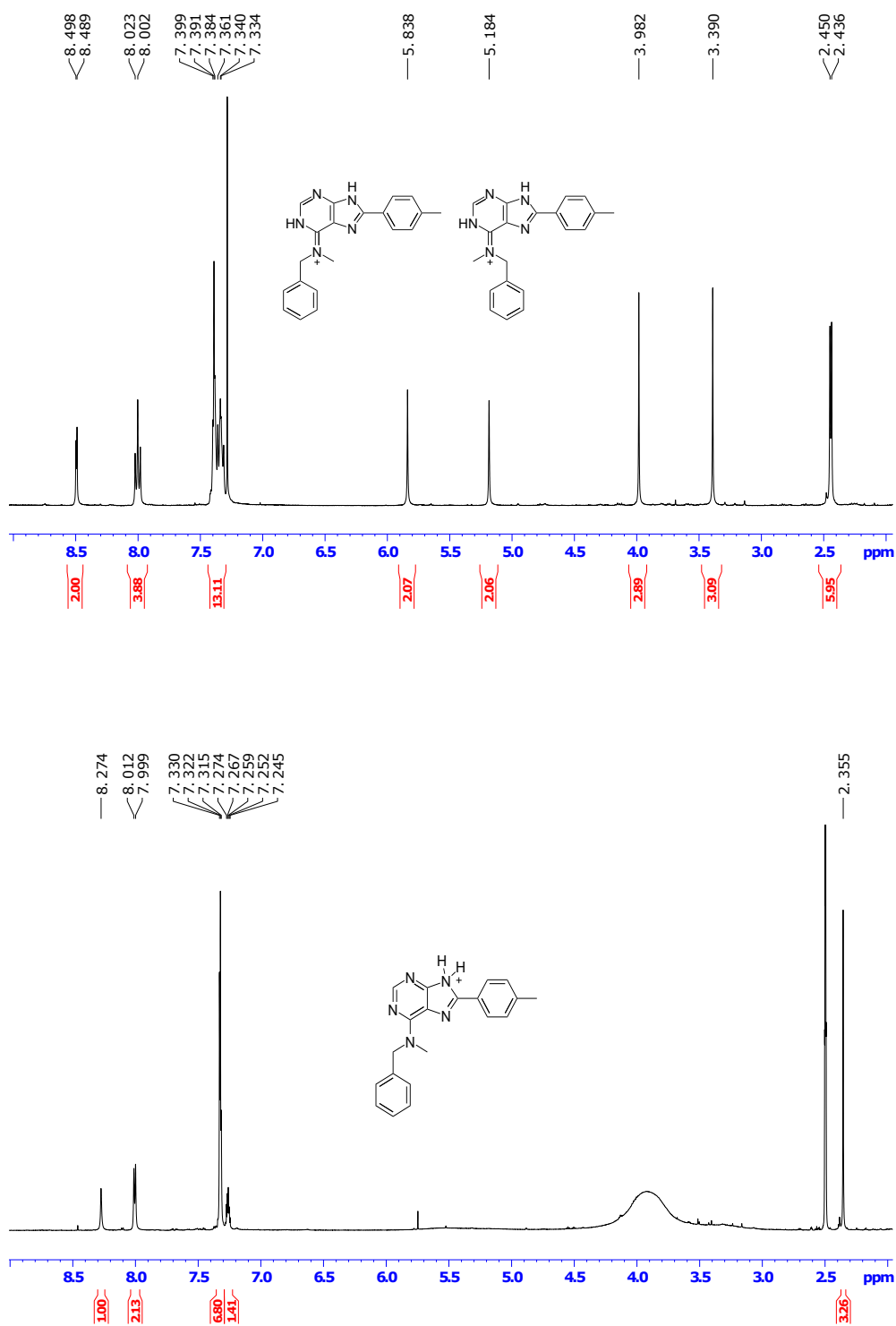


Figure 3.8: ^1H NMR (400 MHz) and suggested conformations of protonated compound **HSB4**. Upper (CDCl_3): Stabilized imine tautomers. Lower ($\text{DMSO-}d_6$): Amine tautomer.

The HCl deprotection protocol described by van Herden *et al.*¹¹⁸ was also tested. Compound **15** was dissolved in equal parts THF and *i*-PrOH, with 10 vol% conc. HCl. ¹H NMR analysis revealed no conversion after 24 h. It was assumed that harsher conditions were required, and the deprotection was reattempted using the conditions described by Auerbach *et al.*¹¹⁹ Compound **15** was stirred in MeOH with 10 vol% conc. HCl at reflux. Full conversion was seen after 3 h, and compound **HSB4** was isolated in 74% yield. MeOH and *i*-PrOH have similar properties,^{120,121} and the increased rate of reaction is mainly attributed to the temperature increase.

Deprotection of compound **18** was also conducted using the method of Auerbach *et al.*¹¹⁹ ¹H NMR analysis showed full conversion after 3 h. With the extra hydroxyl group, there was a fear of increased loss of product to the aqueous phase during work-up. In an effort to keep the yields at acceptable levels, the reaction was quenched with NH₃, concentrated *in vacuo* and purified by silica-gel column chromatography. ¹H NMR analysis revealed the resulting fractions to be more impure than the reaction mixture. After a second column on the most impure fractions, compound **HSB5** was isolated in 20% yield. 2D-TLC analysis indicated decomposition of the product on silica. Due to the small scale, no alternative purification methods were attempted. Higher yields could possibly be achieved using the TFA protocol, as no purification other than work-up was needed for the toluene analog.

3.7 Structure Elucidation

Eight of the compounds synthesized in this project are not reported in the literature. NMR, MS and IR was used to determine the structure of these compounds. 1D ^1H NMR, ^{13}C NMR, and 2D ^1H - ^1H COSY, ^1H - ^{13}C HSQC and ^1H - ^{13}C HMBC were used to assign the chemical shifts. MS was used to confirm the identity of the compounds. All spectra are given in Appendix A to O.

Assigned peaks for compound **3** to **HSB5** are given in Table 3.9 to Table 3.17. All NMR experiments were done in CDCl_3 or $\text{DMSO-}d_6$. Traces of grease and common solvents can be seen in some of the spectra. Chemical shifts of selected solvents and trace impurities are shown in Table 3.8.

Table 3.8: ^1H and ^{13}C shifts of some common solvents and trace impurities.¹²²

	Group	CDCl_3		$\text{DMSO-}d_6$	
		^1H	^{13}C	^1H	^{13}C
Solvent Residual		7.26	77.16	2.50	39.52
Silicone Grease		0.07	1.19	-0.06	
1,4-Dioxane		3.71	67.1	3.57	66.4
CH_2Cl_2		5.30	53.5	5.76	54.8
H_2O		1.56		3.33	
EtOAc	CH_3CO	2.05	21.0	1.99	20.7
	CH_2CH_3	4.12	60.5	4.03	59.7
	CH_2CH_3	1.26	14.2	1.17	14.4
	CO		171.4		170.3
MeOH	CH_3OH	3.49	50.41	3.16	48.59
	OH	1.09		4.01	

3.7.1 General Remarks

^1H - ^{13}C long range coupling was used to determine chemical shift of sp^2 hybridized carbons. For some carbons these couplings were not present and the assignments were made with regards to effect of shielding on value of chemical shift where possible. All sp^2 hybridized purine carbons except C5 are bonded to two electronegative groups. C4 and C6 have less shielding and are expected to have higher shifts. The concentration of NMR samples varied, and some of the sp^2 hybridized carbons were not observed in the ^{13}C spectra. Missing shifts were approximated from HMBC and HSQC analysis wherever possible.

Peak broadening was observed in all compounds containing a C6-amino functionality, stemming from the CH_2 and CH_3 groups on the amino-substituent. These carbons were not observed in ^{13}C NMR. Peak broadening occurs because of chemical or conformational exchange, and is a known occurrence in 6-amino-purines.^{101,102} Broadened signals are labeled "br" in the tables. Heightened integrals in the 0.8 ppm to 3.0 ppm region may be observed, due to traces of the aliphatic amine by-product **7**.

A detailed structure elucidation of every compound containing a new structure element will be given. Structures of compounds containing similar substituents were determined using the same methods and will not be discussed in detail.

3.7.2 Compound 3

In this section a detailed structure elucidation of compound **3** will be given. Previously reported instances of the compound provided insufficient spectroscopic data, so a complete characterisation of the compound was conducted.

The structure of compound **3** with numbered positions is shown in Figure 3.9. HRMS gave m/z 199.0386 $[M+H]^+$. With a calculated value of 199.0387, the molecular formula $C_7H_8N_4OCl$ was confirmed. All 1H NMR, ^{13}C NMR, MS and IR spectra for compound **3** are shown in Appendix A.

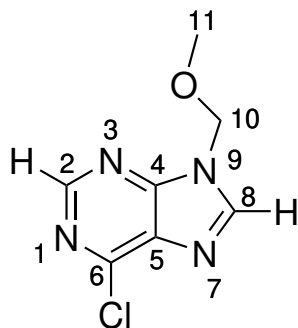


Figure 3.9: Numbering of positions in compound **3**.

^1H NMR spectra of compound **3** showed two singlets with integrals of 1H at 8.79 ppm and 8.27 ppm. These signals must belong to the protons on the purine ring. HSQC analysis revealed that the corresponding carbon shifts were 152.6 ppm and 145.1 ppm respectively. A singlet of integral 2H was observed at 5.64 ppm, with a corresponding carbon shift of 74.6 ppm. This peak must be from the CH_2 ether group at C10. HMBC analysis showed coupling to a singlet at 3.40 ppm with an integral of 3H and a corresponding carbon shift of 57.5 ppm. Which is from the methyl ether group at C11. Additionally HMBC analysis showed coupling between the signal at C10 and the singlet at 8.27. This places the signal at 8.79 ppm at C2 and the signal at 8.27 ppm at C8, see Figure 3.10.

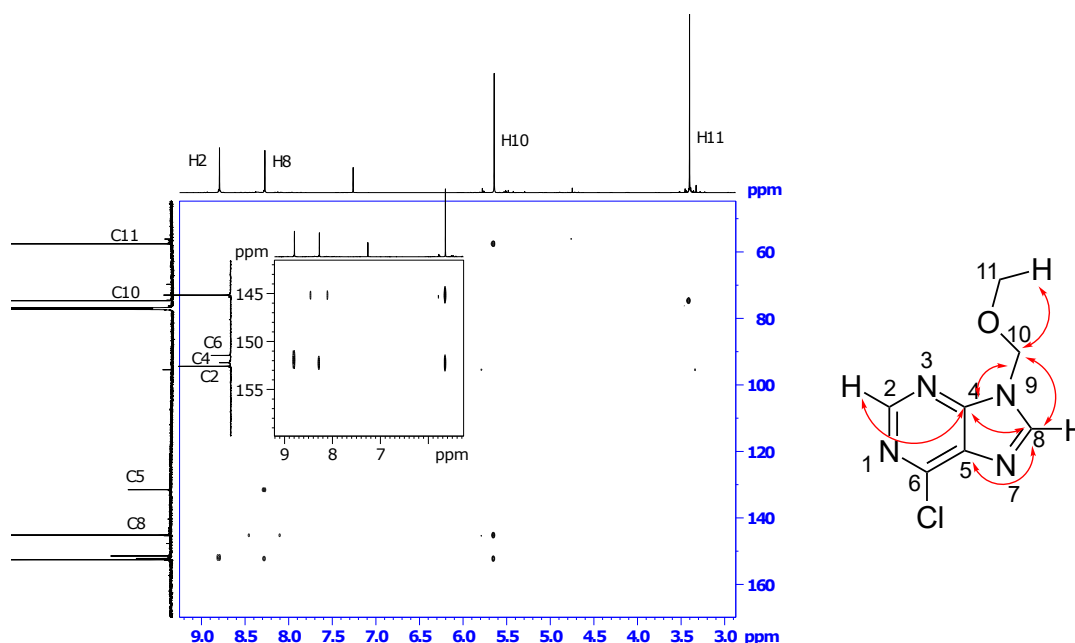


Figure 3.10: Correlation between carbons and protons as seen in the HMBC spectra.

This leaves three sp^2 hybridized carbons to be assigned. C6 and C4 are expected to be close in shifts due to both carbons being bonded to two electron withdrawing groups. The carbon at C5 is more shielded and is expected to have a lower shift. The carbon signals at 152.2 ppm and 151.4 ppm were assigned to C4 and C6.

HMBC coupling to C10 places the signal at 152.2 at C4. Because of the lower shift and coupling to C8 through HMBC, the signal at 131.5 ppm was assigned to C5. Since C10 couples to C4 and not C5, the formation of the N9 isomer is confirmed. Assigned chemical shifts from ^1H and ^{13}C NMR are given in Table 3.9.

Table 3.9: ^1H and ^{13}C shift for compound **3** (CDCl_3 , 400 MHz).

Position	^1H [ppm] (mult., J [Hz], int.)	^{13}C	COSY	HMBC
1		N		
2	8.79 (s, 1H)	152.6		4
3		N		
4		152.2		10, 8, 2
5		131.5		8
6		151.4		
7		N		
8	8.27 (s, 1H)	145.1		10, 5, 4
9		N		
10	5.64 (s, 2H)	74.6		11, 8, 4
11	3.40 (s, 3H)	57.5		10

3.7.3 Compound 10

The structure of compound **10** with numbered positions is shown in Figure 3.11. HRMS gave m/z 410.0479 $[M+H]^+$. With a calculated value of 410.0478, the molecular formula $C_{15}H_{17}N_5OI$ was confirmed. All 1H NMR, ^{13}C NMR, MS and IR spectra for compound **10** are shown in Appendix G.

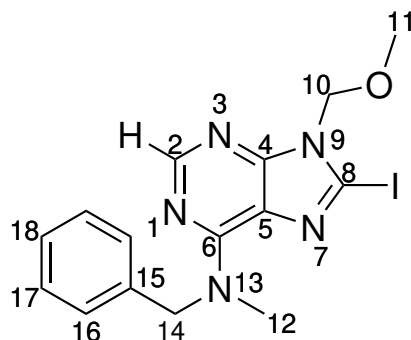


Figure 3.11: Numbering of positions in compound **10**.

The chemical shifts of the purine moiety and the MOM protecting group was assigned as described in section 3.7.2. As previously explained the broad peaks at 5.76 - 4.81 ppm, and 3.92 - 2.97 ppm in the 1H NMR spectra belong to the CH_2 and CH_3 groups of the amine functionality. The methyl group is expected to have a lower shift due to less shielding from anisotropic effects of the phenyl ring,¹²³ and is placed at 5.76 - 4.81 ppm. HSQC analysis revealed the corresponding carbon shift of 67.1 ppm. The methyl group was not seen in the ^{13}C NMR spectrum, and neither show coupling to other groups.

Since the aromatic ring is symmetric it is only expected to give three signals. 1H NMR analysis revealed a multiplet with an integral of 1H at 7.27 - 7.26 ppm, with a corresponding carbon shift of 127.4 ppm. This signal must belong to the proton at C18, and showed coupling through COSY to multiplets at 7.33 - 7.30 ppm and 7.29 - 7.27 ppm with carbon shifts of 128.6 ppm and 127.7 ppm respectively. HMBC analysis showed only coupling to the signal at 7.29 - 7.27 ppm. This leaves the ^{13}C signal at 137.6 ppm which must be at C15, and shows coupling to the signal at 7.33 - 7.30 ppm through HMBC. Both two and three bond correlations can be seen in HMBC, and since accurate coupling constants could not be

extracted, unambiguous assignment for C16 and C17 was not possible. Assigned chemical shifts from ^1H and ^{13}C NMR are given in Table 3.10.

Table 3.10: ^1H and ^{13}C shift for compound **10** (CDCl_3 , 600 MHz).

Position	^1H [ppm] (mult., J [Hz], int.)	^{13}C	COSY	HMBC
1		N		
2	8.31 (s, 1H)	153.6		6, 4
3		N		
4		153.0		
5		122.5		
6		153.0		
7		N		
8		96.5		10
9		N		
10	5.50 (s, 2H)	75.3		11, 8, 4
11	3.41 (s, 3H)	57.2		10
12	3.92 - 2.97 (br, 3H)	* <i>a</i>		
13		N		
14	5.76 - 4.81 (br, 2H)	67.1		
15		137.6		
16	7.29 - 7.27 ^{<i>b</i>} (m, 2H)	127.7 ^{<i>b</i>} (2C)	18, 17	18, 16
17	7.33 - 7.30 ^{<i>b</i>} (m, 2H)	128.6 ^{<i>b</i>} (2C)	18, 16	15
18	7.27 - 7.26 (m, 1H)	127.4	17, 16	18, 16

^{*a*} Signals too weak to be observed in ^{13}C NMR.

^{*b*} May be interchanged.

3.7.4 Compound 12

The structure of compound **12** with numbered positions is shown in Figure 3.12. HRMS gave m/z 456.2758 $[M+H]^+$. With a calculated value of 456.2763, the molecular formula $C_{28}H_{34}N_5O$ was confirmed. All 1H NMR, ^{13}C NMR, MS and IR spectra for compound **12** are shown in Appendix H.

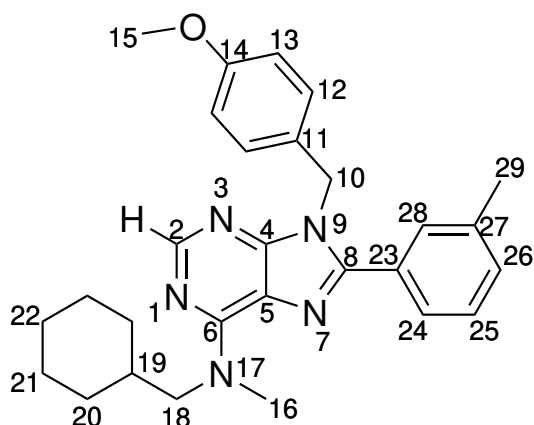


Figure 3.12: Numbering of positions in compound **12**.

The chemical shifts of the purine moiety was assigned as described in section 3.7.2. 1H NMR analysis revealed a signal with integral 2H at 5.29 ppm. This must belong to the benzylic CH_2 group at C10. HSQC analysis gave the corresponding carbon shift of 46.4 ppm. Due to the PMB group being symmetric, only two proton signals are expected from the aromatic ring. The doublets at 7.04 ppm and 6.80 ppm lie in the aromatic region, and show coupling through COSY and coupling constants. These proton signals must stem from position C12 and C13 and were assigned carbon shifts 128.5 ppm and 114.1 ppm respectively. HMBC analysis revealed coupling between C10 and the doublet at 7.04 ppm, but not the signal at 6.80 ppm. Thus the signal at 7.04 ppm was assigned to position C11 while the doublet at 6.80 ppm was assigned to C12. The methoxy group at C15 is responsible for the singlet at 3.77 ppm, with an integral of 3H and corresponding carbon shift of 55.3 ppm. HMBC revealed coupling to 158.4 ppm, which has to be from the carbon at C14.

Since the 3H singlet at 2.39 ppm has a much lower shift than the methoxy group, it must be from the methyl group at C29. HSQC gave the corresponding carbon shift as 21.4 ppm, and HMBC showed coupling to a signal at 138.9 ppm. This signal corresponds to no proton signals, and was assigned to position C27. The singlet at 7.44 ppm with carbon shift 130.0 ppm was placed at C28, considering it shows no coupling to neighbouring protons. This leaves the two doublets at 7.39 ppm and 7.27 ppm and the triplet at 7.27 ppm, with carbon shifts 126.2 ppm, 130.4 ppm and 128.1 ppm respectively. The triplet shows coupling to both the doublets through COSY and coupling constants and was assigned to C25. HMBC revealed coupling from C29 to the doublet at 7.27 ppm, placing it at C26. Thus, the signal at 7.39 was assigned to position C24.

As previously discussed, the broad peak at 4.19 - 3.29 ppm in the ^1H NMR spectra is from the CH_2 and CH_3 groups in the amino functionality. These groups are not seen in the ^{13}C NMR spectrum, and show no coupling to other groups. The multiplet 1.93 - 1.88 ppm had an integral of 1H and belongs to the CH group in the cyclohexane ring, while the multiplets from 1.78 - 1.04 ppm belong to the CH_2 groups on the ring. HSQC analysis gave the corresponding carbon shifts, and multiple proton multiplets were assigned to each carbon. This is because of the difference in chemical shift for protons in axial and equatorial positions due to anisotropic effects.¹²³ Thus, unambiguous assignment of carbon shifts from position 20 to 22 was not possible. Assigned chemical shifts from ^1H and ^{13}C NMR is given in Table 3.11.

Table 3.11: ^1H and ^{13}C shift for compound **12** (CDCl_3 , 400 MHz).

Position	^1H [ppm] (mult., J [Hz], int.)	^{13}C	COSY	HMBC
1		N		
2	8.38 (s, 1H)	152.4		
3		N		
4		152.6		
5		* <i>a</i>		
6		* <i>a</i>		
7		N		
8		149.1		
9		N		
10	5.39 (s, 2H)	46.4		11, 10, 8, 4
11		* <i>a</i>		
12	7.04 (d, $J = 8.7$, 2H)	128.5 (2C)	13	14
13	6.80 (d, $J = 8.7$, 2H)	114.1 (2C)	12	12
14		158.4		
15	3.77 (s, 3H)	55.3		14
16	4.19 - 3.29 (br, 3H)	* <i>a</i>		
17		N		
18	4.19 - 3.29 (br, 2H)	* <i>a</i>		
19	1.93 - 1.88 (m, 1H)	* <i>a</i>		
20	1.78 - 1.66 / 1.14 - 1.04	30.9 ^{<i>b</i>}	22, 21	
21	1.78 - 1.66 / 1.28 - 1.17	26.2 ^{<i>b</i>}	22, 20	
22	1.78 - 1.66 / 1.28 - 1.17	26.0 ^{<i>b</i>}	21, 20	
23		* <i>a</i>		
24	7.39 (d, $J = 7.3$, 1H)	126.2	25	
25	7.31 (t, $J = 7.5$, 1H)	128.1	26, 24	26
26	7.27 (d ^{<i>c</i>} , 1H)	130.4	25	
27		138.9		
28	7.44 (s, 1H)	130.0		
29	2.39 (s, 3H)	21.4		28, 27, 26

^{*a*} Signals too weak to be observed in ^{13}C NMR.

^{*b*} May be interchanged.

^{*c*} Coupling constant not determined due to overlapping solvent signal.

3.7.5 Compound 15

The structure of compound **15** with numbered positions is shown in Figure 3.13. Assigned chemical shifts from ^1H and ^{13}C NMR are given in Table 3.12. HRMS gave m/z 374.977 $[\text{M}+\text{H}]^+$. With a calculated value of 374.1981, the molecular formula $\text{C}_{22}\text{H}_{24}\text{N}_5\text{O}$ was confirmed. All ^1H NMR, ^{13}C NMR, MS and IR spectra for compound **15** are shown in Appendix I.

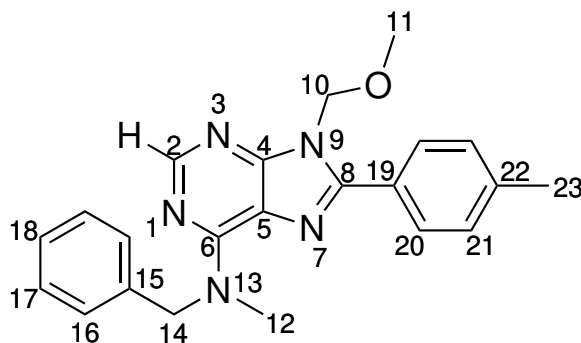


Figure 3.13: Numbering of positions in compound **15**.

Table 3.12: ^1H and ^{13}C shift for compound **15** (CDCl_3 , 400 MHz).

Position	^1H [ppm] (mult., J [Hz], int.)	^{13}C	COSY	HMBC
1		N		
2	8.41 (s, 1H)	152.5		
3		N		
4		153.3		
5		119.5		
6		154.6		
7		N		
8		149.8		
9		N		
10	5.55 (s, 2H)	73.2		11, 8, 4
11	3.56 (s, 3H)	57.1		10
12	3.62 - 3.26 (br, 3H)	* a		
13		N		
14	5.62 - 5.22 (br, 2H)	* a		
15		138.5		
16	7.33 - 7.27 (m, 2H)	128.5 b (2C)	18, 17	18, 17
17	7.33 - 7.27 (m, 2H)	127.8 b (2C)	18, 16	18, 16
18	7.33 - 7.27 (m, 1H)	127.2 b	18, 17	18, 17
19		126.8		21
20	7.33 - 7.27 (m, 2H)	129.2 (2C)	21	23, 21
21	7.88 (d, $J = 8.2$, 2H)	129.5 (2C)	20	22, 8
22		140.2		
23	2.41 (s, 3H)	21.5		22, 21

a Signals too weak to be observed in ^{13}C NMR.

b May be interchanged.

3.7.6 Compound 17

The structure of compound **17** with numbered positions is shown in Figure 3.14. Assigned chemical shifts from ^1H and ^{13}C NMR are given in Table 3.13. HRMS gave m/z 458.2548 $[\text{M}+\text{H}]^+$. With a calculated value of 458.2556, the molecular formula $\text{C}_{27}\text{H}_{32}\text{N}_5\text{O}_2$ was confirmed. All ^1H NMR, ^{13}C NMR, MS and IR spectra for compound **17** are shown in Appendix J.

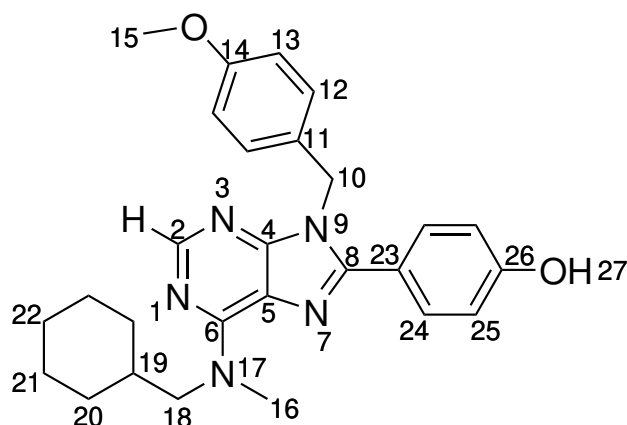


Figure 3.14: Numbering of positions in compound **17**.

Table 3.13: ^1H and ^{13}C shift for compound **17** (CDCl_3 , 400 MHz).

Position	^1H [ppm] (mult., J [Hz], int.)	^{13}C	COSY	HMBC
1		N		
2	8.36 (s, 1H)	152.1		
3		N		
4		152.5		
5		119.7		
6		152.5		
7		N		
8		148.7		
9		N		
10	5.39 (s, 2H)	46.3		12, 11, 8, 4
11		<i>*a</i>		
12	7.01 (d, $J = 8.6$, 2H)	127.9 (2C)	13	
13	6.79 (d, $J = 8.7$, 2H)	114.2 (2C)	12	12
14		159		
15	3.75 (s, 3H)	55.3		14
16	4.27 - 3.17 (br, 3H)	<i>*a</i>		
17		N		
18	4.27 - 3.17 (br, 2H)	<i>*a</i>		
19	1.93 - 1.85 (m, 1H)	<i>*a</i>		
20	1.75 - 1.59 / 1.28 - 1.05	30.7 ^b (2C)	22, 21	
21	1.75 - 1.59 / 1.28 - 1.05	26.6 ^b (2C)	22, 20	
22	1.75 - 1.59 / 1.28 - 1.05	26.0 ^b (2C)	21, 20	
23		122.6		25
24	7.49 (d, $J = 8.6$, 2H)	130.7 (2C)	25	8
25	6.86 (d, $J = 8.6$, 2H)	115.7 (2C)	24	26, 23
26		157.3		25, 24
27	6.01 (br, 1H)	OH		

^a Signals too weak to be observed in ^{13}C NMR.

^b May be interchanged.

3.7.7 Compound 18

The structure of compound **18** with numbered positions is shown in Figure 3.15. Assigned chemical shifts from ^1H and ^{13}C NMR are given in Table 3.14. HRMS gave m/z 376.1769 $[\text{M}+\text{H}]^+$. With a calculated value of 376.1773, the molecular formula $\text{C}_{21}\text{H}_{22}\text{N}_5\text{O}_2$ was confirmed. All ^1H NMR, ^{13}C NMR, MS and IR spectra for compound **18** are shown in Appendix K.

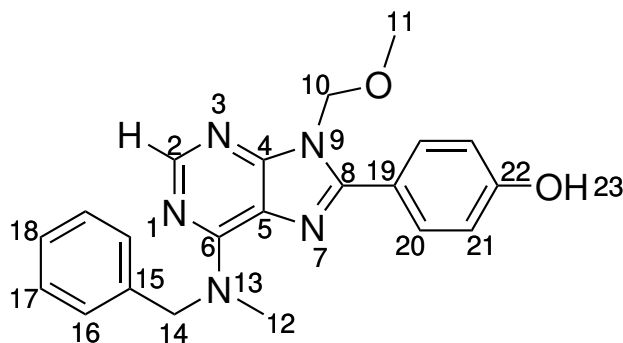


Figure 3.15: Numbering of positions in compound **18**.

Table 3.14: ^1H and ^{13}C shift for compound **18** (DMOS- d_6 , 400 MHz).

Position	^1H [ppm] (mult., J [Hz], int.)	^{13}C	COSY	HMBC
1		N		
2	8.31 (s, 1H)	152.4		6
3		N		
4		153.3		
5		118.9		
6		154.1		
7		N		
8		149.9		
9		N		
10	5.50 (s, 2H)	73.6		11, 8, 4
11	3.42 (s, 3H)	57.1		10
12	3.74 - 2.92 (br, 3H)	* a		
13		N		
14	5.76 - 4.96 (br, 2H)	* a		
15		138.6		
16	7.33 - 7.26 (m, 2H)	129.0 b (2C)	18, 17	18, 17
17	7.33 - 7.26 (m, 2H)	127.9 b (2C)	18, 16	18, 16
18	7.33 - 7.26 (m, 1H)	127.6 b	18, 17	18, 17
19		120.4		21
20	7.78 (d, $J = 8.6$, 2H)	130.9 (2C)	21	22, 8
21	6.92 (d, $J = 8.7$, 2H)	116.1 (2C)	20	19
22		159.8		
23	10.1 (br, 1H)	OH		22, 21

a Signals too weak to be observed in ^{13}C NMR.

b May be interchanged.

3.7.8 Compound HSB2

The structure of compound **HSB2** with numbered positions is shown in Figure 3.16. Assigned chemical shifts from ^1H and ^{13}C NMR are given in Table 3.15. HRMS gave m/z 336.2186 $[\text{M}+\text{H}]^+$. With a calculated value of 336.2188, the molecular formula $\text{C}_{20}\text{H}_{26}\text{N}_5$ was confirmed. All ^1H NMR, ^{13}C NMR, MS and IR spectra for compound **HSB2** are shown in Appendix M.

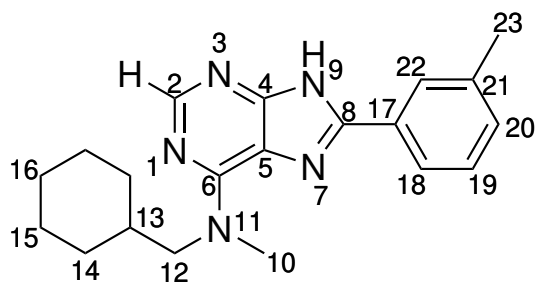


Figure 3.16: Numbering of positions in compound **HSB2**.

Table 3.15: ^1H and ^{13}C shift for compound **HSB2** (DMOS- d_6 , 600 MHz).

Position	^1H [ppm] (mult., J [Hz], int.)	^{13}C	COSY	HMBC
1		N		
2	8.23 (s, 1H)	152.7		6, 4
3		N		
4		154.6		
5		141.7		
6		154.6		
7		N		
8		148.5		
9		N		
10	3.75 - 2.64 (br, 3H)	<i>*a</i>		
11		N		
12	3.75 - 2.64 (br, 2H)	<i>*a</i>		
13	1.95 - 1.82 (m, 1H)	<i>*a</i>		
14	1.73 - 1.57 / 1.32 - 0.99	27.5 ^b (2C)	15	
15	1.73 - 1.57 / 1.32 - 0.99	26.6 ^b (2C)	16, 14	
16	1.73 - 1.57 / 1.32 - 0.99	25.8 ^b	15	
17		130.2		
18	7.92 (d, $J = 7.7$, 1H)	123.8	19	22, 20, 8
19	7.44 - 7.41 (m, 1H)	129.3	20, 18	21, 18, 17
20	7.31 (d, $J = 7.1$, 1H)	19	22, 18	
21		138.6		
22	7.99 (s, 1H)	127.2		23, 21, 18, 8
23	2.4 (s, 3H)	21.5		22, 21, 20, 19

^a Signals too weak to be observed in ^{13}C NMR.

^b May be interchanged.

3.7.9 Compound HSB4

The structure of compound **10** with numbered positions is shown in Figure 3.17. Assigned chemical shifts from ^1H and ^{13}C NMR are given in Table 3.16. HRMS gave m/z 330.1715 $[\text{M}+\text{H}]^+$. With a calculated value of 330.1719, the molecular formula $\text{C}_{20}\text{H}_{20}\text{N}_5$ was confirmed. All ^1H NMR, ^{13}C NMR, MS and IR spectra for compound **HSB4** are shown in Appendix N.

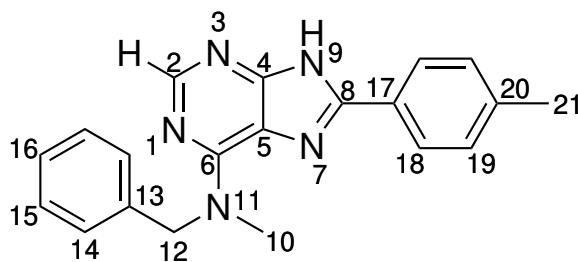


Figure 3.17: Numbering of positions in compound **HSB4**.

Table 3.16: ^1H and ^{13}C shift for compound **HSB4** (CDCl_3 , 600 MHz).

Position	^1H [ppm] (mult., J [Hz], int.)	^{13}C	COSY	HMBC
1		N		
2	8.48 (s, 1H)	151.2		6, 4
3		N		
4		152.5		
5		121.1		
6		154.5		
7		N		
8		148.3		
9	14.41 (s, 1H)	N		
10	4.14 - 3.10 (br, 3H)	* <i>a</i>		
11		N		
12	5.88 - 4.99 (br, 2H)	* <i>a</i>		
13		138.1		
14	7.38 - 7.27 (m, 2H)	128.6 ^{<i>b</i>} (2C)	15	16
15	7.38 - 7.27 (m, 2H)	127.9 ^{<i>b</i>} (2C)	16, 14	13
16	7.38 - 7.27 (m, 1H)	127.3 ^{<i>b</i>}	15	14
17		127.4		
18	8.05 (d, $J = 8.0$, 2H)	126.4 (2C)	19	20, 8
19	7.38 - 7.27 (m, 2H)	129.7 (2C)	18	
20		140.2		
21	2.43 (s, 3H)	21.5		20, 19, 18

^{*a*} Signals too weak to be observed in ^{13}C NMR.

^{*b*} May be interchanged.

3.7.10 Compound HSB5

The structure of compound **HSB5** with numbered positions is shown in Figure 3.18. Assigned chemical shifts from ^1H and ^{13}C NMR are given in Table 3.17. HRMS gave m/z 332.1508 $[\text{M}+\text{H}]^+$. With a calculated value of 332.1511, the molecular formula $\text{C}_{19}\text{H}_{18}\text{N}_5\text{O}$ was confirmed. All ^1H NMR, ^{13}C NMR, MS and IR spectra for compound **HSB5** are shown in Appendix O.

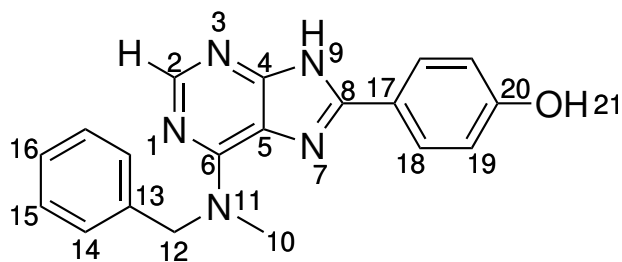


Figure 3.18: Numbering of positions in compound **HSB5**.

Table 3.17: ^1H and ^{13}C shift for compound **HSB5** (DMOS- d_6 , 400 MHz).

Position	^1H [ppm] (mult., J [Hz], int.)	^{13}C	COSY	HMBC
1		N		
2	8.27 (s, 1H)	151.9		6, 4
3		N		
4		153.8		
5		120.2		
6		153.8		
7		N		
8		148.1		
9	13.33 (s, 1H)	N		
10	3.82 - 3.00 (br, 3H)	* a		
11		N		
12	5.72 - 5.26 (br, 2H)	* a		
13		138.8		
14	7.41 - 7.29 (m, 2H)	129.0 b (2C)	15	16
15	7.41 - 7.29 (m, 2H)	127.9 b (2C)	16, 14	13
16	7.41 - 7.29 (m, 1H)	127.5 b	15	14
17		121.0		
18	8.00 (d, $J = 8.7$, 2H)	128.3 (2C)	19	20, 8
19	6.93 (d, $J = 8.7$, 2H)	116.1 (2C)	18	20, 18
20		159.6		
21	10.00 (s, 1H)	OH		

a Signals too weak to be observed in ^{13}C NMR.

b May be interchanged.

3.7.11 IR-Spectroscopy

The compounds discussed in section 3.7.2 to 3.7.10 were analyzed by IR spectroscopy. Absorption bands were assigned using theory from Silverstein *et al.*¹²⁴ Because of structural similarities the same absorption bands are observed in multiple compounds. A summary of the most important bands are found in this section. The spectra are shown in Appendix A to O.

Weak bands stemming from aromatic stretching vibrations in the 3100 cm^{-1} and 3000 cm^{-1} region were seen for almost all compounds. Both the protons in the purine ring and the aryl substituents can give rise to these bands. Aromatic C–H out of plane bending vibrations gave signals in the 900 cm^{-1} to 675 cm^{-1} region. All compounds showed absorption in the 1600 cm^{-1} to 1300 cm^{-1} region, stemming from C=C or C=N stretching vibrations in the purine ring.

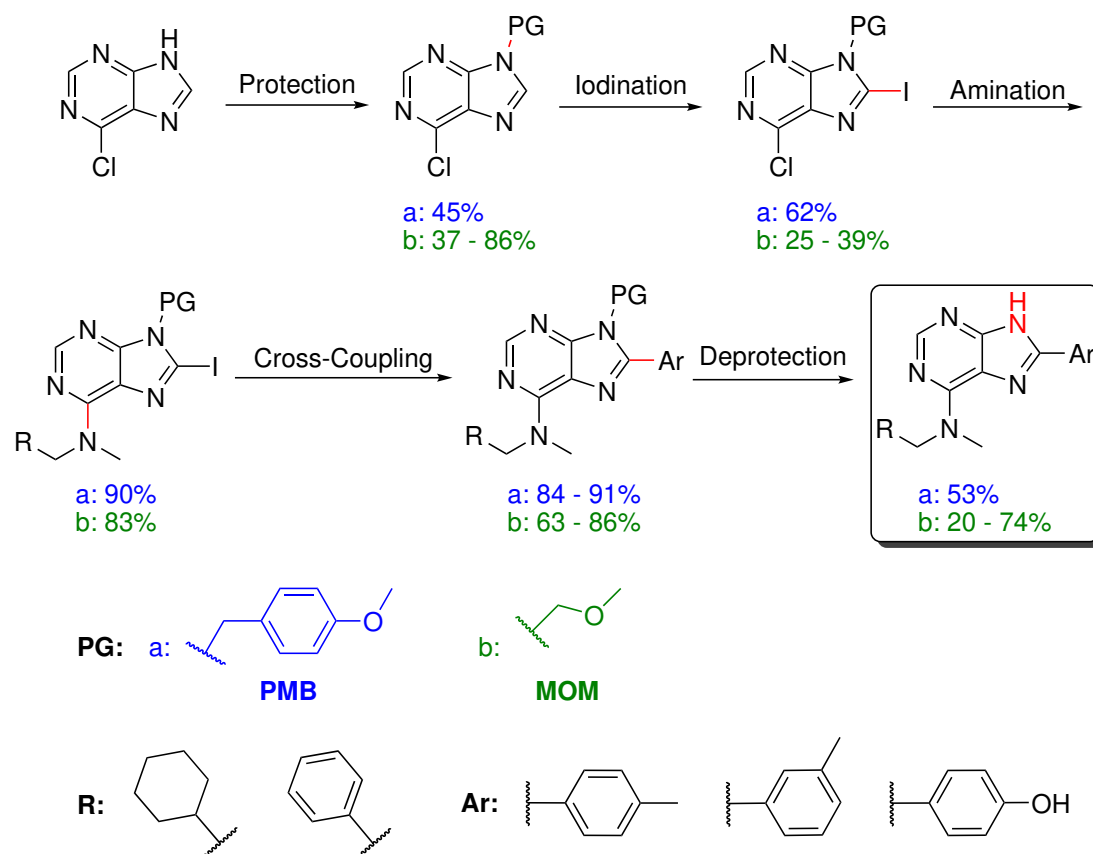
The aliphatic cyclohexane ring in compounds **12**, **17** and **HSB1** gave absorption bands in the 3100 cm^{-1} to 2900 cm^{-1} region. Absorption in the 600 cm^{-1} to 500 cm^{-1} region was seen for compound **10** due to C–I bending vibrations. Broad signals at 3500 cm^{-1} to 3300 cm^{-1} from O–H and N–H stretching vibrations were seen for compounds **17**, **18**, and **HSB1** to **HSB5**.

4 Conclusion and Further Work

4.1 Conclusion

The main purpose of this thesis was to investigate and evaluate the use of *p*-methoxybenzyl (PMB) and methoxymethyl (MOM) as protecting groups in the synthesis of 6-amino-8-arylpurines.

The target compounds were synthesized from 6-chloropurine (**1**) in a five step synthesis, see Scheme 4.1. Utilizing the PMB protecting group, target molecule **HSB2** was isolated in 11% overall yield. The MOM protecting group gave products **HSB4** and **HSB5** in 18% and 4% overall yield, respectively. Loss of material during purification was observed for all reactions purified by silica-gel column chromatography.



Scheme 4.1: Synthetic route towards the target compounds.

The initial step was introduction of a protecting group at the *N*9-position of compound **1**. *N*-Alkylation with PMB-Cl was performed in the pre-master's project and gave a 2:1 mixture of the *N*9 and *N*7 isomers. Compound **2** was isolated in 45% yield.³⁰ MOM alkylation showed complete selectivity towards the *N*9 isomer, and after some optimization a yield of 86% was achieved.

Iodination of the PMB protected analog proceeded without difficulty, and gave compound **4** in 62% yield, corresponding to previously achieved yields.^{27,30} Synthesis of the MOM protected analog was attempted through various metallation reactions. Iodination through *ortho* lithiation proceeded in 37% yield due to by-product formation and difficulties during work-up. Zincation by the synthesized TMPZnCl·LiCl gave a maximum of 70% conversion, and 39% yield. The water sensitive nature of the zinc base made preparation difficult, and is believed to be the main contributing factor to the low conversion and yield. Iodination of compound **3** with TMPZnCl·LiCl has been reported in up to 98% yields,^{57,73} and improved procedures and execution should give better results.

1-Cyclohexyl-*N*-methylethanamine (**6**) was synthesized through reductive amination from cyclohexylcarbaldehyde in 45% yield. The low yield is probably due to the volatility of the compound. Compound **6** and *N*-methyl-1-phenylethanamine were introduced at the C6-position to give compounds **8**, and **10** in 90% and 83% yield, respectively. All aminated purines displayed peak broadening in ¹H NMR due to tautomerism.

Cross-coupling reactions were used to introduce aryl functionalities in the C8-position. Negishi cross-coupling on compound **3** using TMPZnCl·LiCl proved unsuccessful, due to reactive impurities in the zinc base. Suzuki cross-coupling was used to successfully introduce *p*-toluene, *m*-toluene, and *p*-phenol to the iodinated building blocks. Pd(dppf)Cl₂ was used as catalyst and compound **12**, **17**, **15** and **18** were synthesized in 61 - 91% yield. The added polarity from both the MOM- and hydroxyl group gave increased loss of material during work-up and purifica-

tion, which contributed to a mediocre yield of compound **18**.

N-Debenzylation was attempted using catalytic hydrogenation with Pd/C, Pd(OH)₂/C, and a 1:1 mixture of both. No conversion was seen after 24 h at 6 atm H₂ pressure. Transfer hydrogenolysis using formic acid, and acid catalyzed deprotection with TFA and anisole was also unsuccessful. The deprotection was achieved using AlCl₃ and gave target structure **HSB1** in 53% yield. The phenolic derivative **17** partly decomposed during the deprotection, and isolation of compound **HSB3** was not possible.

MOM deprotection was successful using TFA and HCl protocols, and compounds **HSB4** and **HSB5** were isolated in 74% and 20% yield, respectively. Decomposition of **HSB5** during purification is the reason for the low yield. The TFA protocol was only done as a test reaction, but proceeded cleanly at rt. with no need for purification. Removal of the MOM group can be done at milder conditions than *N*-debenzylation, and proceeded in higher yields. With easier deprotection and fully selective *N*-alkylation, the MOM group vastly outperforms PMB in two crucial steps. However, due to the difficulties in the iodination step there was only a difference in overall yield of 7 percentage points. If the literature is to be trusted, the iodination of MOM protected purines can be achieved in high yields with current procedures. Achieving this would place MOM as the definite preferred protecting group for this synthetic route. However, currently the PMB route offers easier execution, for a slight decrease in yield. As long as the desired compound is expected to survive the harsh deprotection conditions, PMB protection might be more efficient.

4.2 Further Work

The mediocre yields in the iodination of the MOM protected analogs is the major bottleneck towards an efficient synthetic route. Iodination was performed through zincation using the method described by Crestey *et al.*,⁵⁷ who reported a 98% yield, in contrast to the 39% achieved in this thesis. Most difficulties were related

to the preparation and quantitative analysis of the zinc base. Further development of methods for high quality preparation of $\text{TMPZnCl}\cdot\text{LiCl}$ should be established. Stathakis *et al.* reported preparation and successful zincation of aromatics with the more air stable zinc base $\text{TMPZnOPic}\cdot\text{LiCl}$.⁹⁶ Higher stability should make it easier to prepare a high quality solution. Previously, the lack of proper quantification methods meant that the amount of zinc base added in the reaction was uncertain. In order to allow study of the iodination reaction under proper conditions, an accurate method of quantification needs to be utilized.

Improved quality of the prepared zinc bases may also allow for successful Negishi cross-coupling reactions. This would shorten the synthetic route by one step, and could greatly improve the overall yield. Further investigations into choice of catalyst, and competing reactions should also be considered. Provided a successful reaction, investigation into the amination at the C6-position with various 8-aryl substituents must be made.

MOM deprotection using TFA as described by Mayrargue *et al.*¹¹³ was only attempted as a test reaction, but showed promising results. The reaction should be scaled-up and investigations into its effect on more labile products like **HSB5** should be made. Improvements to the PMB based route could be achieved by finding milder deprotection conditions. Successful *N*-debenzylation have been reported for both chemical and catalytic hydrogenation, e.g. by using ammonium formate as hydrogen donor,¹²⁵ or Ni, Cu or Pt based catalysts.¹⁰⁷ Further examination of various hydrogenation protocols could prove fruitful.

Loss of material to work-up and purification was seen in all reactions. Alternative purification methods, and work-up procedures should be considered.

5 Experimental

5.1 General Information

The chemicals used were of analytical grade or higher, unless otherwise specified. Accurate concentration of *n*-BuLi was determined by titration with *N*-benzylbenzamide in dry THF as described by Burchat *et al.*⁹⁴ Water used in reactions were filtered and deionized. All reactions were conducted on a teflon coated magnetic stirrer, and an oil bath was used for reactions with a reaction temperature exceeding 20 °C. A Braun MB SPS-800 Solvent Purification System was used to collect dry solvents.

5.1.1 Chromatography

Reactions were monitored using thin layer chromatography (TLC, silica gel on aluminium plates, F254, Merck). Visualization of the plates was done by UV-light at 254 nm and 365 nm, or heat treatment after dipping in a *p*-anisaldehyde solution. Purification of crude products were done using silica-gel column chromatography (40-63 mesh, 60 Å). Eluent systems are specified for each compound.

5.1.2 Spectroscopic Analysis

¹H NMR and ¹³C NMR spectra were recorded using a Bruker Avance III HD instrument. Proton spectra were recorded at 400 or 600 MHz, and carbon spectra on 100 MHz or 150 MHz. Samples were analyzed in either CDCl₃ or DMSO-*d*₆ and are specified for each compound. Chemical shifts are reported in ppm relative to TMS in CDCl₃ (0.00 ppm in ¹H and ¹³C), or solvent peak in DMSO (2.50 ppm in ¹H and 39.52 ppm in ¹³C). Water traces may be observed at 1.56 ppm in CDCl₃ and 3.33 ppm in DMSO-*d*₆. Signals are defined according to multiplicity; s (singlet), d (doublet), t (triplet), pent (pentet), hex (hextet), hept (heptet), br (peak broadening), m (multiplet). Multiplets are defined as intervals, and the coupling constants *J* are given in Hz.

Accurate mass determination in positive and negative mode was performed on a "Synapt G2-S" Q-TOF instrument from Waters TM. Samples were ionized by the use of ASAP probe (APCI) or ESI probe. No chromatographic separation was used previous to the mass analysis. Calculated exact mass and spectra processing was done by Waters TM Software Masslynx V4.1 SCN871.

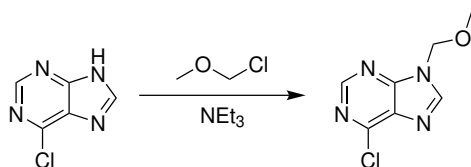
Infrared spectroscopy (IR) was recorded with a Bruker Alpha FT-IR Spectrometer with a Platinum ATR single reflection diamond.

5.1.3 Melting Point

Melting points were determined by using an automatic Stuart SMP40 melting point apparatus.

5.2 Protection

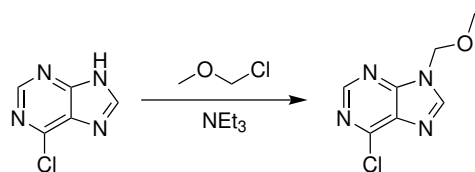
5.2.1 6-Chloro-9-(methoxymethyl)-9H-purine (3) - 150 mg¹²⁶



6-Chloropurine (156 mg, 1 mmol) and K₂CO₃ (210 mg, 1.52 mmol, 1.5 eq) were dissolved in dry DMF (1.5 mL) and stirred for 25 min. Methoxymethyl chloride (0.12 mL, 127 mg, 1.58 mmol, 1.6 eq) technical grade was added dropwise, and the solution stirred at rt for 24 h and 60 °C for another 20 h. The mixture was conc. *in vacuo*, dissolved in H₂O (5 mL) and CH₂Cl₂ (5 mL) and the phases separated. The aqueous phase was extracted with CH₂Cl₂ (10 × 5 mL), and the combined organic phases were washed with brine and dried over Na₂SO₄. Purification by silica-gel column chromatography (EtOAc/n-pentane, 2/1, R_f = 0.22) gave 69.0 mg (0.37 mmol, 37%) of compound **3** as a white solid, mp. 108 - 112 °C (Lit.¹²⁶ 117 °C).

Spectroscopic data for compound **3** (Appendix A): ^1H NMR (400 MHz, CDCl_3) δ : 8.80 (s, 1H), 8.27 (s, 1H), 5.65 (s, 2H), 3.40 (s, 3H); ^{13}C NMR (100 MHz, CDCl_3) δ : 152.6, 145.1, 131.5, 74.6, 57.5; IR (neat, cm^{-1}) ν : 3102 (m), 3069 (m), 2994 (m), 2932 (m), 2826 (m), 1696 (m), 1592 (s), 1560 (s), 1494 (s), 1210 (s), 1027 (s), 938 (s), 916 (s), 752 (s), 672 (s), 471 (m); HRMS (APCI/ASAP+, m/z) detected 199.0386 (calcd. $\text{C}_7\text{H}_8\text{N}_4\text{OCl}$, 199.0387, $[\text{M}+\text{H}]^+$).

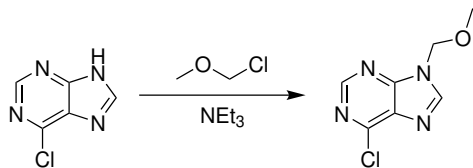
5.2.2 6-Chloro-9-(methoxymethyl)-9H-purine (**3**) - 1 g¹²⁶



6-Chloropurine (1.03 g, 6.69 mmol) was dissolved in dry DMF (10 mL), NEt_3 (1.40 mL, 1.02 g, 10.0 mmol, 1.5 eq) was added dropwise and the solution stirred for 15 min. Methoxymethyl chloride (0.75 mL, 0.80 g, 9.87 mmol, 1.5 eq) technical grade was added dropwise and the solution stirred at 45°C for 22 h. The reaction was quenched with saturated K_2CO_3 solution (40 mL) and extracted with CH_2Cl_2 (7×5 mL). The combined organic phases were washed with brine and dried over Na_2SO_4 and conc. *in vacuo*. Purification by silica-gel column chromatography (EtOAc/n-pentane, 1/2, $R_f = 0.16$), and vacuum distillation at 120°C gave 802 mg (4.35 mmol, 65%) of compound **3** as a white solid, mp. $111 - 115^\circ\text{C}$ (Lit.¹²⁶ 117°C).

Spectroscopic data for compound **3** (Appendix A): ^1H NMR (400 MHz, CDCl_3) δ : 8.79 (s, 1H), 8.26 (s, 1H), 5.64 (s, 2H), 3.40 (s, 3H). ^1H NMR data was in accordance with previously acquired spectra.

5.2.3 6-Chloro-9-(methoxymethyl)-9H-purine (3) - 3 g¹²⁶

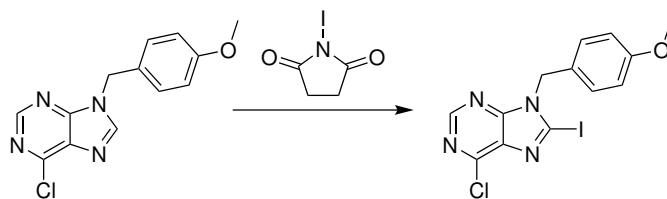


6-Chloropurine (3.03 g, 0.02 mol) was dissolved in dry THF (40 mL) and NEt₃ (4.10 mL, 2.98 g, 0.03 mol, 1.5 eq) added dropwise. The mixture was heated to 40 °C and stirred for 20 min. Methoxymethyl chloride (2.5 mL, 2.65 g, 0.33 mmol, 1.6 eq) was added and the solution stirred for 24.5 h. The mixture was conc. *in vacuo* and dissolved in CH₂Cl₂ (5 mL) and H₂O (5 mL), the phases separated, and the aqueous phase extracted with CH₂Cl₂ (5 × 5 mL). The combined organic phases were washed with brine, dried over Na₂SO₄, and conc. *in vacuo*. Purification by silica-gel column chromatography (EtOAc/n-pentane, 1/1, R_f = 0.14) gave 3.12 g (0.02 mmol, 86%) of compound **3** as a white solid, mp. 112 - 115 °C (Lit.¹²⁶ 117 °C).

Spectroscopic data for compound **3** (Appendix A): ¹H NMR (400 MHz, CDCl₃) δ: 8.79 (s, 1H), 8.26 (s, 1H), 5.64 (s, 2H), 3.40 (s, 3H). ¹H NMR data was in accordance with previously acquired spectra.

5.3 Iodination

5.3.1 6-Chloro-8-iodo-9-(4-methoxybenzyl)-9H-purine (4)²⁷



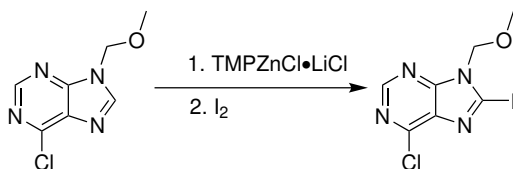
Compound **2** (1.03 g, 3.74 mmol) and NIS (2.46 g, 10.9 mmol, 3 eq) were dissolved in dry THF (40 mL) and stirred at 60 °C for 22 h. The mixture was conc. *in vacuo* and the resulting materials dissolved in CH₂Cl₂ (20 mL) and Na₂S₂O₃ (20 mL,

10%). The aqueous phase was extracted with CH_2Cl_2 (8×10 mL) and the combined organic phases were washed with H_2O (3×10 mL) and brine, dried over Na_2SO_4 and conc. *in vacuo*. Purification by silica-gel column chromatography (EtOAc/n-pentane, 1/3, $R_f = 0.20$) gave 0.93 g (2.32 mmol, 62%) of compound **4** as a white solid, mp. 140 - 144 °C (Lit.²⁷ 106 - 108 °C).

Spectroscopic data for compound **4** (Appendix B): ^1H NMR (400 MHz, CDCl_3) δ : 8.71 (s, 1H), 7.33 (d, $J = 8.8$, 2H), 6.85 (d, $J = 8.8$, 2H), 5.41 (s, 2H), 3.78 (s, 3H). ^1H NMR data was in accordance with previously reported spectra.²⁷

5.3.2 6-Chloro-8-iodo-9-(methoxymethyl)-9H-purine (**5**)

- Zincation 300 mg^{57,73}



TMP (1.00 mL, 0.84 g, 5.93 mmol) was dissolved in dry THF (6 mL) and cooled to -44 °C under an N_2 atmosphere. *n*-BuLi (5.20 mL, 1.4 M, 7.28 mmol, 1.2 eq) was added dropwise. The mixture was allowed to reach -10 °C over 1.5 h. Then, ZnCl_2 (1.22 g, 8.82 mmol, 1.5 eq) dissolved in dry THF (9 mL) was added dropwise. The solution was stirred for 30 min, and allowed to heat to rt. over 30 min, and conc. *in vacuo*. The resulting orange solid was dissolved in dry THF (5 mL) under an N_2 atmosphere.

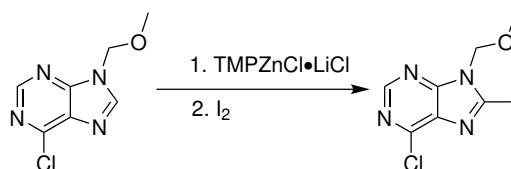
Compound **3** (0.30 g, 1.51 mmol) was dissolved in dry THF (4 mL) and the TMPZnCl·LiCl solution (2.5 mL) was added dropwise at rt, and stirred for 40 min. Then, I_2 (0.81 g, 3.19 mmol, 2 eq) dissolved in dry THF (11 mL) was added dropwise to the reaction mixture. The solution was stirred for 16 h, and quenched with $\text{Na}_2\text{S}_2\text{O}_3$ (20 mL, 10%). The phases were separated and the aqueous phase was extracted with Et_2O (5×10 mL), the combined organic phases were washed with H_2O (2×10 mL) and brine, and dried over Na_2SO_4 . Purification by silica-

gel column chromatography (EtOAc/n-pentane, 1/2, $R_f = 0.20$) gave 0.12 g (0.39 mmol, 25%) of compound **5** as a white solid, mp. 137 - 140 (Lit.⁵⁷ 125 - 127 °C).

Spectroscopic data for compound **5** (Appendix C: ^1H NMR (400 MHz, CDCl_3) δ : 8.71 (s, 1H), 5.61 (s, 2H), 3.42 (s, 3H). ^1H NMR spectra was in accordance with previously reported spectra.⁵⁷

5.3.3 6-Chloro-8-iodo-9-(methoxymethyl)-9H-purine (**5**)

- Zincation 900 mg^{57,73}



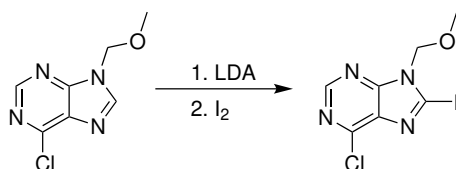
TMP (3.00 mL, 2.51 g, 17.8 mmol) diluted in dry THF (17 mL) was cooled to -44 °C. n-BuLi (15 mL, 1.4 M, 21.0 mmol, 1.2 eq) was added dropwise and stirred for 30 min under an N₂ atmosphere. The solution was allowed to reach -10 °C and stirred for 30 min. ZnCl₂ (2.81 g, 20.6 mmol, 1.2 eq) dried at 140 °C *in vacuo* was weighed out in a glove box and dissolved in dry THF (23 mL). The ZnCl₂ solution was added dropwise to the reaction mixture, and the solution stirred for 30 min, and allowed to reach rt and stirred for another 30 min. The solution was conc. *in vacuo*, dissolved in dry THF (18 mL) and stored under an N₂ atmosphere.

Compound **3** (0.90 g, 4.87 mmol) was dissolved in dry THF (7 mL). TMPZnCl·LiCl (11 mL) was added dropwise and the solution stirred for 30 min at rt. I₂ (1.7 g, 6.70 mmol, 1.4 eq) was dissolved in dry THF (20 mL) and added dropwise to the reaction mixture. The solution was stirred for 1 h under an N₂ atmosphere, and quenched with Na₂S₂O₃ (50 mL, 10%). The phases were separated and the aqueous phase was extracted with CH₂Cl₂ (3 × 10 mL). The combined organic phases were washed with H₂O (10 mL) and brine, dried over Na₂SO₄, and conc.

in vacuo. Purification by silica-gel column chromatography (EtOAc/*n*-pentane, 1/2, $R_f = 0.27$) gave 0.59 (1.89 mmol, 39%) of compound **5** as a white solid, mp. 155 - 157 (Lit.⁵⁷ 125 - 127 °C).

Spectroscopic data for compound **5** (Appendix C): ¹H NMR (400 MHz, CDCl₃) δ : 8.71 (s, 1H), 5.61 (s, 2H), 3.42 (s, 3H). ¹H NMR data was in accordance with previously reported spectra.⁵⁷

5.3.4 6-Chloro-8-iodo-9-(methoxymethyl)-9*H*-purine (**5**) - *Ortho* Lithiation⁶¹

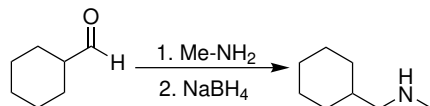


Compound **3** (0.30 g, 1.65 mmol) was dissolved in dry THF (5 mL) and cooled to -78 °C and LDA (2 M, 1.35 mL, 2.70 mmol, 1.6 eq) was added over 30 min, and the solution stirred for 2.5 h. I₂ (0.54 g, 2.12 mmol, 1.3 eq) dissolved in dry THF (5 mL) was added to the reaction mixture over 30 min, and stirred for 1.5 h. The reaction was quenched with saturated NH₄Cl solution (10 mL), and conc. *in vacuo*. Na₂S₂O₄ (15 mL) was added and the aqueous phase was extracted with CH₂Cl₂ (8 × 5 mL). The combined organic phases were washed with brine, dried over Na₂SO₄ and conc. *in vacuo*. Purification by silica-gel column chromatography (Et₂O/*n*-pentane, 1/1, $R_f = 0.15$) gave 0.19 g (0.61 mmol, 37%) of compound **5** as a white solid, mp. 154 - 156 °C (Lit.⁵⁷ 125 - 127 °C).

Spectroscopic data for compound **5** (Appendix C): ¹H NMR (400 MHz, CDCl₃) δ : 8.71 (s, 1H), 5.61 (s, 2H), 3.42 (s, 3H). ¹H NMR data was in accordance with previously reported spectra.⁵⁷

5.4 Amination

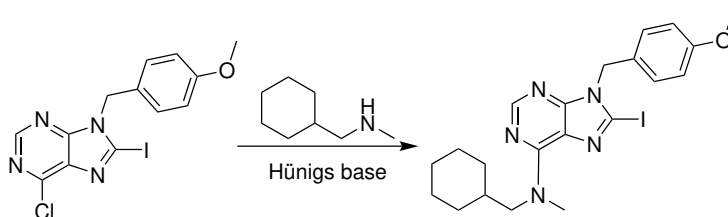
5.4.1 1-Cyclohexyl-*N*-methylethanamine (**6**)⁹⁷



Cyclohexanecarbaldehyde (3.25 mL, 3.01 g, 26.8 mmol) was diluted in dry MeOH (100 mL) and MeNH₂ (2M, 17.0 mL, 34.0 mmol, 1.3 eq) in MeOH was added dropwise. The solution was stirred at rt. for 2.5 h, cooled to 0 °C and NaBH₄ (2.05 g, 0.05 mol, 2 eq) was added. The mixture was stirred for 2.5 h, heated to rt and conc. *in vacuo*. H₂O (20 mL) was added, and conc. HCl was added dropwise until pH 0. The solution was stirred for 1 h and Et₂O (15 mL) was added, the phases separated and the aqueous phase washed with Et₂O (5 × 10 mL). NaOH (5 M) was added dropwise to pH 12, and the aqueous phase was extracted with CH₂Cl₂ (10 × 5 mL). The combined organic phases were washed with brine, dried over Na₂SO₄ and conc. *in vacuo*. This gave 1.55 g (12.2 mmol, 45%) of compound **6** as a clear liquid.

Spectroscopic data for compound **6** (Appendix D: ¹H NMR (400 MHz, DMSO-*d*₆) δ: 3.30 (br, 1H), 2.27 (d, *J* = 6.6, 2H), 2.24 (s, 3H), 1.72 - 1.60 (m, 5H), 1.40 - 1.30 (m, 1H), 1.20 - 1.09 (m, 3H), 0.88 - 0.79 (m, 2H). The ¹H NMR data was in accordance with the data acquired from a commercial sample of compound **6**, see Appendix D.

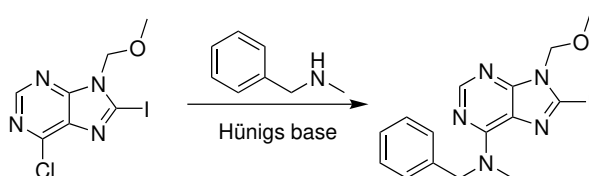
5.4.2 *N*-(Cyclohexylmethyl)-8-iodo-9-(4-methoxybenzyl)-*N*-methyl-9*H*-purin-6-amine (**8**)



Compound **4** (0.85 g, 2.11 mmol) was dissolved in 1,4-dioxane (17 mL). Hünigs base (0.55 mL, 0.42 g, 3.12 mmol, 1.5 eq) and 1-cyclohexyl-*N*-methylethylamine (0.50 mL, 0.42 g, 3.27 mmol, 1.5 eq) were added dropwise. The solution was heated to 60 °C and stirred for 24 h. The reaction mixture was conc. *in vacuo*, dissolved in CH₂Cl₂ (10 mL) and H₂O (10 mL) and the phases separated. The aqueous phase was extracted with CH₂Cl₂ (5 × 5 mL), and the combined organic phases were washed with brine, dried over Na₂SO₄, and conc. *in vacuo*. Purification by silica-gel column chromatography (EtOAc/*n*-pentane, 1/3, R_f = 0.12) gave 0.94 g (1.91 mmol, 90%) of compound **8** as a light yellow solid, mp. 97 - 100 °C.

Spectroscopic data for compound **8** (Appendix E): ¹H NMR: (400 MHz, CDCl₃) δ: 8.27 (s, 1H), 7.29 (d, *J* = 5.72, 2H), 6.83 (d, *J* = 5.76, 2H), 5.28 (s, 2H), 3.77 (s, 3H), 4.20 - 3.20 (br, 5H), 1.82 (br, 1H), 1.72 - 1.65 (m, 5H), 1.25 - 1.16 (m, 4H), 1.05 - 0.99 (m, 2H). ¹H NMR data was in accordance with previously reported spectra.³⁰

5.4.3 *N*-Benzyl-8-iodo-9-(methoxymethyl)-*N*-methyl-9*H*-purin-6-amine (**10**)



Compound **5** (0.50 g, 1.61 mmol) was dissolved in 1,4-dioxane (16 mL), and Hünigs base (0.40 mL, 0.30 g, 2.33 mmol, 1.5 eq) and *N*-methyl-1-phenylethylamine (0.40 mL, 0.38 g, 3.10 mmol, 1.9 eq) were added. The solution was stirred at 60 °C under an N₂ atmosphere for 2 h, and conc. *in vacuo*. The resulting oil was dissolved in CH₂Cl₂ (20 mL) and H₂O (20 mL), and the phases separated. The aqueous phase was extracted with CH₂Cl₂ (5 × 5 mL), and the combined organic phases were washed with brine, dried over Na₂SO₄ and conc. *in vacuo* to give 0.55 g (1.34 mmol, 83%) of compound **10** as an amber solid, mp. 113 - 116 °C.

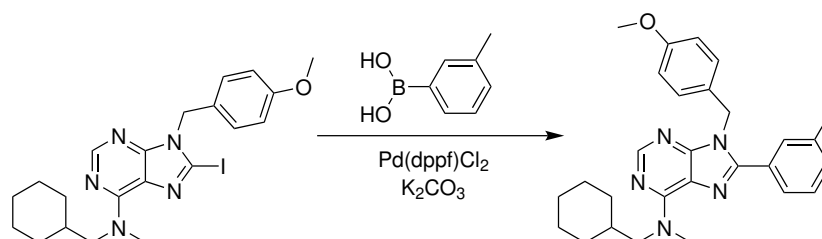
Spectroscopic data for compound **10** (Appendix G: ^1H NMR (600 MHz, CDCl_3) δ : 8.31 (s, 1H), 7.33 - 7.30 (m, 2H), 7.29 - 7.27 (m, 2H), 7.27 - 7.26 (m, 1H), 5.76 - 4.81 (br, 2H), 5.50 (s, 2H), 3.92 - 2.97 (br, 3H), 3.41 (s, 3H); ^{13}C NMR (150 MHz, CDCl_3) δ : 153.6, 153.0, 137.6, 128.6 (2C), 127.7 (2C), 127.4, 122.5, 96.5, 75.3, 67.1, 57.2; IR (neat, cm^{-1}): ν : 3053 (w), 2983 (w), 2305 (w), 1726 (w), 1591 (s), 1510 (m), 1212 (s), 1107 (m), 1053 (m), 704 (s), 614 (s); HRMS (APCI/ASAP +, m/z) detected 410.0479 (calcd. 410.0478, $\text{C}_{15}\text{H}_{17}\text{N}_5\text{OI}$, $[\text{M}+\text{H}]^+$).

5.5 Suzuki Cross-Coupling

5.5.1 General procedure

A mixture of compound **8** or **9**, arylboronic acid (1.2 eq), $\text{Pd}(\text{dppf})\text{Cl}_2$ (5 mol%), K_2CO_3 (3 eq) were dissolved in 1,4-dioxane/ H_2O . The reaction mixture was stirred at 80 °C under an N_2 atmosphere for 30 min. Solvents were removed and residues extracted with CH_2Cl_2 (3 - 5 mL). The combined organic phases were washed with brine, dried over Na_2SO_4 , filtered and conc. *in vacuo*. Purification was performed as described for each compound. Solvents were degassed with a subsurface nitrogen sparge in an ultrasound bath for minimum 30 min prior to use.

5.5.2 *N*-(Cyclohexylmethyl)-9-(4-methoxybenzyl)-*N*-methyl-8-(*m*-tolyl)-9*H*-purin-6-amine (**12**)

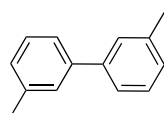


According to the general procedure in section 5.5.1 compound **12** was obtained from compound **8** (509 mg, 1.04 mmol), *m*-tolylboronic acid (170 mg, 1.26 mmol, 1.2 eq), K_2CO_3 (431 mg, 3.12 mmol, 3 eq) and $\text{Pd}(\text{dppf})\text{Cl}_2$ (39.7 mg, 0.05 mmol, 0.05 eq) dissolved in 1,4-dioxane/ H_2O (3 mL, 2:1). Full conversion was achieved after 30 min. Purification by silica-gel column chromatography (EtOAc/n -pentane,

1/4, $R_f = 0.14$) gave 397 mg (0.87 mmol, 84%) of compound **12** as a white wax.

Spectroscopic data for compound **12** (Appendix H): ^1H NMR (400 MHz, CDCl_3) δ : 8.38 (s, 1H), 7.44 (s, 1H), 7.39 (d, $J = 7.3$, 1H) 7.31 (t, $J = 7.5$, 1H), 7.27 (dⁱ, 1H), 7.04 (d, $J = 8.6$, 2H), 6.80 (d, $J = 8.7$, 2H), 5.39 (s, 2H), 4.19 - 3.29 (br, 5H), 3.77 (s, 3H), 2.36 (s, 3H), 1.93 - 1.88 (m, 1H), 1.78 - 1.66 (m, 4H), 1.28 - 1.17 (m, 4H), 1.14 - 1.04 (m, 2H); ^{13}C NMR (100 MHz, CDCl_3) δ : 159.0, 152.4, 130.0, 128.1, 55.3, 30.9, 26.0; IR (neat, cm^{-1}) ν : 2921 (w), 2849 (w), 1610 (s), 1583 (m), 1559 (m), 1511 (m), 1447 (m), 1422 (w), 1406 (w), 1328 (m), 1298 (m), 1246 (s), 1034 (m), 792 (m), 718 (m), 699 (m), 681 (m), 569 (w); HRMS (APCI/ASAP+, m/z) detected 456.2758 (calcd. $\text{C}_{28}\text{H}_{34}\text{N}_5\text{O}$, 456.2763, $[\text{M}+\text{H}]^+$).

5.5.3 3,3'-Dimethyl-1,1'-biphenyl (**13**)

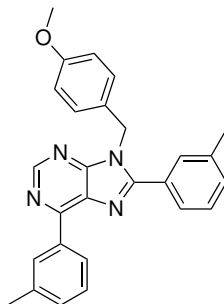


Compound **13** was isolated in semi-pure form (10 mg) as the minor product in the reaction described in section 5.5.5.

Spectroscopic data for compound **13** (Appendix H): ^1H NMR (400 MHz, CDCl_3) δ : 7.40 (s, 2H), 7.38 (d, $J = 8$, 2H), 7.32 (t, $J = 7.4$, 2H), 7.16 (d, $J = 7.36$, 2H), 2.42 (s, 6H). ^1H NMR data was in accordance with previously reported spectra.¹²⁷

ⁱOverlaps with solvent signal.

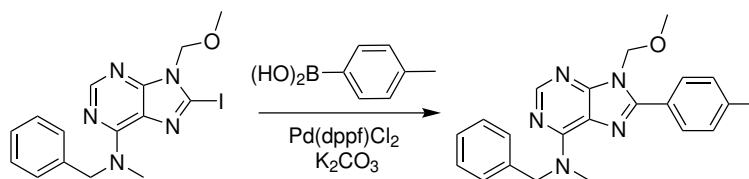
5.5.4 9-(4-Methoxybenzyl)-6,8-di-*m*-tolyl-9*H*-purine (**14**)



Compound **14** was isolated in semi-pure form (8.6 mg) as the minor product in the reaction described in section 5.5.5.

Spectroscopic data for compound **14** (Appendix H): ^1H NMR (400 MHz, CDCl_3) δ : 9.07 (s, 1H), 8.79 (d, $J = 7.8$, 1H), 8.64 (s, 1H), 7.58 (s, 1H), 7.54 - 7.35 (m, 6H), 7.08 (d, $J = 8.8$, 2H), 6.84 (d, $J = 8.7$, 2H), 5.54 (s, 2H), 3.79 (s, 3H), 2.52 (s, 2H), 2.44 (s, 3H); HRMS (APCI/ASAP+, m/z) detected 421.2028 (calcd. $\text{C}_{27}\text{H}_{25}\text{N}_4\text{O}$, 421.2028, $[\text{M}+\text{H}]^+$).

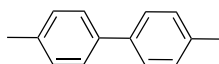
5.5.5 *N*-Benzyl-9-(methoxymethyl)-*N*-methyl-8-(*p*-tolyl)-9*H*-purin-6-amine (**15**)



Following the general procedure in section 5.5.1 compound **15** was obtained from compound **10** (99.5 mg, 0.24 mmol), *p*-tolylboronic acid (41.8 mg, 0.31 mmol, 1.3 eq), K_2CO_3 (102 mg, 0.74 mmol, 3 eq) and $\text{Pd}(\text{dppf})\text{Cl}_2$ (9.8 mg, 0.01 mmol, 0.04 eq) dissolved in 1,4-dioxane/ H_2O (2 mL, 1:1). Full conversion was achieved after 30 min. Purification by silica-gel plug filtration (CH_2Cl_2 , $R_f = 0$, EtOAc, $R_f = 0.57$) gave 78.5 mg (0.21 mmol, 86%) of compound **15** as a burgundy solid, mp. 82 - 84°C.

Spectroscopic data for compound **15** (Appendix I): ^1H NMR (400 MHz, CDCl_3) δ : 8.41 (s, 1H), 7.88 (d, $J = 8.2$, 2H), 7.33 - 7.27 (m, 7H), 5.62 - 5.22 (br, 2H), 5.55 (s, 2H), 3.62 - 3.26 (br, 3H), 3.56 (s, 3H), 2.42 (s, 2H); ^{13}C NMR (100 MHz, CDCl_3) δ : 154.6, 152.5, 153.3, 149.8, 140.2, 138.5, 129.5 (2C), 129.2 (2C), 128.5 (2C), 127.8 (2C), 127.2 (2C), 119.5, 73.2, 57.1, 30.9, 21.5; IR (neat, cm^{-1}) ν : 3002 (w), 2920 (w), 2863 (w), 1587 (s), 1560 (s), 1511 (m), 1478 (m), 1209 (m), 1155 (m), 1036 (m), 1020 (m), 955 (m), 875 (s), 725 (m), 703 (m), 677 (m), 654 (m), 572 (m), 531 (m), 513 (w), 499 (m), 474 (w); HRMS (APCI/ASAP+, m/z) detected 374.1977 (calcd. $\text{C}_{22}\text{H}_{24}\text{N}_5\text{O}$, 374.1981, $[\text{M}+\text{H}]^+$).

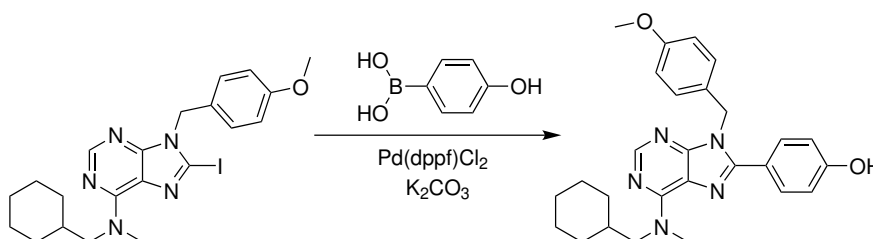
5.5.6 4,4'-Dimethyl-1,1'-biphenyl (**16**)



Compound **16** was isolated in semi-pure form (2.6 mg) as the minor product in the reaction described in section 5.5.5.

Spectroscopic data for compound **16** (Appendix I): ^1H NMR (400 MHz, CDCl_3) δ : 7.47 (d, $J = 8.1$, 4H), 7.23 (d, $J = 8.5$, 4H), 2.39 (s, 6H). ^1H NMR data was in accordance with previously reported spectra.¹²⁷

5.5.7 4-(6-((Cyclohexylmethyl)(methyl)amino)-9-(4-methoxybenzyl)-9H-purin-8-yl)phenol (**17**)

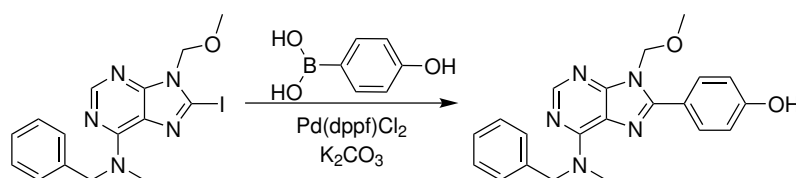


According to the general procedure in section 5.5.1 compound **17** was obtained from compound **8** (198 mg, 0.40 mmol), (4-hydroxyphenyl)boronic acid (67.7 mg, 0.49 mmol, 1.2 eq), K_2CO_3 (197 mg, 1.43 mmol, 3 eq) and $\text{Pd}(\text{dppf})\text{Cl}_2$ (39.7 mg,

0.05 mmol, 0.05 eq) dissolved in 1,4-dioxane/H₂O (3 mL, 2:1). Full conversion was achieved after 30 min. Purification by silica-gel plug filtration (CH₂Cl₂, R_f = 0.00, 5% MeOH/CH₂Cl₂, R_f = 0.68) gave 168 mg (0.37 mmol, 91%) of compound **17** as a beige solid, mp. 168 - 172 °C.

Spectroscopic data for compound **17** (Appendix J): ¹H NMR (400 MHz, CDCl₃) δ: 8.36 (s, 1H), 7.49 (d, *J* = 8.6, 2H), 7.01 (d, *J* = 8.6, 2H), 6.86 (d, *J* = 8.6, 2H), 6.79 (d, *J* = 8.7, 2H), 6.01 (br, 1H) 5.39 (s, 2H), 4.27 - 3.17 (br, 5H), 3.75 (s, 3H), 1.93 - 1.85 (m, 1H), 1.75 - 1.59 (m, 4H), 1.28 - 1.05 (m, 6H); ¹³C NMR (100 MHz, CDCl₃) δ: 159.0, 152.1, 130.7 (2C), 129.0, 127.9 (2C), 122.6, 119.7, 115.7 (2C), 114.2 (2C), 55.3, 46.3, 30.7 (2C), 26.6 (2C), 26.0; IR (neat, cm⁻¹) ν: 3002 (m), 2921 (s), 2848 (s), 2670 (m), 2596 (m), 1586 (s), 1562 (s), 1538 (s), 1391 (s), 1362 (s), 1277 (s), 1033 (s), 909 (s), 897 (s), 837 (m), 631 (s), 524 (m), 510 (m), 463 (w), 443 (w); HRMS (APCI/ASAP+, *m/z*) detected 458.2548 (calcd. C₂₇H₃₂N₅O₂, 458.2556, [M+H]⁺).

5.5.8 4-(6-(Benzyl(methyl)amino)-9-(methoxymethyl)-9*H*-purin-8-yl)phenol (**18**)



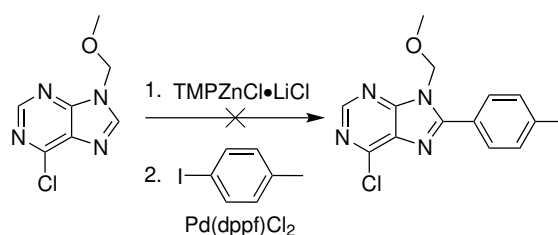
Following the general procedure in section 5.5.1 compound **18** was obtained from compound **10** (203 mg, 0.50 mmol), (4-hydroxyphenyl)boronic acid (83.9 mg, 0.61 mmol, 1.2 eq), K₂CO₃ (230 mg, 1.66 mmol, 3 eq) and Pd(dppf)Cl₂ (18.4 mg, 0.03 mmol, 0.05 eq) dissolved in 1,4-dioxane/H₂O (3 mL, 2:1). Full conversion was achieved after 30 min. Purification by silica-gel plug filtration (CH₂Cl₂, R_f = 0.00, 5% MeOH/CH₂Cl₂, R_f = 0.59) gave 114 mg (0.31 mmol, 61%) of compound **18** as a beige solid, mp. 169 - 173 °C.

Spectroscopic data for compound **18** (Appendix K): ¹H NMR (400 MHz, DMSO-

d_6) δ : 10.01 (s, 1H), 8.31 (s, 1H), 7.78 (d, $J = 8.6$, 2H), 7.33 - 7.26 (m, 5H), 6.92 (d, $J = 8.7$, 2H), 5.76 - 4.96 (br, 2H), 5.50 (s, 2H), 3.74 - 2.92 (br, 3H), 3.42 (s, 3H); ^{13}C NMR (100 MHz, DMSO- d_6) δ : 159.8, 154.1, 153.3, 152.4, 149.9, 138.6, 130.9 (2C), 129.0 (2C), 127.9 (2C), 127.6, 120.4, 118.9, 116.1 (2C), 73.6, 57.1; IR (neat, cm^{-1}) ν : 3195 (m), 2998 (m), 2984 (m), 2924 (m), 2826 (m), 1613 (s), 1583 (s), 1485 (s), 1250 (s), 1206, 1172 (s), 1141 (s), 955 (s), 919 (s), 792 (s), 680 (s), 630 (s), 578 (m), 514 (m), 478 (m), 431 (m); HRMS (APCI/ASAP+, m/z) detected 376.1769 (calcd. $\text{C}_{21}\text{H}_{22}\text{N}_5\text{O}_2$, 376.1773, $[\text{M}+\text{H}]^+$).

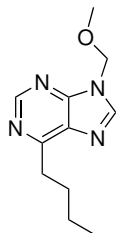
5.6 Negishi Cross-Coupling

5.6.1 6-Chloro-9-(methoxymethyl)-8-(*p*-tolyl)-9*H*-purine (**19**)⁵⁷



Compound **3** (95.4 mg, 0.52 mmol) and Pd(dppf)Cl₂ (18.9 mg, 0.03 mmol, 0.05 eq) was dissolved in dry THF (1 mL) under an N₂ atmosphere. TMPZnCl·LiCl (1.6 mL) was added dropwise and the solution stirred 1.75 h. Then, 4-iodotoluene (186 mg, 0.85 mmol, 1.6 eq) dissolved in dry THF (2 mL) was added, and the reaction mixture stirred for 1 h. The reaction was quenched with sat. NH₄Cl solution (5 mL), and the phases separated. The aqueous phase was extracted with CH₂Cl₂ (3 × 5 mL), and the combined organic phases were washed with H₂O (5 mL) and brine, filtered, dried over Na₂SO₄ and conc. *in vacuo*. ^1H NMR showed no formation of compound **19**.

5.6.2 6-Butyl-9-(methoxymethyl)-9H-purine (20)

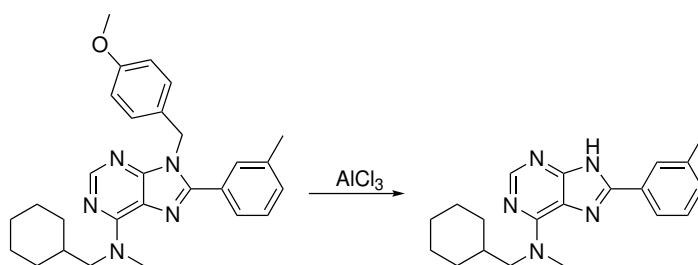


Purification of the crude from section 5.6.1 by silica-gel column chromatography (EtOAc/*n*-pentane, 5/1, $R_f = 0.16$), gave compound **20** (150 mg) in semi-pure form.

Spectroscopic analysis of compound **20** (Appendix L): ^1H NMR (400 MHz, CDCl_3) δ : 8.92 (s, 1H), 8.16 (s, 1H), 5.62 (s, 2H), 3.40 (s, 3H), 3.22 (t, $J = 7.8$, 2H), 1.93 - 1.84 (m, 2H), 1.46 (hex, $J = 7.4$, 2H), 0.97 (t, $J = 7.3$, 3H); ^{13}C NMR (100 MHz, CDCl_3) δ : 153.0, 143.6, 74.1, 57.3, 33.1, 30.7, 22.8, 13.9; HRMS (APCI/ASAP+, m/z) detected 221.1400 (calcd. $\text{C}_{11}\text{H}_{17}\text{N}_4\text{O}$, 221.1402, $[\text{M}+\text{H}]^+$).

5.7 Deprotection

5.7.1 *N*-(Cyclohexylmethyl)-*N*-methyl-8-(*m*-tolyl)-9H-purin-6-amine (HSB2)⁶⁸

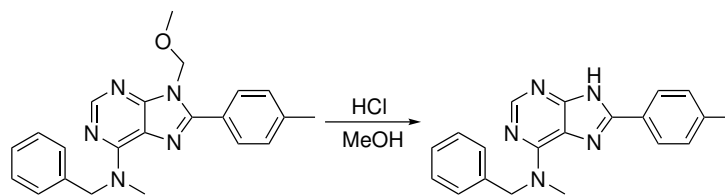


Compound **12** (26.8 mg, 0.06 mmol) was dissolved in 1,2-dichlorobenzene (3 mL) and AlCl_3 (67.8 mg, 0.51 mmol, 8.0 eq) was added, and the solution was stirred at 160 °C for 2.5 h. The reaction mixture was then cooled to rt, and ice water (2 mL) added. The aqueous phase was extracted with CH_2Cl_2 (5×5 mL). The combined organic phases were washed with brine, dried over anhydrous Na_2SO_4 , filtered and conc. *in vacuo*. Purification by silica-gel plug filtration (CH_2Cl_2 , $R_f = 0.00$, 5%

MeOH/CH₂Cl₂, R_f = 0.40) gave 10.5 mg (0.03 mmol, 53%) of compound **HSB2** as a light grey solid. Not enough material for accurate mp. determination.

Spectroscopic data for compound **HSB2** (Appendix M): ¹H NMR (600 MHz, DMSO-*d*₆) δ: 13.37 (br, 1H), 8.23 (s, 1H), 7.99 (s, 1H), 7.92 (d, *J* = 7.7, 1H), 7.42 (t, *J* = 7.6, 1H), 7.31 (d, *J* = 7.1, 1H), 3.75 - 2.64 (br, 5H), 2.40 (s, 3H), 1.95 - 1.82 (m, 1H), 1.73 - 1.57 (m, 4H), 1.32 - 0.99 (m, 6H); ¹³C NMR (150 MHz, DMSO-*d*₆) δ: 152.7, 141.7, 138.6, 130.9, 130.2, 129.3, 127.2, 123.8, 27.5, 26.6, 25.8, 21.5; IR (neat, cm⁻¹) ν: 3368 (m), 2921 (m), 2851 (m), 1676 (s), 1590 (s), 1541 (s), 1466 (s), 1196 (s), 1142 (s), 850 (s), 801 (s), 688 (m), 668 (m), 519 (m), 468 (m), 445 (m); HRMS (APCI/ASAP+, *m/z*) detected 336.2186 (calcd. C₂₀H₂₆N₅, 336.2188, [M+H]⁺).

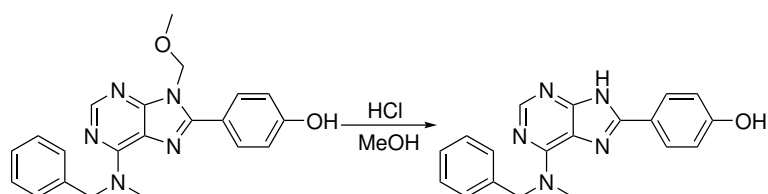
5.7.2 *N*-Benzyl-*N*-methyl-8-(*p*-tolyl)-9*H*-purin-6-amine (**HSB4**)¹¹⁹



Compound **15** (19.0 mg, 0.05 mmol) was dissolved in MeOH (4 mL) and conc. HCl (0.4 mL) and stirred at 60 °C. Full conversion was obtained after 3 h. The mixture was quenched with NaHCO₃ and conc. *in vacuo*. The residue was dissolved in H₂O (3 mL) and CH₂Cl₂ (3 mL). Then, the phases were separated and the aqueous phase extracted with CH₂Cl₂ (5×3 mL). The combined organic phases were washed with brine and dried over Na₂SO₄, and conc. *in vacuo*. Purification by silica-gel column chromatography (2.5% MeOH/CH₂Cl₂, R_f = 0.14) gave 12.33 mg (0.04 mmol, 74%) of compound **HSB4** as a beige solid. Not enough material for accurate mp. determination.

Spectroscopy data for compound **HSB4** (Appendix N): ^1H NMR (600 MHz, CDCl_3) δ : 14.41 (br, 1H), 8.48 (s, 1H), 8.05 (d, $J = 8.0$, 2H), 7.38 - 7.27 (m, 7H), 5.88 - 4.99 (br, 2H), 4.14 - 3.10 (br, 3H), 2.43 (s, 3H); ^{13}C NMR (150 MHz, CDCl_3) δ : 154.5, 152.5, 151.2, 148.4, 140.2, 129.7, 128.6, 127.9, 127.3, 126.4, 121.1, 21.5; IR (neat, cm^{-1}) ν : 3063 (w), 3028 (w), 2924 (m), 2853 (m), 2719 (w), 1734 (w), 1591 (s), 1537 (m), 1514 (m), 1495 (m), 1091 (m), 1027 (m), 932 (m), 912, 884 (m), 755 (m), 698 (m), 647 (m), 635 (w), 570 (w), 503 (w); HRMS (APCI/ASAP+, m/z) detected 330.1715 (calcd. $\text{C}_{20}\text{H}_{20}\text{N}_5$, 330.1719, $[\text{M}+\text{H}]^+$).

5.7.3 4-(6-(Benzyl(methyl)amino)-9H-purin-8-yl)phenol (**HSB5**)¹¹⁹



Compound **18** (40.3 mg, 0.11 mmol) was dissolved in MeOH (5 mL) and conc. HCl (0.5 mL) and stirred at 60 °C. Full conversion was achieved after 3 h. Mixture was quenched with NH_3 and conc. *in vacuo*. Purification by silica-gel column chromatography (2.5% MeOH/ CH_2Cl_2 , $R_f = 0.12$) gave 7.1 mg (0.02 mmol, 20%) of compound **HSB5** as a beige solid. Not enough material for accurate mp. determination.

Spectroscopy data for compound **HSB5** (Appendix O): ^1H NMR (400 MHz, $\text{DMSO}-d_6$) δ : 13.33 (s, 1H), 10.00 (s, 1H), 8.27 (s, 1H), 8.00 (d, $J = 8.7$, 2H), 7.41 - 7.29 (m, 5H), 6.93 (d, $J = 8.7$, 2H), 5.72 - 5.26 (br, 2H), 3.82 - 3.00 (br, 3H); ^{13}C NMR (100 MHz, $\text{DMSO}-d_6$) δ : 159.6, 153.8, 151.9, 148.1, 138.8, 129.0 (2C), 128.3 (2C), 127.9 (2C), 127.5, 121.0, 120.2, 116.1 (2C); IR (neat, cm^{-1}) ν : 3085 (m), 2850 (m), 1595 (s), 1537 (s), 1486 (s), 1407 (s), 1157 (s), 951 (s), 896 (s), 725 (s), 676 (s), 619 (m), 566 (m), 456 (m); HRMS (APCI/ASAP+, m/z) detected 332.1508 (calcd. $\text{C}_{19}\text{H}_{18}\text{N}_5\text{O}$, 332.1511, $[\text{M}+\text{H}]^+$).

References

1. Popat, K.; McQueen, K.; Feeley, T. The global burden of cancer. *Best Pract. Res. Clin. Anaesthesiol.* **2013**, *27*, 399–408.
2. Cheetham, G. M. Novel protein kinases and molecular mechanisms of autophosphorylation. *Curr. Opin. Struct. Biol.* **2004**, *14*, 700–705.
3. Kondapalli, L.; Soltani, K.; Lacouture, M. E. The promise of molecular targeted therapies: Protein kinase inhibitors in the treatment of cutaneous malignancies. *J. Am. Acad. Dermatol.* **2005**, *53*, 291–302.
4. Deininger, M. W. N.; Goldman, J. M.; Melo, J. V. The molecular biology of chronic myeloid leukemia. *Blood* **2000**, *96*, 3343–3356.
5. Cohen, P. Protein kinases – the major drug targets of the twenty-first century? *Nat. Rev. Drug Discov.* **2002**, *1*, 309–315.
6. El-Gamal, M. I.; Anbar, H. S.; Yoo, K. H.; Oh, C. FMS kinase inhibitors: current status and future prospects. *Med. Res. Rev.* **2013**, *33*, 599–636.
7. Roesch, S.; Rapp, C.; Dettling, S.; Herold-Mende, C. When immune cells turn bad—tumor-associated microglia/macrophages in glioma. *Int. J. Mol. Sci.* **2018**, *19*, 1–20.
8. Chen, X.; Liu, H.; Focia, P. J.; Shim, A. H.-R.; He, X. Structure of macrophage colony stimulating factor bound to FMS: Diverse signaling assemblies of class III receptor tyrosine kinases. *Proc. Natl. Acad. Sci. USA* **2009**, *105*, 18267 – 18272.
9. Stanley, E. R.; Chitu, V. CSF-1 receptor signaling in myeloid cells. *Cold. Spring Harb. Perspect. Biol.* **2014**, *6*, 1–21.
10. Avendano, J. C., Carmen ; Menendez *Medicinal chemistry of anticancer drugs*, 2nd ed.; Elsevier Science, 2015; pp 392 – 402.
11. Blagden, S.; de Bono, J. Drugging cell cycle kinases in cancer therapy. *Curr. Drug Targets* **2005**, *6*, 325–335.

12. Hume, D.; Macdonald, K. Therapeutic applications of macrophage colony-stimulating factor-1 (CSF-1) and antagonists of CSF-1 receptor (CSF-1R) signaling. *Blood* **2012**, *119*, 1810–1820.
13. Xu, J.; Escamilla, J.; Mok, S.; David, J.; Priceman, S.; West, B.; Bollag, G.; McBride, W.; Wu, L. CSF1R signaling blockade stanches tumor-infiltrating myeloid cells and improves the efficacy of radiotherapy in prostate cancer. *Cancer Res.* **2013**, *73*, 2782–2794.
14. Müller, A.; Strauss, L.; Greter, M.; Gast, H.; Recher, M.; Becher, B.; Fontana, A. Neutralization of colony-stimulating factor 1 receptor prevents sickness behavior syndrome by reprogramming inflammatory monocytes to produce IL-10. *Brain Behav. Immun.* **2015**, *48*, 78–85.
15. Gómez-Nicola, D.; Fransen, N. L.; Suzzi, S.; Perry, V. H. Regulation of microglial proliferation during chronic neurodegeneration. *J. Neurosci.* **2013**, *33*, 2481–2493.
16. Cannarile, M. A.; Weisser, M.; Jacob, W.; Jegg, A.-M.; Ries, C. H.; Rüttinger, D. Colony-stimulating factor 1 receptor (CSF1R) inhibitors in cancer therapy. *J. Immunother. Cancer* **2017**, *5*, 1–13.
17. Conway, J. G. et al. Inhibition of colony-stimulating-factor-1 signaling in vivo with the orally bioavailable cFMS kinase inhibitor GW2580. *Proc. Natl. Acad. Sci. U.S.A.* **2005**, *102*, 16078–16083.
18. Ohno, H.; Kubo, K.; Murooka, H.; Kobayashi, Y.; Nishitoba, T.; Shibuya, M.; Yoneda, T.; Isoe, T. A c-fms tyrosine kinase inhibitor, Ki20227, suppresses osteoclast differentiation and osteolytic bone destruction in a bone metastasis model. *Mol. Cancer Ther.* **2006**, *5*, 2634–2643.
19. Lee, H. J.; Seo, A. N.; Kim, E. J.; Jang, M. H.; Kim, Y. J.; Kim, J. H.; Kim, S.-W.; Ryu, H. S.; Park, I. A.; Im, S.-A.; Gong, G.; Jung, K. H.; Kim, H. J.; Park, S. Y. Prognostic and predictive values of EGFR overexpression and EGFR copy number alteration in HER2-positive breast cancer. *Br. J. Cancer* **2014**, *112*, 103–111.

20. Cook, N.; Frese, K.; Moore, M. Assessing the role of the EGF receptor in the development and progression of pancreatic cancer. *Gastrointest. Cancer* **2014**, *2014*, 23–37.
21. Siwak, D. R.; Carey, M.; Hennessy, B. T.; Nguyen, C. T.; Murray, M. J. M.; Nolden, L.; Mills, G. B. Targeting the Epidermal Growth Factor Receptor in Epithelial Ovarian Cancer: Current Knowledge and Future Challenges. *J. Oncol.* **2010**, *2010*, 1–21.
22. Red Brewer, M.; Yun, C.-H.; Lai, D.; Lemmon, M. A.; Eck, M. J.; Pao, W. Mechanism for activation of mutated epidermal growth factor receptors in lung cancer. *Proc. Natl. Acad. Sci.* **2013**, *110*, E3595–E3604.
23. Pao, W.; Chmielecki, J. Rational, biologically based treatment of EGFR-mutant non-small-cell lung cancer. *Nat. Rev. Cancer* **2010**, *10*, 760.
24. Bugge, S.; Buene, A. F.; Jurisch-Yaksi, N.; Moen, I. U.; Skjønsvjell, E. M.; Sundby, E.; Hoff, B. H. Extended structure-activity study of thienopyrimidine-based EGFR inhibitors with evaluation of drug-like properties. *Eur. J. Med. Chem.* **2016**, *107*, 255–274.
25. Han, J.; Kaspersen, S. J.; Nervik, S.; Nørsett, K. G.; Sundby, E.; Hoff, B. H. Chiral 6-aryl-furo[2,3-d]pyrimidin-4-amines as EGFR inhibitors. *Eur. J. Med. Chem.* **2016**, *119*, 278–299.
26. Sundby, E.; Han, J.; Kaspersen, S. J.; Hoff, B. H. In vitro baselining of new pyrrolopyrimidine EGFR-TK inhibitors with Erlotinib. *Eur. J. Pharm. Sci.* **2015**, *80*, 56–65.
27. Skinderhaug, J. K. Synthetic strategies towards substituted purines and their CSF1R activity. M.Sc. thesis, Norwegian University of Science and Technology, 2018.
28. Manolikakes, G.; Muñoz Hernandez, C.; Schade, M. A.; Metzger, A.; Knochel, P. Palladium- and nickel-catalyzed cross-couplings of unsaturated halides bearing relatively acidic protons with organozinc reagents. *J. Org. Chem.* **2008**, *73*, 8422–8436.

29. Manolikakes, G.; Schade, M. A.; Hernandez, C. M.; Mayr, H.; Knochel, P. Negishi cross-couplings of unsaturated halides bearing relatively acidic hydrogen atoms with organozinc reagents. *Org. Lett.* **2008**, *10*, 2765–2768.
30. Bygdås, H. S. Evaluation of protective groups for purines in synthesis of CSF1R inhibitors. 2018; Pre-Master's project; Norwegian University of Science and Technology.
31. Blackburn, G. M. *Nucleic Acids in Chemistry and Biology*, 3rd ed.; Royal Society Of Chemistry, 2006; pp 14–19.
32. Joule, J. A. *Heterocyclic Chemistry*, 5th ed.; Wiley: Chichester, 2010; pp 515–539, 629–649.
33. Robak, T.; Lech-Maranda, E.; Korycka, A.; Robak, E. Purine nucleoside analogs as immunosuppressive and antineoplastic agents: Mechanism of action and, clinical activity. *Curr. Med. Chem.* **2006**, *13*, 3165–3189.
34. Celik, G. D.; Disli, A.; Oner, Y.; Acik, L. Synthesis of some novel amino and thiotetrazole purine derivatives and investigation of their antimicrobial activity and DNA interactions. *Med. Chem. Res.* **2013**, *22*, 1470–1479.
35. Hu, Y. L.; Ge, Q.; Lu, M.; Lu, H. F. Synthesis and biological activities of O 6 -alkylguanine derivatives. *B. Chem. Soc. Ethiopia.* **2010**, *24*, 425–432.
36. Rida, S. M.; Ashour, F. A.; El-Hawash, S. A. M.; El-Semary, M. M.; Badr, M. H. Synthesis of some novel substituted purine derivatives as potential anticancer, anti-HIV-1 and antimicrobial agents. *Arch. Pharm.* **2007**, *340*, 185–194.
37. Mitra, S.; Kaina, B. In *Regulation of repair of alkylation damage in mammalian genomes*; Cohn, W. E., Moldave, K., Eds.; Progress in Nucleic Acid Research and Molecular Biology; Academic Press, 1993; Vol. 44; pp 109–142.
38. Morimoto, K.; Dolan, M. E.; Scicchitano, D.; Pegg, A. E. Repair of O 6 -propylguanine and O 6 -butylguanine in DNA by O 6 -alkylguanine-DNA

- alkyltransferases from rat liver and *E. coli*. *Carcinogenesis* **1985**, *6*, 1027–1031.
39. Carmo, A. M. L.; Braga, F. G.; Paula, M. L. D.; Ferreira, A. P.; Teixeira, H. C.; da Silva, A. D.; Coimbra, E. S. Synthesis and biological activity of new tricyclic purine derivatives obtained by intramolecular N-7 alkylation. *Lett. Drug. Des. Discov.* **2008**, *5*, 122–126.
40. Moss, G. P.; Smith, P. A. S.; Tavernier, D. Glossary of class names of organic compounds and reactive intermediates based on structure. *Pure Appl. Chem.* **1995**, *Vol. 67*, 1307–1375.
41. Lister, J. H.; Lawley, P. D.; Jones, R. L.; Brown, D. J. In *Fused Pyrimidines*; Brown, D. J., Ed.; Interscience, 1971; Vol. 2; pp 10–13, 31–33, 117–132, 158.
42. Katritzky, A. R.; Ramsden, C. A.; Joule, J. A.; Zhdankin, V. V. *Handbook of Heterocyclic Chemistry*, 3rd ed.; Elsevier: Amsterdam, 2010; pp 490, 836–838.
43. Geen, R., Graham; Gritnet, T. J.; Knicey, P. M.; Jarvest, R. L. The effect of the C-6 substituent on the regioselectivity of N-alkylation of 2-aminopurines. *Tetrahedron* **1990**, *46*, 6903–6914.
44. Hocková, D.; Buděšínský, M.; Marek, R.; Marek, J.; Holý, A. Regioselective preparation of N7- and N9-alkyl derivatives of N6-[(dimethylamino)methylene]adenine bearing an active methylene group and their further derivatization leading to α -branched acyclic nucleoside analogues. *Eur. J. Org. Chem.* **1999**, 2675–2682.
45. Kjellberg, J.; Liljenberg, M. Regioselective alkylation of 6-(8-methoxy)ethoxylguanine to give the 9-alkylguanine derivative. *Tetrahedron Lett.* **1986**, *27*, 877–880.
46. Traube, W. Ueber eine neue synthese des guanins und xanthins. *Chem. Ber.* **1900**, *33*, 1371–1383.

47. Haggerty, W. J.; Springer, R. H.; Cheng, C. C. Studies on 2-(α -hydroxybenzyl)benzimidazole (HBB) analogs. I. Synthesis of 8-(α -hydroxybenzyl)purines, the diaza analogs of HBB1a,b. *J. Med. Chem.* **1965**, *8*, 797–802.
48. Traube, W. Der synthetische aufbau der harnsäure, des xanthins, theobromins, theophyllins und caffeïns aus der cyanessigsäure. *Chem. Ber.* **1900**, *33*, 3035–3056.
49. Daves, G. D.; Noell, C. W.; Robins, R. K.; Koppel, H. C.; Beaman, A. G. Potential purine antagonists. XXII. The preparation and reactions of certain derivatives of 2-amino-6-purinethiol. *J. Am. Chem. Soc.* **1960**, *82*, 2633–2640.
50. Gabriel, S.; Colman, J. Synthesen in der purinreihe. *Chem. Ber.* **1901**, *34*, 1234–1257.
51. Maddila, S.; Valand, J.; Bandaru, H.; Yalagala, K.; Lavanya, P. Ag Loaded on SiO₂ as an efficient and recyclable heterogeneous catalyst for the synthesis of chloro-8-substituted-9 H-purines. *J. Heterocycl. Chem.* **2016**, *53*, 319 – 324.
52. Ibrahim, N.; Legraverend, M. High-yielding two-step synthesis of 6,8-disubstituted N-9-unprotected purines. *J. Comb. Chem.* **2009**, *11*, 658–666.
53. Capek, P.; Vrabel, M.; Hasnik, Z.; Pohl, R.; Hocek, M. Aqueous-phase Suzuki–Miyaura cross-coupling reactions of free halopurine bases. *Synthesis* **2006**, 3515–3526.
54. Steklov, M. Y.; Tararov, V. I.; Romanov, G. A.; Mikhailov, S. N. Facile synthesis of 8-azido-6-benzylaminopurine. *Nucleos. Nucleot. Nucl.* **2011**, *30*, 503–511.
55. Qu, G.-R.; Mao, Z.-J.; Niu, H.-Y.; Wang, D.-C.; Xia, C.; Guo, H.-M. Straightforward and highly efficient catalyst-free one-step synthesis of

- 2-(purin-6-yl)acetoacetic acid ethyl esters, (purin-6-yl)acetates, and 6-methylpurines through S_NAr-based reactions of 6-halopurines with ethyl acetoacetate. *Org. Lett.* **2009**, *11*, 1745–1748.
56. Robins, R. K.; Godefroi, E. F.; Taylor, E. C.; Lewis, L. R.; Jackson, A. Purine Nucleosides. I. The Synthesis of Certain 6-Substituted-9-(tetrahydro-2-pyranyl)-purines as Models of Purine Deoxynucleosides 1. *J. Am. Chem. Soc.* **1961**, *83*, 2574–2579.
57. Crestey, F.; Zimdars, S.; Knochel, P. Regioselective functionalization of purine derivatives at positions 8 and 6 using hindered TMP-amide bases of Zn and Mg. *Synthesis* **2013**, *45*, 3029–3037.
58. Wuts, P. G. M.; Greene, T. W. *Greene's protective groups in organic synthesis*, fifth edition. ed.; John Wiley & Sons Inc, 2014; pp 1120–1143.
59. Wang, S.-B.; Deng, X.-Q.; Liu, D.-C.; Zhang, H.-J.; Quan, Z.-S. *Med. Chem. Res.* **2014**, *23*, 4619–4626.
60. Taddei, D.; Kilian, P.; Slawin, A. M. Z.; Derek Woollins, J. Synthesis and full characterisation of 6-chloro-2-iodopurine, a template for the functionalisation of purines. *Org. Biomol. Chem.* **2004**, *2*, 665–670.
61. Ibrahim, N.; Chevot, F.; Legraverend, M. Regioselective Sonogashira cross-coupling reactions of 6-chloro-2,8-diiodo-9-THP-9H-purine with alkyne derivatives. *Tetrahedron Lett.* **2011**, *52*, 305–307.
62. Haddach, A. A.; Kelleman, A.; Deaton-Rewolinski, M. V. An efficient method for the N-debenzylation of aromatic heterocycles. *Tetrahedron Lett.* **2002**, *43*, 399–402.
63. Wang, S.-B.; Deng, X.-Q.; Liu, D.-C.; Zhang, H.-J.; Quan, Z.-S. Synthesis and evaluation of anticonvulsant and antidepressant activities of 7-alkyl-7H-tetrazolo[1,5-g]purine derivatives. *Med. Chem. Res.* **2014**, *23*, 4619–4626.
64. Qu, G.-R.; Mao, Z.-J.; Niu, H.-Y.; Wang, D.-C.; Xia, C.; Guo, H.-M. Straightforward and highly efficient catalyst-free one-step synthesis of

- 2-(purin-6-yl)acetoacetic acid ethyl esters, (purin-6-yl)acetates, and 6-methylpurines through S_NAr-based reactions of 6-halopurines with ethyl acetoacetate. *Org. Lett.* **2009**, *11*, 1745–1748.
65. Dvořák, D.; Hocek, M.; Havelková, M. The Suzuki–Miyaura cross-coupling reactions of 2-, 6- or 8-halopurines with boronic acids leading to 2-, 6- or 8-aryl- and -alkenylpurine derivatives. *Synthesis* **2001**, *2001*, 1704–1710.
66. Canela, M.-D.; Liekens, S.; Camarasa, M.-J.; Priego, E. M.; Pérez-Pérez, M.-J. Synthesis and antiproliferative activity of 6-phenylaminopurines. *Eur. J. Med. Chem.* **2014**, *87*, 421–428.
67. Merz, A.; Schropp, R.; Dotterl, E. 3,4-Dialkoxypyrroles and 2,3,7,8,12,13,17,18-octaalkoxyporphyrins. *Synthesis* **1995**, 795–800.
68. Girardet, J. L.; Koh, Y.-H.; Shaw, S.; Kim, H. W. Preparation of purines, azapurines, and deazapurines as non-nucleoside reverse transcriptase inhibitors for treatment of HIV infection. Patent WO 122003, 2006.
69. Jones, M. I.; Froussios, C.; Evans, D. A. A short, versatile synthesis of porphobilinogen. *Chem. Commun.* **1976**, 472–473.
70. Forbes, I. T.; Johnson, C. N.; Thompson, M. Syntheses of functionalised pyrido[2,3-b]indoles. *J. Chem. Soc., Perkin Trans. 1* **1992**, 275–281.
71. Remers, W. A.; Roth, R. H.; Gibbs, G. J.; Weiss, M. J. Synthesis of indoles from 4-oxo-4,5,6,7-tetrahydroindoles. II. Introduction of substituents into the 4 and 5 positions. *J. Org. Chem.* **1971**, *36*, 1232–1240.
72. Gigg, R.; Conant, R. Conversion of the N-benzylacetamido group into the acetamido group by autoxidation in potassium t-butoxide–dimethyl sulphoxide. *Chem. Commun.* **1983**, 465–466.
73. Mosrin, M.; Bresser, T.; Knochel, P. Regio- and chemoselective multiple functionalization of chloropyrazine derivatives. Application to the synthesis of coelenterazine. *Org. Lett.* **2009**, *11*, 3406–3409.

74. Brown, D. G.; Boström, J. Analysis of past and present synthetic methodologies on medicinal chemistry: Where have all the new reactions gone?: Miniperspective. *J. Med. Chem.* **2016**, *59*, 4443–4458.
75. Bunnett, J. F.; Zahler, R. E. Aromatic nucleophilic substitution reactions. *Chem. Rev.* **1951**, *49*, 273–412.
76. Artamkina, G. A.; Egorov, M. P.; Beletskaya, I. P. Some aspects of anionic σ -complexes. *Chem. Rev.* **1982**, *82*, 427–459.
77. Miller, J.; Parker, A. Dipolar aprotic solvents in bimolecular aromatic nucleophilic substitution reactions. *J. Am. Chem. Soc.* **1961**, *83*, 117–123.
78. Clayden, J.; Greeves, N.; Warren, S., *Organic Chemistry*, 2nd ed.; Oxford University Press, 2012; pp 514–526.
79. Senger, N. A.; Bo, B.; Cheng, Q.; Keeffe, J. R.; Gronert, S.; Wu, W. The element effect revisited: Factors determining leaving group ability in activated nucleophilic aromatic substitution reactions. *J. Org. Chem.* **2012**, *77*, 9535–9540.
80. Anslyn, E. V. *Modern Physical Organic Chemistry*; University Science Books: Sausalito, Cal, 2006; pp 611 – 617.
81. Acevedo, O.; Jorgensen, W. L. Solvent effects and mechanism for a nucleophilic aromatic substitution from QM/MM simulations. *Org. Lett.* **2004**, *6*, 2881–2884.
82. Wu, X.; Anbarasan, P.; Neumann, H.; Beller, M. From noble metal to nobel prize: palladium-catalyzed coupling reactions as key methods in organic synthesis. *Angew. Chem. Int. Ed. Engl.* **2010**, *49*, 9047–9050.
83. Garcia-Melchor, M.; Braga, A.; Lledos, A.; Ujaque, G.; Maseras, F. Computational Perspective on Pd-Catalyzed C–C Cross-Coupling Reaction Mechanisms. *Acc. Chem. Res.* **2013**, *46*, 2626–2634.

84. Kürti, L. *Strategic applications of named reactions in organic synthesis : background and detailed mechanisms : 250 named reactions*; Elsevier Academic Press: Amsterdam, 2005; pp 448 – 449.
85. Jedinak, L.; Zatopkova, R.; Zemankova, H.; Sustkova, A.; Cankar, P. "The Suzuki Miyaura cross-coupling reaction of halogenated aminopyrazoles: Method development, scope, and mechanism of dehalogenation side reaction". *J. Org. Chem.* **2017**, *82*, 157–169.
86. Miller, W.; Fray, A.; Quatroche, J.; Sturgill, C. Suppression of a palladium-mediated homocoupling in a Suzuki cross-coupling reaction. Development of an impurity control strategy supporting synthesis of LY451395. *Org. Process Res. Dev.* **2007**, *11*, 359–364.
87. Ahmadi, Z.; McIndoe, J. S. A mechanistic investigation of hydrodehalogenation using ESI-MS. *Chem. Commun.* **2013**, *49*, 11488–11490.
88. Braga, A. A. C.; Ujaque, G.; Maseras, F. A DFT study of the full catalytic cycle of the Suzuki–Miyaura cross-coupling on a model system. *Organometallics* **2006**, *25*, 3647–3658.
89. Christmann, U.; Vilar, R. Monoligated palladium species as catalysts in cross-coupling reactions. *Angew. Chem. Int. Ed. Engl.* **2005**, *44*, 366–374.
90. Martin, R.; Buchwald, S. L. Palladium-catalyzed Suzuki–Miyaura cross-coupling reactions employing dialkylbiaryl phosphine ligands. *Acc. Chem. Res.* **2008**, *41*, 1461–1473.
91. Kode, N. R.; Phadtare, S. Synthesis and cytotoxic activity of some new 2,6-substituted purines. *Molecules* **2011**, *16*, 5840–5860.
92. Guthmann, H.; Könemann, M.; Bach, T. Synthesis of a cyclic tetrameric purine by successive cross-coupling reactions and subsequent Pd-catalyzed cyclization. *Eur. J. Org. Chem.* *2007*, 632–638.
93. Greibrokk, T. *Kromatografi*, 2nd ed.; Universitetsforlaget: Oslo, 1987; pp 112 – 114.

94. Burchat, A. F.; Chong, J.; Nielsen, N. Titration of alkyllithiums with a simple reagent to a blue endpoint. *J. Organomet. Chem.* **1997**, *542*, 281–283.
95. Hammett, L.; Walden, G.; Edmonds, S. New indicators for oxidimetry: Some phenanthroline and diphenylamine derivatives. *J. Am. Chem. Soc.* **1934**, *56*, 1092–1094.
96. Stathakis, C. I.; Manolikakes, S. M.; Knochel, P. TMPZnOPiv • LiCl: A new base for the preparation of air-stable solid zinc pivalates of sensitive aromatics and heteroaromatics. *Org. Lett.* **2013**, *15*, 1302–1305.
97. Ehrhardt, C.; Irie, O.; Lorthiois, J.; Maibaum, K.; Ostermann, N.; Sellner, H. Preparation of 3,4-substituted pyrrolidines for treatment of hypertension. Patent WO 2006100036, 2006.
98. Tsui, H. M. H. Synthetic strategy towards substituted pyrrolo[2,3-d]pyrimidine as potential CSF-1R inhibitor. 2018; Pre-Master's project; Norwegian University of Science and Technology.
99. Brown, H. C.; Narasimhan, S.; Choi, Y. M. Improved procedure for borane-dimethyl sulfide reduction of tertiary and secondary amides in the presence of boron trifluoride etherate. *Synthesis* **1981**, *1981*, 996–997.
100. Meanwell, N. Improving drug candidates by design: A focus on physicochemical properties as a means of improving compound disposition and safety. *Chem. Res. Toxicol.* **2011**, *24*, 1420–1456.
101. Pitner, T. P.; Sternglanz, H.; Bugg, C. E.; Glickson, J. D. Proton nuclear magnetic resonance study of hindered internal rotation of the dimethylamino group of N6,N6-dimethyladenine hydrochloride in aqueous solution. *J. Am. Chem. Soc.* **1975**, *97*, 885–888.
102. Neiman, Z.; Bergmann, F. Restricted rotation of a dimethyl group in a purine with a diazafulvene-like structure. *Chem. Commun.* **1968**, 1002–1003.

103. Bugge, S.; Kaspersen, S. J.; Sundby, E.; Hoff, B. H. Route selection in the synthesis of C-4 and C-6 substituted thienopyrimidines. *Tetrahedron* **2012**, *68*, 9226–9233.
104. Adamo, C.; Amatore, C.; Ciofini, I.; Jutand, A.; Lakmini, H. Mechanism of the Palladium-Catalyzed Homocoupling of Arylboronic Acids: Key Involvement of a Palladium Peroxo Complex. *J. Am. Chem. Soc.* **2006**, *128*, 6829–6836.
105. Audran, G.; Brémond, P.; Marque, S. R.; Siri, D.; Santelli, M. Calculated linear free energy relationships in the course of the Suzuki–Miyaura coupling reaction. *Tetrahedron* **2014**, *70*, 2272–2279.
106. Li, Y.; Manickam, G.; Ghoshal, A.; Subramaniam, P. More efficient palladium catalyst for hydrogenolysis of benzyl groups. *Synth. Commun.* **2006**, *36*, 925–928.
107. Hartung, W. H.; Simonoff, R. *Organic Reactions*; American Cancer Society, 2011; Chapter 5, pp 263–326.
108. Gray, B. D.; Jeffs, P. W. Alkylation and condensation reactions of N,N-dibenzylglycine esters: Synthesis of α -amino acid derivatives. *Chem. Commun.* **1987**, 1329–1330.
109. Elamin, B.; Anantharamaiah, G. M.; Royer, G. P.; Means, G. E. Removal of benzyl-type protecting groups from peptides by catalytic transfer hydrogenation with formic acid. *J. Org. Chem.* **1979**, *44*, 3442–3444.
110. Miki, Y.; Hachiken, H.; Kashima, Y.; Sugimura, W.; Yanase, N. p-Methoxybenzyl group as a protecting group of the nitrogen in indole derivatives: Deprotection by DDQ or trifluoroacetic acid. *Heterocycles* **1998**, *48*, 1–4.
111. Kawakita, Y.; Seto, M.; Ohashi, T.; Tamura, T.; Yusa, T.; Miki, H.; Iwata, H.; Kamiguchi, H.; Tanaka, T.; Sogabe, S.; Ohta, Y.; Ishikawa, T. Design and synthesis of novel pyrimido[4,5-b]azepine derivatives as HER2/EGFR dual inhibitors. *Bioorg. Med. Chem.* **2013**, *21*, 2250–2261.

112. Watanabe, T.; Kobayashi, A.; Nishiura, M.; Takahashi, H.; Usui, T.; Izumi, K.; Mochizuki, N.; Noritake, K.; Yokoyama, Y.; Murakami, Y. Synthetic studies on indoles and related compounds. XXVI. The debenylation of protected indole nitrogen with aluminum chloride. *Chem. Pharm. Bull.* **1991**, *39*, 1152–1156.
113. Mayrargue, J.; Essamkaoui, M.; Moskowitz, H. An unexpected difficulty in the use of MEM as a protective group for phenolic hydroxyl. *Tetrahedron Lett.* **1989**, *30*, 6867–6868.
114. Dreyfus, M.; Dodin, G.; Bensaude, O.; Dubois, J. E. Tautomerism of purines. 2. Amino–imino tautomerism in 1–alkyladenines. *J. Am. Chem. Soc.* **1977**, *99*, 7027–7037.
115. Gundersen, L.-L.; Görbitz, C.; Neier, L.; Roggen, H.; Tamm, T. *Calculated tautomeric equilibria and X-ray structures of 2-substituted N-methoxy-9-methyl-9H-purin-6-amines*; Springer-Verlag: Berlin/Heidelberg, 2011; Vol. 129; pp 349–358.
116. Houben, L.; Schoone, K.; Smets, J.; Adamowicz, L.; Maes, G. Combined matrix–isolation FT–IR and ab–initio 6–31++G** studies on tautomeric properties of nucleic acid bases and simpler model molecules. *J. Mol. Struct.* **1997**, *410*, 397–401.
117. Procházková, E.; Šála, M.; Nencka, R.; Dračinský, M. C6–Substituted purine derivatives: and experimental and theoretical ¹H, ¹³C and ¹⁵N NMR study. *Magn. Reson. Chem.* **2012**, *50*, 181–186.
118. Yardley, P., John; Fletcher, P., Horace Introduction of the methoxymethyl ether protecting group. *Synthesis* **1976**, *1976*, 244–244.
119. Auerbach, J.; Weinreb, S. M. Synthesis of terrein, a metabolite of *Aspergillus terreus*. *Chem. Commun.* **1974**, 298–299.
120. Brauman, J. I.; Blair, L. K. Gas–phase acidities of alcohols. Effects of alkyl groups. *J. Am. Chem. Soc.* **1968**, *90*, 6561–6562.

121. Brauman, J. I.; Blair, L. K. Gas-phase acidities of alcohols. *J. Am. Chem. Soc.* **1970**, *92*, 5986–5992.
122. Fulmer, G. R.; Miller, A. J. M.; Sherden, N. H.; Gottlieb, H. E.; Nudelman, A.; Stoltz, B. M.; Bercaw, J. E.; Goldberg, K. I., NMR chemical shifts of trace impurities: Common laboratory solvents, organics, and gases in deuterated solvents relevant to the organometallic chemist. *Organometallics* **2010**, *29*, 2176–2179.
123. Friebolin, H. *Basic one- and two-dimensional NMR spectroscopy*, 5th ed.; Wiley-VCH: Weinheim, 2011; pp 47–52.
124. Silverstein, R. M.; Webster, F. X.; Kiemle, D. J. *Spectrometric identification of organic compounds*, 8th ed.; Wiley, 2005; pp 71–125.
125. Ram, S.; D. Spicer, L. Debenzylation of N-benzylamino derivatives by catalytic transfer hydrogenation with ammonium Formate. *Synth. Commun.* **1987**, *17*, 415–418.
126. Waldhof, Z. Improvements in and relating to the preparation of purines. Patent GB 1029696, 1966.
127. Ma, N.; Zhu, Z.; Wu, Y. Cyclopalladated ferrocenyimine: a highly effective catalyst for the borylation/suzuki coupling reaction. *Tetrahedron* **2007**, *63*, 4625 – 4629.

Appendices

A Spectroscopic Data for Compound 3

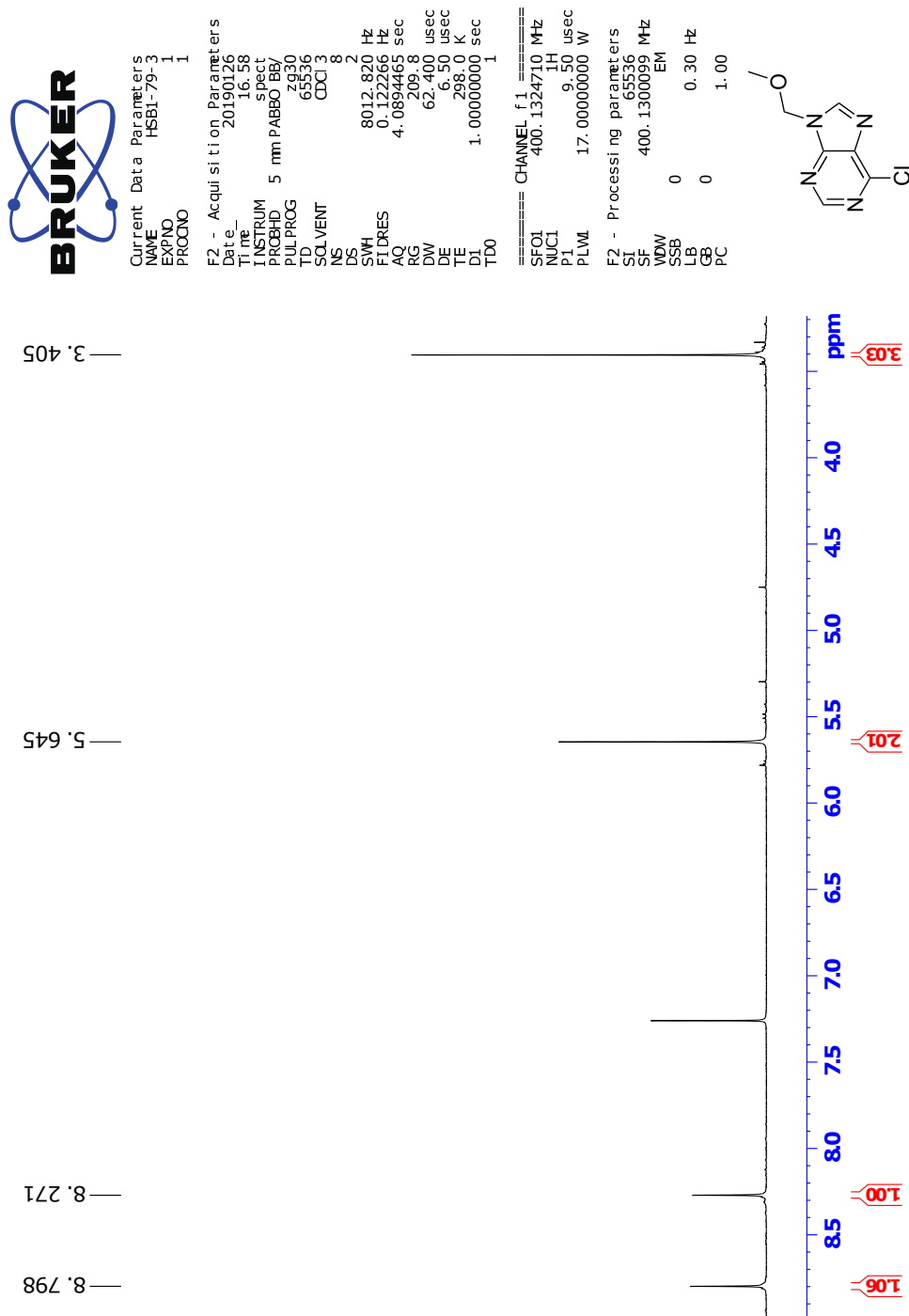


Figure A.1: ^1H NMR specter of compound **3** (CDCl_3 , 400 MHz).

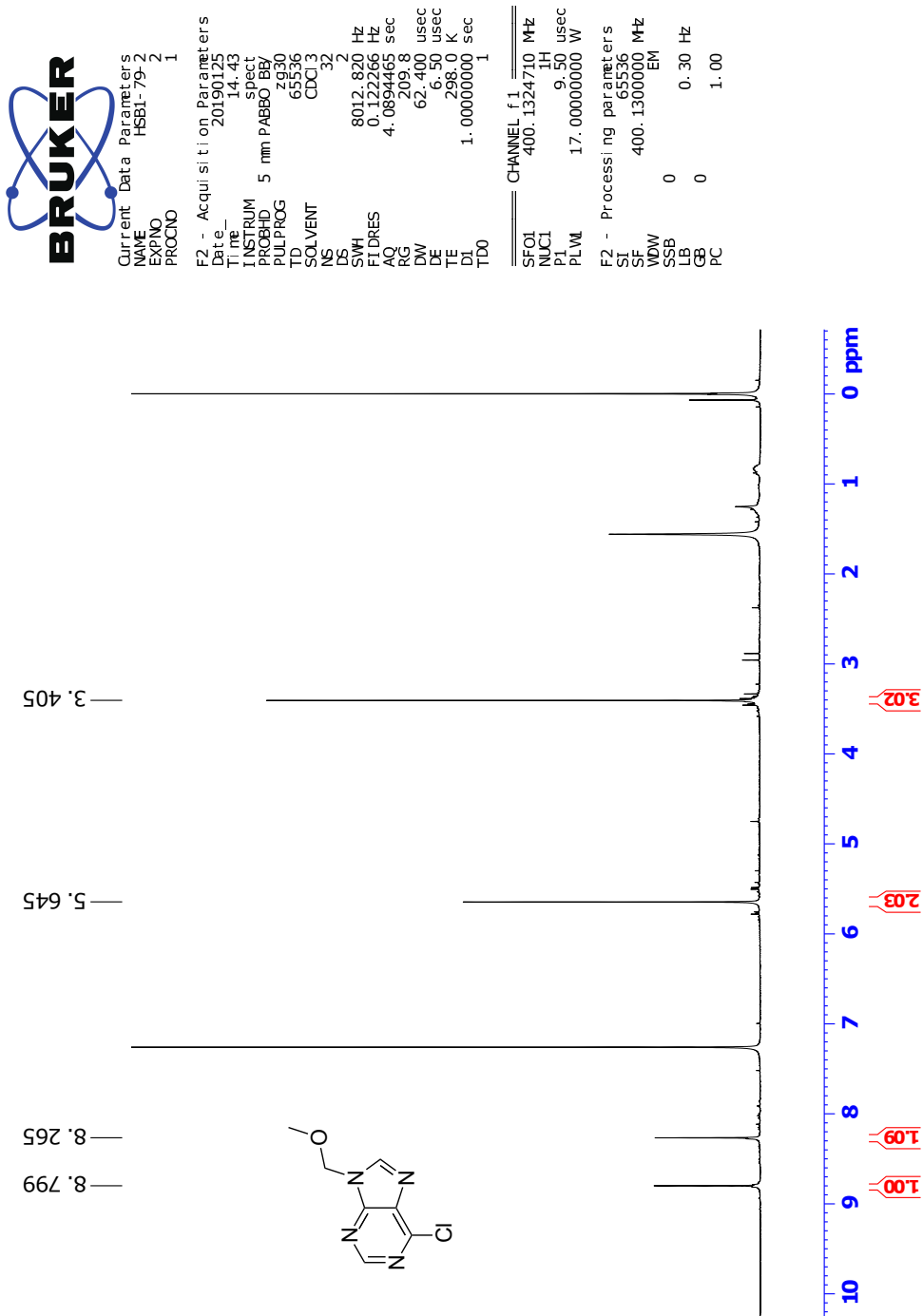


Figure A.2: ^1H NMR spectrum of the crude material in synthesis of compound **3** (CDCl_3 , 400 MHz).



Current Parameters
NAME HEB1-79-3
EXPNO 2
PROCNO 1

F2 - Acquisition Parameters

Date_ 20190126
Time 17.29
INSTRUM spect
PROBHD 5 mm PABBO BB/
PULPROG zgpg30
TD 65536
SOLVENT CDCl3
NS 512
DS 4
SWH 24038.461 Hz
FIDRES 0.366798 Hz
AQ 1.3631488 sec
RG 209.8
DW 20.800 usec
DE 6.50 usec
TE 298.0 K
D1 2.0000000 sec
D11 0.03000000 sec
TDO 1

CHANNEL f1
SFO1 100.6228293 MHz
NUC1 13C
P1 9.50 usec
PLW1 71.00000000 W

CHANNEL f2
SFO2 400.1316005 MHz
NUC2 1H
CPDPRG2 waltz16
PCPDZ 90.00 usec
PLW2 17.00000000 W
PLW3 0.18941000 W
PLW4 0.15343000 W

F2 - Processing parameters
SI 32768
SF 100.6127685 MHz
WDW EM
SSB 0
LB 0
GB 0
PC 1.40

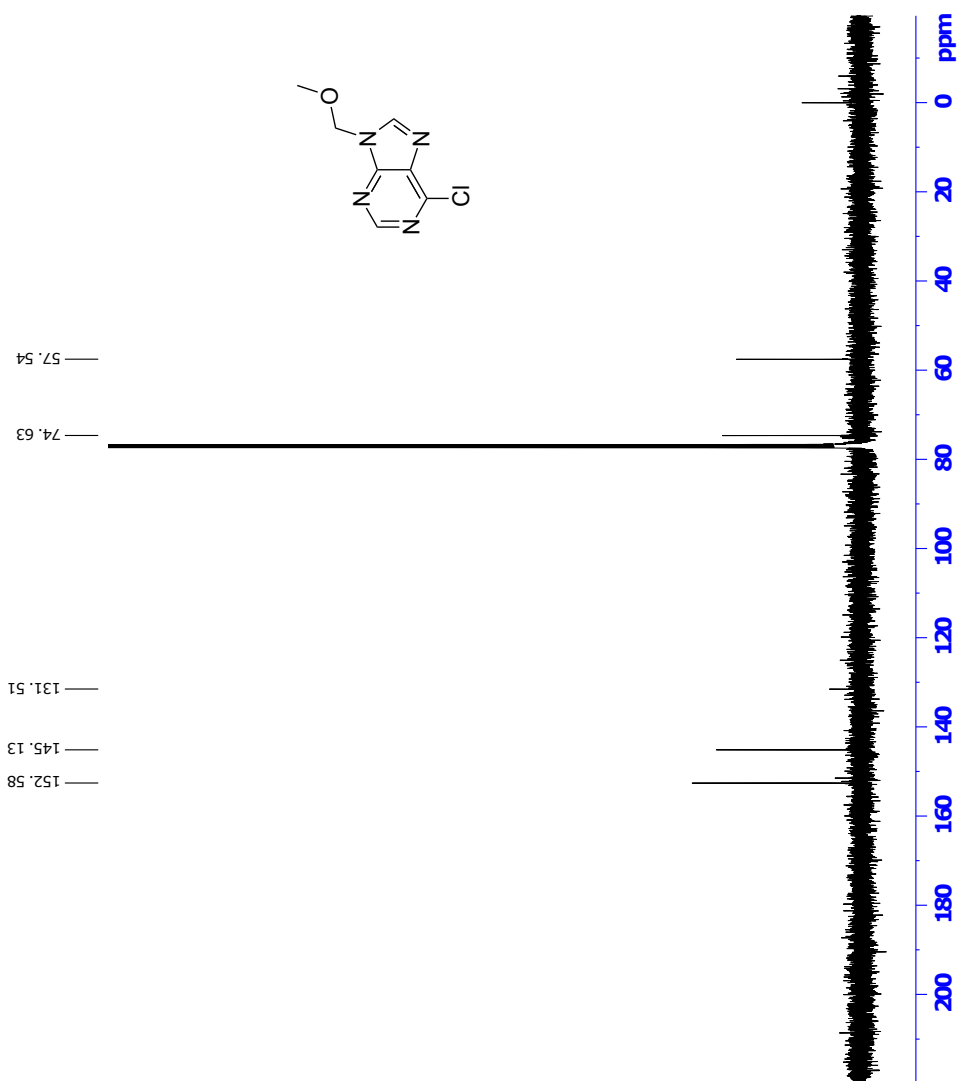


Figure A.3: ^{13}C NMR spectrum of compound **3** (CDCl_3 , 100 MHz).



Current Data Parameters
 NAME HEBL-79-3
 EXPNO 1
 PROCNO 1

F2 - Acquisition Parameters
 Date_ 20190126
 Time 13:21
 INSTRUM spect
 PROBHD 5 mm PABBO BB/
 PULPROG zgpg30
 TD 65536
 SOLVENT CDCl3
 NS 8
 DS 8
 SWH 5102.041 Hz
 FIDRES 0.100000 Hz
 AQ 0.2007040 sec
 RG 64.34
 DW 98.000 usec
 DE 6.50 usec
 TE 296.2 K
 D0 0.0000300 sec
 D1 1.9909897 sec
 D11 0.0300000 sec
 D12 0.0000000 sec
 D13 0.0000400 sec
 D16 0.0002000 sec
 D19 0.00019600 sec

===== CHANNEL f1 =====
 SFO1 400.1322183 MHz
 NUC1 1H
 P0 9.50 usec
 PL1 1.00 usec
 PL17 2500.00 usec
 PLW1 17.00000000 W
 PLW10 2.26959991 W

===== GRADIENT CHANNEL =====
 GNM1 11 SWSFO10.100
 GP21 10.00 %
 P16 1000.00 usec

F1 - Acquisition parameters
 TD 128
 SFO1 400.1322 MHz
 FIDRES 0.100000 Hz
 SWH 5102.041 Hz
 FWHM 12.7 Hz

F2 - Processing parameters
 SF 400.130079 MHz
 DS 8
 WSW 0 Hz
 SSB 0 Hz
 GB 0 Hz
 PC 1.40

F1 - Processing parameters
 TD 128
 SFO1 400.130079 MHz
 FIDRES 0.100000 Hz
 SWH 5102.041 Hz
 WSW 0 Hz
 SSB 0 Hz
 GB 0 Hz

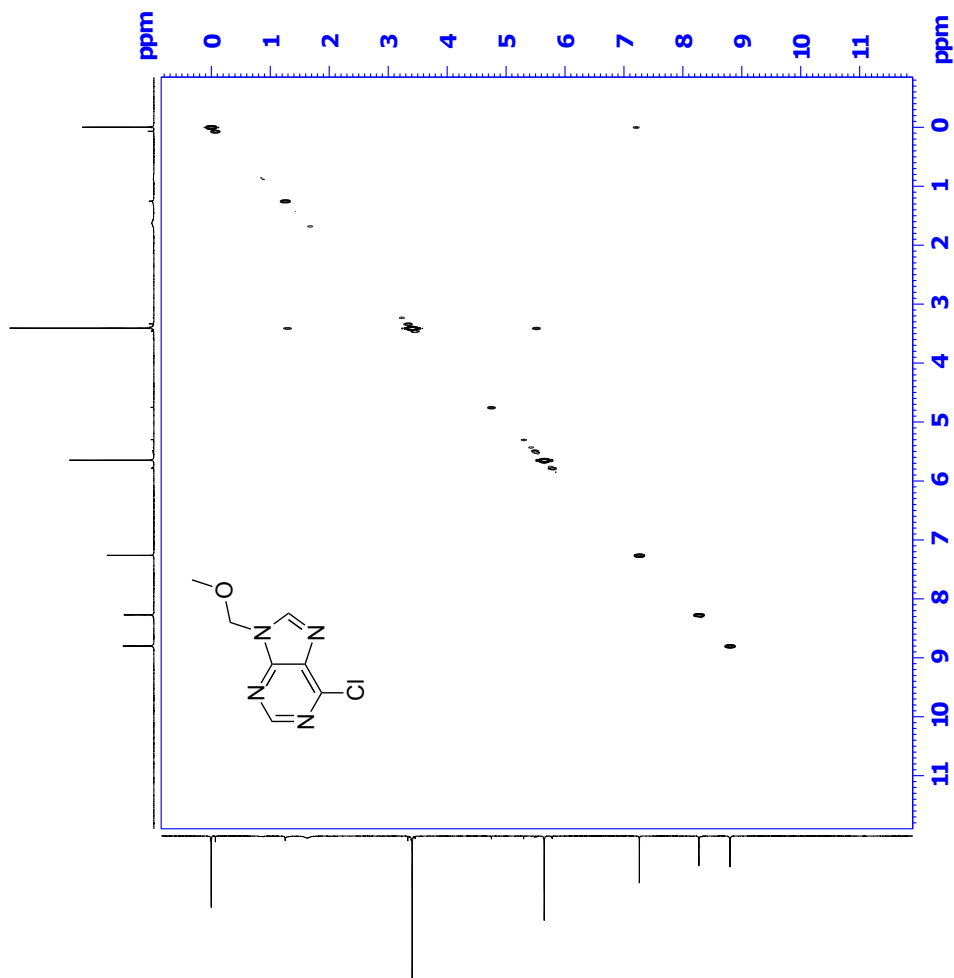


Figure A.4: COSY spectrum compound **3** (CDCl₃, 400 MHz).

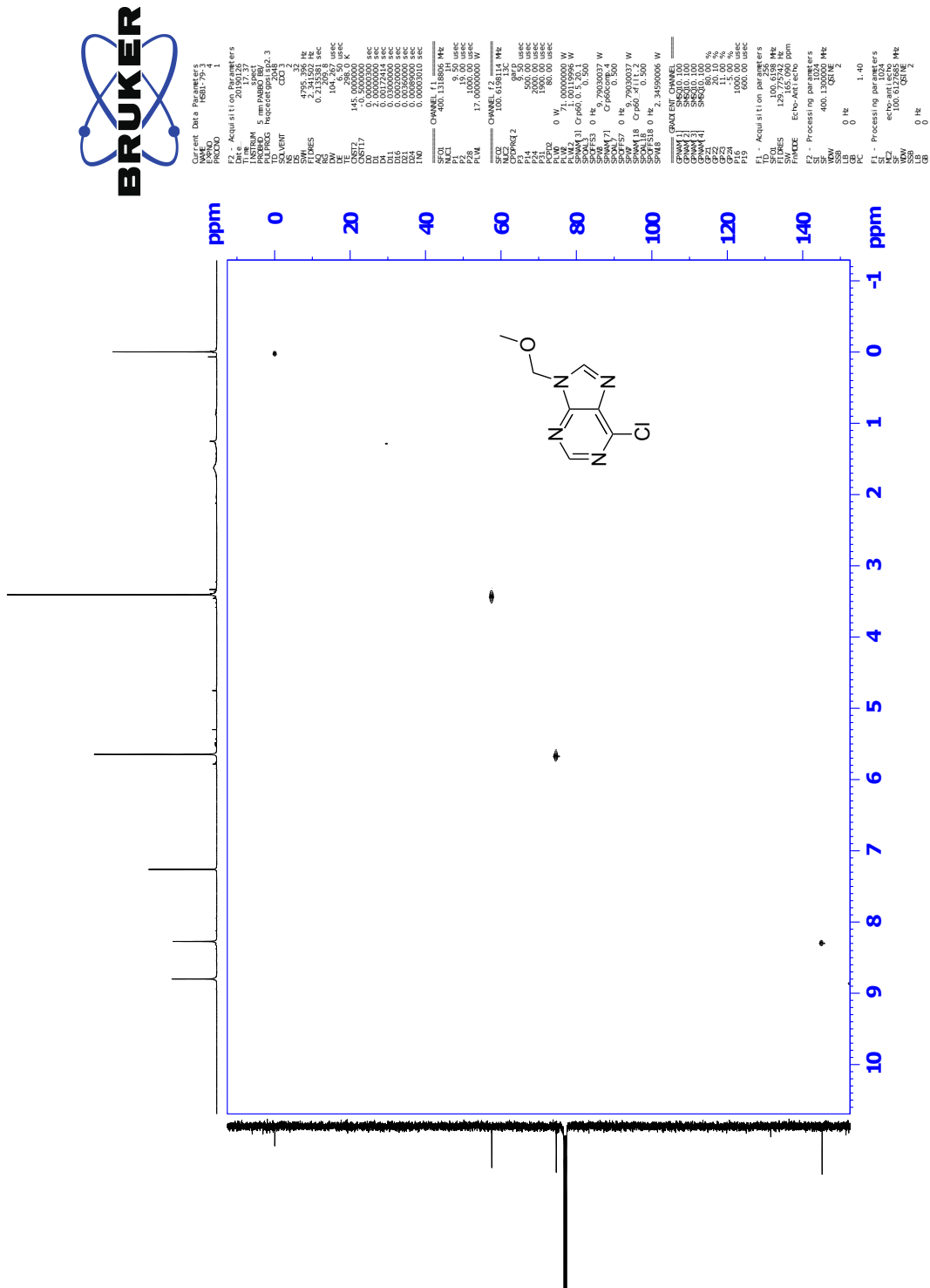


Figure A.5: HSQC spectrum of compound 3 (CDCl₃, 400 MHz).

Single Mass Analysis

Tolerance = 2.0 PPM / DBE: min = -2.0, max = 50.0

Element prediction: Off

Number of isotope peaks used for i-FIT = 3

Monoisotopic Mass, Even Electron Ions

788 formula(e) evaluated with 1 results within limits (all results (up to 1000) for each mass)

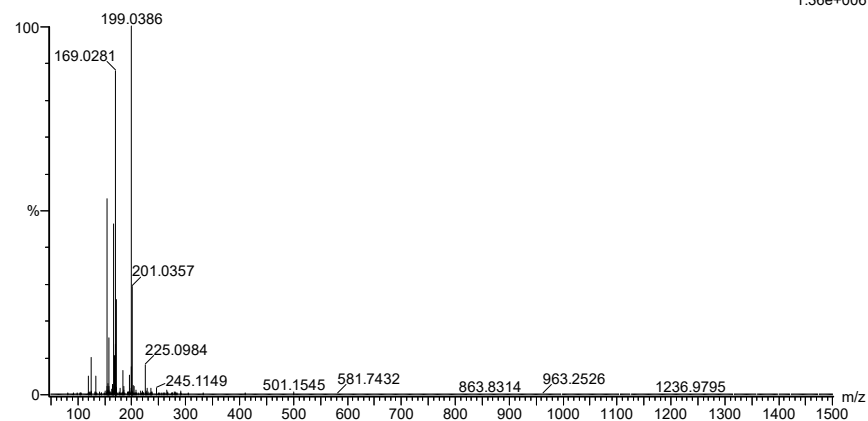
Elements Used:

C: 0-100 H: 0-150 N: 0-10 O: 0-10 Na: 0-1 Cl: 0-3 Au: 0-2

2019-42 17 (0.364)AM2 (Ar,35000.0,0.00,0.00); Cm (17:21)

1: TOF MS ASAP+

1.36e+006



Minimum: -2.0
Maximum: 50.0

Mass	Calc. Mass	mDa	PPM	DBE	i-FIT	Norm	Conf (%)	Formula
199.0386	199.0387	-0.1	-0.5	5.5	1802.7	n/a	n/a	C7 H8 N4 O Cl

Figure A.7: MS specter of compound 3.

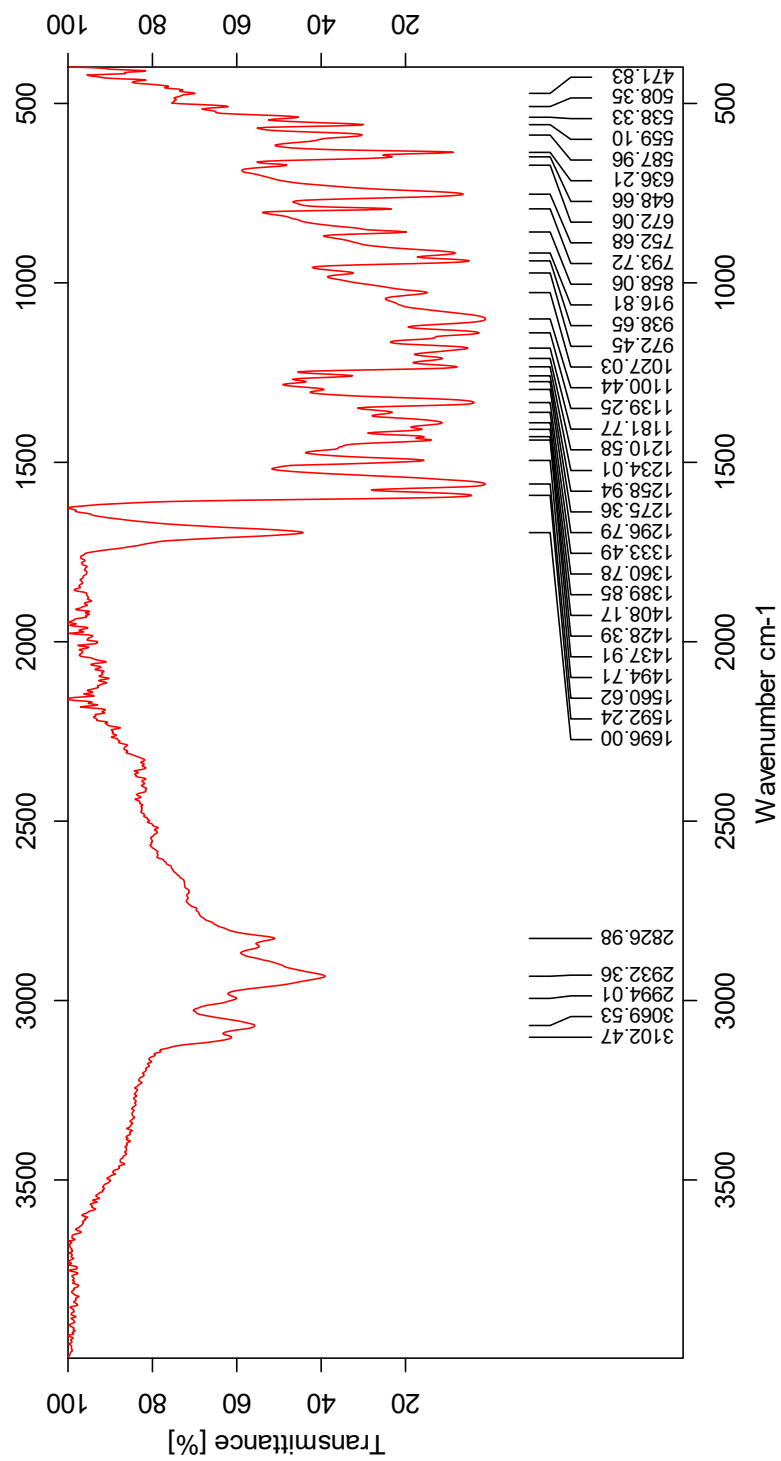


Figure A.8: IR specter of compound 3.

B Spectroscopic Data for Compound 4

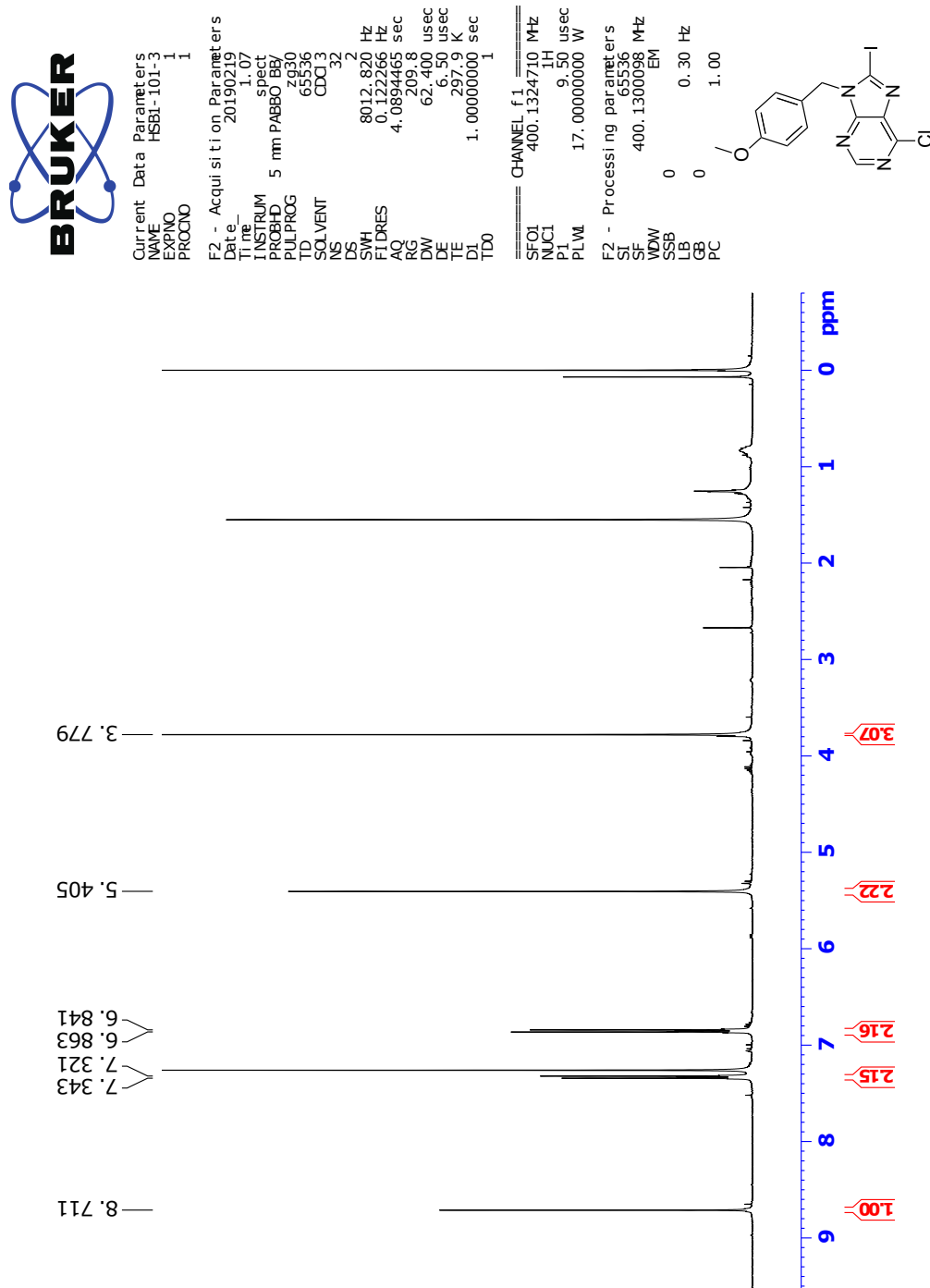


Figure B.1: ¹H NMR specter of compound 4 (CDCl₃, 400 MHz).

C Spectroscopic Data for Compound 5

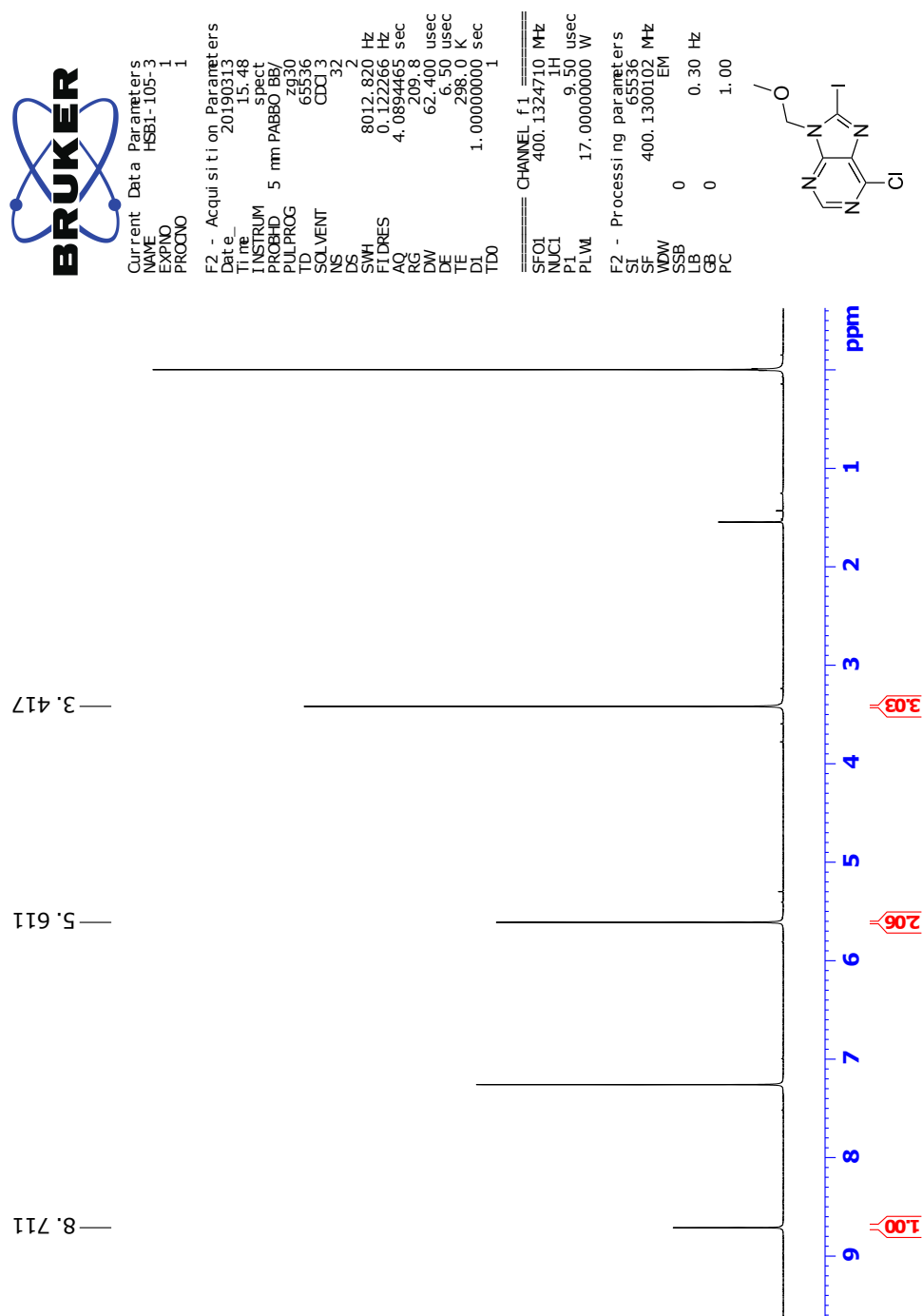


Figure C.1: ¹H NMR specter of compound 5 (CDCl₃, 400 MHz).

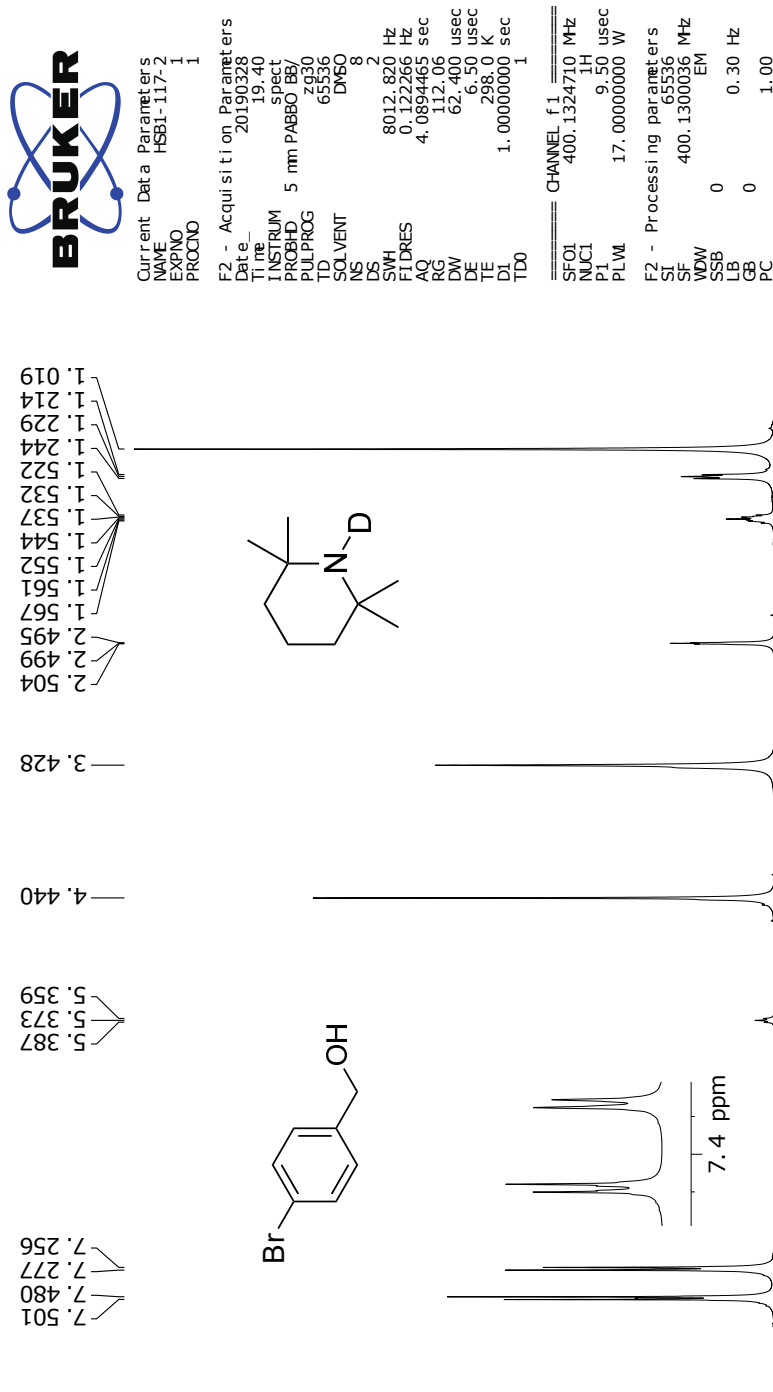


Figure C.2: ^1H NMR spectrum of $\text{TMPZnCl}\cdot\text{LiCl}$ quenched with D_2O and the internal standard 4-bromobenzyl alcohol. (DMSO- d_6 , 400 MHz).

D Spectroscopic Data for Compound 6

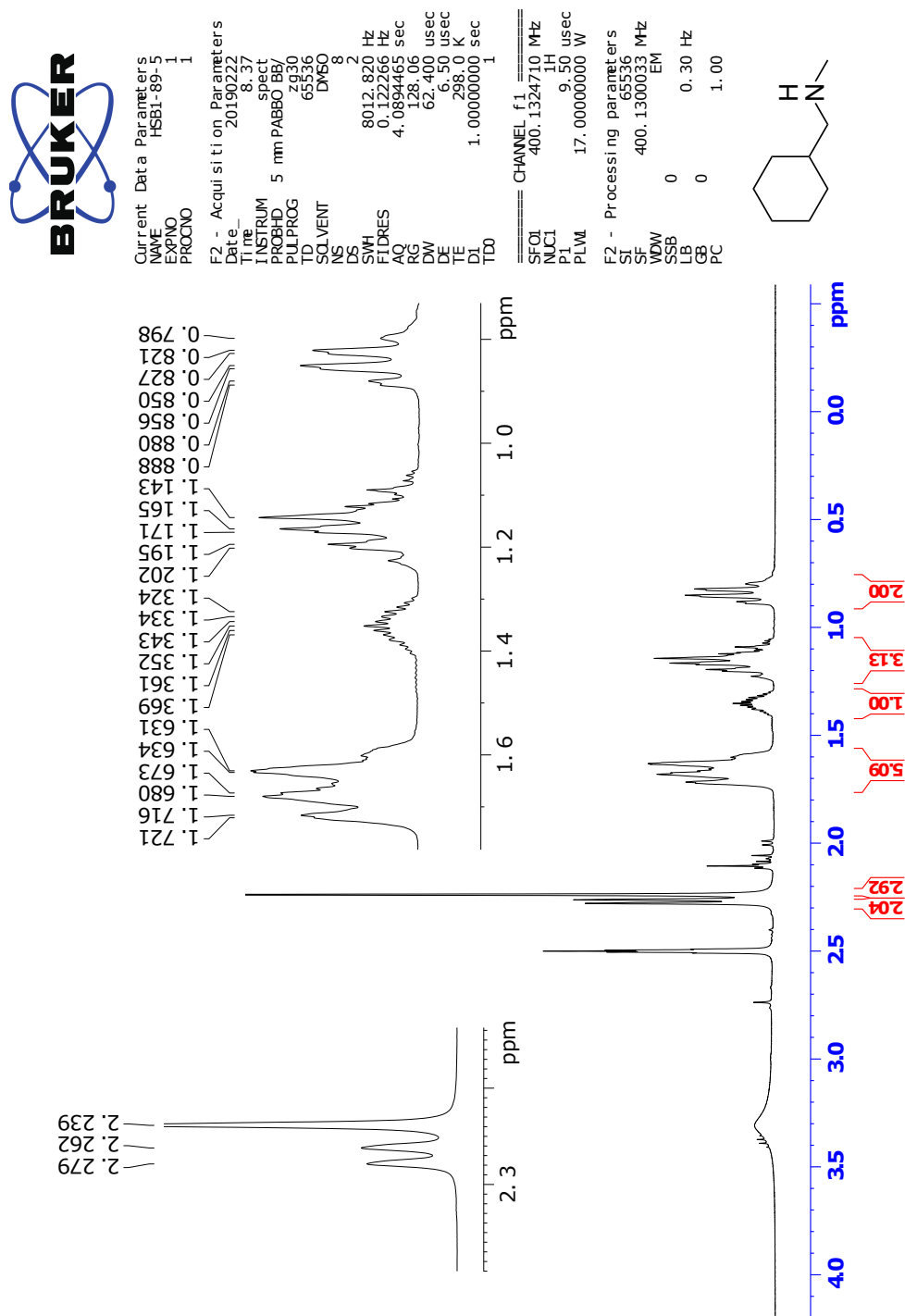


Figure D.1: ¹H NMR specter of compound 6 (DMSO-*d*₆, 400 MHz).

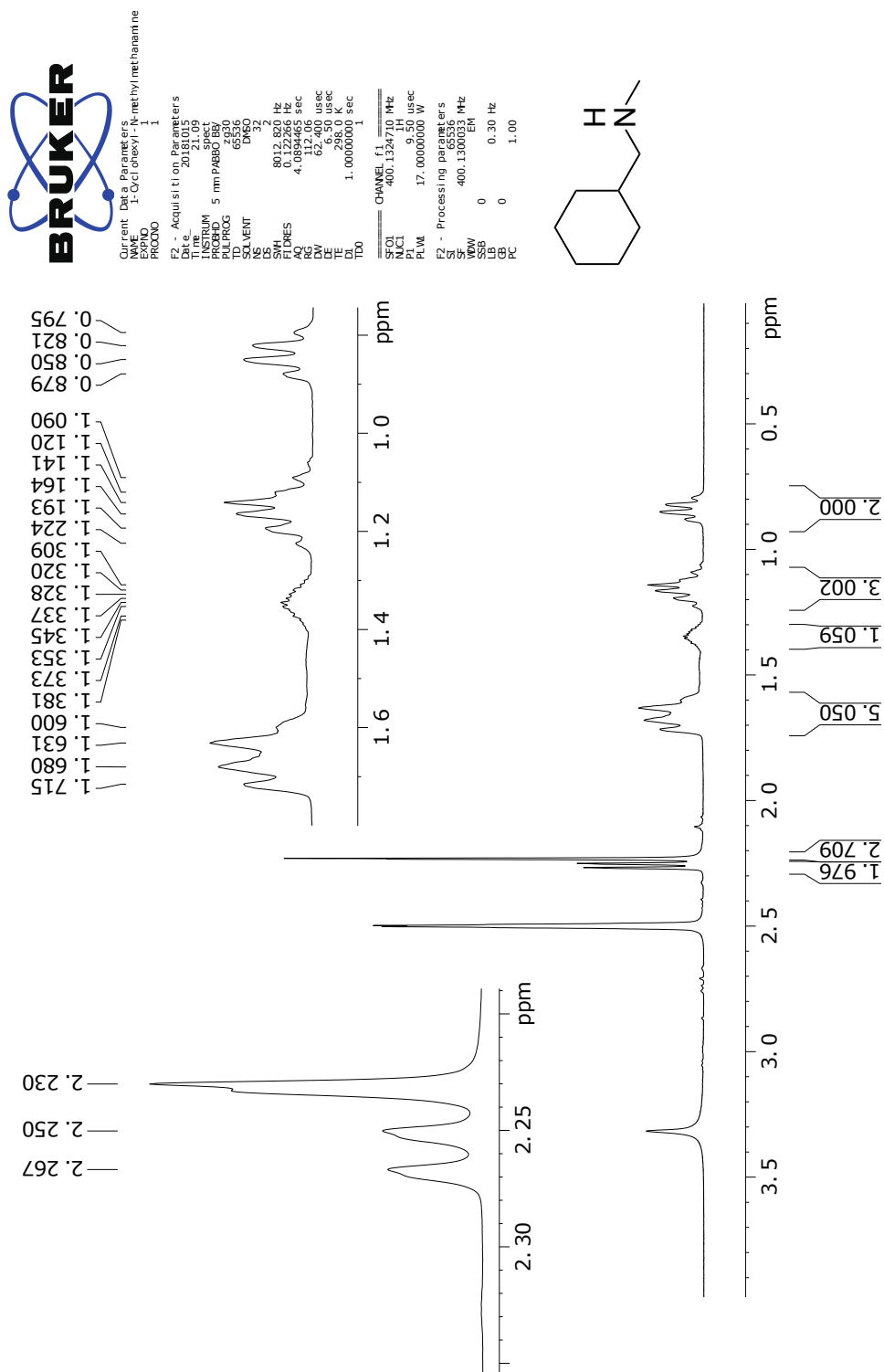


Figure D.2: ^1H NMR spectrum of standard of compound **6** ($\text{DMSO-}d_6$, 400 MHz).

E Spectroscopic Data for Compound 8

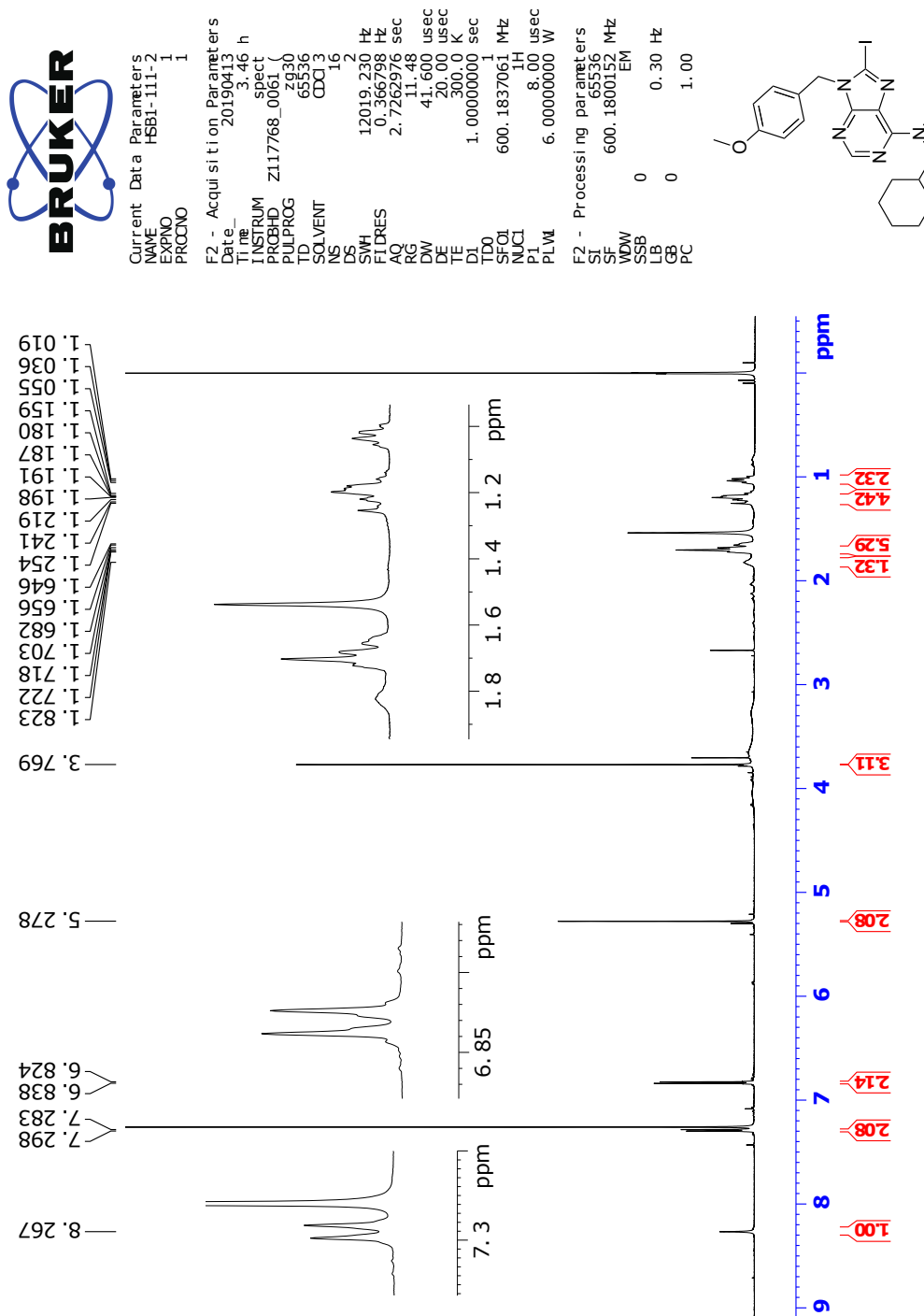


Figure E.1: ¹H NMR spectrum of compound 8 (CDCl₃, 400 MHz).

F Spectroscopic Data for Compound 9

Elemental Composition Report

Page 1

Single Mass Analysis

Tolerance = 2.0 PPM / DBE: min = -50.0, max = 50.0

Element prediction: Off

Number of isotope peaks used for i-FIT = 3

Monoisotopic Mass, Even Electron Ions

1404 formula(e) evaluated with 3 results within limits (all results (up to 1000) for each mass)

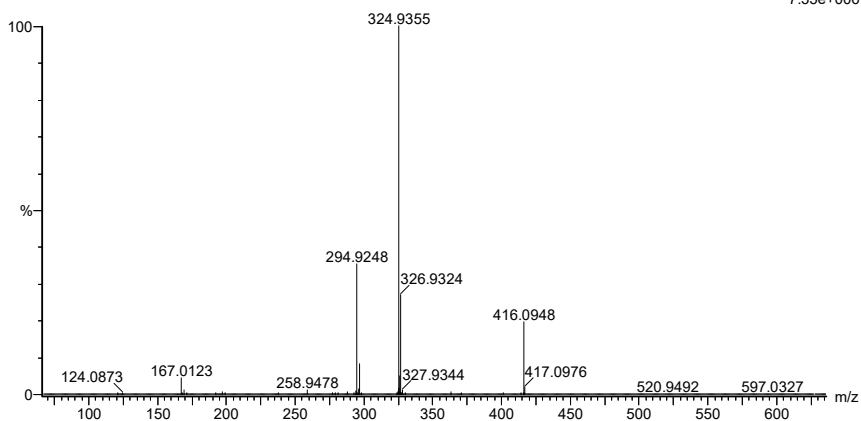
Elements Used:

C: 0-100 H: 0-150 N: 0-6 O: 0-6 I: 0-2

2019-320 40 (0.792) AM2 (Ar,35000.0,0.00,0.00); Cm (40:50)

1: TOF MS ASAP+

7.35e+006



Minimum: -50.0
Maximum: 5.0 2.0 50.0

Mass	Calc. Mass	mDa	PPM	DBE	i-FIT	Norm	Conf (%)	Formula
416.0948	416.0947	0.1	0.2	6.5	1142.3	0.406	66.65	C15 H23 N5 O I
	416.0949	-0.1	-0.2	-49.5	1145.8	3.934	1.96	C17 H139 N4 O
	416.0945	0.3	0.7	-18.5	1143.1	1.159	31.39	C H40 N O6 I2

Figure F.1: MS specter of compound 9.

G Spectroscopic Data for Compound 10

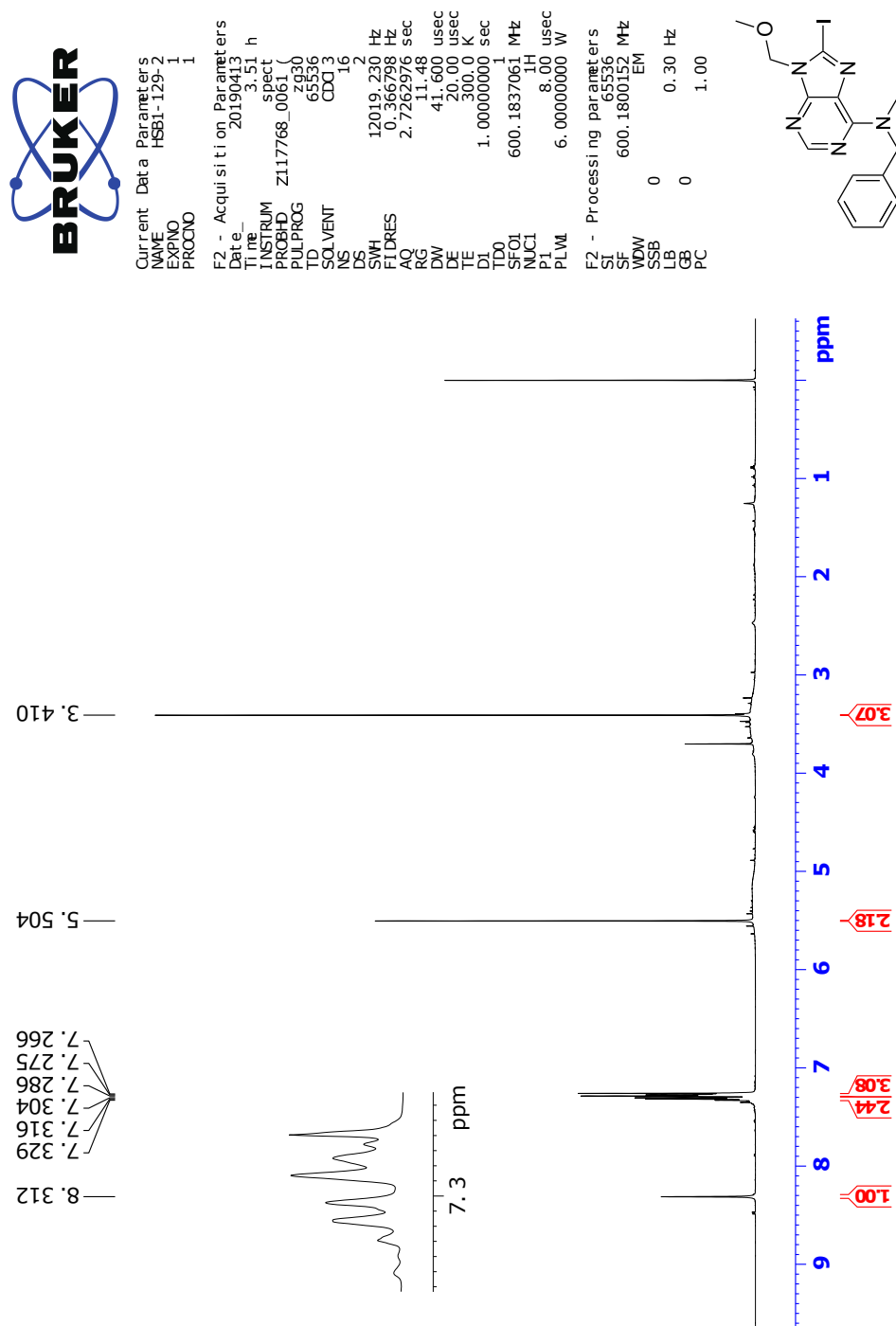


Figure G.1: ¹H NMR specter of compound **10** (CDCl₃, 600 MHz).



Current Data Parameters
NAME HSB1-129-2
EXPNO 2
PROCNO 1

F2 - Acquisition Parameters
Date_ 20190413
Time_ 4.16 h
INSTRUM spect
PROBHD Z117768.0061
PULPROG zgpg30
TD 65536
SOLVENT CDCl3
NS 512
DS 4
SWH 36057.691 Hz
FIDRES 1.100393 Hz
AQ 0.9087659 sec
RG 197.14
DW 13.867 usec
DE 18.00 usec
TE 300.0 K
D1 2.0000000 sec
D11 0.0300000 sec
TD0 1
SFO1 150.9304719 MHz
NUC1 13C
P1 11.40 usec
PLW1 80.0000000 W
SFO2 600.1824007 MHz
NUC2 1H
PCPD2 val tz16
PCPD2 70.00 usec
PLW2 6.0000000 W
PLW3 0.07836700 W
PLW3 0.03941800 W

F2 - Processing parameters
SI 32768
SF 150.9155808 MHz
WDW 0
SSB 0
LB 1.00 Hz
GB 0
PC 1.40

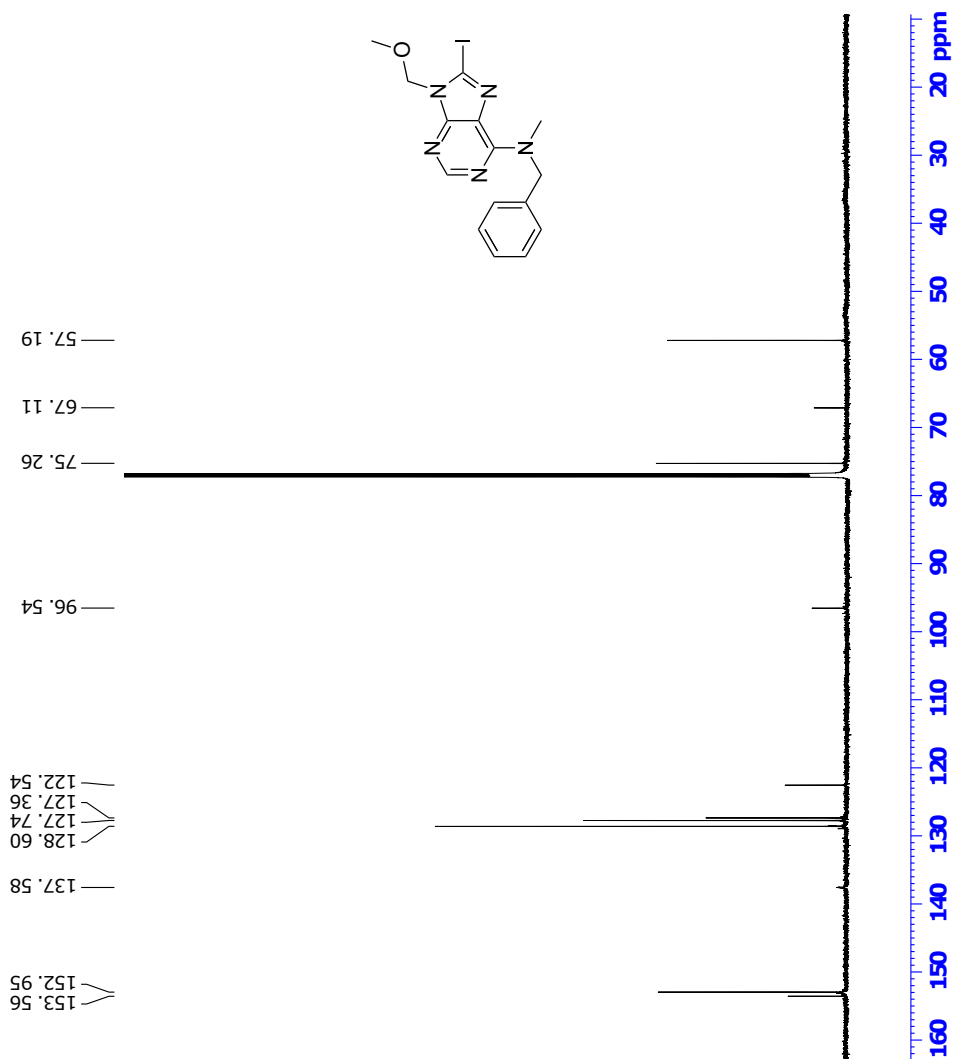


Figure G.2: ^{13}C NMR spectrum of compound **10** (CDCl_3 , 150 MHz).



Current Data Parameters
 NAME HSB1-129-2
 EXPNO 1
 PROCNO 1

F2 - Acquisition Parameters
 Date_ 20190413
 Time 4.18 h
 INSTRUM spect
 PROBHD Z117768.0061
 PULPROG cosygppbf
 TD 2048
 SOLVENT CDCl3
 NS 16
 DS 16
 SWH 6410.256 Hz
 FIDRES 6.260016 Hz
 AQ 0.1597440 sec
 RG 327.500
 DW 78.000 usec
 DE 20.000 usec
 TE 300.0 K
 D0 0.0000300 sec
 D1 1.133802 sec
 D2 0.0000000 sec
 D3 0.0002000 sec
 D4 0.0000400 sec
 D5 0.0002000 sec
 D6 0.0002000 sec
 D7 0.00015600 sec
 Delay 600.182525 MHz
 SF01 1H
 P0 8.00 usec
 P1 8.00 usec
 P2 250.000000 usec
 PL1 6.0000000 W
 PL2 0.61440003 W
 PLW0
 GPMAM 1
 GPZ1 SWSQ0, 100
 P16 10.00 %
 1000.00 usec

F1 - Acquisition parameters
 TD 128
 SFO1 600.1826 MHz
 DRES 100.160251 Hz
 SWH 10.061 ppm
 FWH0

F2 - Processing parameters
 SI 1024
 SF 600.180112 MHz
 WDW COSYNE
 SSB 0 Hz
 LB 0 Hz
 GB 0
 PC 1.40

F1 - Processing parameters
 SI 1024
 ACZ 0
 WDW 600.180112 MHz
 SSB 0 Hz
 LB 0 Hz
 GB 0

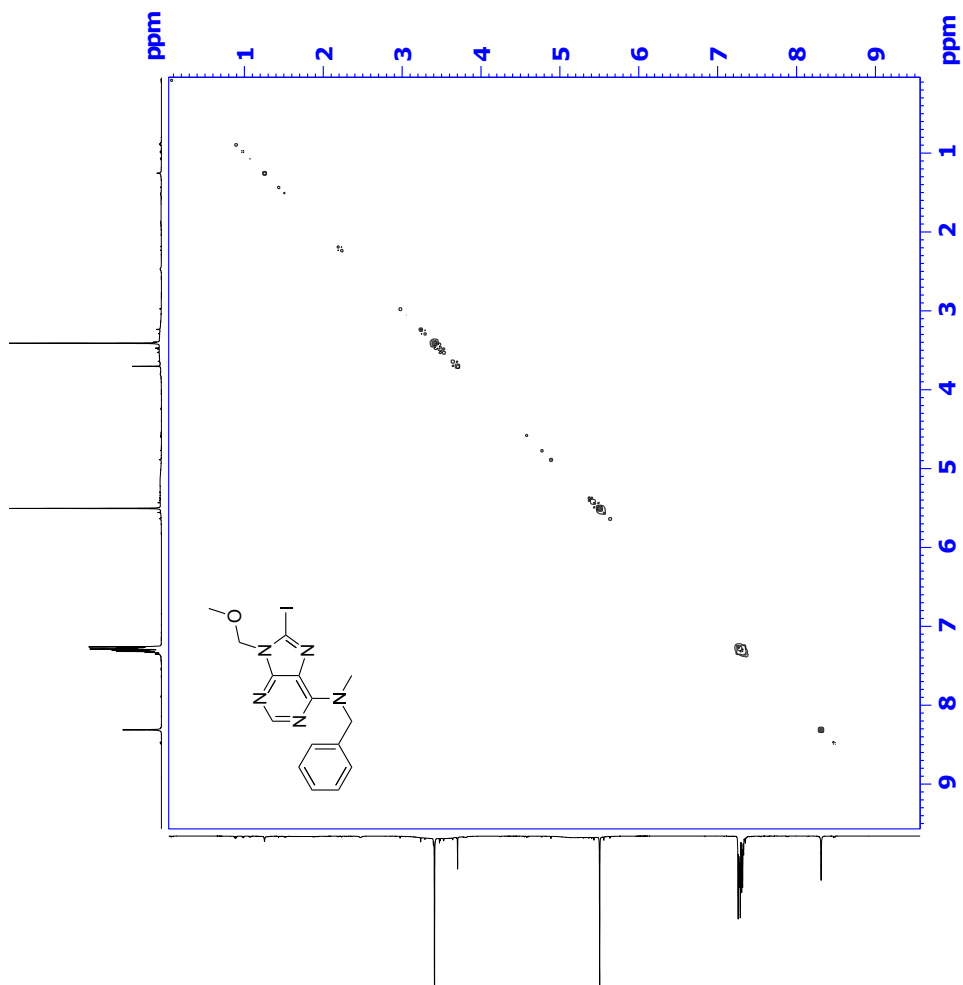


Figure G.3: COSY spectrum compound **10** (CDCl₃, 600 MHz).

Single Mass Analysis

Tolerance = 2.0 PPM / DBE: min = -50.0, max = 50.0

Element prediction: Off

Number of isotope peaks used for i-FIT = 3

Monoisotopic Mass, Even Electron Ions

2995 formula(e) evaluated with 3 results within limits (all results (up to 1000) for each mass)

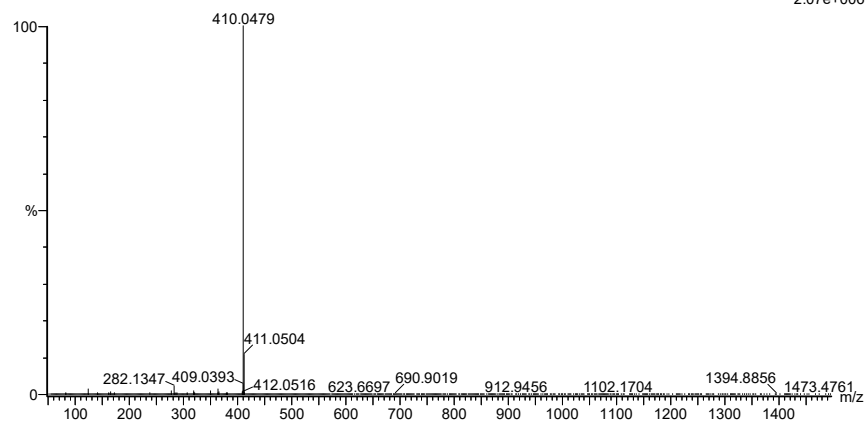
Elements Used:

C: 2-100 H: 0-150 N: 0-5 O: 0-10 S: 0-1 I: 0-2

2019-339 40 (0.792)AM2 (Ar,35000.0,0.00,0.00); Cm (35:40)

1: TOF MSASAP+

2.07e+006



Minimum: -50.0
Maximum: 50.0

Mass	Calc. Mass	mDa	PPM	DBE	i-FIT	Norm	Conf (%)	Formula
410.0479	410.0479	0.0	0.0	-46.5	1041.9	2.944	5.26	C17 H133 N4 O
	410.0478	0.1	0.2	9.5	1039.0	0.055	94.68	C15 H17 N5 O I
	410.0487	-0.8	-2.0	19.5	1046.4	7.453	0.06	C24 H12 N O4 S

Figure G.6: MS specter of compound 10.

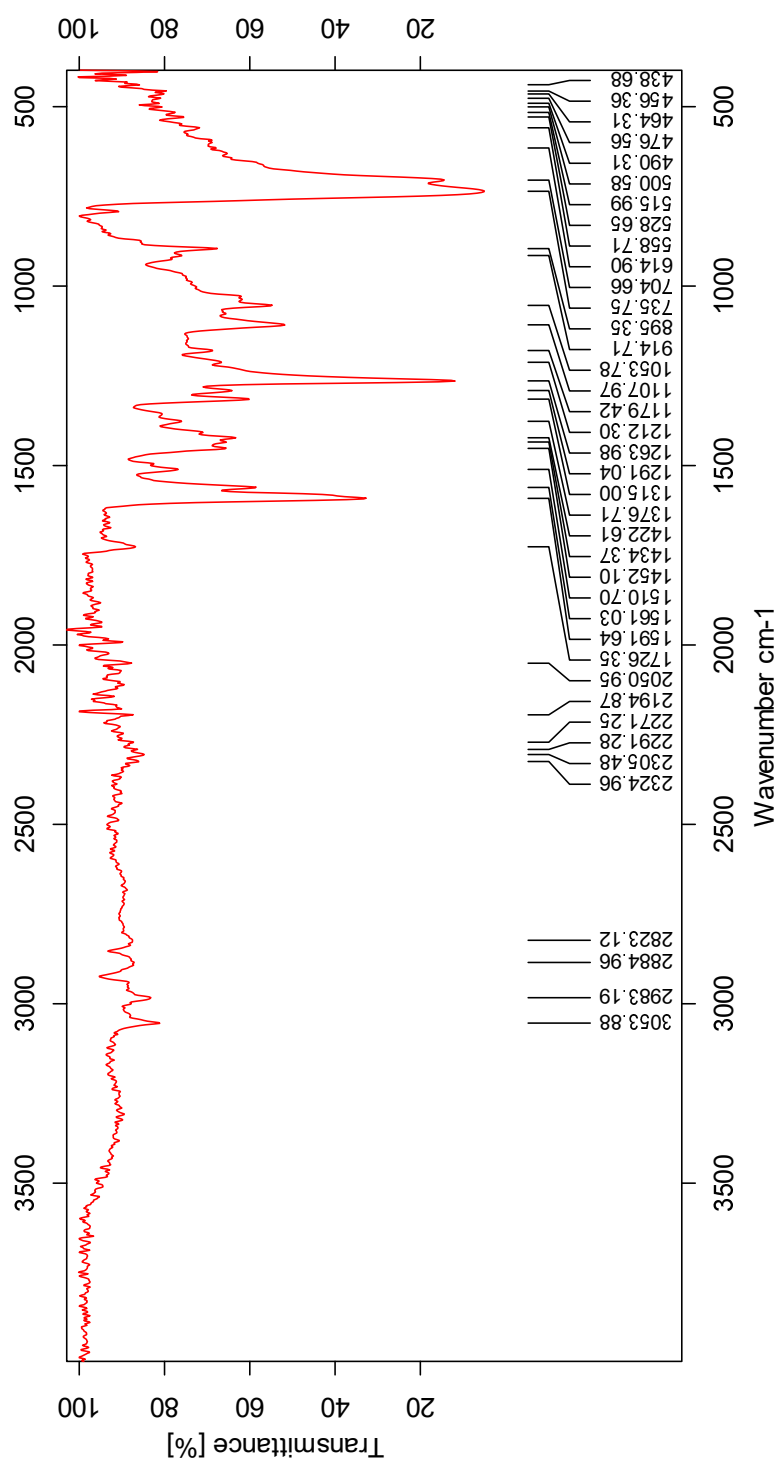


Figure G.7: IR specter of compound 10.

H Spectroscopic Data for Compound 12

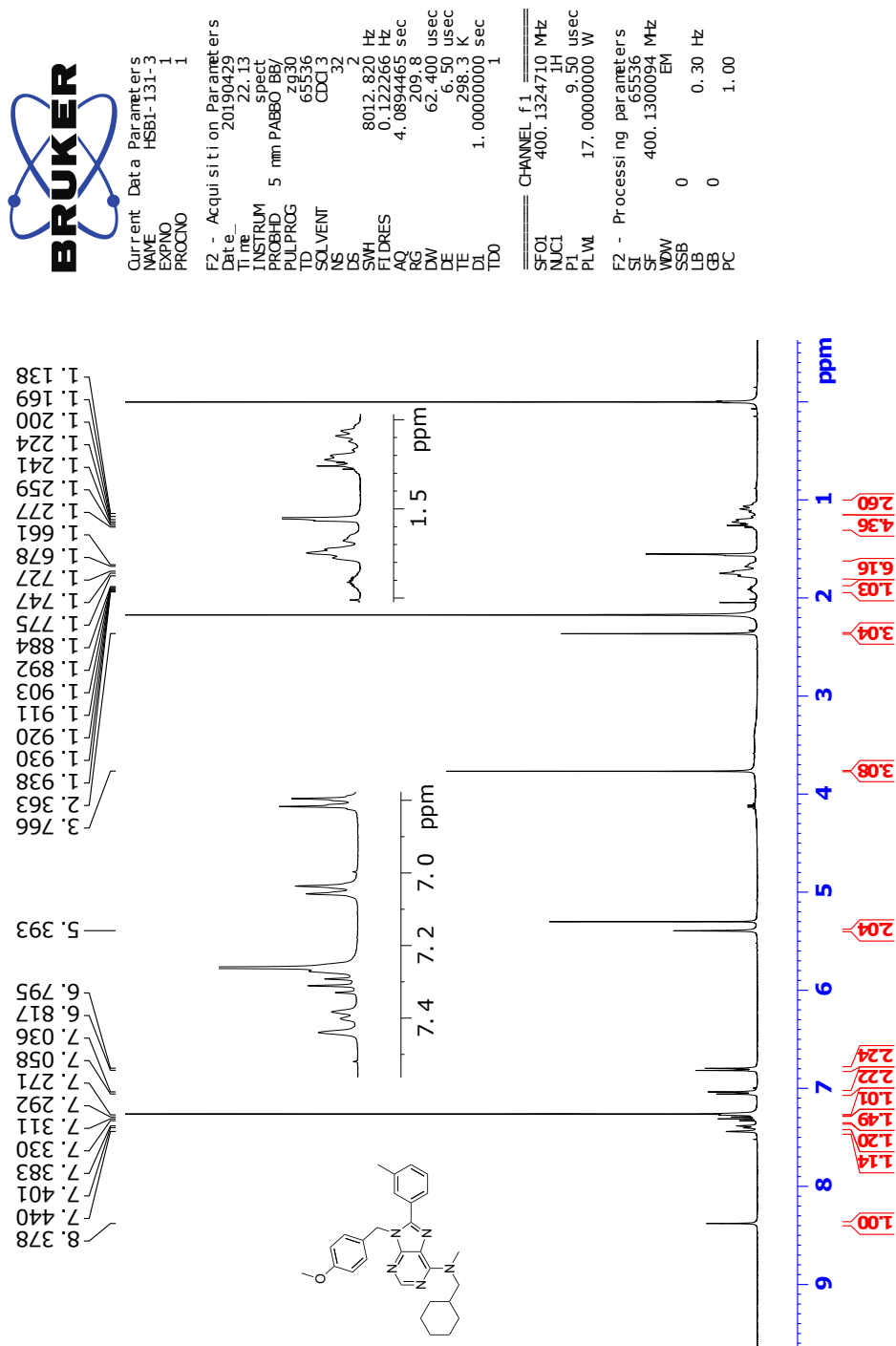


Figure H.1: ¹H NMR spectrum of compound 12 (CDCl₃, 400 MHz).



Current Data Parameters
NAME HSB1-131-3
EXPNO 2
PROCNO 1

F2 - Acquisition Parameters
Date_ 20190429
Time 23.13
INSTRUM spect
PROBHD 5 mm PABBO BB/
PULPROG zgpg30
TD 65536
SOLVENT CDCl3
NS 1024
DS 4
SWH 24038.461 Hz
FIDRES 0.366798 Hz
AQ 1.3631488 sec
RG 209.8
DW 20.800 usec
DE 6.50 usec
TE 298.3 K
D1 2.00000000 sec
D11 0.03000000 sec
TD0 1

==== CHANNEL f1 =====
SF01 100.6228293 MHz
NUC1 13C
P1 9.50 usec
PLW1 71.00000000 W

==== CHANNEL f2 =====
SF02 400.1316005 MHz
NUC2 1H
CPDPRG2 waltz16
PCPD2 90.00 usec
PLW2 17.00000000 W
PLW3 0.18941000 W
PLW4 0.15343000 W

F2 - Processing parameters
SI 32768
SF 100.6127685 MHz
WDW EM
SSB 0
LB 0
GB 0
PC 1.40

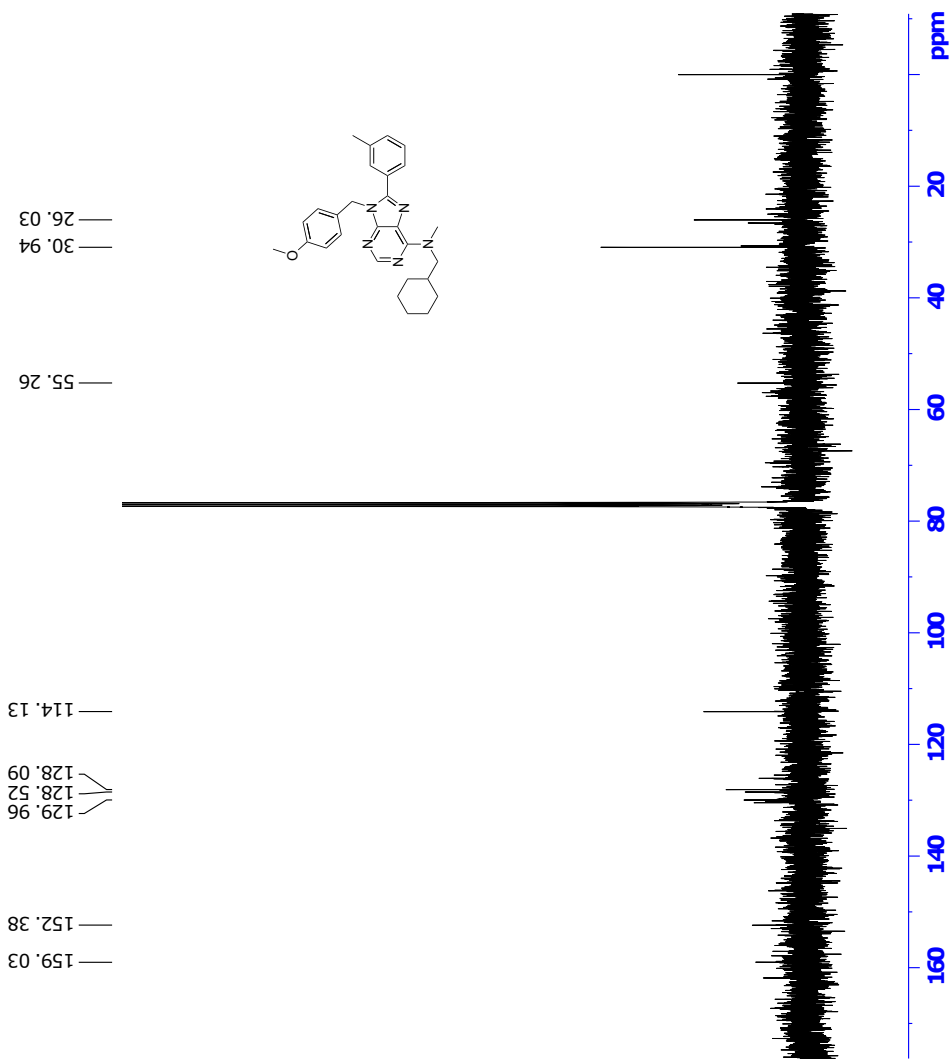


Figure H.2: ^{13}C NMR spectrum of compound **12** (CDCl_3 , 100 MHz).



```

Current Data Parameters
=====
EXPNO      3
PROCNO     1
F2 - Acquisition Parameters
=====
Date_      20160314
Time       23.14
INSTRUM    spect
PROBHD     5 mm PABBO BB/
PULPROG    zgpg30
TD         65536
SOLVENT    CDCl3
NS         1
DS         4
SWH         3875.968 Hz
FIDRES     1.892563 Hz
AQ         0.2641920 sec
RG         64.34
RGW        129.650 usec
DE         6.50 usec
TE         298.3 K
D0         0.0000300 sec
D1         1.9270006 sec
D11        0.0000000 sec
D12        0.0002000 sec
D13        0.00000400 sec
D16        0.00020000 sec
D19        0.00025800 sec
=====
CHANNEL f1
SFO1       400.1316681 MHz
NUC1       13C
P1         9.50 usec
PL1        0.00 dB
PL12       2500.00 usec
PL17       17.00000000 W
PL19       2.28959951 W
=====
GRABM 1]  SHM6Q0.100
P16        0.00 %
P16        1000.00 usec
F1 - Acquisition parameters
=====
NUC1       13C
SFO1       400.1316681 MHz
FIDRES     1.892563 Hz
SOLVENT    CDCl3
SWH         3875.968 Hz
=====
F2 - Processing parameters
=====
SI         1024
SF         400.1300094 MHz
WDW        0 Hz
SSB        0 Hz
GB         0
PC         1.40
=====
F1 - Processing parameters
=====
SI         1024
SF         400.1300094 MHz
WDW        0 Hz
SSB        0 Hz
GB         0

```

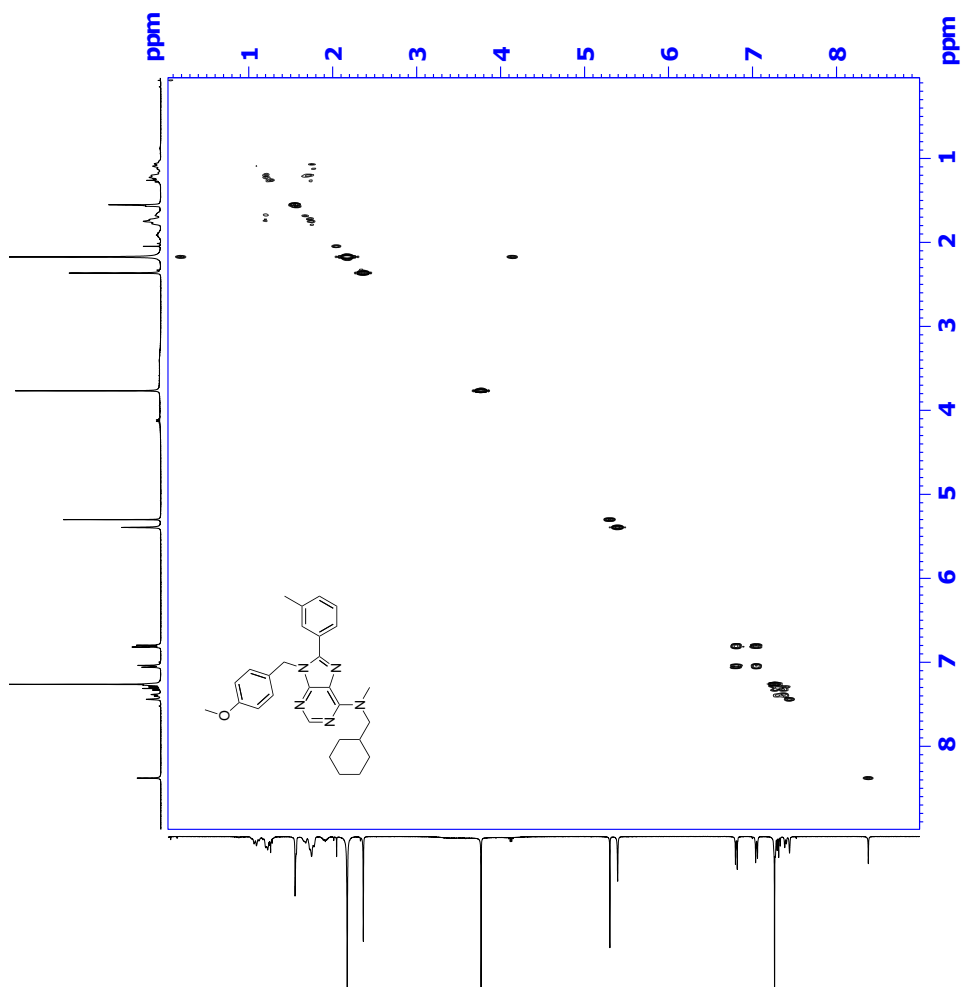


Figure H.3: COSY spectrum of compound **12** (CDCl_3 , 400 MHz).

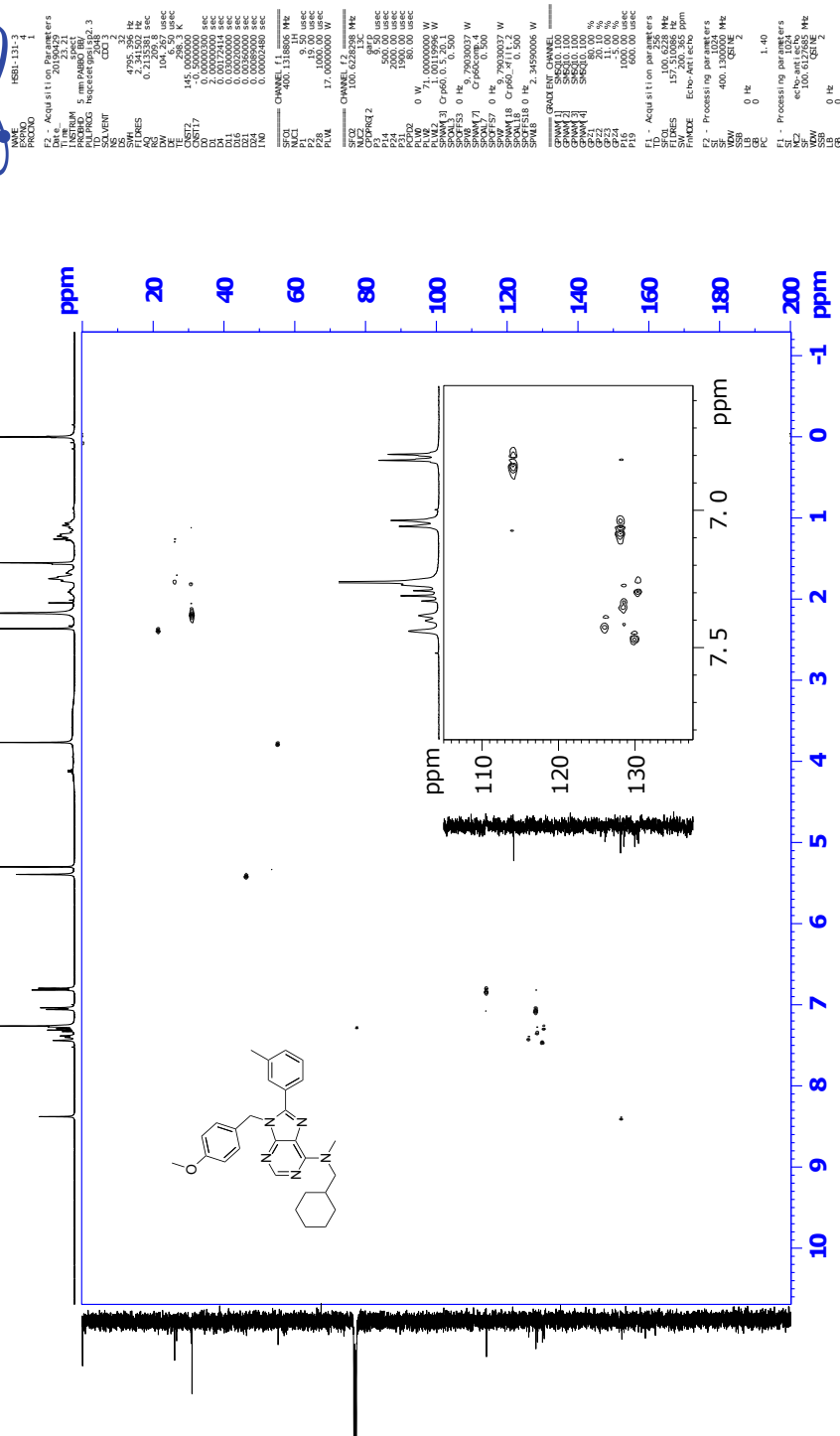


Figure H.4: HSQC spectrum of compound 12 (CDCl₃, 400 MHz).



Current Data Parameters
 Name: HS81-131-3
 PROCNO: 1
 F2 - Acquisition Parameters
 Date_: 20190429
 Time: 10.00
 INSTRUM: spect
 PULPROG: zgpg30
 TD: 65536
 SFO: 400.130094
 NS: 4096
 DS: 4
 SWH: 38705.989 Hz
 FIDRES: 0.3945281 Hz
 AQC: 0.529578 sec
 RG: 2052.8
 DW: 129.000 usec
 DE: 1.900 usec
 TE: 300.2 K
 D1: 0.2983 sec
 D11: 170.000000 sec
 D12: 8.000000 sec
 D13: 0.0000300 sec
 D14: 0.0000000 sec
 D15: 0.8525000 sec
 D16: 0.0000000 sec
 L16: 0.0002240 sec
 ===== CHANNEL f1 =====
 SFO1: 400.130094 MHz
 NUC1: 13C
 P1: 0.311 usec
 PL1: 19.00 usec
 PLW: 17.0000000 W
 ===== CHANNEL f2 =====
 SFO2: 100.628133 MHz
 NUC2: 1H
 P2: 5.50 usec
 PL2: 200.000000 W
 PLW2: 71.0000000 W
 SFOA1: 400.130094 MHz
 SFOA2: 100.628133 MHz
 SFOF57: 0 Hz
 SFOF58: 0 Hz
 SFOF59: 0 Hz
 SFOF60: 0 Hz
 SFOF61: 0 Hz
 SFOF62: 0 Hz
 SFOF63: 0 Hz
 SFOF64: 0 Hz
 SFOF65: 0 Hz
 SFOF66: 0 Hz
 SFOF67: 0 Hz
 SFOF68: 0 Hz
 SFOF69: 0 Hz
 SFOF70: 0 Hz
 SFOF71: 0 Hz
 SFOF72: 0 Hz
 SFOF73: 0 Hz
 SFOF74: 0 Hz
 SFOF75: 0 Hz
 SFOF76: 0 Hz
 SFOF77: 0 Hz
 SFOF78: 0 Hz
 SFOF79: 0 Hz
 SFOF80: 0 Hz
 SFOF81: 0 Hz
 SFOF82: 0 Hz
 SFOF83: 0 Hz
 SFOF84: 0 Hz
 SFOF85: 0 Hz
 SFOF86: 0 Hz
 SFOF87: 0 Hz
 SFOF88: 0 Hz
 SFOF89: 0 Hz
 SFOF90: 0 Hz
 SFOF91: 0 Hz
 SFOF92: 0 Hz
 SFOF93: 0 Hz
 SFOF94: 0 Hz
 SFOF95: 0 Hz
 SFOF96: 0 Hz
 SFOF97: 0 Hz
 SFOF98: 0 Hz
 SFOF99: 0 Hz
 SFOF100: 0 Hz
 ===== GRAB F1 =====
 GRAB1: 100.628133 MHz
 GRAB2: 100.628133 MHz
 GRAB3: 100.628133 MHz
 GRAB4: 100.628133 MHz
 GRAB5: 100.628133 MHz
 GRAB6: 100.628133 MHz
 GRAB7: 100.628133 MHz
 GRAB8: 100.628133 MHz
 GRAB9: 100.628133 MHz
 GRAB10: 100.628133 MHz
 GRAB11: 100.628133 MHz
 GRAB12: 100.628133 MHz
 GRAB13: 100.628133 MHz
 GRAB14: 100.628133 MHz
 GRAB15: 100.628133 MHz
 GRAB16: 100.628133 MHz
 GRAB17: 100.628133 MHz
 GRAB18: 100.628133 MHz
 GRAB19: 100.628133 MHz
 GRAB20: 100.628133 MHz
 GRAB21: 100.628133 MHz
 GRAB22: 100.628133 MHz
 GRAB23: 100.628133 MHz
 GRAB24: 100.628133 MHz
 GRAB25: 100.628133 MHz
 GRAB26: 100.628133 MHz
 GRAB27: 100.628133 MHz
 GRAB28: 100.628133 MHz
 GRAB29: 100.628133 MHz
 GRAB30: 100.628133 MHz
 GRAB31: 100.628133 MHz
 GRAB32: 100.628133 MHz
 GRAB33: 100.628133 MHz
 GRAB34: 100.628133 MHz
 GRAB35: 100.628133 MHz
 GRAB36: 100.628133 MHz
 GRAB37: 100.628133 MHz
 GRAB38: 100.628133 MHz
 GRAB39: 100.628133 MHz
 GRAB40: 100.628133 MHz
 GRAB41: 100.628133 MHz
 GRAB42: 100.628133 MHz
 GRAB43: 100.628133 MHz
 GRAB44: 100.628133 MHz
 GRAB45: 100.628133 MHz
 GRAB46: 100.628133 MHz
 GRAB47: 100.628133 MHz
 GRAB48: 100.628133 MHz
 GRAB49: 100.628133 MHz
 GRAB50: 100.628133 MHz
 GRAB51: 100.628133 MHz
 GRAB52: 100.628133 MHz
 GRAB53: 100.628133 MHz
 GRAB54: 100.628133 MHz
 GRAB55: 100.628133 MHz
 GRAB56: 100.628133 MHz
 GRAB57: 100.628133 MHz
 GRAB58: 100.628133 MHz
 GRAB59: 100.628133 MHz
 GRAB60: 100.628133 MHz
 GRAB61: 100.628133 MHz
 GRAB62: 100.628133 MHz
 GRAB63: 100.628133 MHz
 GRAB64: 100.628133 MHz
 GRAB65: 100.628133 MHz
 GRAB66: 100.628133 MHz
 GRAB67: 100.628133 MHz
 GRAB68: 100.628133 MHz
 GRAB69: 100.628133 MHz
 GRAB70: 100.628133 MHz
 GRAB71: 100.628133 MHz
 GRAB72: 100.628133 MHz
 GRAB73: 100.628133 MHz
 GRAB74: 100.628133 MHz
 GRAB75: 100.628133 MHz
 GRAB76: 100.628133 MHz
 GRAB77: 100.628133 MHz
 GRAB78: 100.628133 MHz
 GRAB79: 100.628133 MHz
 GRAB80: 100.628133 MHz
 GRAB81: 100.628133 MHz
 GRAB82: 100.628133 MHz
 GRAB83: 100.628133 MHz
 GRAB84: 100.628133 MHz
 GRAB85: 100.628133 MHz
 GRAB86: 100.628133 MHz
 GRAB87: 100.628133 MHz
 GRAB88: 100.628133 MHz
 GRAB89: 100.628133 MHz
 GRAB90: 100.628133 MHz
 GRAB91: 100.628133 MHz
 GRAB92: 100.628133 MHz
 GRAB93: 100.628133 MHz
 GRAB94: 100.628133 MHz
 GRAB95: 100.628133 MHz
 GRAB96: 100.628133 MHz
 GRAB97: 100.628133 MHz
 GRAB98: 100.628133 MHz
 GRAB99: 100.628133 MHz
 GRAB100: 100.628133 MHz
 ===== Acquisition parameters =====
 SFO1: 400.130094 MHz
 SFO2: 100.628133 MHz
 SWH1: 38705.989 Hz
 SWH2: 17721.833 ppm
 FIMODE: ECHO-ANTI ECHO
 F2 - Processing parameters
 SF: 400.130094 MHz
 SI: 1024
 SF2: 100.617695 MHz
 SW2: 17721.833 ppm
 LB: 0 Hz
 GB: 0 Hz
 PC: 1.40
 F1 - Processing parameters
 SI: 1024
 SF: 100.617695 MHz
 SW: 17721.833 ppm
 LB: 0 Hz
 GB: 0 Hz

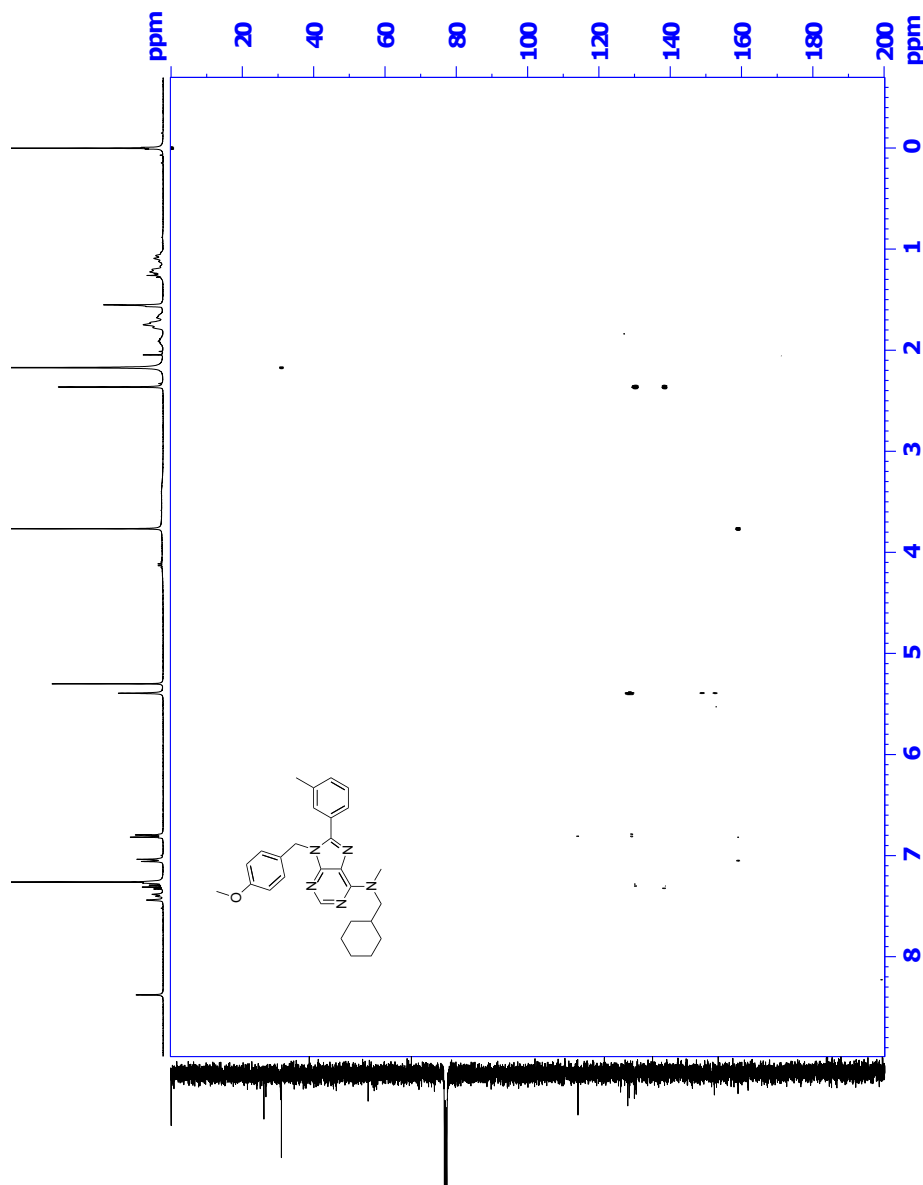


Figure H.5: HMBC spectrum of compound 12 (CDCl₃, 400 MHz).

Single Mass Analysis

Tolerance = 2.0 PPM / DBE: min = -50.0, max = 50.0

Element prediction: Off

Number of isotope peaks used for i-FIT = 3

Monoisotopic Mass, Even Electron Ions

704 formula(e) evaluated with 1 results within limits (all results (up to 1000) for each mass)

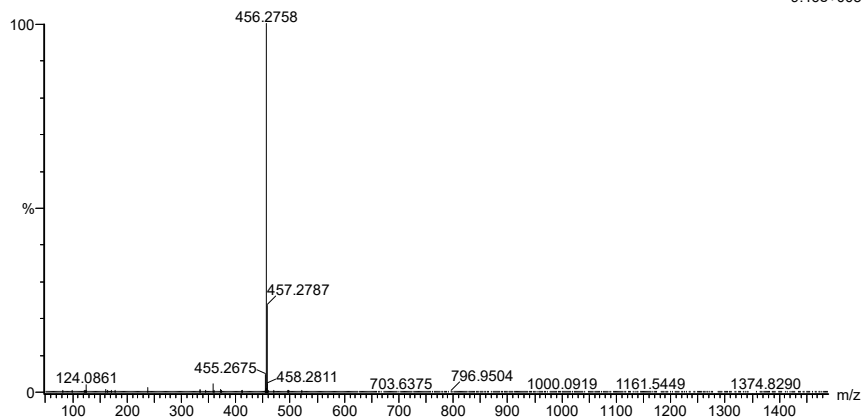
Elements Used:

C: 0-100 H: 0-150 N: 0-6 O: 0-3 Na: 0-1

2019-387 113 (2.225) AM2 (Ar,35000.0,0.00,0.00); Cm (107:114)

1: TOF MS ASAP+

9.46e+005



Minimum: -50.0
Maximum: 5.0 2.0 50.0

Mass	Calc. Mass	mDa	PPM	DBE	i-FIT	Norm	Conf (%)	Formula
456.2758	456.2763	-0.5	-1.1	14.5	899.3	n/a	n/a	C28 H34 N5 O

Figure H.6: MS specter of compound 12.

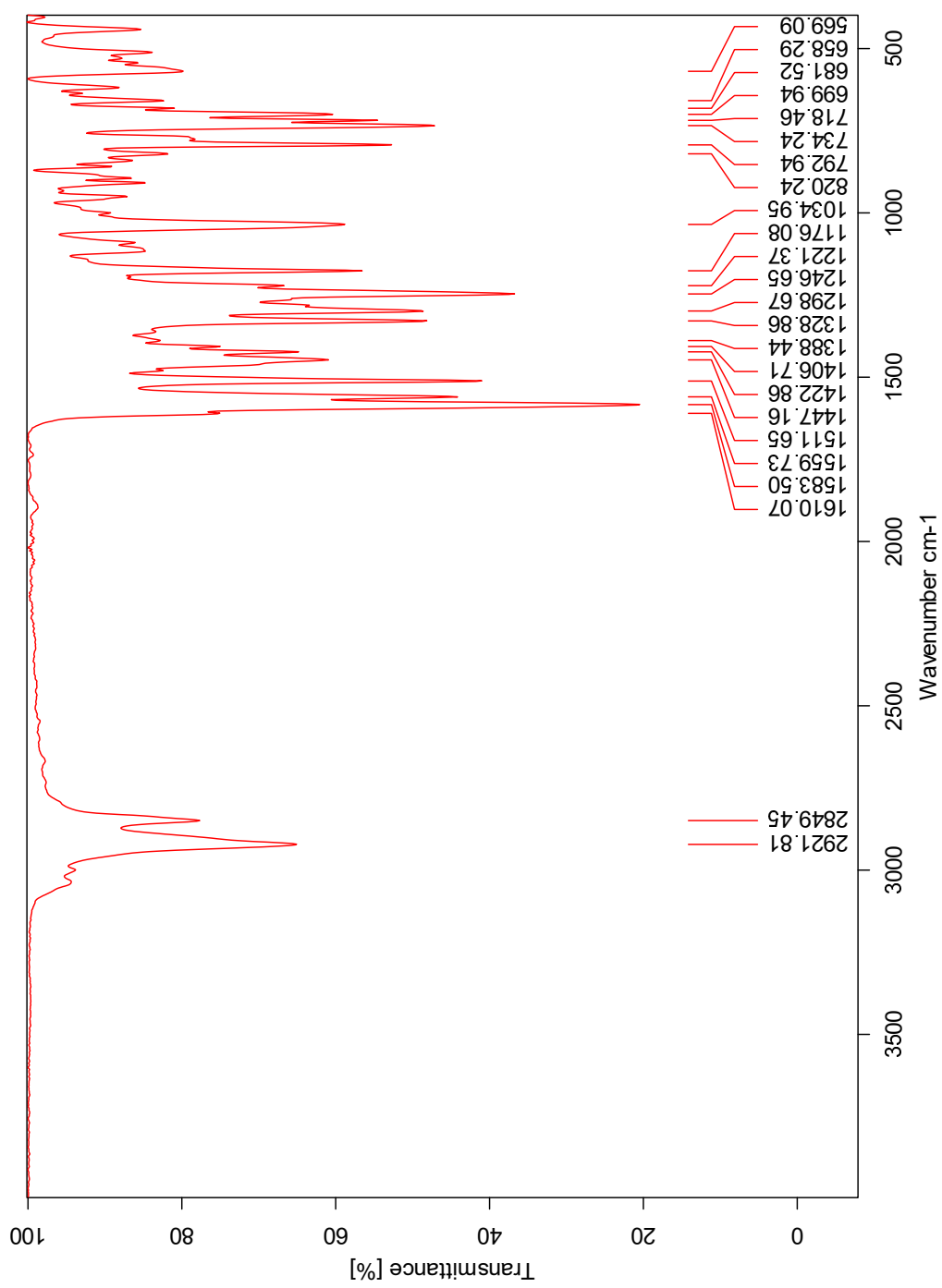


Figure H.7: IR specter of compound 12.

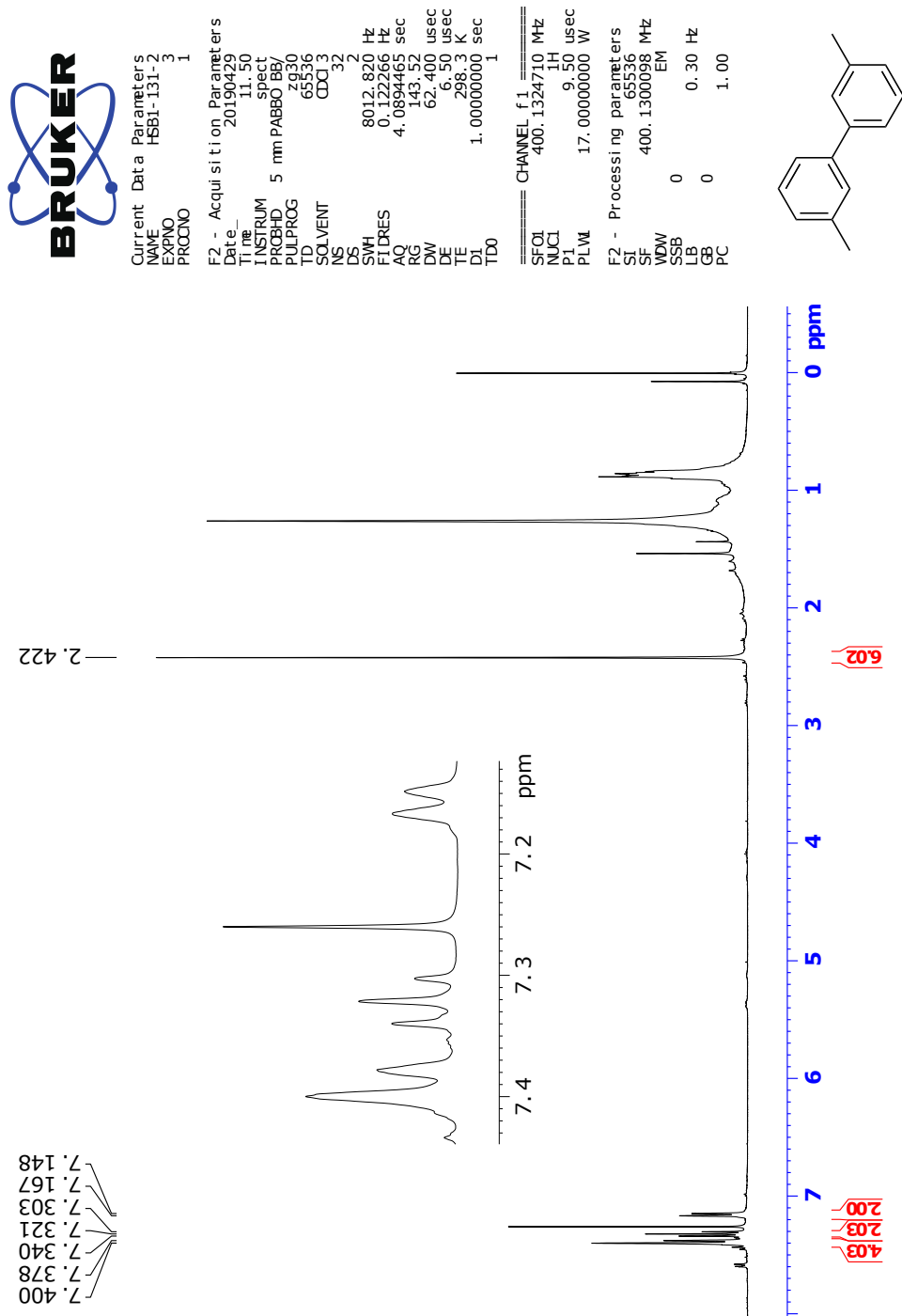


Figure H.8: ^1H NMR spectrum of by-product **13** from the synthesis of compound **12** (CDCl_3 , 400 MHz).

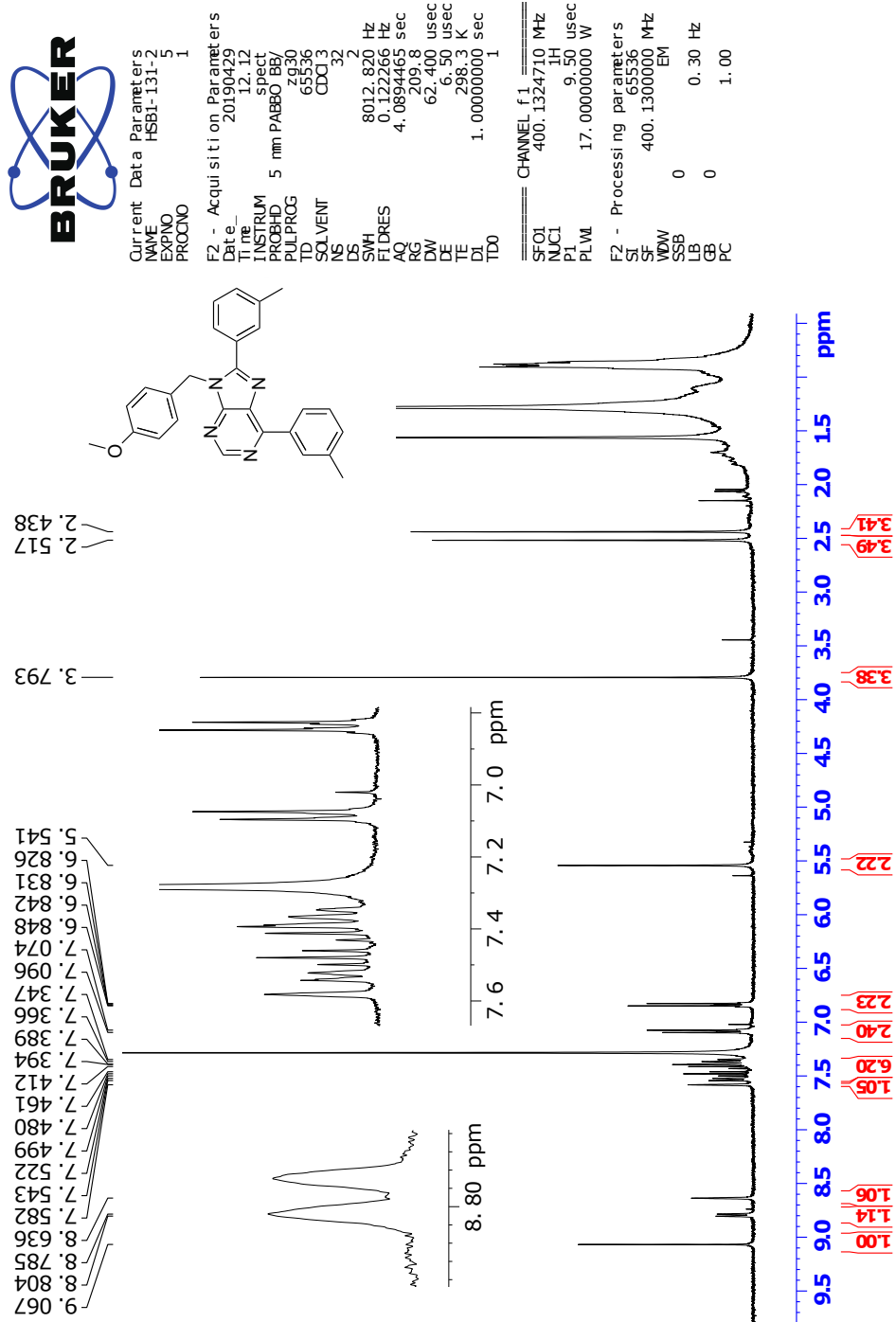


Figure H.9: ^1H NMR spectrum of by-product **14** from the synthesis of compound **12** (CDCl_3 , 400 MHz).

Single Mass Analysis

Tolerance = 3.0 PPM / DBE: min = -50.0, max = 50.0

Element prediction: Off

Number of isotope peaks used for i-FIT = 3

Monoisotopic Mass, Even Electron Ions

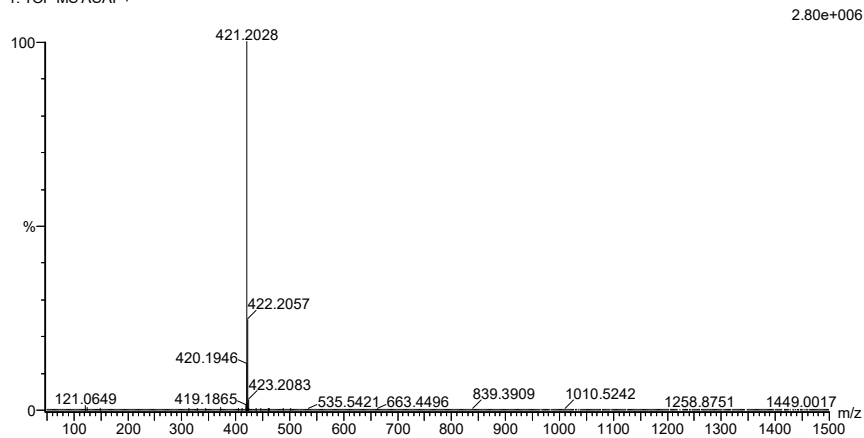
1140 formula(e) evaluated with 1 results within limits (all results (up to 1000) for each mass)

Elements Used:

C: 0-100 H: 0-150 N: 0-5 O: 0-7 Na: 0-1

2019-533 135 (2.636)AM2 (Ar,35000.0,0.00,0.00); Cm (135:139)

1: TOF MS ASAP+



Minimum: -50.0
 Maximum: 5.0 3.0 50.0

Mass	Calc. Mass	mDa	PPM	DBE	i-FIT	Norm	Conf (%)	Formula
421.2028	421.2028	0.0	0.0	17.5	1095.3	n/a	n/a	C27 H25 N4 O

Figure H.10: MS spectrum of by-product **14** from the synthesis of compound **12**.

I Spectroscopic Data for Compound 15

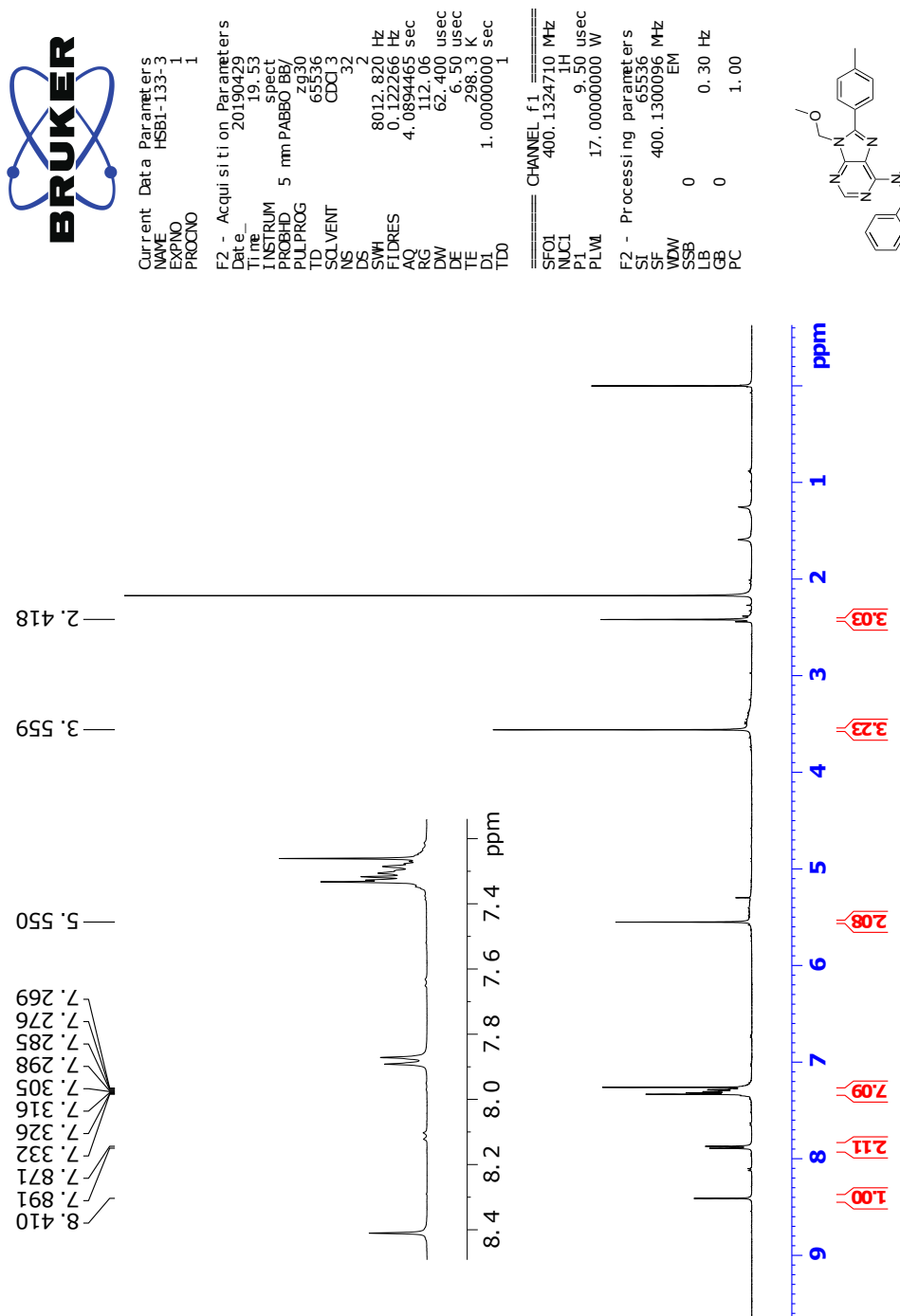


Figure I.1: ¹H NMR specter of compound **15** (CDCl₃, 400 MHz).



Current Parameters
 NAME HSB1-133-3
 EXPNO 2
 PROCNO 1

F2 - Acquisition Parameters

Date_ 20190429
 Time 20.53
 INSTRUM spect
 PROBH 5 mm PABBO BB
 PULPROG zgpg30
 TD 65536
 SOLVENT CDCl3
 NS 1024
 DS 4
 SWH 24038.461 Hz
 FLDRES 0.366798 Hz
 AQ 1.3631488 sec
 RG 209.8
 DW 20.800 usec
 DE 6.50 usec
 TE 298.3 K
 D1 2.000000 sec
 D11 0.03000000 sec
 TDO 1

CHANNEL f1
 SFO1 100.6228293 MHz
 NUC1 13C
 P1 9.50 usec
 PLW1 71.00000000 W

CHANNEL f2
 SFO2 400.1316005 MHz
 NUC2 1H
 CPDPRG2 waltz16
 PCPDZ 90.00 usec
 PLW2 17.00000000 W
 PLW3 0.18941000 W
 PLW4 0.15343000 W

F2 - Processing parameters
 SI 32768
 SF 100.6127685 MHz
 VDW 0
 SSB 0
 LB 0
 GB 0
 PC 1.40

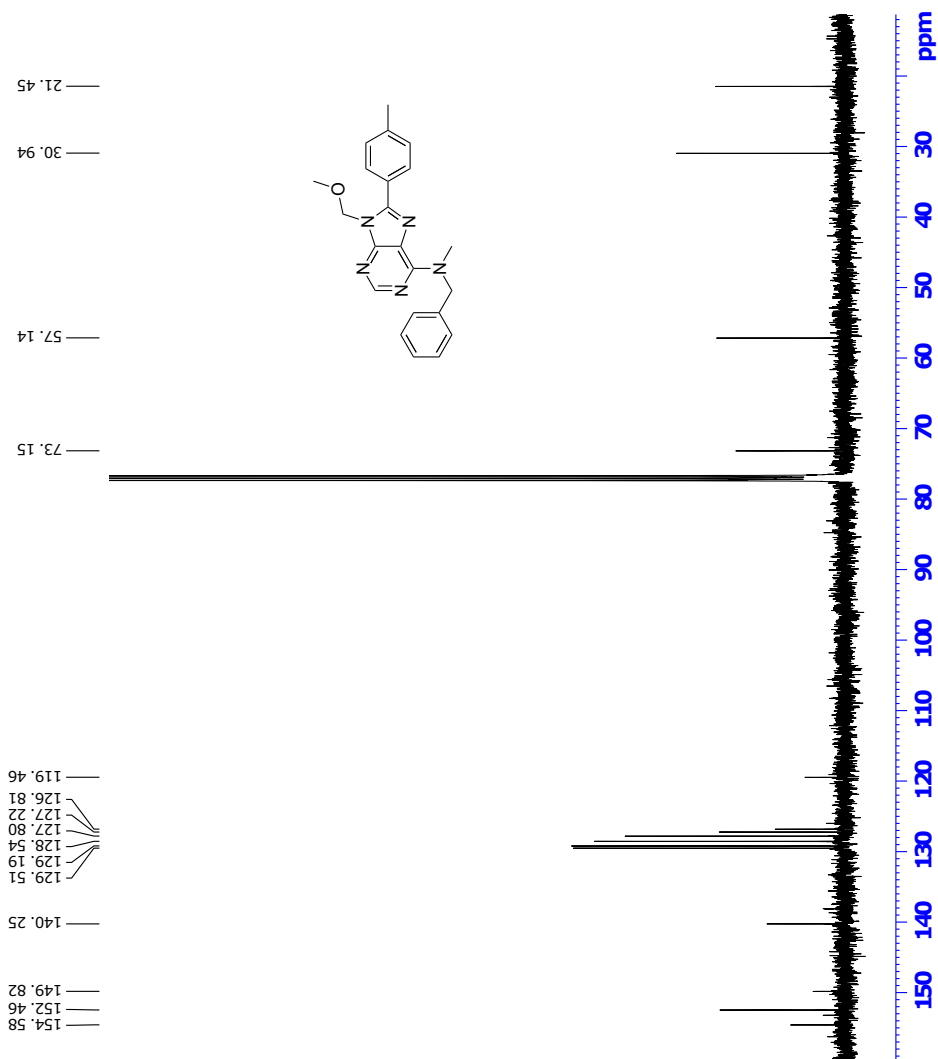


Figure I.2: ^{13}C NMR spectrum of compound **15** (CDCl_3 , 100 MHz).



Current Data Parameters
 NAME HSEI-133-3
 EXPNO 1
 PROCNO 1

F2 - Acquisition Parameters
 Date_ 20190429
 Time 17:55:24
 INSTRUM spect
 PRCBHID 5 mmPA6BBO BBY
 PULPROG cosygpp0qf
 SOLVENT CDCl3
 NS 1
 DS 8
 SWH 3968.7234 Hz
 FIDRES 0.19574234 Hz
 AQ 0.25280480 sec
 RG 0.25280480 sec
 DW 126.000 usec
 DE 19.39 usec
 TE 296.2 K
 D0 0.00000300 sec
 D1 1.93364501 sec
 D11 0.00000000 sec
 D12 0.00000000 sec
 D13 0.00000400 sec
 D16 0.00020000 sec
 INO 0.00025200 sec

==== CHANNEL f1 =====
 SFOL 400.1316796 MHz
 NUC1 1H
 P1 9.50 usec
 PL1 0.00 dB
 P17 2500.00 usec
 PL10 0.00 dB
 PL16 17.00000000 W
 PL100 2.26959991 W

==== GRADIENT CHANNEL =====
 GPMAX11 SINEQ0.100
 GPZ1 10.00 %
 P16 1000.00 usec

F1 - Acquisition parameters
 TD 128
 SFOL 400.1317 MHz
 FIDRES 0.19574234 Hz
 SW 3968.7234 Hz
 FWHM 9.917 ppm
 FWHMDE CF

F2 - Processing parameters
 SI 1024
 SF 400.1300096 MHz
 WDW 0 Hz
 SSB 0 Hz
 GB 0 Hz
 PC 1.40

F1 - Processing parameters
 SI 1024
 SF 400.1300096 MHz
 WDW 0 Hz
 SSB 0 Hz
 LB 0 Hz
 GB 0 Hz

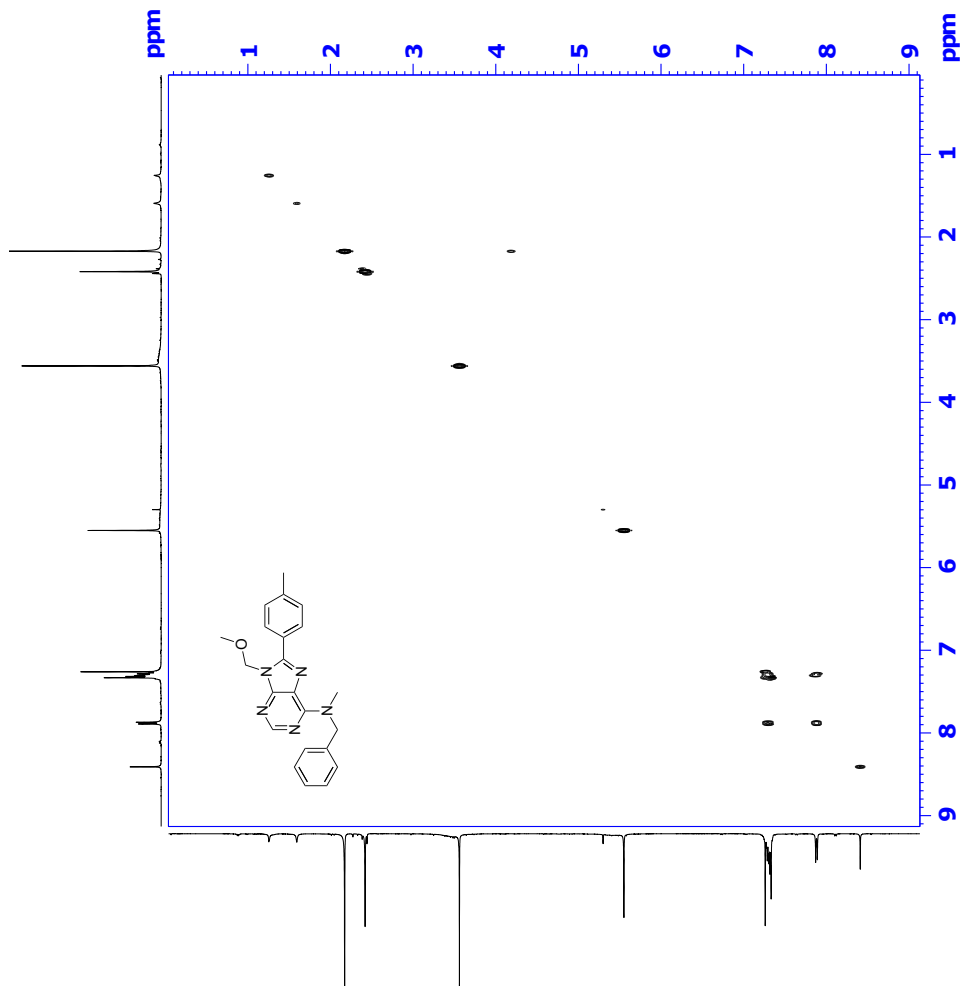


Figure I.3: COSY specter compound **15** (CDCl₃, 400 MHz).



Current Data Parameters
 EXPNO 4
 PROCNO 1
 Data Acquisition Parameters
 Date_ 20190428
 Time 11:55:11
 INSTRUM spect
 F1PRG00 f2prg00
 PULPROG zgpg30
 SFO 400.136460983
 CDCL3
 DS 2
 SWH1 4795.395 Hz
 AQ 0.3138381 sec
 LW 104.767 usec
 TE 300.2 K
 T1 145.736 sec
 CONS17 1.0000000
 D1 2.0000000 sec
 D11 0.0333333 sec
 D21 0.0333333 sec
 D31 0.0333333 sec
 T20 0.0000000 sec
 T30 0.0000000 sec

===== CHANNEL f1 =====
 RQ1 400.136460983 MHz
 P1 9.50 usec
 PC16 17.00000000 usec
 ===== CHANNEL f2 =====
 SFO2 100.626262626 MHz
 CPDPRG2 8pt4
 P14 9.50 usec
 PC14 17.00000000 usec
 P31 100.00 usec
 P32 100.00 usec
 P33 100.00 usec
 P34 80.00 usec
 P35 80.00 usec
 P36 0 W
 P37 1.00000000 W
 P38 1.00000000 W
 P39 1.00000000 W
 P40 1.00000000 W
 SFOF53 0 Hz, 70000007 W
 SFOF57 0 Hz, 70000007 W
 SFOF58 0 Hz, 70000007 W
 SFOF59 0 Hz, 70000007 W
 SFOF60 0 Hz, 70000007 W
 SFOF61 0 Hz, 2489006 W
 SFOF62 0 Hz, 2489006 W
 SFOF63 0 Hz, 70000007 W
 SFOF64 0 Hz, 70000007 W
 SFOF65 0 Hz, 70000007 W
 SFOF66 0 Hz, 70000007 W
 SFOF67 0 Hz, 70000007 W
 SFOF68 0 Hz, 70000007 W
 SFOF69 0 Hz, 70000007 W
 SFOF70 0 Hz, 70000007 W
 SFOF71 0 Hz, 70000007 W
 SFOF72 0 Hz, 70000007 W
 SFOF73 0 Hz, 70000007 W
 SFOF74 0 Hz, 70000007 W
 SFOF75 0 Hz, 70000007 W
 SFOF76 0 Hz, 70000007 W
 SFOF77 0 Hz, 70000007 W
 SFOF78 0 Hz, 70000007 W
 SFOF79 0 Hz, 70000007 W
 SFOF80 0 Hz, 70000007 W
 SFOF81 0 Hz, 70000007 W
 SFOF82 0 Hz, 70000007 W
 SFOF83 0 Hz, 70000007 W
 SFOF84 0 Hz, 70000007 W
 SFOF85 0 Hz, 70000007 W
 SFOF86 0 Hz, 70000007 W
 SFOF87 0 Hz, 70000007 W
 SFOF88 0 Hz, 70000007 W
 SFOF89 0 Hz, 70000007 W
 SFOF90 0 Hz, 70000007 W
 SFOF91 0 Hz, 70000007 W
 SFOF92 0 Hz, 70000007 W
 SFOF93 0 Hz, 70000007 W
 SFOF94 0 Hz, 70000007 W
 SFOF95 0 Hz, 70000007 W
 SFOF96 0 Hz, 70000007 W
 SFOF97 0 Hz, 70000007 W
 SFOF98 0 Hz, 70000007 W
 SFOF99 0 Hz, 70000007 W
 SFOF100 0 Hz, 70000007 W
 SFOF101 0 Hz, 70000007 W
 SFOF102 0 Hz, 70000007 W
 SFOF103 0 Hz, 70000007 W
 SFOF104 0 Hz, 70000007 W
 SFOF105 0 Hz, 70000007 W
 SFOF106 0 Hz, 70000007 W
 SFOF107 0 Hz, 70000007 W
 SFOF108 0 Hz, 70000007 W
 SFOF109 0 Hz, 70000007 W
 SFOF110 0 Hz, 70000007 W
 SFOF111 0 Hz, 70000007 W
 SFOF112 0 Hz, 70000007 W
 SFOF113 0 Hz, 70000007 W
 SFOF114 0 Hz, 70000007 W
 SFOF115 0 Hz, 70000007 W
 SFOF116 0 Hz, 70000007 W
 SFOF117 0 Hz, 70000007 W
 SFOF118 0 Hz, 70000007 W
 SFOF119 0 Hz, 70000007 W
 SFOF120 0 Hz, 70000007 W
 SFOF121 0 Hz, 70000007 W
 SFOF122 0 Hz, 70000007 W
 SFOF123 0 Hz, 70000007 W
 SFOF124 0 Hz, 70000007 W
 SFOF125 0 Hz, 70000007 W
 SFOF126 0 Hz, 70000007 W
 SFOF127 0 Hz, 70000007 W
 SFOF128 0 Hz, 70000007 W
 SFOF129 0 Hz, 70000007 W
 SFOF130 0 Hz, 70000007 W
 SFOF131 0 Hz, 70000007 W
 SFOF132 0 Hz, 70000007 W
 SFOF133 0 Hz, 70000007 W
 SFOF134 0 Hz, 70000007 W
 SFOF135 0 Hz, 70000007 W
 SFOF136 0 Hz, 70000007 W
 SFOF137 0 Hz, 70000007 W
 SFOF138 0 Hz, 70000007 W
 SFOF139 0 Hz, 70000007 W
 SFOF140 0 Hz, 70000007 W
 SFOF141 0 Hz, 70000007 W
 SFOF142 0 Hz, 70000007 W
 SFOF143 0 Hz, 70000007 W
 SFOF144 0 Hz, 70000007 W
 SFOF145 0 Hz, 70000007 W
 SFOF146 0 Hz, 70000007 W
 SFOF147 0 Hz, 70000007 W
 SFOF148 0 Hz, 70000007 W
 SFOF149 0 Hz, 70000007 W
 SFOF150 0 Hz, 70000007 W
 SFOF151 0 Hz, 70000007 W
 SFOF152 0 Hz, 70000007 W
 SFOF153 0 Hz, 70000007 W
 SFOF154 0 Hz, 70000007 W
 SFOF155 0 Hz, 70000007 W
 SFOF156 0 Hz, 70000007 W
 SFOF157 0 Hz, 70000007 W
 SFOF158 0 Hz, 70000007 W
 SFOF159 0 Hz, 70000007 W
 SFOF160 0 Hz, 70000007 W
 SFOF161 0 Hz, 70000007 W
 SFOF162 0 Hz, 70000007 W
 SFOF163 0 Hz, 70000007 W
 SFOF164 0 Hz, 70000007 W
 SFOF165 0 Hz, 70000007 W
 SFOF166 0 Hz, 70000007 W
 SFOF167 0 Hz, 70000007 W
 SFOF168 0 Hz, 70000007 W
 SFOF169 0 Hz, 70000007 W
 SFOF170 0 Hz, 70000007 W
 SFOF171 0 Hz, 70000007 W
 SFOF172 0 Hz, 70000007 W
 SFOF173 0 Hz, 70000007 W
 SFOF174 0 Hz, 70000007 W
 SFOF175 0 Hz, 70000007 W
 SFOF176 0 Hz, 70000007 W
 SFOF177 0 Hz, 70000007 W
 SFOF178 0 Hz, 70000007 W
 SFOF179 0 Hz, 70000007 W
 SFOF180 0 Hz, 70000007 W
 SFOF181 0 Hz, 70000007 W
 SFOF182 0 Hz, 70000007 W
 SFOF183 0 Hz, 70000007 W
 SFOF184 0 Hz, 70000007 W
 SFOF185 0 Hz, 70000007 W
 SFOF186 0 Hz, 70000007 W
 SFOF187 0 Hz, 70000007 W
 SFOF188 0 Hz, 70000007 W
 SFOF189 0 Hz, 70000007 W
 SFOF190 0 Hz, 70000007 W
 SFOF191 0 Hz, 70000007 W
 SFOF192 0 Hz, 70000007 W
 SFOF193 0 Hz, 70000007 W
 SFOF194 0 Hz, 70000007 W
 SFOF195 0 Hz, 70000007 W
 SFOF196 0 Hz, 70000007 W
 SFOF197 0 Hz, 70000007 W
 SFOF198 0 Hz, 70000007 W
 SFOF199 0 Hz, 70000007 W
 SFOF200 0 Hz, 70000007 W

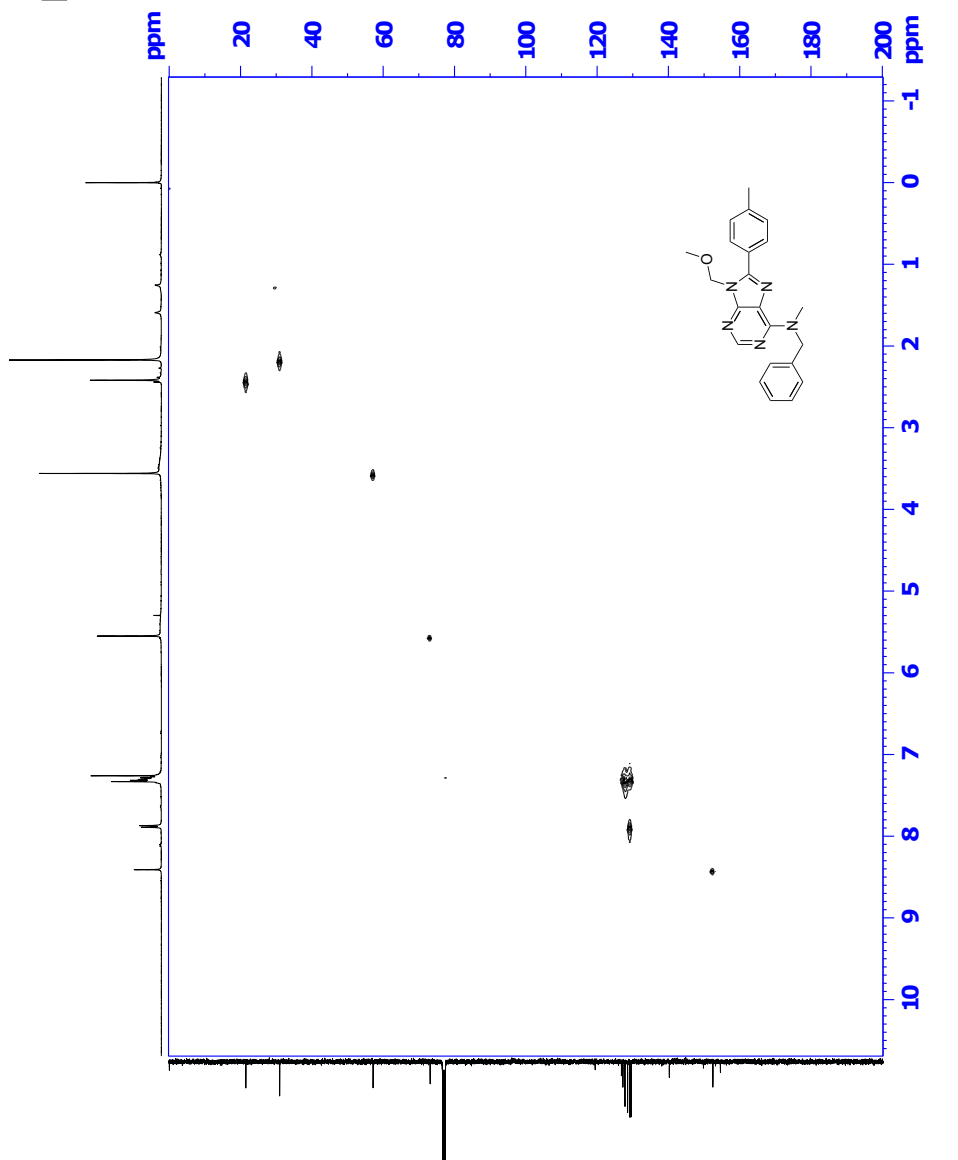


Figure I.4: HSQC spectrum of compound **15** (CDCl₃, 400 MHz).

Single Mass Analysis

Tolerance = 2.0 PPM / DBE: min = -50.0, max = 50.0

Element prediction: Off

Number of isotope peaks used for i-FIT = 3

Monoisotopic Mass, Even Electron Ions

654 formula(e) evaluated with 1 results within limits (all results (up to 1000) for each mass)

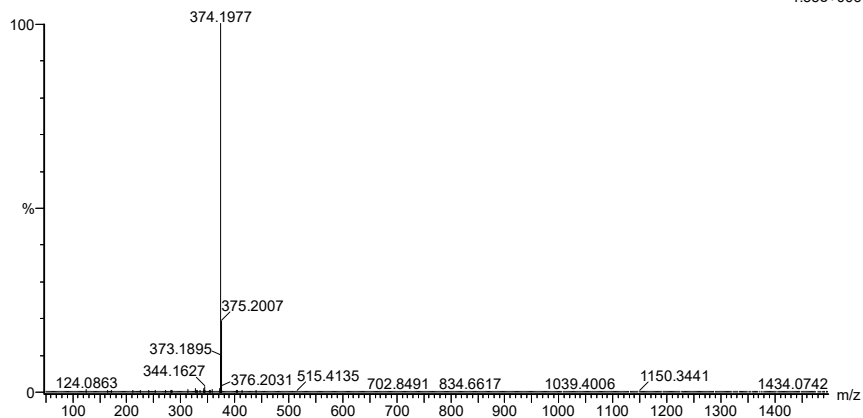
Elements Used:

C: 0-100 H: 0-150 N: 0-6 O: 0-3 Na: 0-1

2019-388 73 (1.449)AM2 (Ar,35000.0,0.00,0.00); Cm (69:79)

1: TOF MS ASAP+

4.35e+006



Minimum: -50.0
Maximum: 5.0 2.0 50.0

Mass	Calc. Mass	Mass mDa	PPM	DBE	i-FIT	Norm	Conf (%)	Formula
374.1977	374.1981	-0.4	-1.1	13.5	1332.5	n/a	n/a	C22 H24 N5 O

Figure I.6: MS specter of compound 15.

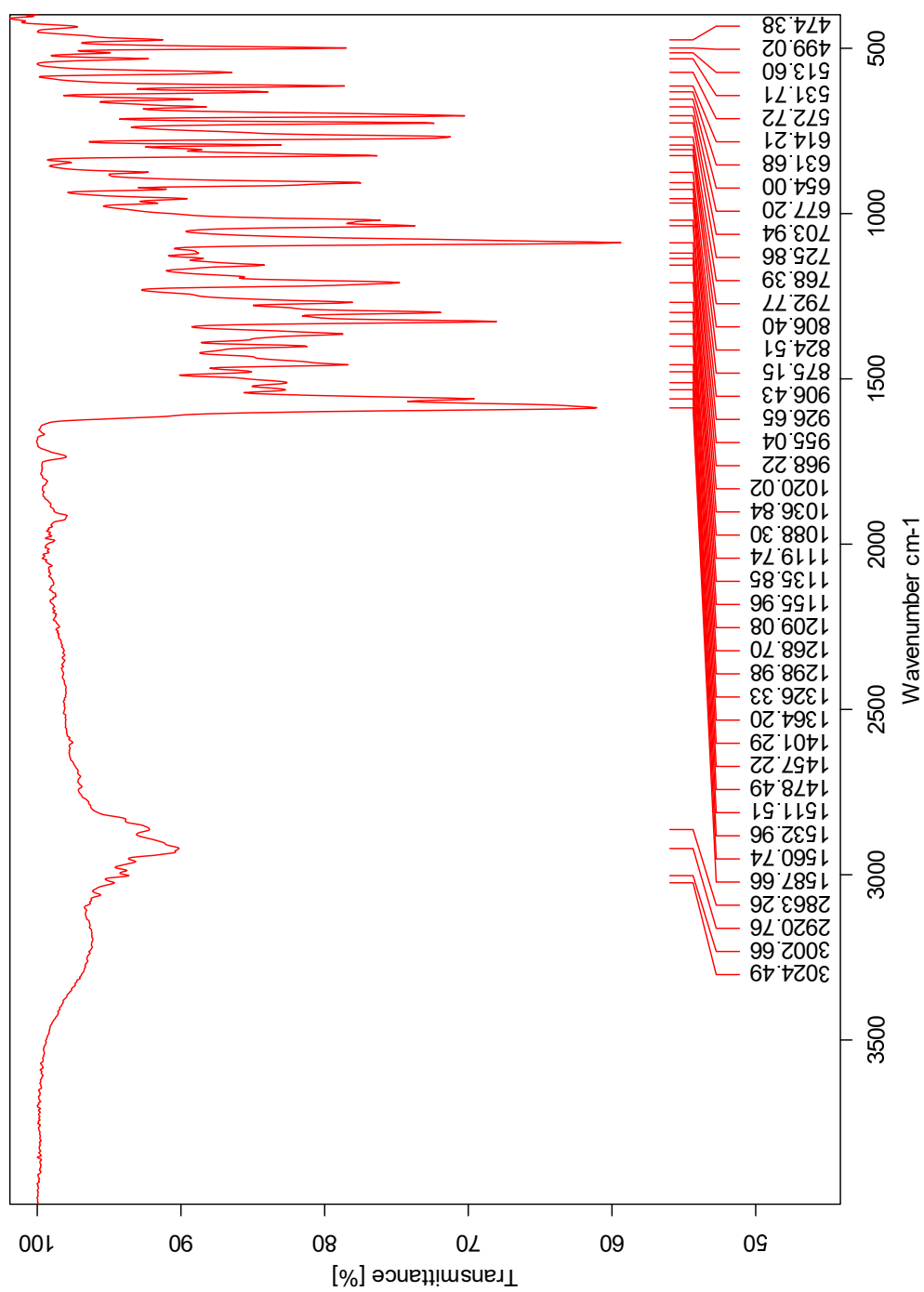


Figure I.7: IR specter of compound 15.

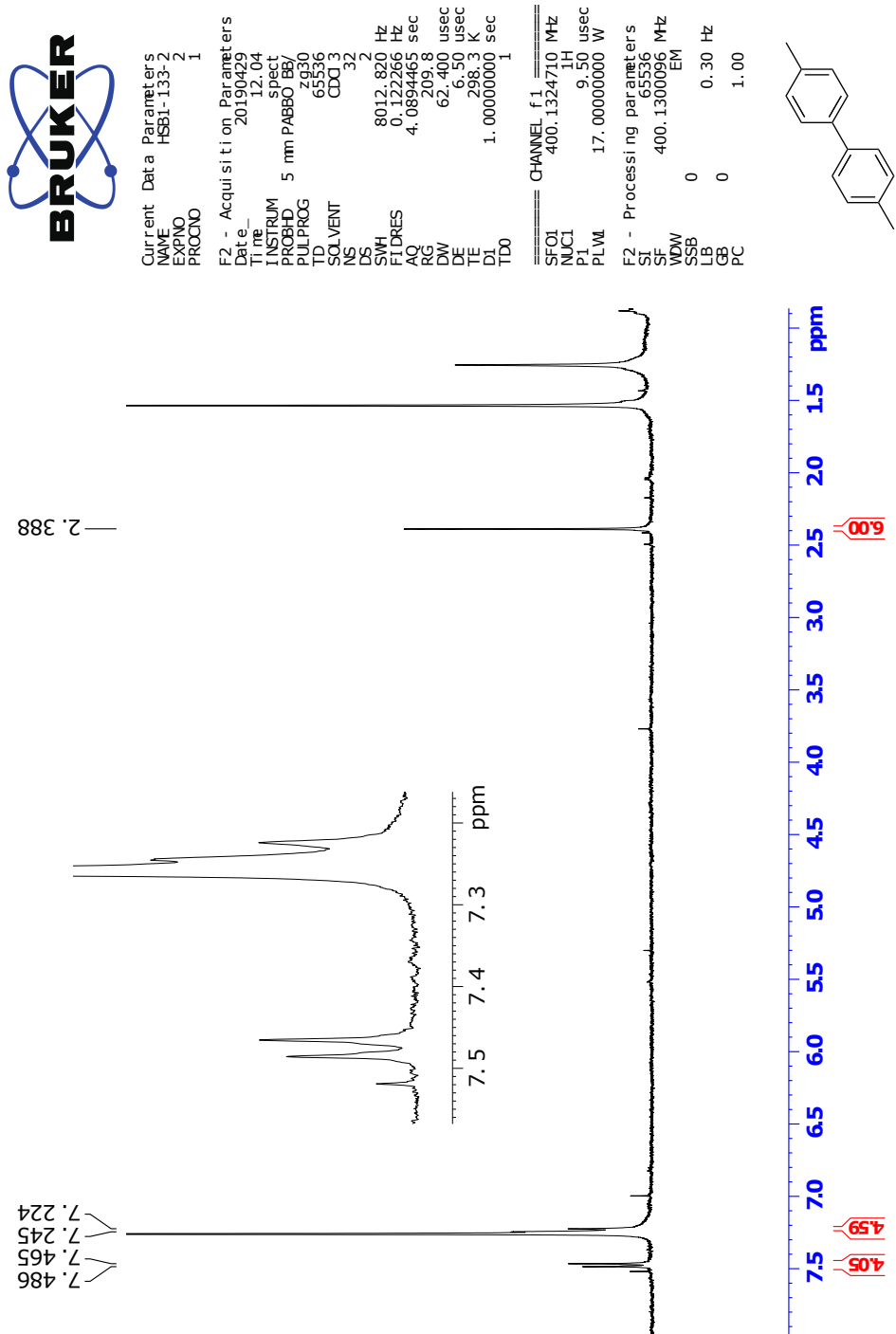


Figure I.8: ^1H NMR spectrum of by-product **16**, from the synthesis of compound **15** (CDCl_3 , 400 MHz).

J Spectroscopic Data for Compound 17

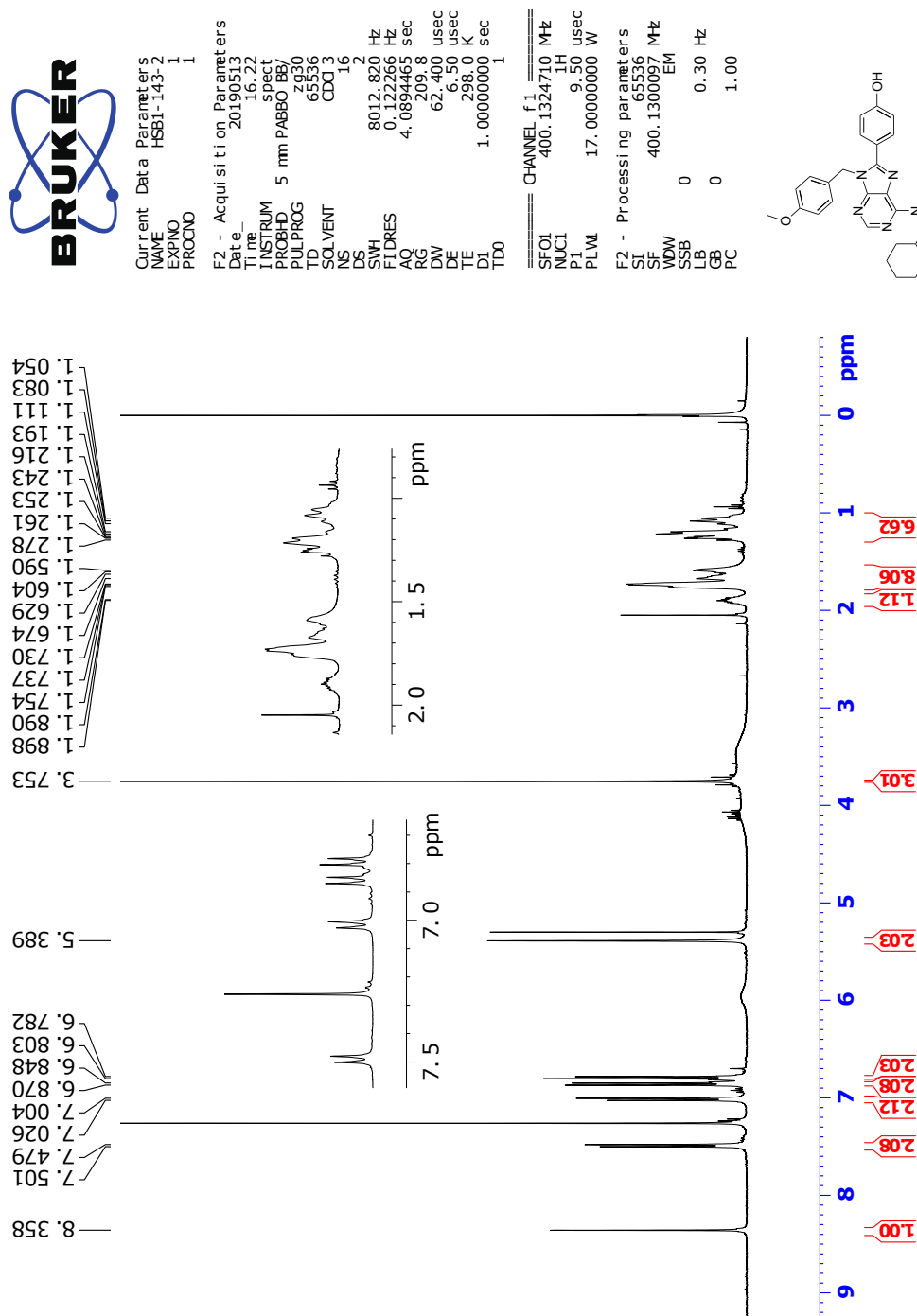


Figure J.1: ¹H NMR specter of compound **17** (CDCl₃, 400 MHz).



Current Data Parameters
NAME HSB1-143-2
EXPNO 2
PROCNO 1

F2 - Acquisition Parameters

Date_ 20190513
Time 17.22
INSTRUM spect
PROBHD 5 mm PABBO BE/
PULPROG zgpg30
TD 65536
SOLVENT CDCl3
NS 1024
DS 4
SWH 24038.461 Hz
FIDRES 0.366708 Hz
AQ 1.3651488 sec
RG 209.8
DW 20.800 usec
DE 6.50 usec
TE 298.0 K
D1 2.0000000 sec
D11 0.0300000 sec
TDO 1

==== CHANNEL f1 =====
SFO1 100.6228293 MHz
NUC1 13C
P1 9.50 usec
PLW1 71.0000000 W

==== CHANNEL f2 =====
SFO2 400.1316005 MHz
NUC2 1H
PCPDPRG2 waltz16
PCPD2 90.00 usec
PLW2 17.0000000 W
PLW2 0.18941000 W
PLW3 0.15343000 W

F2 - Processing parameters
SI 32768
SF 100.6127685 MHz
WDW EM
SSB 0
LB 0
GB 0
PC 1.40

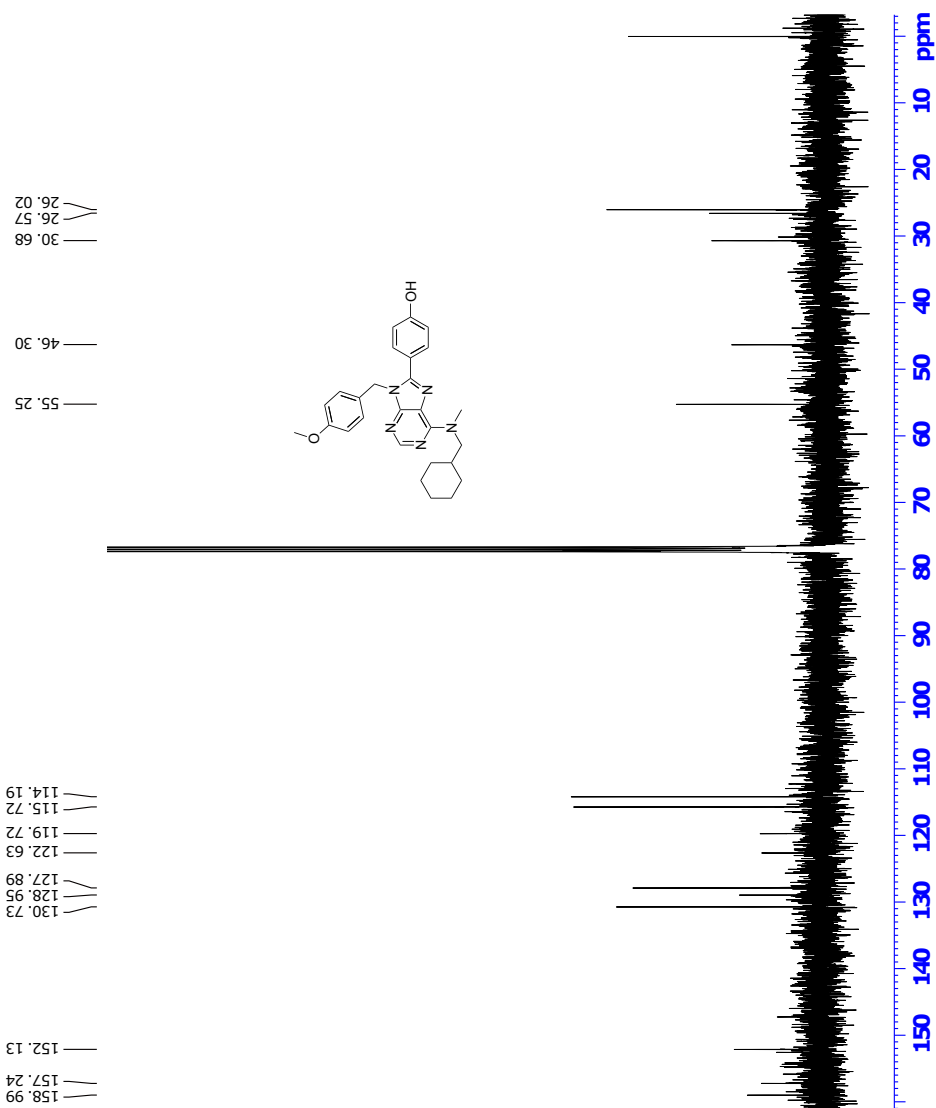


Figure J.2: ^{13}C NMR spectrum of compound **17** (CDCl_3 , 100 MHz).



```

Current Data Parameters
Name: HSEI-143-2
EXPNO: 1
PROCNO: 1

F2 - Acquisition Parameters
Date_ 20110723
Time 17:23
INSTRUM spect
PROBHD 5 mm PA6BBO BB
PULPROG cosygprf18
TD 65536
SOLVENT CDCl3
NS 1
DS 8
SWH 3968.258 Hz
FIDRES 1.937624 Hz
AQ 0.2580480 sec
RG 104.62
DF 126.150 usec
TE 298.0 K
D0 0.0000300 sec
D1 0.3364500 sec
D12 0.0002000 sec
D13 0.0000400 sec
D16 0.0002000 sec
LN0 0.0002500 sec

===== CHANNEL f1 =====
SFO1 400.1316318 MHz
NUC1 1H
P1 9.50 usec
PL1 2500.00 usec
PLW0 17.0000000 W
PLM0 2.2695991 W

===== GRADIENT CHANNEL =====
GPM1 1J
GZ1 10.00 %
P16 1000.00 usec

F1 - Acquisition parameters
SFO1 400.1316318 MHz
FIDRES 62.003967 Hz
SW 9.917 ppm
F1NDC0 QF

F2 - Processing parameters
SI 1024
SF 400.1300097 MHz
WDW QFT
SSB 0 Hz
LB 0
GB 0
PC 1.40

F1 - Processing parameters
SI 1024
SF 400.1300097 MHz
WDW QFT
SSB 0 Hz
LB 0
GB 0
  
```

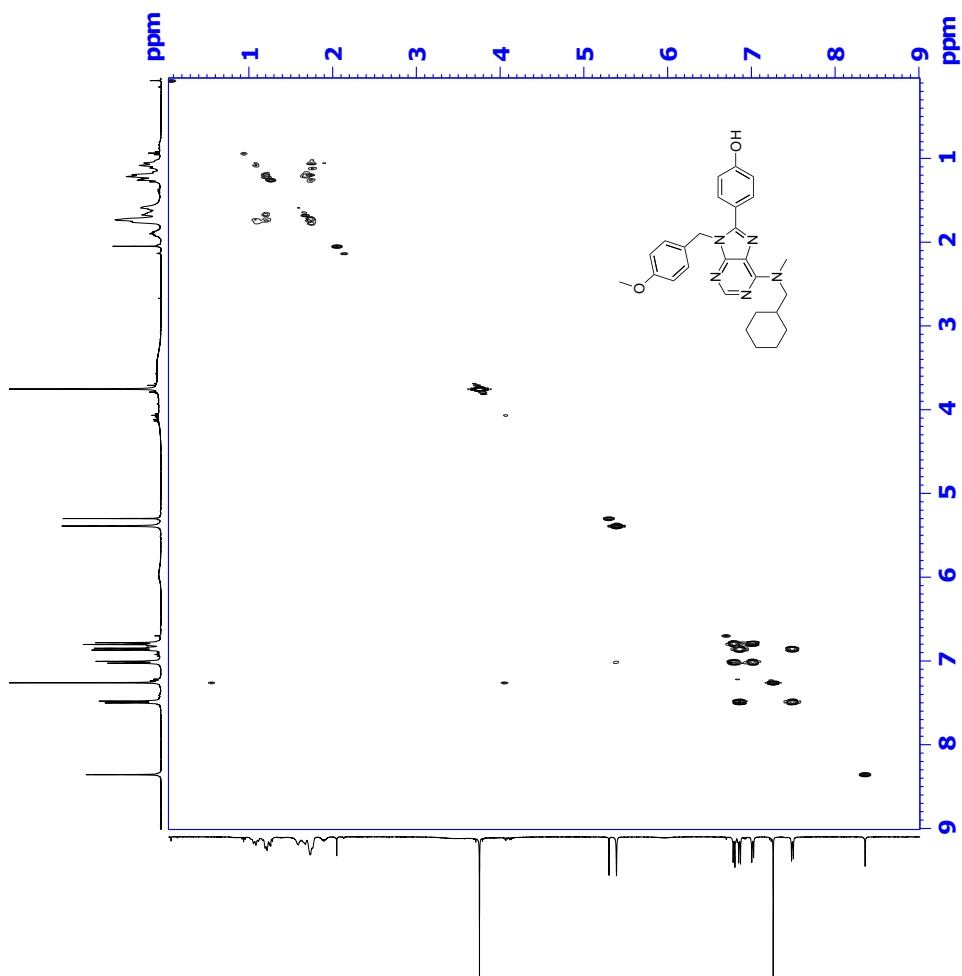


Figure J.3: COSY spectrum of compound 17 (CDCl₃, 400 MHz).

Single Mass Analysis

Tolerance = 2.0 PPM / DBE: min = -50.0, max = 50.0

Element prediction: Off

Number of isotope peaks used for i-FIT = 3

Monoisotopic Mass, Even Electron Ions

1434 formula(e) evaluated with 2 results within limits (all results (up to 1000) for each mass)

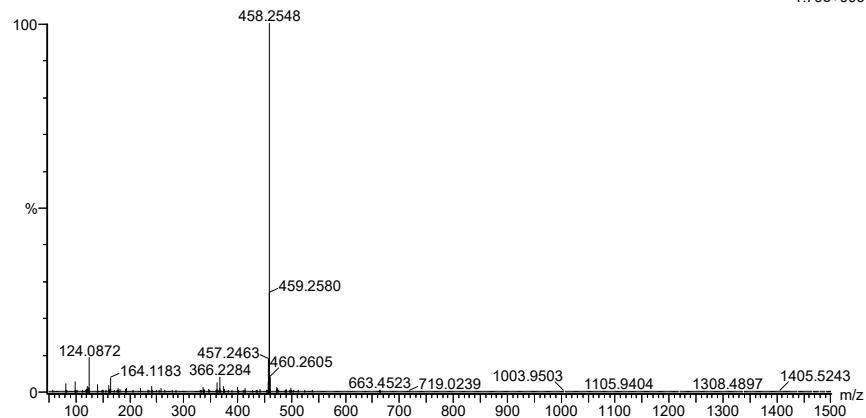
Elements Used:

C: 0-100 H: 0-150 N: 0-10 O: 0-10

2019-470 145 (2,845)AM2 (Ar,35000.0,0.00,0.00); Cm (119:145)

1: TOF MS ASAP+

1.79e+006



Minimum: -50.0
Maximum: 5.0 2.0 50.0

Mass	Calc. Mass	mDa	PPM	DBE	i-FIT	Norm	Conf (%)	Formula
458.2548	458.2543	0.5	1.1	9.5	1086.4	0.111	89.47	C26 H36 N O6
	458.2556	-0.8	-1.7	14.5	1088.6	2.251	10.53	C27 H32 N5 O2

Figure J.6: MS specter of compound 17.

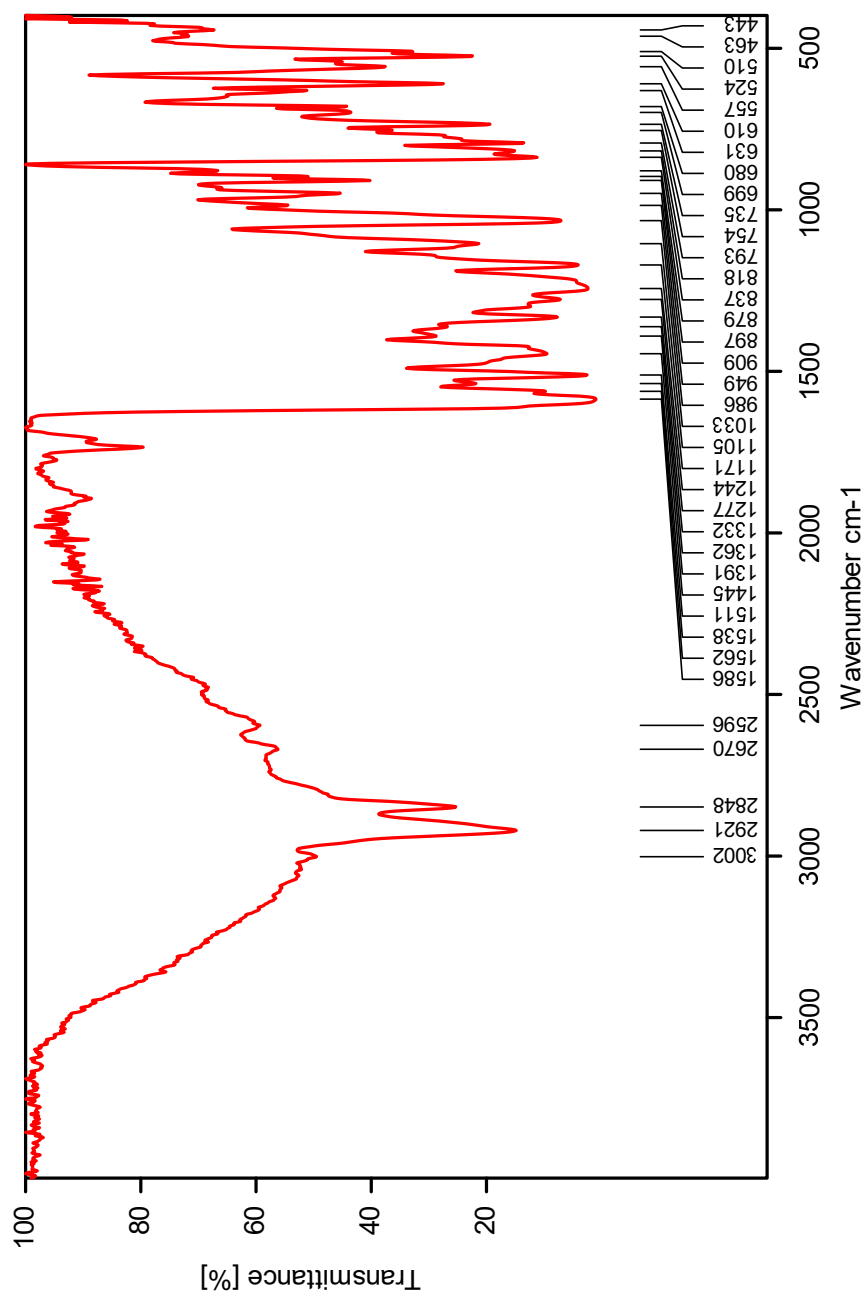


Figure J.7: IR specter of compound 17.

K Spectroscopic Data for Compound 18

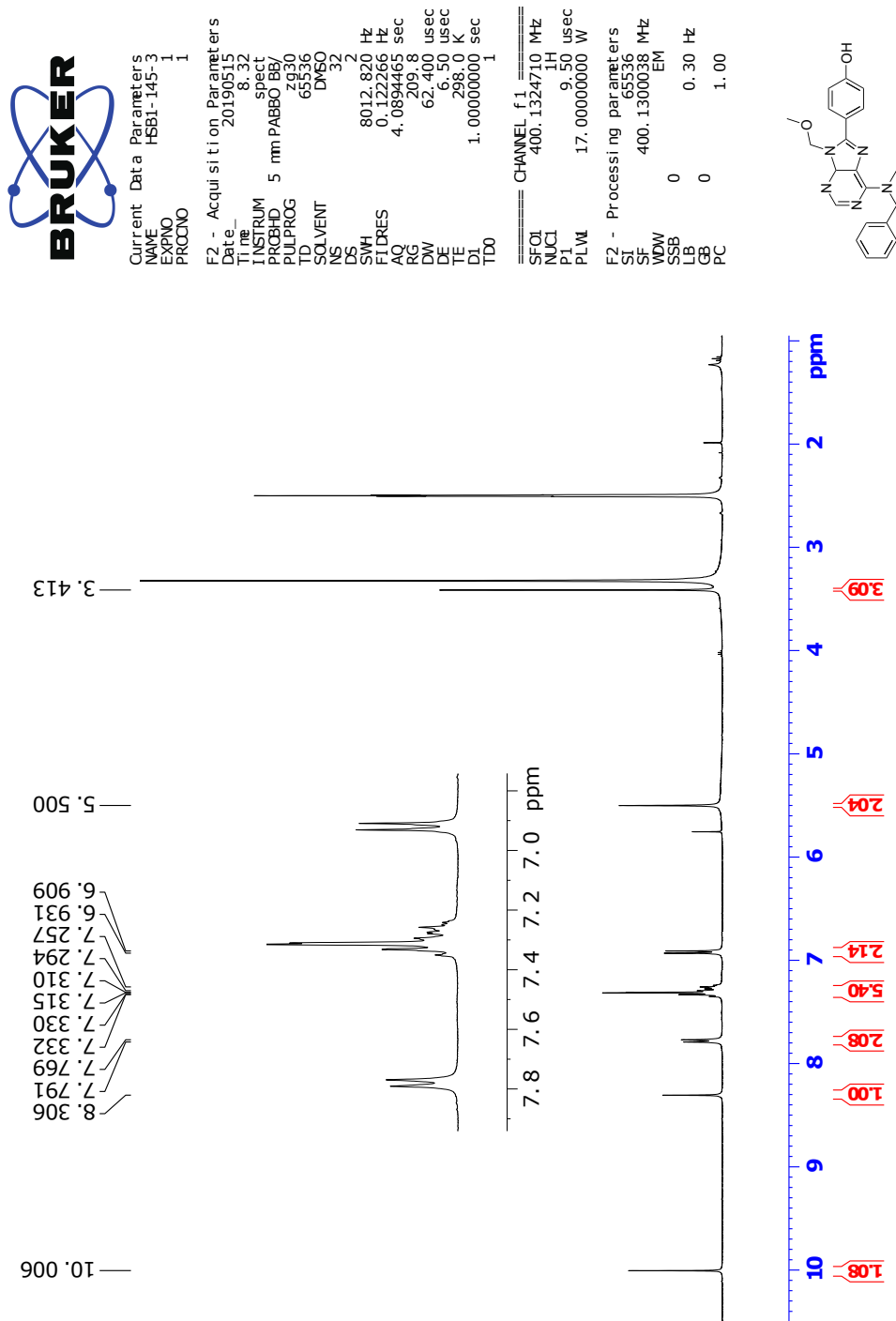


Figure K.1: ¹H NMR specter of compound **18** (DMSO-*d*₆, 400 MHz).

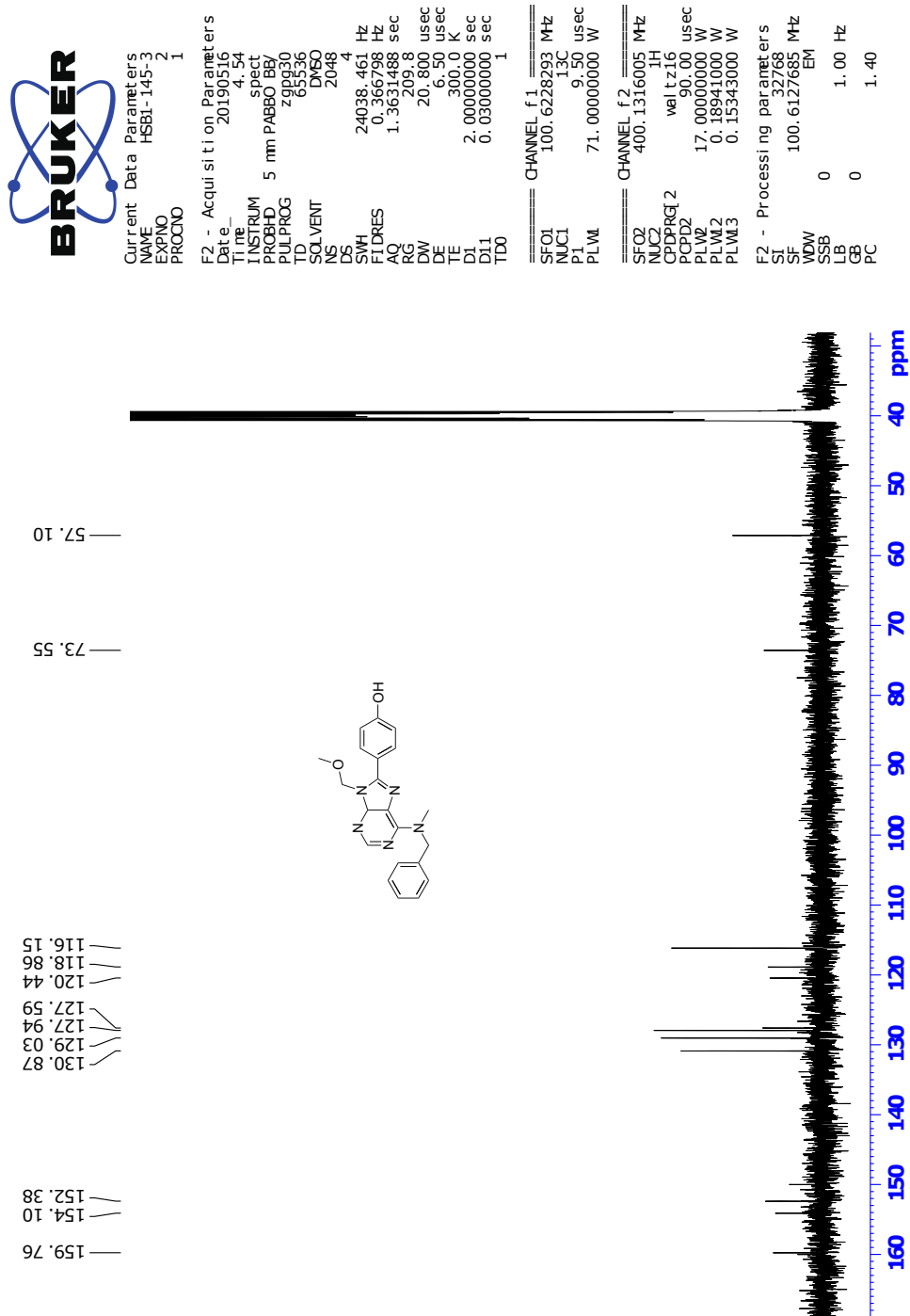


Figure K.2: ¹³C NMR spectrum of compound **18** (DMSO-*d*₆, 100 MHz).



```

Current Data Parameters:
NAME      PAB18-145-3
EXPNO    1
PROCNO   1

F2 - Acquisition Parameters
Date_    20190516
Time     4.55
INSTRUM spect
PROBHD   5 mm PABBO BB
PULPROG zgpg30
TD        65536
SOLVENT  DMSO
NS        1
DS        4
SWH       4201.681 Hz
FIDRES   0.051602 Hz
AQ        0.2437120 sec
RG         655
DE         119.100 usec
TE         300.0 K
D0         0.0000000 sec
DELTA     0.0000000 sec
D11        0.0300000 sec
D12        0.0000000 sec
D13        0.0000000 sec
D16        0.0000000 sec
LW         0.0002860 sec

===== CHANNEL f1 =====
NUC1      13C
P1         9.50 usec
PL1        0.0000000
PL12       2500.00 usec
PL14       17.00 usec
PL16       2.26959991 W

===== GRADIENT CHANNEL =====
GAMMA1    13C
P16        9.50 usec
PL16       1000.00 usec

F1 - Acquisition parameters
SFO1      400.1322 MHz
FIDRES    65.1260 Hz
SW        10.501 ppm
F1MODE    CF

F2 - Processing parameters
SI         1024
SF        400.1300000 MHz
AQ         0.2437120 sec
RG         655
DE         119.100 usec
TE         300.0 K
D0         0.0000000 sec
DELTA     0.0000000 sec
D11        0.0300000 sec
D12        0.0000000 sec
D13        0.0000000 sec
D16        0.0000000 sec
LW         0.0002860 sec

F1 - Processing parameters
SI         1024
SF        400.1300000 MHz
AQ         0.2437120 sec
RG         655
DE         119.100 usec
TE         300.0 K
D0         0.0000000 sec
DELTA     0.0000000 sec
D11        0.0300000 sec
D12        0.0000000 sec
D13        0.0000000 sec
D16        0.0000000 sec
LW         0.0002860 sec
  
```

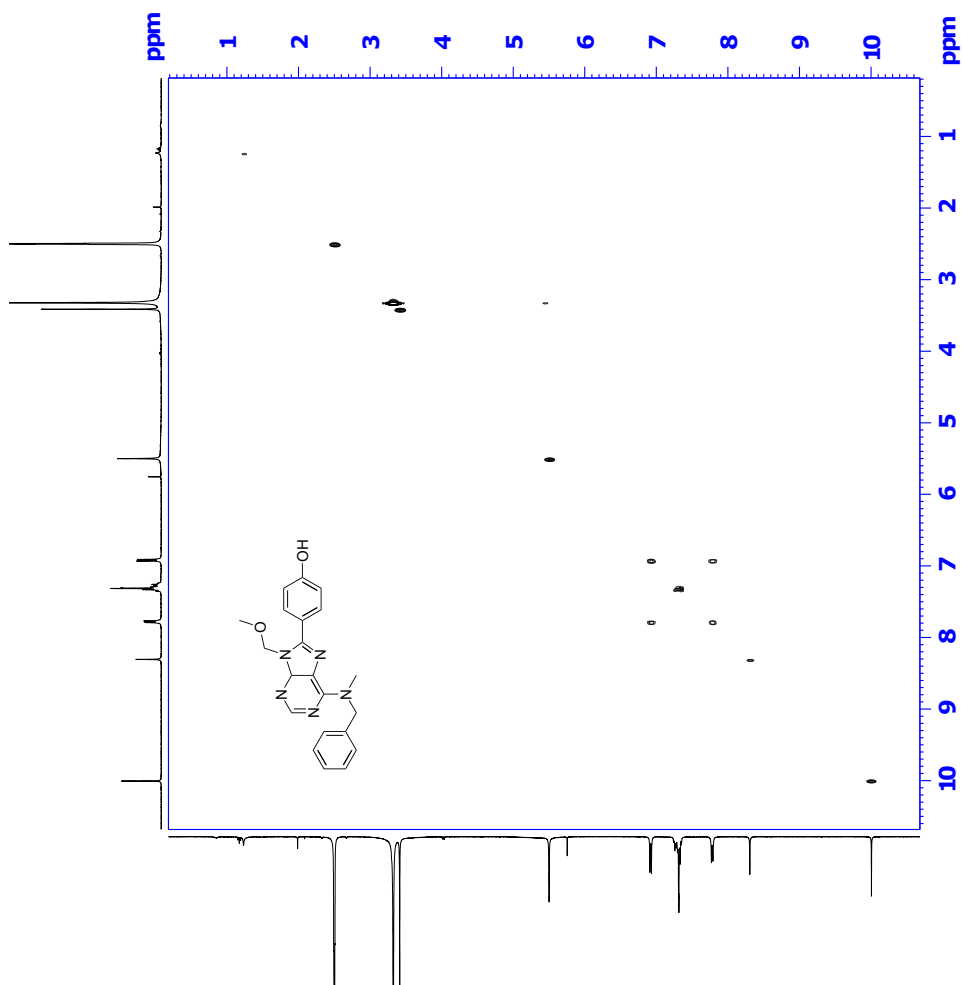


Figure K.3: COSY spectrum compound **18** (DMSO- d_6 , 400 MHz).



```

Current Data Parameters
NAME      HSEI-145-3
EXPNO    1
PROCNO   1
Date_    20190915
Time     5.23
PROBHD   5 mm PABBO BBI
PULPROG  hmczgpr02
TD        65536
SOLVENT  DMSO
DS        4
AQ        16
F1RES    402.861 Hz
F2RES    402.861 Hz
AQ       0.4874240 sec
DELTA    119.000 usec
DE        3.50 usec
TE        120.000000 K
CST16    178.000000
CST17    18.000000
CST18    0.5961156 sec
CST19    1.93856001 sec
DI        0.000000 sec
DI16     0.000000 sec
DI17     0.000000 sec
DI18     0.0002240 sec
LN0       0.0002240 sec

===== CHANNEL f1 =====
NUC1      13C
P1        9.50 usec
PL1       0.0000000 W
PL12      17.0000000 W
===== CHANNEL f2 =====
SFO2     100.628128 MHz
P2        9.50 usec
PL2       0.0000000 W
===== CHANNEL f3 =====
SFO3     400.136199 MHz
P3        9.50 usec
PL3       0.0000000 W
===== CHANNEL f4 =====
SFO4     71.000000 MHz
P4        0.500 usec
PL4       0.0000000 W
===== CHANNEL f5 =====
SFO5     9.79030037 MHz
P5        0.500 usec
PL5       0.0000000 W

===== GRABENT CHANNEL =====
GRAB1    100.628128 MHz
SFO1     100.628128 MHz
P1        9.50 usec
PL1       0.0000000 W
GRAB2    100.628128 MHz
SFO2     100.628128 MHz
P2        9.50 usec
PL2       0.0000000 W
GRAB3    100.628128 MHz
SFO3     100.628128 MHz
P3        9.50 usec
PL3       0.0000000 W
GRAB4    100.628128 MHz
SFO4     100.628128 MHz
P4        9.50 usec
PL4       0.0000000 W
GRAB5    100.628128 MHz
SFO5     100.628128 MHz
P5        9.50 usec
PL5       0.0000000 W

===== Acquisition parameters =====
SFO1     100.628128 MHz
FIDRES   174.386154 Hz
AQ        0.4874240 sec
PR        1.0000000
PULPROG  hmczgpr02
F2 - Processing parameters
SFO2     400.136199 MHz
WDW       SINE
SSB       0
GB        0
PC        1.40

===== Processing parameters =====
F1 - Processing parameters
SFO1     100.628128 MHz
FIDRES   174.386154 Hz
AQ        0.4874240 sec
PR        1.0000000
PULPROG  hmczgpr02
F2 - Processing parameters
SFO2     400.136199 MHz
WDW       SINE
SSB       0
GB        0
PC        1.40
  
```

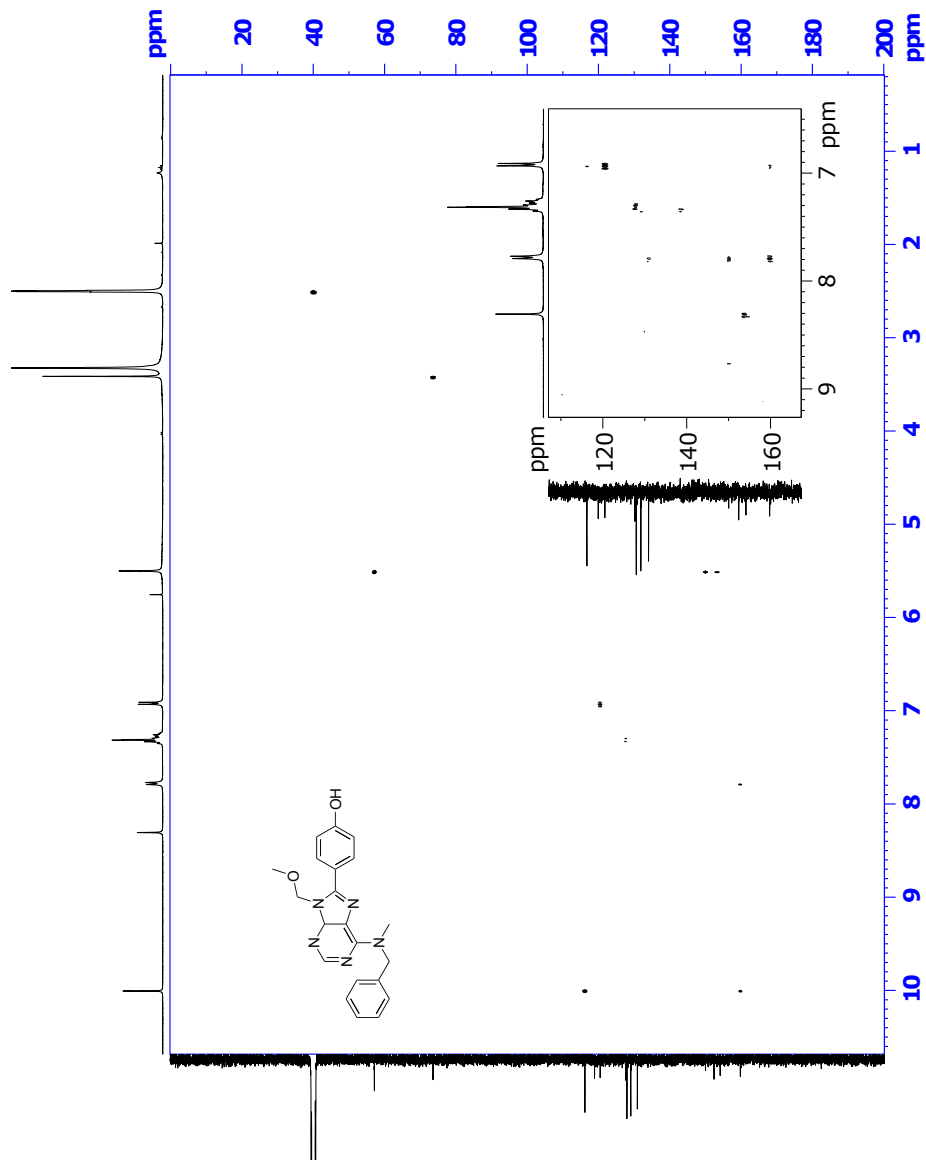


Figure K.5: HMBC spectrum of compound **18** (DMSO- d_6 , 400 MHz).

Single Mass Analysis

Tolerance = 2.0 PPM / DBE: min = -50.0, max = 50.0

Element prediction: Off

Number of isotope peaks used for i-FIT = 3

Monoisotopic Mass, Even Electron Ions

1319 formula(e) evaluated with 1 results within limits (all results (up to 1000) for each mass)

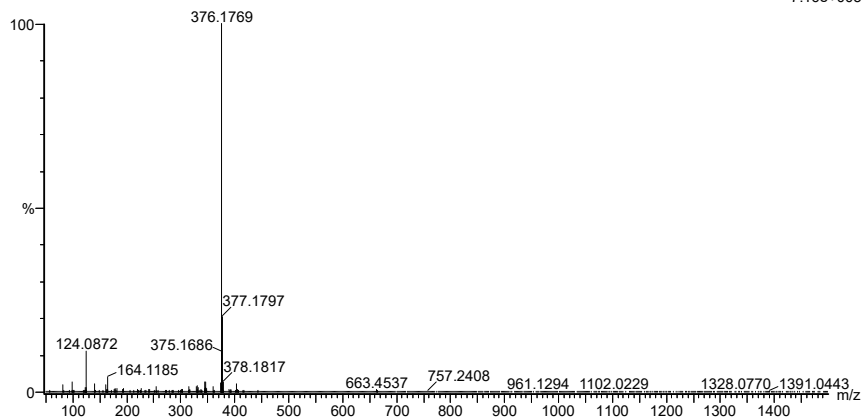
Elements Used:

C: 0-100 H: 0-150 N: 0-10 O: 0-10

2019-471 105 (2.069)AM2 (Ar,35000.0,0.00,0.00); Cm (104:111)

1: TOF MS ASAP+

7.16e+005



Minimum: -50.0
Maximum: 5.0 2.0 50.0

Mass	Calc. Mass	mDa	PPM	DBE	i-FIT	Norm	Conf (%)	Formula
376.1769	376.1773	-0.4	-1.1	13.5	1104.6	n/a	n/a	C21 H22 N5 O2

Figure K.6: MS specter of compound 18.

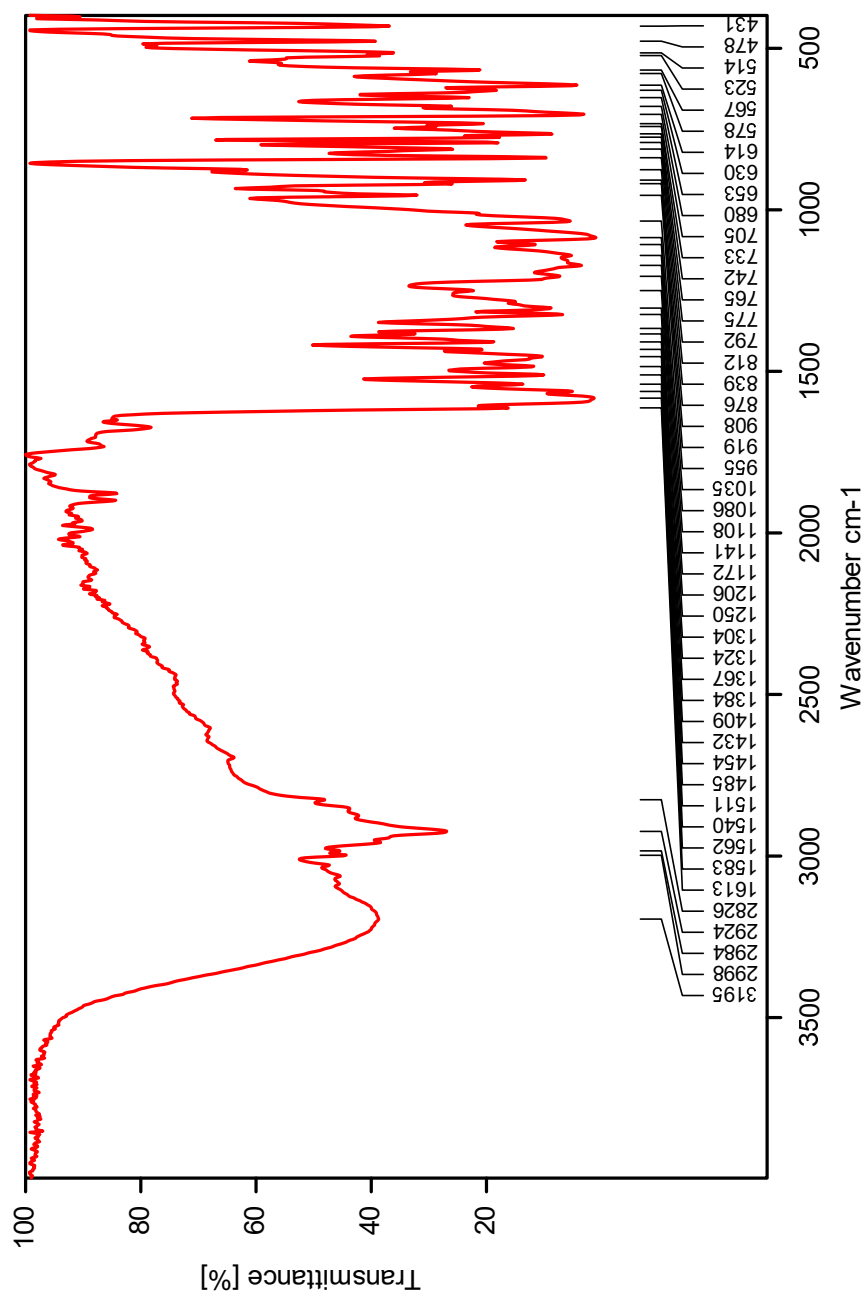


Figure K.7: IR specter of compound 18.

L Spectroscopic Data for Compound 20

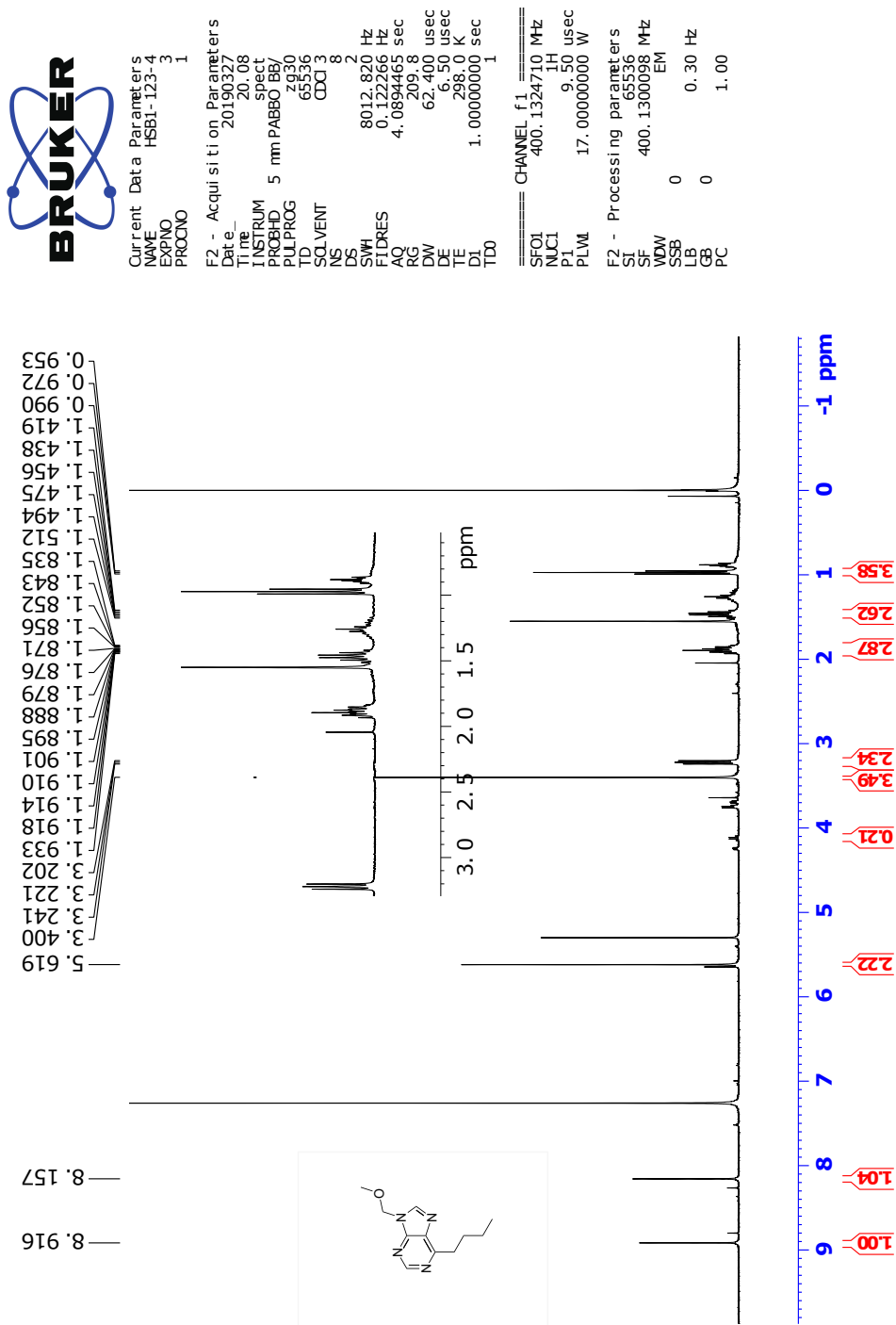


Figure L.1: ¹H NMR specter of compound **20** (CDCl₃, 400 MHz).



Current Data Parameters
NAME HSBI-123-5
EXPNO 3
PROCNO 1

F2 - Acquisition Parameters
Date_ 20190329
Time 7.20
INSTRUM spect
PROBHD 5 mm PABBO BB/
PULPROG zgpg30
TD 65536
SOLVENT CDCl3
NS 2048
DS 4
SWH 24038.461 Hz
FIDRES 0.366798 Hz
AQ 1.3631488 sec
RG 209.8
DW 20.800 usec
TE 6.50 usec
DE 298.0 K
DI 2.0000000 sec
D11 0.0300000 sec
TD0 1

==== CHANNEL f1 ====
SFO1 100.628293 MHz
NUC1 13C
P1 9.50 usec
PLM 71.0000000 W

==== CHANNEL f2 ====
SFO2 400.1316005 MHz
NUC2 1H
CPDPRG2 waltz16
PCPD2 90.00 usec
PLW 17.0000000 W
PLW2 0.18941000 W
PLW3 0.15343000 W

F2 - Processing parameters
SI 32768
SF 100.6127685 MHz
WDW EM
SSB 0
LB 0
GB 0
PC 1.40

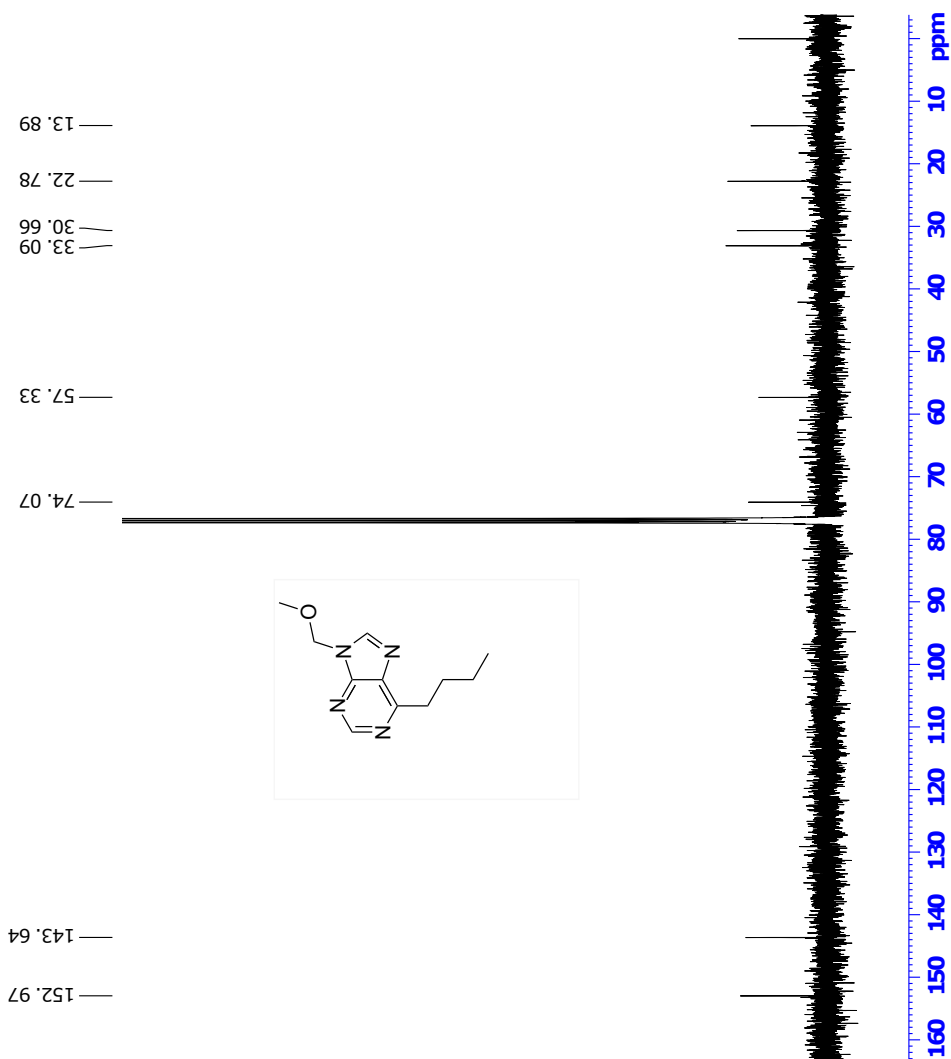


Figure L.2: ^{13}C NMR spectrum of compound **20** (CDCl_3 , 100 MHz).

Single Mass Analysis

Tolerance = 4.0 PPM / DBE: min = -2.0, max = 50.0

Element prediction: Off

Number of isotope peaks used for i-FIT = 3

Monoisotopic Mass, Even Electron Ions

644 formula(e) evaluated with 1 results within limits (up to 50 closest results for each mass)

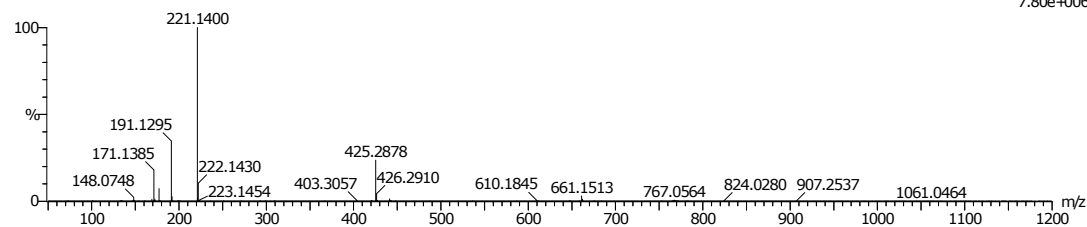
Elements Used:

C: 0-500 H: 0-1000 N: 0-6 O: 0-5 Na: 0-1 Cl: 0-3

svg_20190403_2019_279_34 (0.636)AM2 (Ar,35000.0,0.00,0.00); Cm (31:37)

1: TOF MS ES+

7.80e+006



Mass	Cal. Mass	nDa	PPM	DBE	i-FIT	Norm	Conf (%)	Formula
221.1400	221.1402	-0.2	-0.9	5.5	1689.1	n/a	n/a	C11 H17 N4 O

Figure L.3: MS specter of compound 20.

M Spectroscopic Data for Compound HSB2

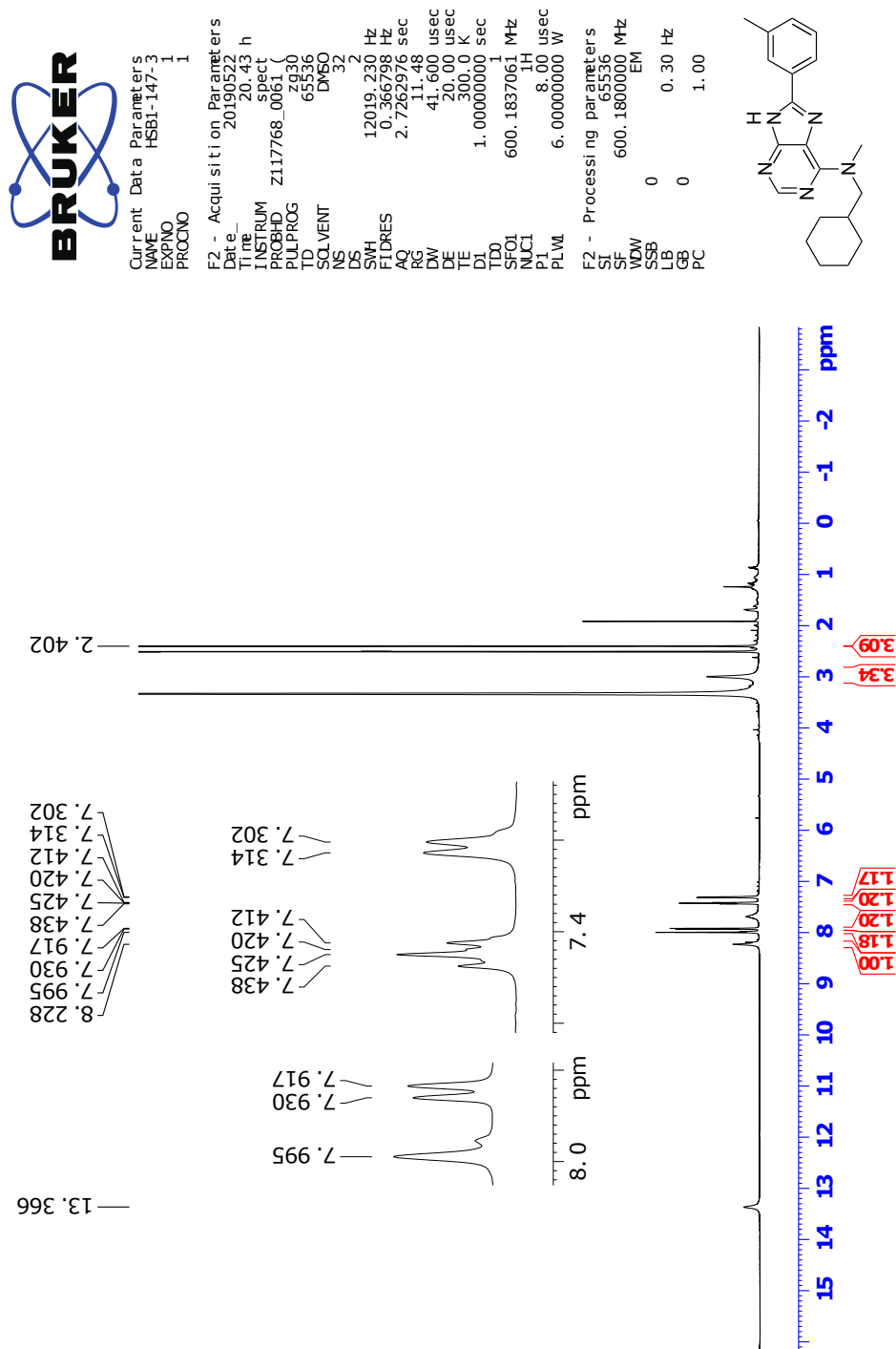


Figure M.1: ¹H NMR specter of compound **HSB2** (DMSO-*d*₆, 600 MHz).

BRUKER

Current Data Parameters
 NAME HSB1-147-3
 EXPNO 2
 PROCNO 1

F2 - Acquisition Parameters
 Date_ 20190522
 Time_ 22.26 h
 INSTRUM spect
 PROBHD Z117768.0061
 PULPROG zgpg30
 TD 81926
 SFO2 125.26
 SOLVENT DMSO
 NS 2048
 DS 4
 SWH 36057.691 Hz
 FIDRES 1.100393 Hz
 AQ 0.9087659 sec
 RG 197.14
 DW 13.867 usec
 DE 18.00 usec
 TE 300.0 K
 D1 2.0000000 sec
 D11 0.0300000 sec
 TD0 1
 SFO1 150.9304719 MHz
 NUC1 13C
 P1 11.40 usec
 PLW 80.0000000 W
 SFO2 600.1824007 MHz
 NUC2 1H
 CPDPRG2 waltz16
 PCPD2 70.00 usec
 PLW2 6.0000000 W
 PLW3 0.07836700 W
 PLW4 0.03941800 W

F2 - Processing parameters
 SF 32768
 WDW EM
 SSB 0
 LB 0
 GB 0
 PC 1.40

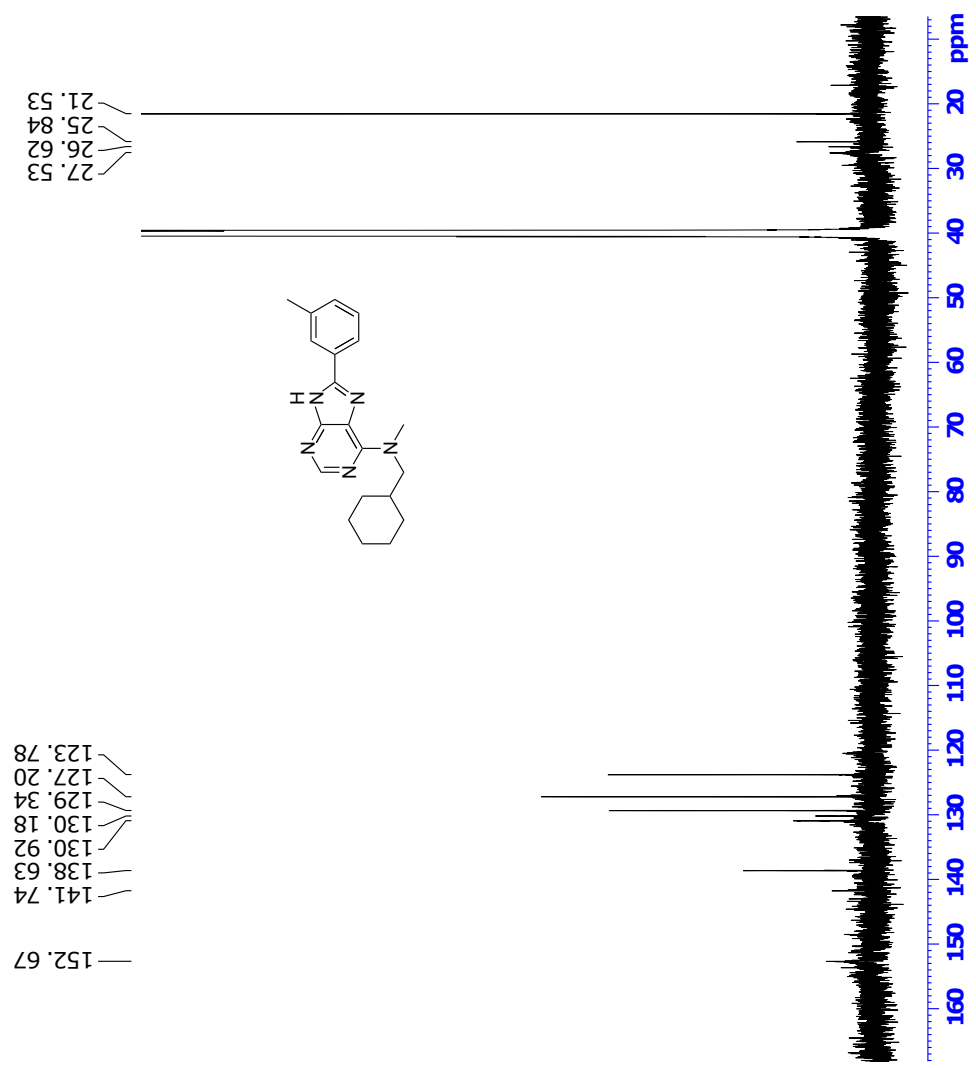


Figure M.2: ¹³C NMR spectrum of compound **HSB2** (DMSO-*d*₆, 150 MHz).



```

Current Data Parameters
NAME      HSB1-147-3
EXPNO    3
PROCNO   1

F2 - Acquisition Parameters
Date_    20190522
Time     22.27 h
INSTRUM  spect
PROBHD   Z11768.0061
PULPROG  zgpg30
TD        65536
SOLVENT  DMSO
NS        1
DS        4
SWH       9615.385 Hz
FIDRES    0.3910024 Hz
AQ         0.1064960 sec
RG         56.06
DW         52.000 usec
DE         300.0 K
TE         300.0 K
D0         0.00000300 sec
D1         2.02457585 sec
D11        0.0300000 sec
D12        0.0000000 sec
D13        0.0000000 sec
D14        0.0000000 sec
D15        0.0000000 sec
D16        0.0002000 sec
IND        0.00010400 sec
TD0        1
SFO1      600.1843671 MHz
NUC1       13C
P0         8.00 usec
P1         8.00 usec
P17        2500.00 usec
PL1        0.0000000 W
PL12       0.0000000 W
PL14       0.0000000 W
PREAMP    GPRNAM(1)
GRZ1       10.00 %
P16        1000.00 usec

F1 - Acquisition parameters
TD         128
SFO1      600.1844 MHz
FIDRES    150.240387 Hz
SW         16.021 ppm
F1MODE    CF

F2 - Processing parameters
SI         1024
SF         600.1800000 MHz
SSB        0 Hz
LB         0
GB         0
PC         1.40

F1 - Processing parameters
SI         1024
SF         600.1800000 MHz
SSB        0 Hz
LB         0
GB         0
  
```

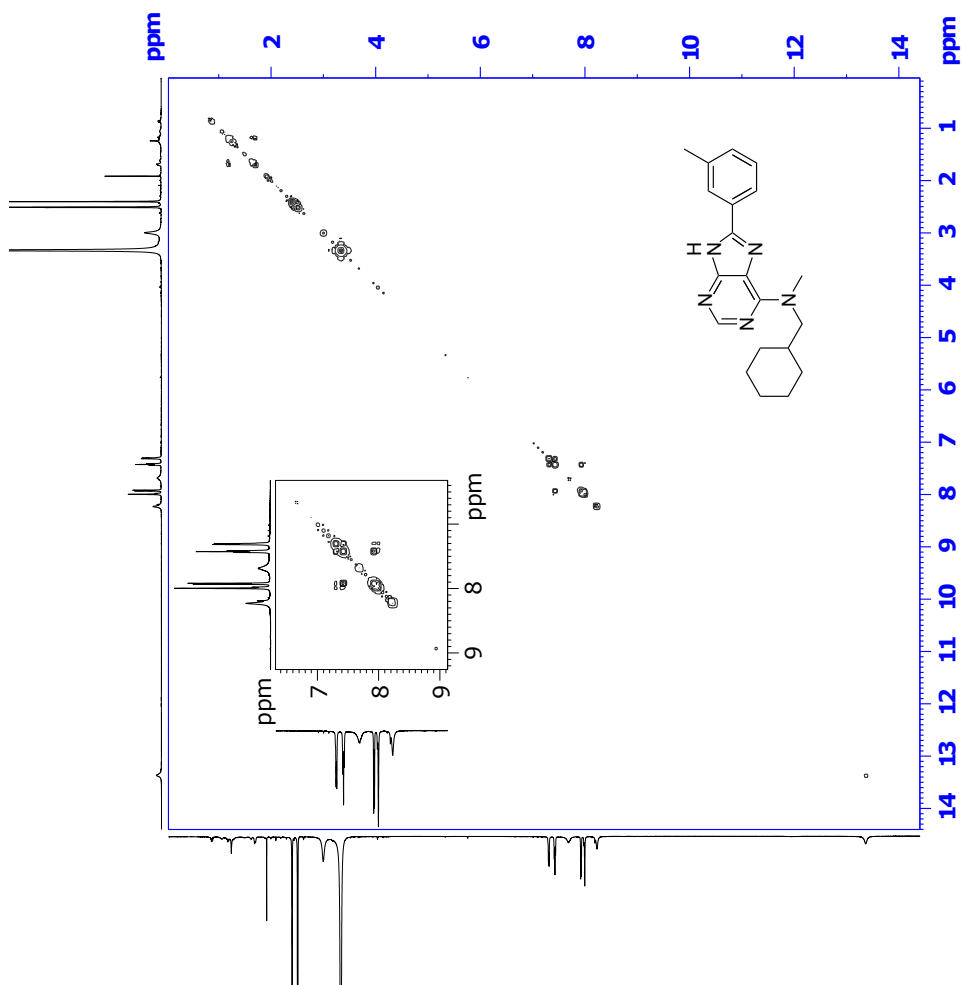


Figure M.3: COSY specter compound **HSB2** (DMSO- d_6 , 600 MHz).



Current Date Parameters
 Name HSB2-147-5
 EXPNO 1
 PROCNO 1
 F2 - Acquisition Parameters
 Date_ 20190522
 Time 12:52 h
 INSTRUM spect
 PROBDI Z11768.0061
 TD 65536
 FIDPROC hmcdec914095
 SOLVENT DMSO
 DS 16
 SWH 9615.365 Hz
 AQ 0.2129970 sec
 RG 57.14 usec
 DE 20.00 usec
 L1 30000 K
 CGST6 120.000000
 ON 170.000000
 CGST13 8.000000
 D1 0.000000 sec
 D11 2.04915190 sec
 D12 0.850000 sec
 D16 0.0002000 sec
 D17 0.0001510 sec
 INJ 600.1843671 MHz
 SEQU 1H
 NUC1 1H usec
 P2 16.00 usec
 PL1 6.0000000 W
 PL2 130.9300000 MHz
 NUC2 13C
 P3 11.40 usec
 PL3 88.0000000 W
 PL4 211.40 usec
 PL5 88.0000000 W
 CPMPCOMB4
 SFOFF57 0 Hz
 SP1 6400093 W
 SP1M11 80.00 %
 SP1M12 80.00 %
 SP1M13 80.00 %
 SP1M14 80.00 %
 SP1M15 80.00 %
 SP1M16 80.00 %
 SP1M17 80.00 %
 SP1M18 80.00 %
 SP1M19 80.00 %
 SP1M20 80.00 %
 SP1M21 80.00 %
 SP1M22 80.00 %
 SP1M23 80.00 %
 SP1M24 80.00 %
 SP1M25 80.00 %
 SP1M26 80.00 %
 SP1M27 80.00 %
 SP1M28 80.00 %
 SP1M29 80.00 %
 SP1M30 80.00 %
 F1 - Acquisition parameters
 TD 65536
 FIDRES 150.226 MHz
 SFOFF 238.692047 Hz
 SFOFF2 219.390 ppm
 FIDPROC Echo-Anti Echo
 F2 - Processing parameters
 SF 600.1800000 MHz
 WDW SINE
 LB 0 Hz
 GB 0 Hz
 PC 1.40
 F1 - Processing parameters
 SI echo-anti echo
 MC 150.533810 MHz
 WDW GAUSS
 SSB 0 Hz
 GB 0 Hz

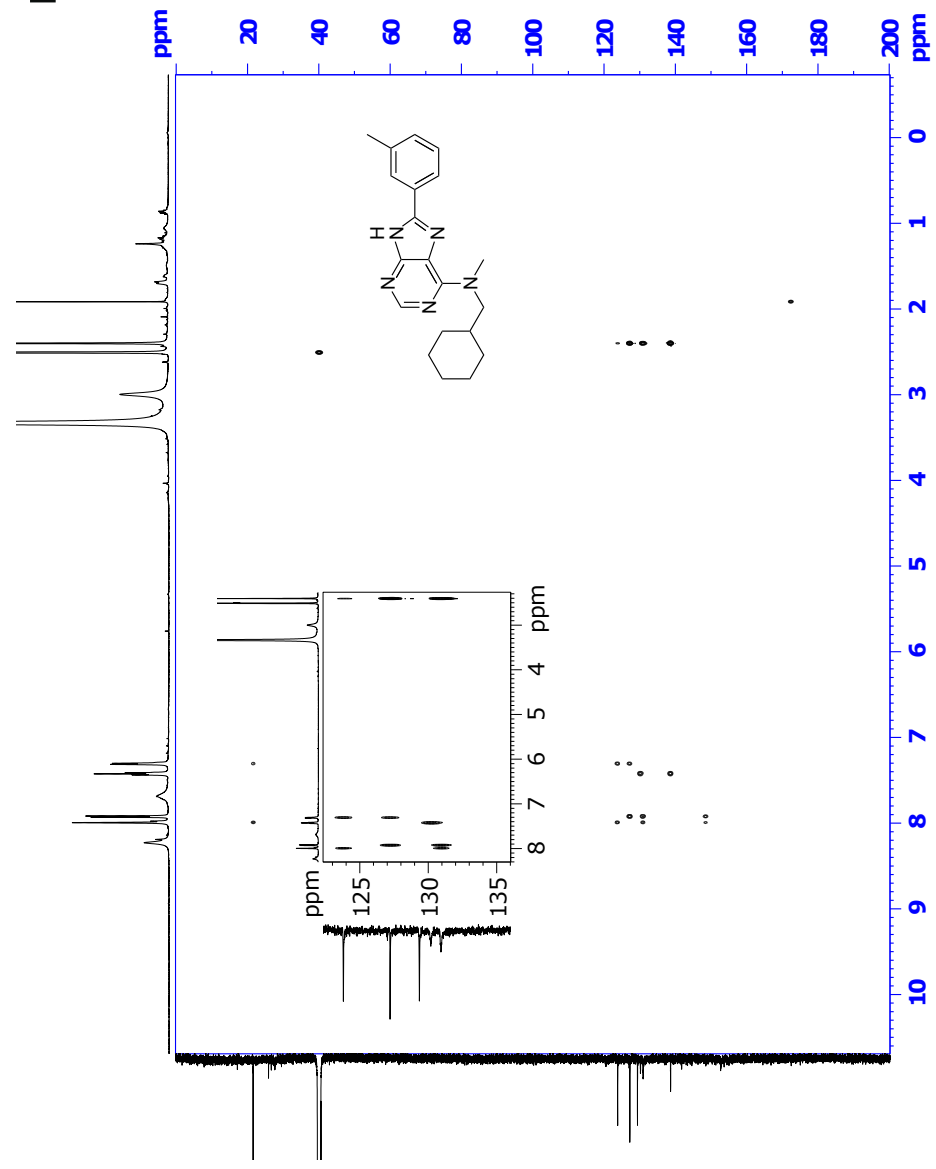


Figure M.5: HMBC spectrum of compound **HSB2** (DMSO-*d*₆, 600 MHz).

Single Mass Analysis

Tolerance = 2.0 PPM / DBE: min = -50.0, max = 50.0

Element prediction: Off

Number of isotope peaks used for i-FIT = 3

Monoisotopic Mass, Even Electron Ions

1234 formula(e) evaluated with 1 results within limits (all results (up to 1000) for each mass)

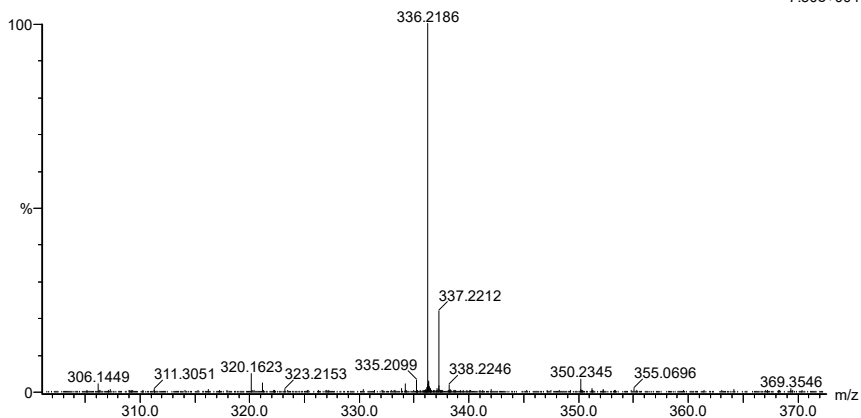
Elements Used:

C: 0-100 H: 0-150 N: 0-10 O: 0-10

2019-510 177 (3.465)AM2 (Ar,35000.0,0.00,0.00); Cm (165:179)

1: TOF MS ASAP+

7.50e+004



Minimum: -50.0
Maximum: 5.0 2.0 50.0

Mass	Calc. Mass	mDa	PPM	DBE	i-FIT	Norm	Conf (%)	Formula
336.2186	336.2188	-0.2	-0.6	10.5	693.4	n/a	n/a	C20 H26 N5

Figure M.6: MS specter of compound HSB2.

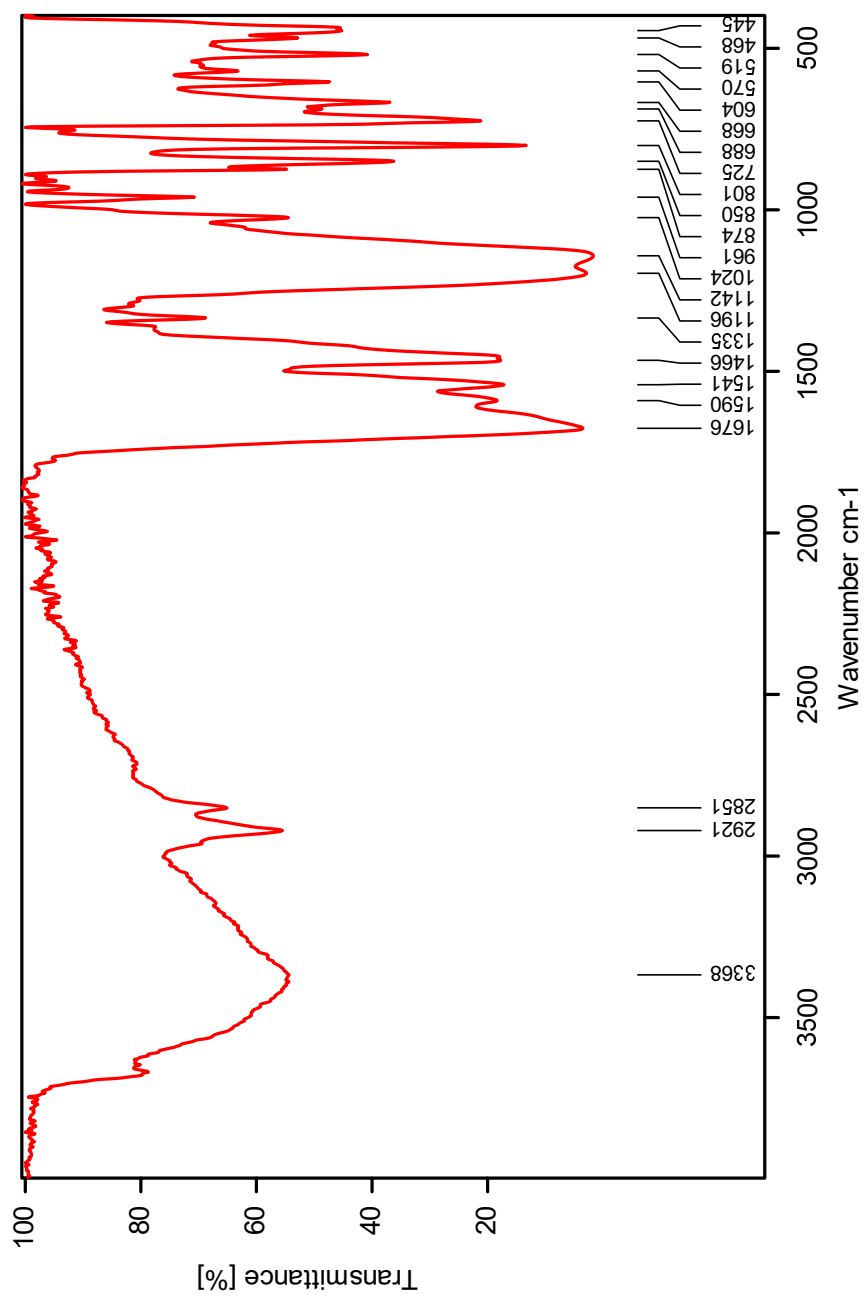


Figure M.7: IR specter of compound **HSB2**.

N Spectroscopic Data for Compound HSB4

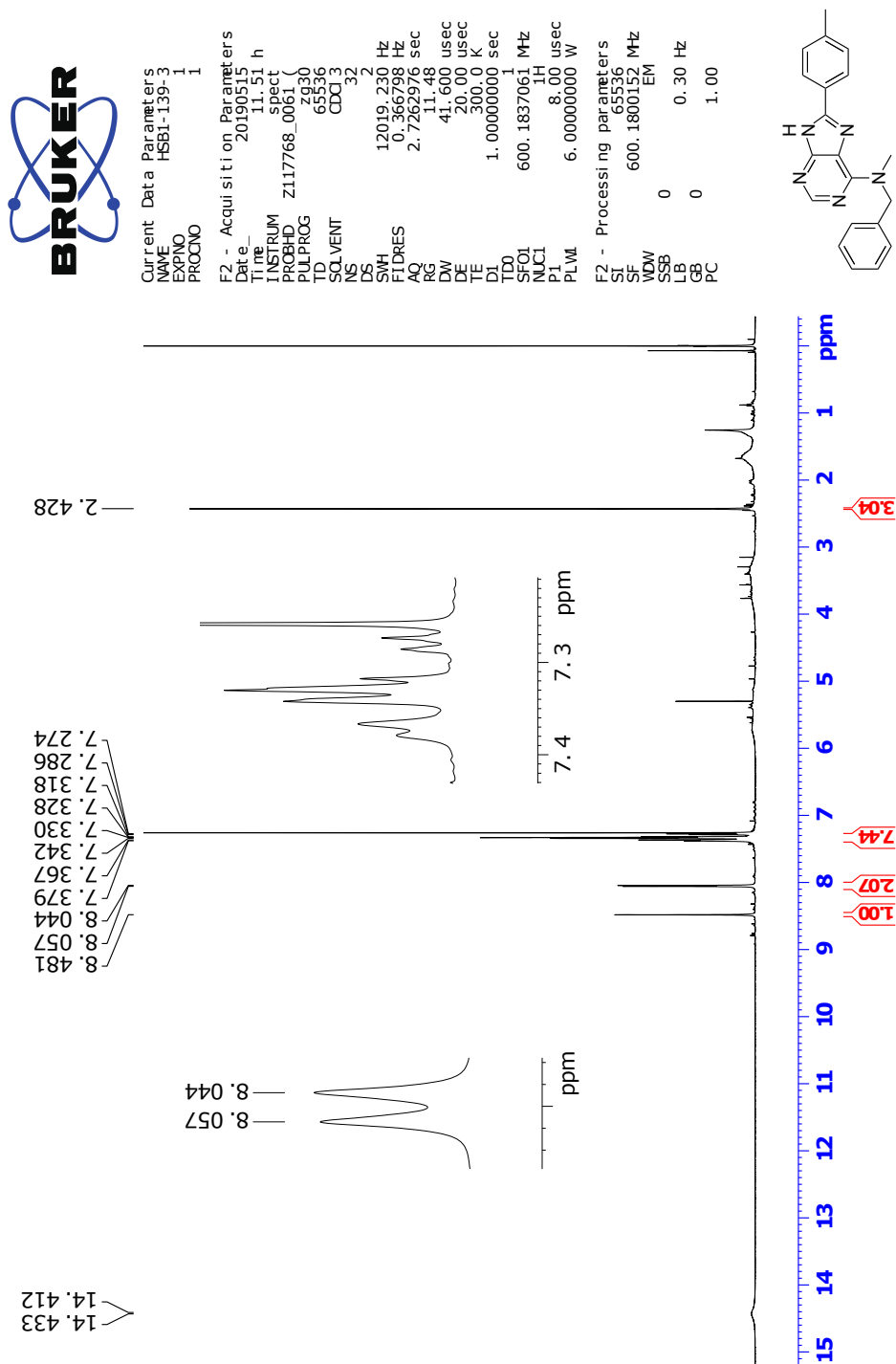


Figure N.1: ¹H NMR specter of compound **HSB4** (CDCl₃, 600 MHz).



Current Data Parameters
 NAME HSB1-I39-3
 EXPNO 2
 PROCNO 1

F2 - Acquisition Parameters
 Date_ 20190515
 Time 12.43 h
 INSTRUM spect
 PROBHD Z117768_0061
 PULPROG zgpg30
 TD 65536
 SOLVENT CDCl3
 NS 1024
 DS 4
 SWH 36057.691 Hz
 FIDRES 1.100393 Hz
 AQ 0.9087659 sec
 RG 197.14
 DW 13.867 usec
 DE 18.00 usec
 TE 300.0 K
 D1 2.0000000 sec
 D11 0.03000000 sec
 TDO
 SFO1 150.9304719 MHz
 NUC1 13C
 PL 11.40 usec
 PLVM 80.0000000 W
 SFO2 600.1824007 MHz
 NUC2 1H
 CPDPRG2 waltz16
 PPD2 70.00 usec
 PLW2 6.0000000 W
 PLW3 0.07836700 W
 PLW4 0.03941800 W

F2 - Processing parameters
 SI 32768
 SF 150.9153824 MHz
 EM
 WDW 0
 SSB 0
 LB 1.00 Hz
 GB 0
 PC 1.40

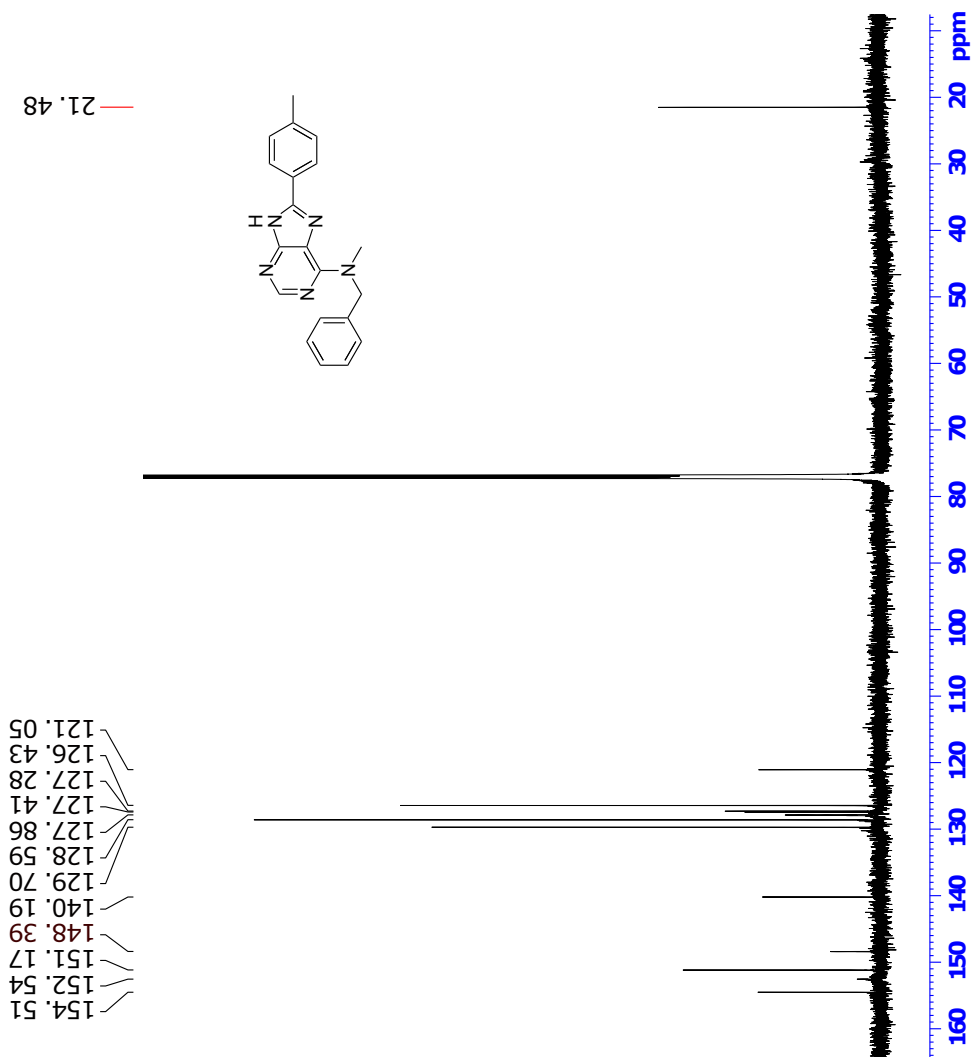


Figure N.2: ^{13}C NMR spectrum of compound **HSB4** (CDCl_3 , 150 MHz).



Current Data Parameters
 NAME HSB1-139-3
 EXPNO 3
 PROCNO 1

F2 - Acquisition Parameters
 Date_ 20190515
 Time 12.43 h
 INSTRUM spect
 PULPROG zgpg30
 TD 65536
 SOLVENT CDCl3
 NS 1
 DS 16
 SWH 11111.16 Hz
 FIDRES 10.857695 Hz
 AQ 0.0921600 sec
 RG 64.33
 DW 45.000 usec
 DE 19.00 usec
 TE 300.0 Ksec
 D0 0.00000000 sec
 D1 2.03891206 sec
 D11 0.03000000 sec
 D12 0.00000000 sec
 D13 0.00000000 sec
 D16 0.00020000 sec
 D19 0.00000000 sec
 INU 0.00009000 sec
 TDel 1
 SFO1 600.1843997 MHz
 P1 11.00 usec
 P2 8.00 usec
 P3 8.00 usec
 P4 8.00 usec
 P5 8.00 usec
 P6 8.00 usec
 P7 2500.00 usec
 P8 6.00000000 W
 PL1 10.00000000 W
 PL2 10.00000000 W
 PL3 10.00000000 W
 PL4 10.00000000 W
 PL5 10.00000000 W
 PL6 10.00000000 W
 PL7 10.00000000 W
 PL8 10.00000000 W
 PL9 10.00000000 W
 PL10 10.00000000 W
 PL11 10.00000000 W
 PL12 10.00000000 W
 PL13 10.00000000 W
 PL14 10.00000000 W
 PL15 10.00000000 W
 PL16 10.00000000 W
 PL17 10.00000000 W
 PL18 10.00000000 W
 PL19 10.00000000 W
 PL20 10.00000000 W
 PL21 10.00000000 W
 PL22 10.00000000 W
 PL23 10.00000000 W
 PL24 10.00000000 W
 PL25 10.00000000 W
 PL26 10.00000000 W
 PL27 10.00000000 W
 PL28 10.00000000 W
 PL29 10.00000000 W
 PL30 10.00000000 W
 PL31 10.00000000 W
 PL32 10.00000000 W
 PL33 10.00000000 W
 PL34 10.00000000 W
 PL35 10.00000000 W
 PL36 10.00000000 W
 PL37 10.00000000 W
 PL38 10.00000000 W
 PL39 10.00000000 W
 PL40 10.00000000 W
 PL41 10.00000000 W
 PL42 10.00000000 W
 PL43 10.00000000 W
 PL44 10.00000000 W
 PL45 10.00000000 W
 PL46 10.00000000 W
 PL47 10.00000000 W
 PL48 10.00000000 W
 PL49 10.00000000 W
 PL50 10.00000000 W
 PL51 10.00000000 W
 PL52 10.00000000 W
 PL53 10.00000000 W
 PL54 10.00000000 W
 PL55 10.00000000 W
 PL56 10.00000000 W
 PL57 10.00000000 W
 PL58 10.00000000 W
 PL59 10.00000000 W
 PL60 10.00000000 W
 PL61 10.00000000 W
 PL62 10.00000000 W
 PL63 10.00000000 W
 PL64 10.00000000 W
 PL65 10.00000000 W
 PL66 10.00000000 W
 PL67 10.00000000 W
 PL68 10.00000000 W
 PL69 10.00000000 W
 PL70 10.00000000 W
 PL71 10.00000000 W
 PL72 10.00000000 W
 PL73 10.00000000 W
 PL74 10.00000000 W
 PL75 10.00000000 W
 PL76 10.00000000 W
 PL77 10.00000000 W
 PL78 10.00000000 W
 PL79 10.00000000 W
 PL80 10.00000000 W
 PL81 10.00000000 W
 PL82 10.00000000 W
 PL83 10.00000000 W
 PL84 10.00000000 W
 PL85 10.00000000 W
 PL86 10.00000000 W
 PL87 10.00000000 W
 PL88 10.00000000 W
 PL89 10.00000000 W
 PL90 10.00000000 W
 PL91 10.00000000 W
 PL92 10.00000000 W
 PL93 10.00000000 W
 PL94 10.00000000 W
 PL95 10.00000000 W
 PL96 10.00000000 W
 PL97 10.00000000 W
 PL98 10.00000000 W
 PL99 10.00000000 W
 PL100 10.00000000 W

F1 - Acquisition parameters
 SFO1 600.1844 MHz
 FIDRES 173.611115 Hz
 SW 18.513 ppm
 FWHM 0.4 Hz
 GB 0 Hz
 PC 1.40

F2 - Processing parameters
 SI 1024
 SF 600.1800152 MHz
 DS 4
 LB 0 Hz
 GB 0 Hz
 PC 1.40

F1 - Processing parameters
 SI 1024
 SF 600.1800152 MHz
 DS 4
 LB 0 Hz
 GB 0 Hz
 PC 1.40

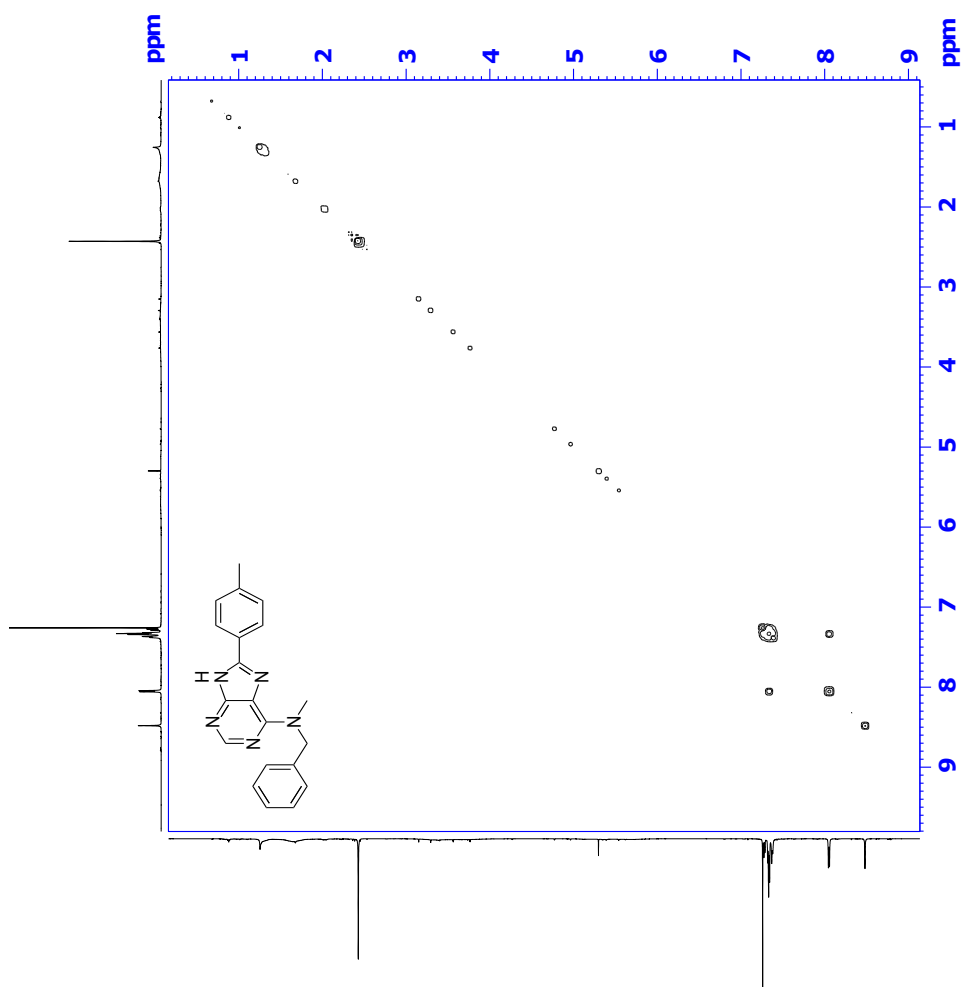


Figure N.3: COSY specter compound **HSB4** (CDCl₃, 600 MHz).



Current Data Parameters
 EXPNO 3
 PROCNO 1
 F2 - Acquisition Parameters
 Date_ 20190515
 Time 16:54:11 h
 INSTRUM spect
 PRBHD Z11768_0061_C
 TD 65536
 FIDRES 0.09094095
 SOLVENT CDCl3
 US 16
 SWH 1111.111 Hz
 FIDRES 0.1843200 sec
 RG 197.14 usec
 DE 4.20.00 usec
 TE 300.0 K
 T1 120.013000 sec
 T1RHO 170.0000000
 CNST13 8.0000000
 DI 2.07782413 sec
 D1 0.0032000 sec
 D16 0.0032000 sec
 T1RHO 0.00001510 sec
 Delay 600.1843997 MHz
 NUC1 13C
 P1 8.11 usec
 P2 16.00 usec
 PL1 6.0000000 V
 PL2 150.9304132 MHz
 P3 11.40 usec
 P4 88.0000000 V
 PL4 C1600-0rb.4
 SFOF57 0 Hz
 SFOF57 0 Hz
 SPW171 17.47200093 W
 SPW172 17.47200093 W
 SPW173 17.47200093 W
 SPW174 17.47200093 W
 SPW175 17.47200093 W
 SPW176 17.47200093 W
 SPW177 17.47200093 W
 SPW178 17.47200093 W
 SPW179 17.47200093 W
 SPW180 17.47200093 W
 SPW181 17.47200093 W
 SPW182 17.47200093 W
 SPW183 17.47200093 W
 SPW184 17.47200093 W
 SPW185 17.47200093 W
 SPW186 17.47200093 W
 SPW187 17.47200093 W
 SPW188 17.47200093 W
 SPW189 17.47200093 W
 SPW190 17.47200093 W
 SPW191 17.47200093 W
 SPW192 17.47200093 W
 SPW193 17.47200093 W
 SPW194 17.47200093 W
 SPW195 17.47200093 W
 SPW196 17.47200093 W
 SPW197 17.47200093 W
 SPW198 17.47200093 W
 SPW199 17.47200093 W
 SPW200 17.47200093 W
 E1 - Acquisition parameters
 TD 256
 FIDRES 0.1843200 sec
 FTRES 258.9304132 MHz
 SW 219.390 ppm
 FWHM 0.1843200 sec
 F2 - Processing parameters
 SF 600.1800152 MHz
 DS 4
 SINE SINE
 GB 0 Hz
 LB 0 Hz
 PC 1.40
 E1 - Processing parameters
 MC2 echo-anti echo
 SF 600.1800152 MHz
 SSB 0 Hz
 GB 0 Hz

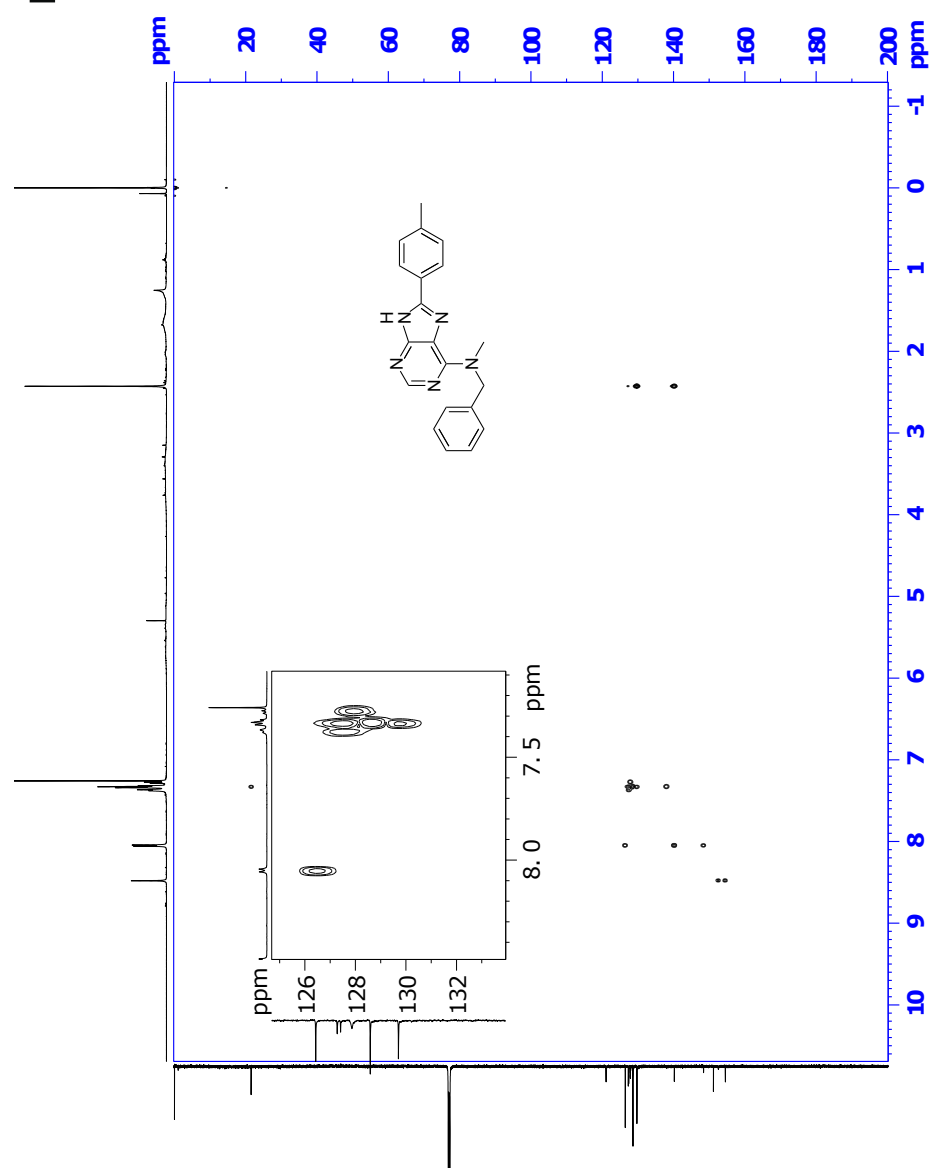


Figure N.5: HMBC spectrum of compound **HSB4** (CDCl₃, 600 MHz).

Single Mass Analysis

Tolerance = 2.0 PPM / DBE: min = -50.0, max = 50.0

Element prediction: Off

Number of isotope peaks used for i-FIT = 3

Monoisotopic Mass, Even Electron Ions

1209 formula(e) evaluated with 1 results within limits (all results (up to 1000) for each mass)

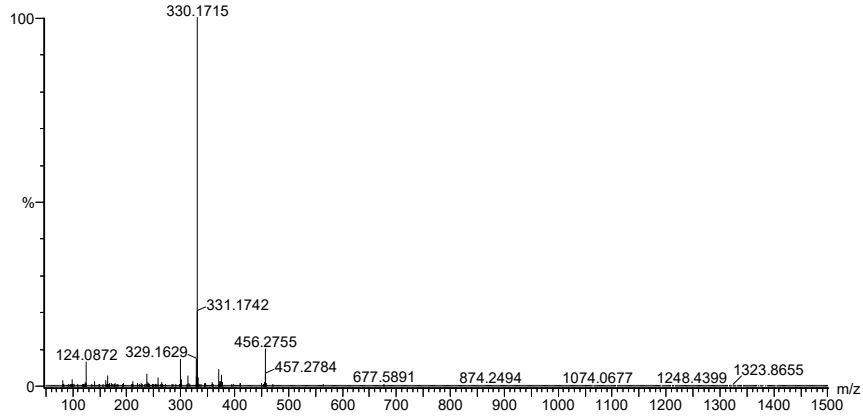
Elements Used:

C: 0-100 H: 0-150 N: 0-10 O: 0-10

2019-469 151 (2.946)AM2 (Ar,35000.0,0.00,0.00); Cm (137:152)

1: TOF MS ASAP+

1.47e+006



Minimum: -50.0
Maximum: 5.0 2.0 50.0

Mass	Calc. Mass	mDa	PPM	DBE	i-FIT	Norm	Conf (%)	Formula
330.1715	330.1719	-0.4	-1.2	13.5	1236.0	n/a	n/a	C20 H20 N5

Figure N.6: MS specter of compound HSB4.

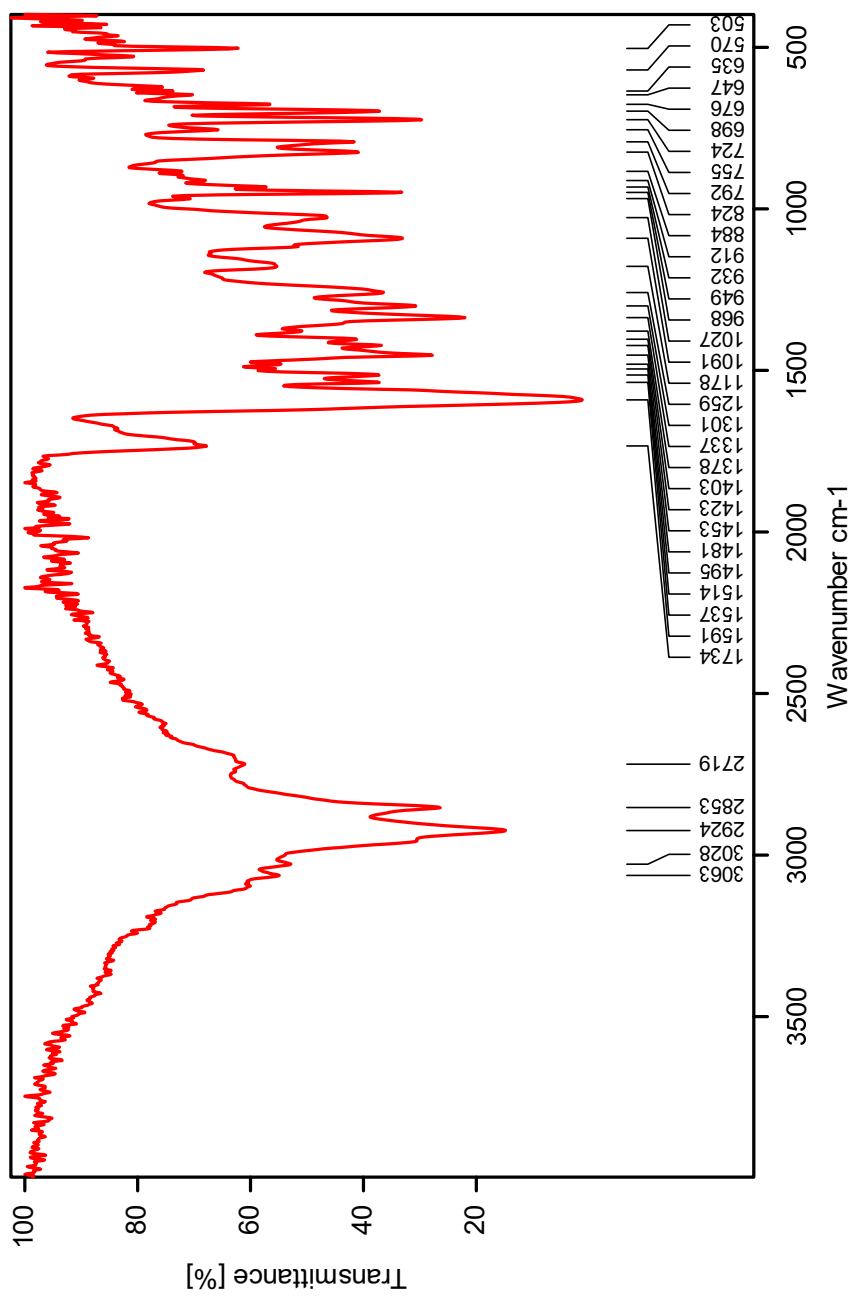


Figure N.7: IR specter of compound **HSB4**.

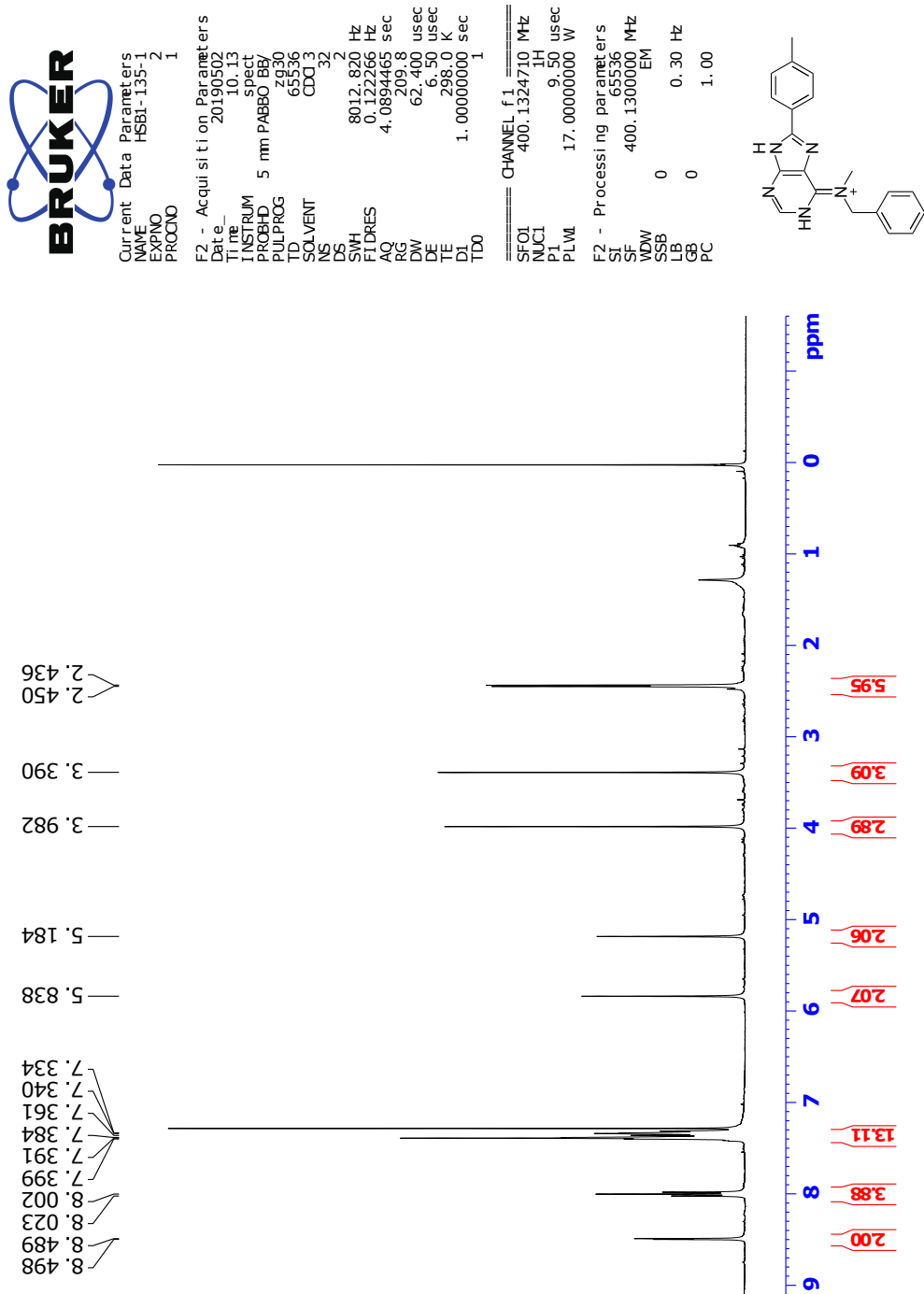


Figure N.8: ¹H NMR spectrum of suspected imine tautomer of compound **HSB4** (CDCl₃, 400 MHz).

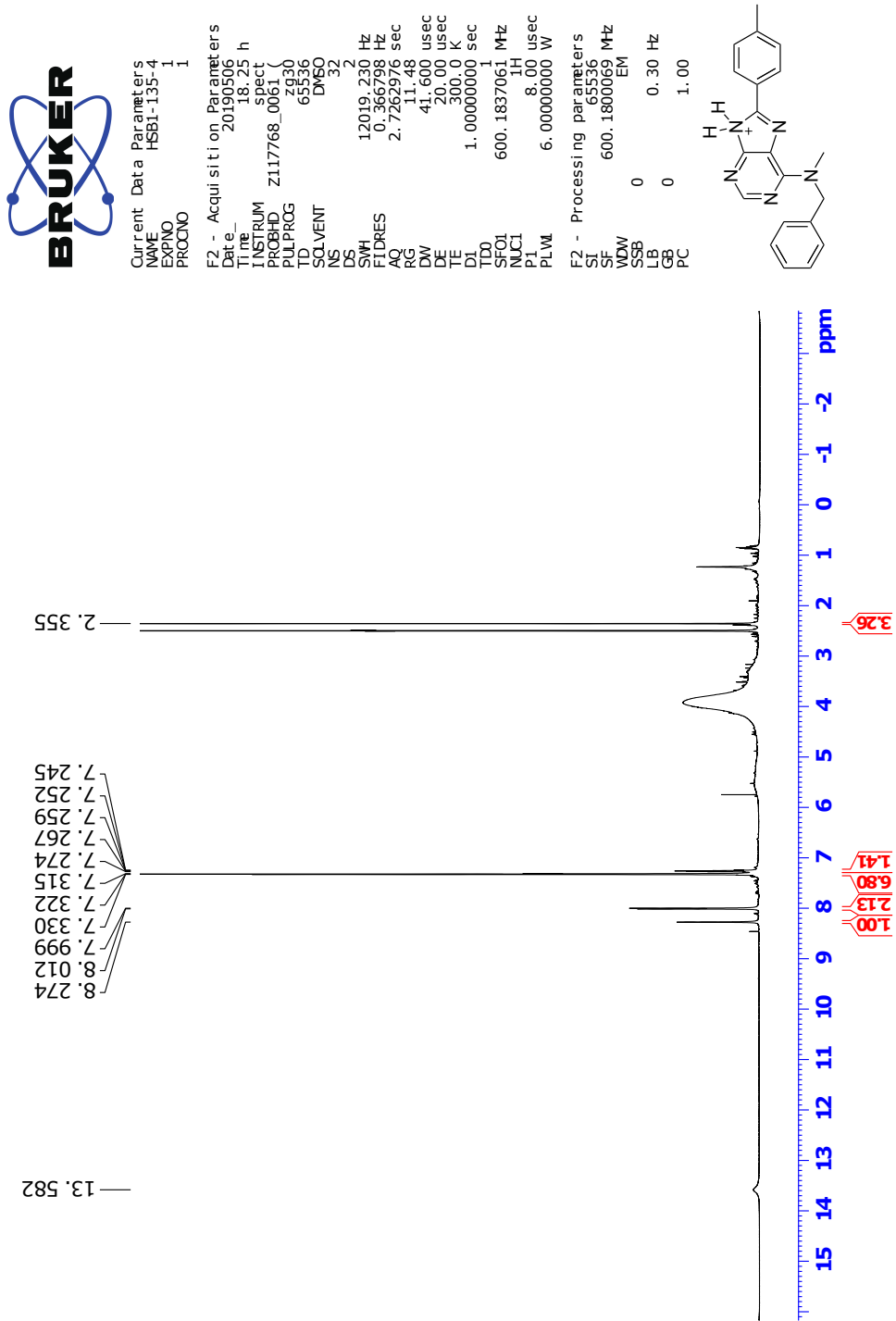


Figure N.9: ¹H NMR spectrum of suspected amine tautomer of compound HSB4 (DMSO-*d*₆, 400 MHz).

O Spectroscopic Data for Compound HSB5

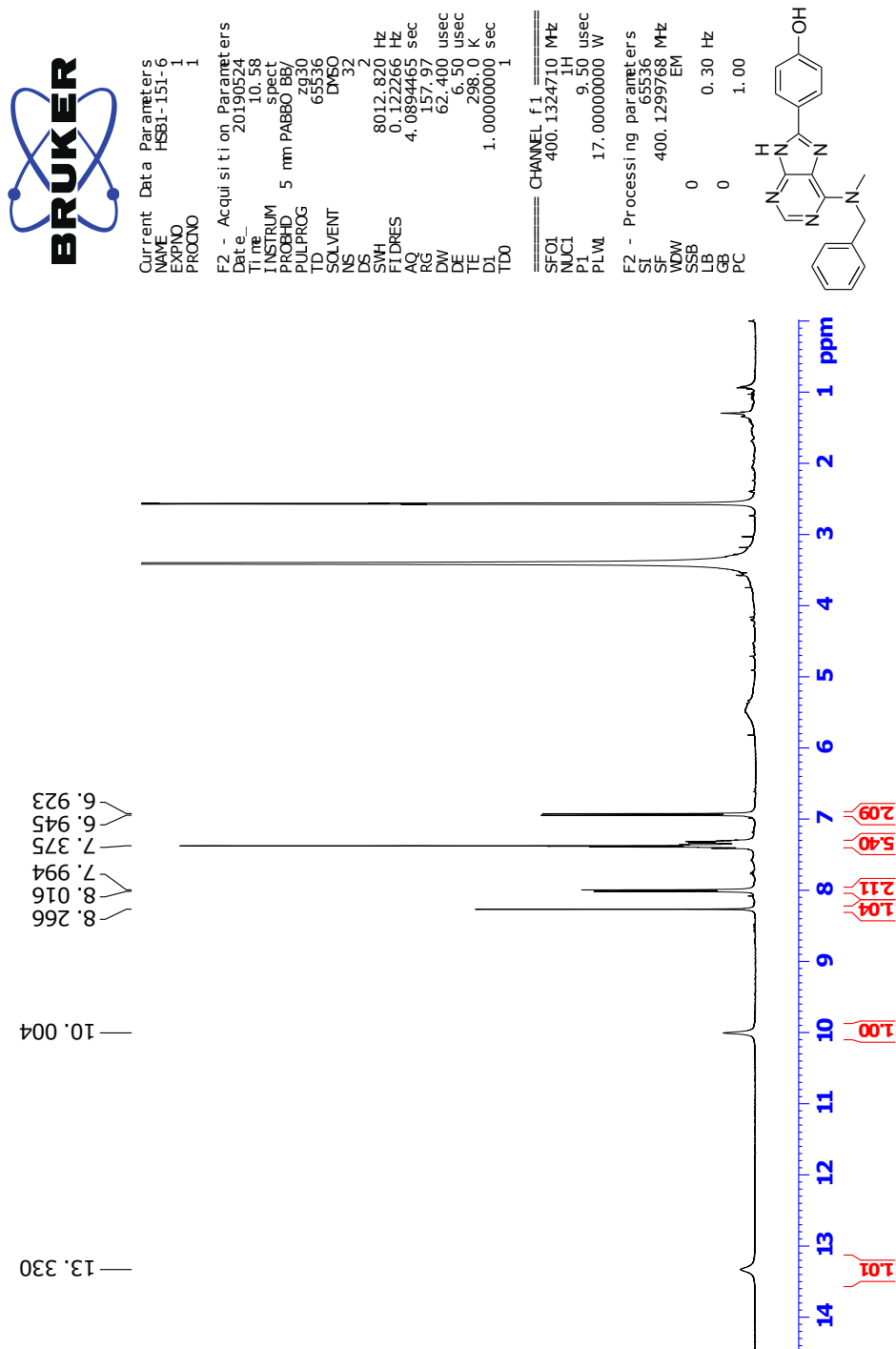


Figure O.1: ¹H NMR specter of compound **HSB5** (DMSO-*d*₆, 400 MHz).



Current Data Parameters
NAME HSB1-151-6
EXPNO 2
PROCNO 1

F2 - Acquisition Parameters
Date_ 20190524
Time_ 19.48
INSTRUM spect
PROBHD 5 mm PABBO BB/
PULPROG zgpg30
TD 65536
SOLVENT DMSO
NS 2048
DS 4
SWH 24038.461 Hz
FIDRES 0.366798 Hz
AQ 1.3031488 sec
RG 2708
RW 20.800 usec
DE 6.50 usec
TE 298.0 K
D1 2.0000000 sec
D11 0.03000000 sec
TD0 1

==== CHANNEL f1 =====
SFO1 100.6228293 MHz
NUC1 13C
P1 9.50 usec
PLW1 71.00000000 W

==== CHANNEL f2 =====
SFO2 400.1316005 MHz
NUC2 1H
CPDPRG2 waltz16
PCPDZ 90.00 usec
PLW2 17.00000000 W
PLW3 0.18941000 W
PLW3 0.15343000 W

F2 - Processing parameters
SI 32768
SF 100.6127685 MHz
WDW 0
SSB 0
LB 1.00 Hz
GB 0
PC 1.40

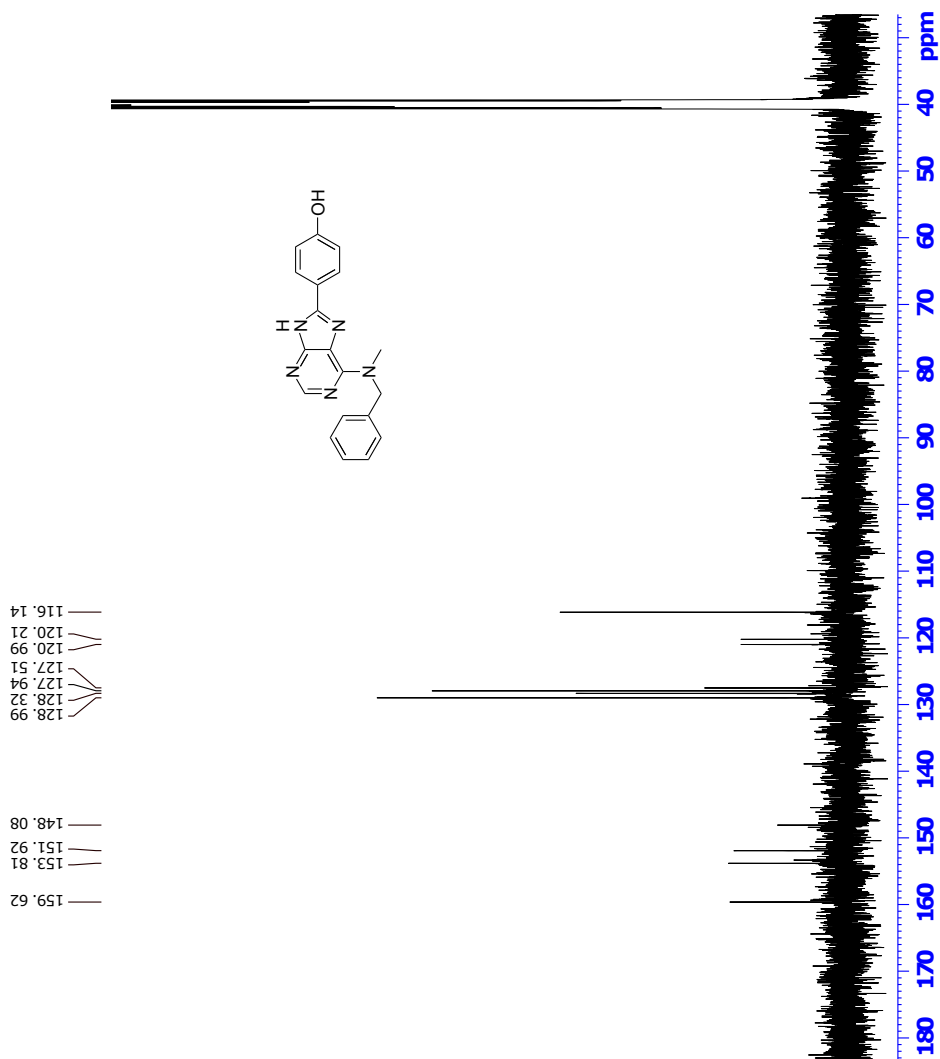


Figure O.2: ^{13}C NMR specter of compound **HSB5** (DMSO- d_6 , 100 MHz).



Current Data Parameters
 NAME HSB1-151-6
 EXPNO 3
 PROCNO 1

F2 - Acquisition Parameters
 Date_ 20190524
 Time 19.50
 INSTRUM spect
 PULPROG zgpg30
 TD 65536
 SOLVENT DMSO
 NS 8
 DS 8
 SWH 5747.126 Hz
 FLDRES 2.806214 Hz
 AQ 0.1781790 sec
 RG 717.000
 DW 67.000 usec
 DE 6.50 usec
 TE 298.0 K
 D0 0.03000000 sec
 D1 0.03000000 sec
 D11 0.03000000 sec
 D12 0.00020000 sec
 D13 0.00004000 sec
 D14 0.00000000 sec
 D15 0.00000000 sec
 D16 0.00000000 sec
 D17 0.00000000 sec
 D18 0.00000000 sec
 D19 0.00000000 sec
 D20 0.00000000 sec
 D21 0.00000000 sec
 D22 0.00000000 sec
 D23 0.00000000 sec
 D24 0.00000000 sec
 D25 0.00000000 sec
 D26 0.00000000 sec
 D27 0.00000000 sec
 D28 0.00000000 sec
 D29 0.00000000 sec
 D30 0.00000000 sec
 D31 0.00000000 sec
 D32 0.00000000 sec
 D33 0.00000000 sec
 D34 0.00000000 sec
 D35 0.00000000 sec
 D36 0.00000000 sec
 D37 0.00000000 sec
 D38 0.00000000 sec
 D39 0.00000000 sec
 D40 0.00000000 sec
 D41 0.00000000 sec
 D42 0.00000000 sec
 D43 0.00000000 sec
 D44 0.00000000 sec
 D45 0.00000000 sec
 D46 0.00000000 sec
 D47 0.00000000 sec
 D48 0.00000000 sec
 D49 0.00000000 sec
 D50 0.00000000 sec
 D51 0.00000000 sec
 D52 0.00000000 sec
 D53 0.00000000 sec
 D54 0.00000000 sec
 D55 0.00000000 sec
 D56 0.00000000 sec
 D57 0.00000000 sec
 D58 0.00000000 sec
 D59 0.00000000 sec
 D60 0.00000000 sec
 D61 0.00000000 sec
 D62 0.00000000 sec
 D63 0.00000000 sec
 D64 0.00000000 sec
 D65 0.00000000 sec
 D66 0.00000000 sec
 D67 0.00000000 sec
 D68 0.00000000 sec
 D69 0.00000000 sec
 D70 0.00000000 sec
 D71 0.00000000 sec
 D72 0.00000000 sec
 D73 0.00000000 sec
 D74 0.00000000 sec
 D75 0.00000000 sec
 D76 0.00000000 sec
 D77 0.00000000 sec
 D78 0.00000000 sec
 D79 0.00000000 sec
 D80 0.00000000 sec
 D81 0.00000000 sec
 D82 0.00000000 sec
 D83 0.00000000 sec
 D84 0.00000000 sec
 D85 0.00000000 sec
 D86 0.00000000 sec
 D87 0.00000000 sec
 D88 0.00000000 sec
 D89 0.00000000 sec
 D90 0.00000000 sec
 D91 0.00000000 sec
 D92 0.00000000 sec
 D93 0.00000000 sec
 D94 0.00000000 sec
 D95 0.00000000 sec
 D96 0.00000000 sec
 D97 0.00000000 sec
 D98 0.00000000 sec
 D99 0.00000000 sec
 D100 0.00000000 sec

CHANNEL F1
 SFOL 400.1328600 MHz
 NUC1 1H
 P0 9.50 usec
 P1 9.50 usec
 P17 9.50 usec
 P18 9.50 usec
 PL1 2000.00 usec
 PL2 2000.00 usec
 PL3 2000.00 usec
 PL4 2000.00 usec
 PL5 2000.00 usec
 PL6 2000.00 usec
 PL7 2000.00 usec
 PL8 2000.00 usec
 PL9 2000.00 usec
 PL10 2000.00 usec
 PL11 2000.00 usec
 PL12 2000.00 usec
 PL13 2000.00 usec
 PL14 2000.00 usec
 PL15 2000.00 usec
 PL16 2000.00 usec
 PL17 2000.00 usec
 PL18 2000.00 usec
 PL19 2000.00 usec
 PL20 2000.00 usec
 PL21 2000.00 usec
 PL22 2000.00 usec
 PL23 2000.00 usec
 PL24 2000.00 usec
 PL25 2000.00 usec
 PL26 2000.00 usec
 PL27 2000.00 usec
 PL28 2000.00 usec
 PL29 2000.00 usec
 PL30 2000.00 usec
 PL31 2000.00 usec
 PL32 2000.00 usec
 PL33 2000.00 usec
 PL34 2000.00 usec
 PL35 2000.00 usec
 PL36 2000.00 usec
 PL37 2000.00 usec
 PL38 2000.00 usec
 PL39 2000.00 usec
 PL40 2000.00 usec
 PL41 2000.00 usec
 PL42 2000.00 usec
 PL43 2000.00 usec
 PL44 2000.00 usec
 PL45 2000.00 usec
 PL46 2000.00 usec
 PL47 2000.00 usec
 PL48 2000.00 usec
 PL49 2000.00 usec
 PL50 2000.00 usec
 PL51 2000.00 usec
 PL52 2000.00 usec
 PL53 2000.00 usec
 PL54 2000.00 usec
 PL55 2000.00 usec
 PL56 2000.00 usec
 PL57 2000.00 usec
 PL58 2000.00 usec
 PL59 2000.00 usec
 PL60 2000.00 usec
 PL61 2000.00 usec
 PL62 2000.00 usec
 PL63 2000.00 usec
 PL64 2000.00 usec
 PL65 2000.00 usec
 PL66 2000.00 usec
 PL67 2000.00 usec
 PL68 2000.00 usec
 PL69 2000.00 usec
 PL70 2000.00 usec
 PL71 2000.00 usec
 PL72 2000.00 usec
 PL73 2000.00 usec
 PL74 2000.00 usec
 PL75 2000.00 usec
 PL76 2000.00 usec
 PL77 2000.00 usec
 PL78 2000.00 usec
 PL79 2000.00 usec
 PL80 2000.00 usec
 PL81 2000.00 usec
 PL82 2000.00 usec
 PL83 2000.00 usec
 PL84 2000.00 usec
 PL85 2000.00 usec
 PL86 2000.00 usec
 PL87 2000.00 usec
 PL88 2000.00 usec
 PL89 2000.00 usec
 PL90 2000.00 usec
 PL91 2000.00 usec
 PL92 2000.00 usec
 PL93 2000.00 usec
 PL94 2000.00 usec
 PL95 2000.00 usec
 PL96 2000.00 usec
 PL97 2000.00 usec
 PL98 2000.00 usec
 PL99 2000.00 usec
 PL100 2000.00 usec

GRADIENT CHANNEL
 G1 10.00 %
 G2 10.00 %
 G3 10.00 %
 G4 10.00 %
 G5 10.00 %
 G6 10.00 %
 G7 10.00 %
 G8 10.00 %
 G9 10.00 %
 G10 10.00 %
 G11 10.00 %
 G12 10.00 %
 G13 10.00 %
 G14 10.00 %
 G15 10.00 %
 G16 10.00 %
 G17 10.00 %
 G18 10.00 %
 G19 10.00 %
 G20 10.00 %
 G21 10.00 %
 G22 10.00 %
 G23 10.00 %
 G24 10.00 %
 G25 10.00 %
 G26 10.00 %
 G27 10.00 %
 G28 10.00 %
 G29 10.00 %
 G30 10.00 %
 G31 10.00 %
 G32 10.00 %
 G33 10.00 %
 G34 10.00 %
 G35 10.00 %
 G36 10.00 %
 G37 10.00 %
 G38 10.00 %
 G39 10.00 %
 G40 10.00 %
 G41 10.00 %
 G42 10.00 %
 G43 10.00 %
 G44 10.00 %
 G45 10.00 %
 G46 10.00 %
 G47 10.00 %
 G48 10.00 %
 G49 10.00 %
 G50 10.00 %
 G51 10.00 %
 G52 10.00 %
 G53 10.00 %
 G54 10.00 %
 G55 10.00 %
 G56 10.00 %
 G57 10.00 %
 G58 10.00 %
 G59 10.00 %
 G60 10.00 %
 G61 10.00 %
 G62 10.00 %
 G63 10.00 %
 G64 10.00 %
 G65 10.00 %
 G66 10.00 %
 G67 10.00 %
 G68 10.00 %
 G69 10.00 %
 G70 10.00 %
 G71 10.00 %
 G72 10.00 %
 G73 10.00 %
 G74 10.00 %
 G75 10.00 %
 G76 10.00 %
 G77 10.00 %
 G78 10.00 %
 G79 10.00 %
 G80 10.00 %
 G81 10.00 %
 G82 10.00 %
 G83 10.00 %
 G84 10.00 %
 G85 10.00 %
 G86 10.00 %
 G87 10.00 %
 G88 10.00 %
 G89 10.00 %
 G90 10.00 %
 G91 10.00 %
 G92 10.00 %
 G93 10.00 %
 G94 10.00 %
 G95 10.00 %
 G96 10.00 %
 G97 10.00 %
 G98 10.00 %
 G99 10.00 %
 G100 10.00 %

F1 - Acquisition parameters
 SFOL 400.1329 MHz
 FLDRES 89.798851 Hz
 SW 14.363 ppm
 FWHM 0.4 Hz
 GB 0 Hz
 PC 1.40

F2 - Processing parameters
 SL 1024
 SF 400.1292769 MHz
 SSB 0 Hz
 LB 0 Hz
 GB 0 Hz
 PC 1.40

F1 - Processing parameters
 SL 1024
 SF 400.1292769 MHz
 SSB 0 Hz
 LB 0 Hz
 GB 0 Hz
 PC 1.40

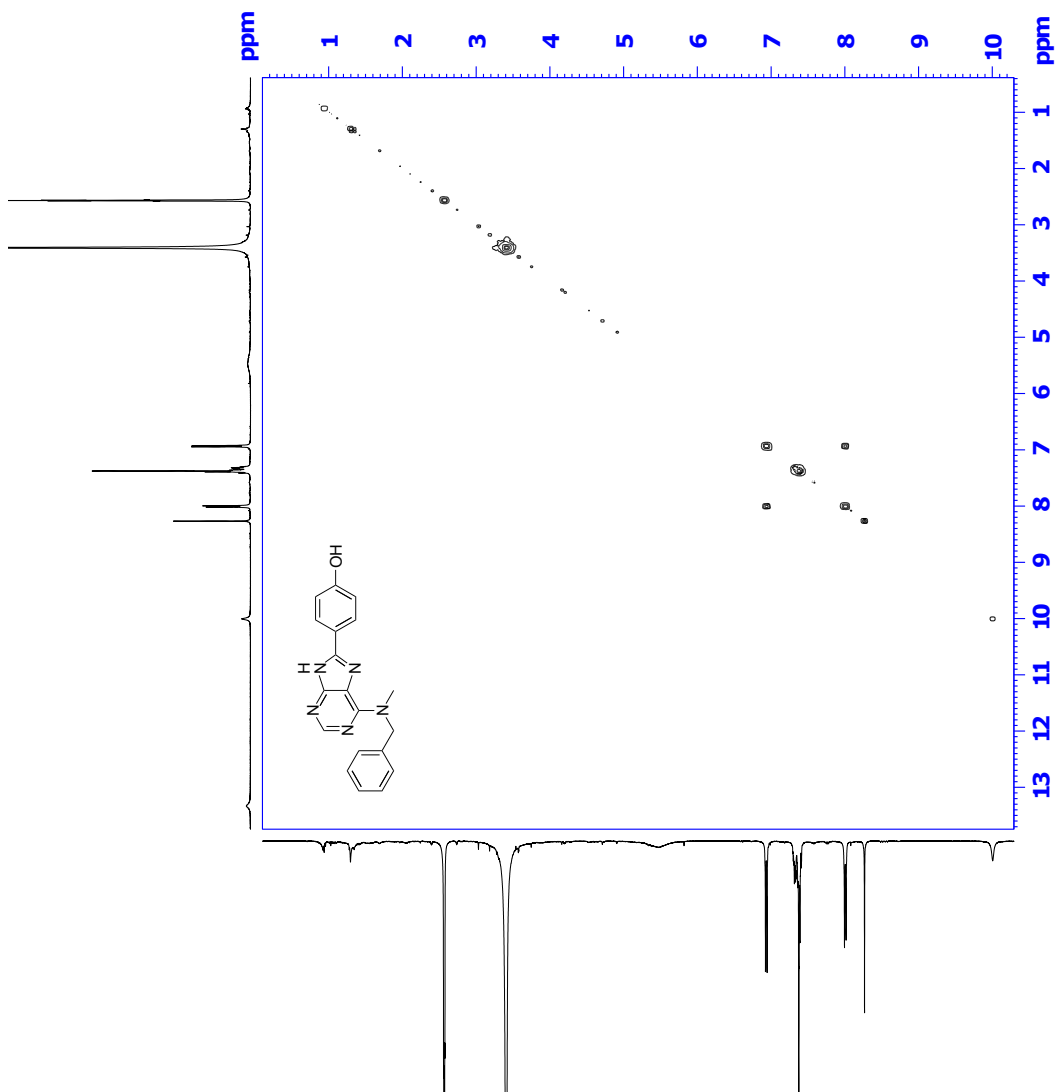


Figure O.3: COSY specter compound **HSB5** (DMSO- d_6 , 400 MHz).

Single Mass Analysis

Tolerance = 2.0 PPM / DBE: min = -50.0, max = 50.0

Element prediction: Off

Number of isotope peaks used for i-FIT = 3

Monoisotopic Mass, Even Electron Ions

1220 formula(e) evaluated with 1 results within limits (all results (up to 1000) for each mass)

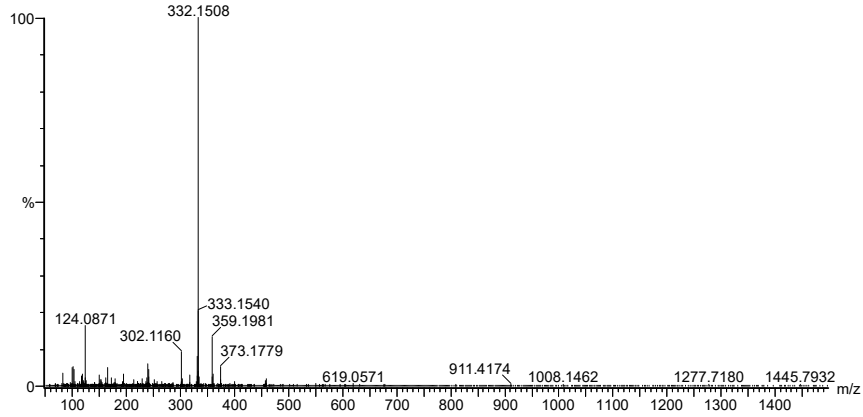
Elements Used:

C: 0-100 H: 0-150 N: 0-10 O: 0-10

2019-511 180 (3.516) AM2 (Ar,35000.0,0.00,0.00); Cm (167:197)

1: TOF MS ASAP+

1.37e+005



Minimum: -50.0
Maximum: 5.0 2.0 50.0

Mass	Calc. Mass	mDa	PPM	DBE	i-FIT	Norm	Conf (%)	Formula
332.1508	332.1511	-0.3	-0.9	13.5	89.0.2	n/a	n/a	C19 H18 N5 O

Figure O.6: MS specter of compound HSB5.

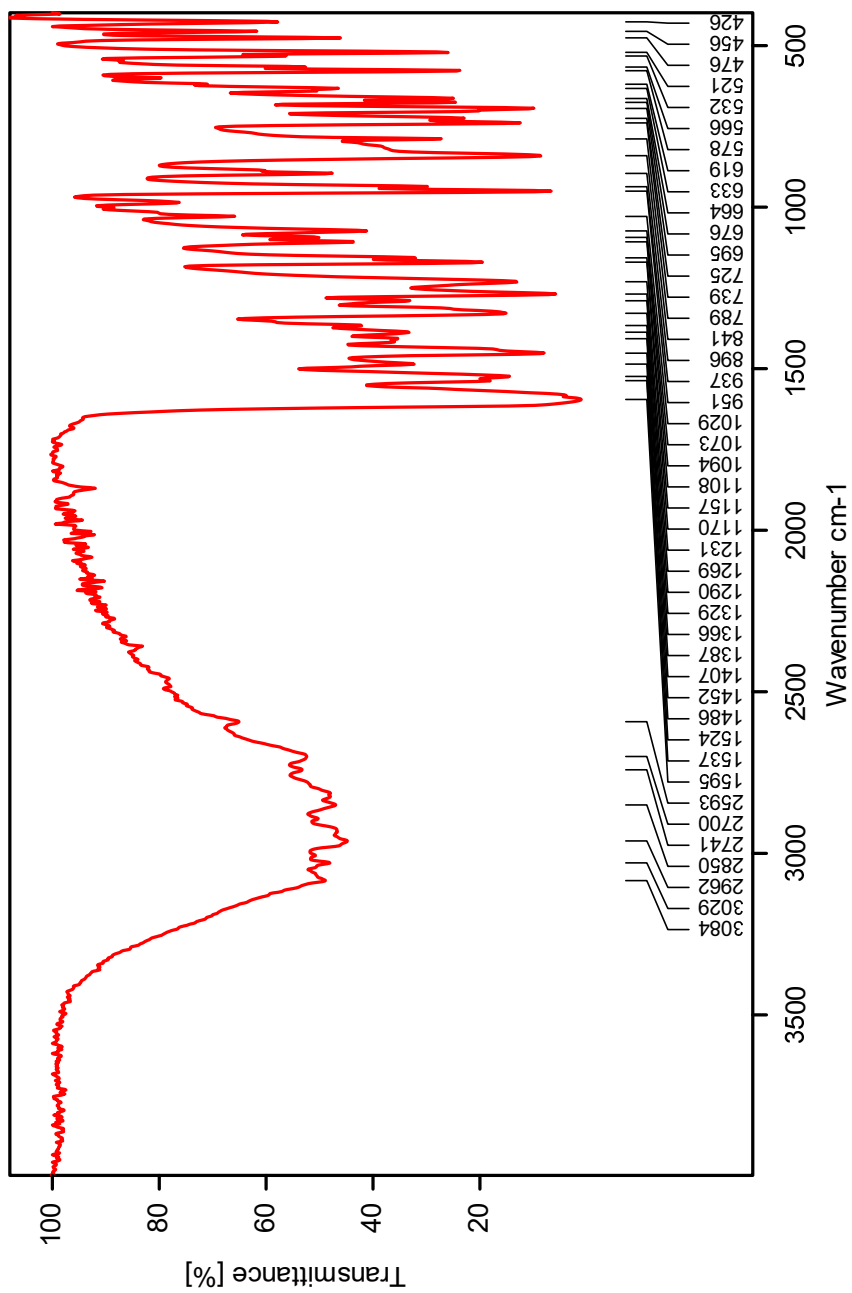


Figure O.7: IR specter of compound **HSB5**.

